Analysis of Cell Cycle Associated Proteins from

Theileria annulata

Geoffrey Malcolm Ingram

PhD

Wellcome Unit of Molecular Parasitology

Anderson College

University of Glasgow

March 1997

ProQuest Number: 11007672

ProQuest 11007672

I would like to dedicate this thesis to my grand-parents, my mother and father and my little brother Michael.

"What we are today comes from our thoughts of yesterday, and our present thoughts build our life of tomorrow: our life is the creation of our mind"

The Dhammapada

Summary

The protozoan parasite, *Theileria annulata*, is a tick transmitted intracellular pathogen of domestic cattle in tropical regions of Africa and Asia. The parasite life cycle within the bovine host involves proliferative phases within the host lymphocytes and erythrocytes. As a means of characterising cdc2-related kinases (CRKs) involved in these stages which would control the parasite division cycle, p13^{suc1} affinity columns have been used to show binding and activity of parasite proteins which are likely to have a role in the cell cycle. Further experiments showed the existence of at least two p13^{suc1} binding kinases in *T. annulata*, together with possible substrate specificities of these polypeptides. Another gene involved in replication and division has been isolated, namely the large subunit of ribonucleotide reductase (R1) which encodes a unique N terminal extension to the predicted amino acid sequence compared to higher eukaryotes. The role of this extension is unknown but could serve in the allosteric regulation of the parasite enzyme. It is also feasible that this region could be used as a target for peptidomimetic inhibitors specific for the parasite enzyme. The R1 polypeptide immunolocalises to the parasite nuclei whereas the host R1 remains in the cytoplasm.

Using anti-sera generated against a range of host and parasite cell cycle associated proteins it was possible to gain a picture of changes occuring during the intracellular differentiation of the parasite within the lymphocyte. These results show that the intracellular differentiation initially involves both host and parasite cell cycles but there is an early decline in the amounts of two polypeptide markers of the host cell cycle whilst the parasite continues to undergo repeated nuclear division prior to the differentiation into the merozoite stage. Attempts were made to synchronise infected cells using aphidicolin and the effects of this drug on the expression of cell cycle associated genes in *T. annulata* was also examined.

Declaration

This thesis and the results herein are entirely my own work except where otherwise stated.

Acknowledgements

CONTENTS

Page Number

Chapter One :   Introduction

Chapter Two : Materials and Methods

Chapter Five :   Regulation of expression of the large subunit of
                    ribonucleotide reductase from *Theileria annulata*

Chapter Six :   Expression of cell cycle related proteins during differentiation

List of Figures :

List of Abbreviations :

ADP:	Adenosine diphosphate
ATP:	Adenosine triphosphate
BrdU:	5-Bromo-2-deoxyuridine
BSA:	Bovine serum albumin
CDK:	Cyclin dependent kinase
cDNA:	Complementary DNA
CRK:	cdc2-related kinase
DAPI:	4',6'-diamino-2-phenylindole dihydrochloride
DNA:	Deoxyribonucleic acid
dNTP:	Deoxynucleotide triphosphate
DTT:	Dithiothreitol
EDTA:	Ethylenediamine tetra-acetic acid
EGTA:	Ethylene glycol-bis(β-aminoethyl ether)-N,N,N,N-tetraacetic acid
FCS:	Foetal calf serum
FPLC:	Fast performance liquid chromatography
GST:	Glutathionine-S-transferase
IPTG:	Isopropyl-thio-β-D-galactoside
IL-2:	Interleukin 2
mAb:	Monoclonal antibody
MOPS:	4-Morphinepropanesulphonic acid
mRNA:	messenger RNA
NP-40:	Nonidet P-40
ORF:	Open reading frame
PAGE:	Polyacrylamide gel electrophoresis
PBS:	Phosphate buffered saline
PCR:	Polymerase chain reaction
PKC:	Protein kinase C
PMSF:	Phenylmethylsulfonyl fluoride
poly(A)$^+$:	polyadenylated
RACE:	Rapid amplification of cDNA ends

RNA: Ribonucleic acid

SDS: Sodium dodecyl sulphate

TaR1:   *T. annulata* large subunit ribonucleotide reductase

TEMED: Tetra-methyl-1,2-diaminoethane

ThaCRK2:   *T. annulata* cdc2-related kinase 2

Tris: Tris (hydroxymethyl) amino methane

UV: Ultraviolet

X-gal: 5-bromo-4-chloro-3-indolyl-β-D-galactoside

Chapter One

Introduction

1.1 *Theileria annulata*

The protozoan parasite *Theileria annulata* is the causative agent of tropical theileriosis, a debilitating and frequently fatal disease of cattle. It has been estimated that there are more than 250 million cattle across the globe that are at risk from this disease (Tait & Hall, 1990). Endemic regions stretch from the Moroccan Atlantic coast to the Pacific in a broad band encompassing Saharan North Africa, India, Byelorussia and into China (Dolan, 1992).

1.1.2 History

Theileriosis was first described as tropical bovine piroplasmosis by Dschunkowsky & Luhs in 1904 in Transcaucasia in southern Russia. The haemo-protozoan parasite responsible was named *Piroplasma annulatum* by Bettencourt in 1907 (cited in Irvin, 1987).

Experimental evidence showing *P. annulatum* to be similar to the *Theileria parva* parasite was published by Theiler in 1904 and the presence of a schizont stage resulted in *P. annulatum* being re-assigned as *Theileria* and hence its name today as *Theileria annulata*.

1.1.3 Classification of the Theileria Genus

Traditionally the taxonomic classification of protozoa depended upon criteria such as ecology, morphology, pathology and immunology. With the advent of molecular biology, more detailed studies at a genetic and biochemical level have resolved long standing disputes over certain *Theileria* species and sub-species designations.

1.1.4 Taxonomic Hierarchy

The currently accepted *Theileria* classification is as given below: (Levine, 1980).

Sub-kingdom	Protozoa
Phylum	Apicomplexa
Class	Aconoidasida
Order	Piroplasmorida
Family	Theileriidae
Genus	Theileria

1.1.5 Theilerial Parasites of Domestic Animals

There are six species of *Theileria* infectious for bovine hosts: *T. annulata, T. parva, T. sergenti, T. mutans, T. taurotragi* and *T. velifera* (Irvin, 1987). Of the six, the first two are the most serious pathogens. There are other *Theileria* species of ruminants which are not pathogenic but which could confuse a correct diagnosis - these are *T. ovis, T. recondita* and *T.separata* (Dolan, 1989, Papadopoulos *et al.,* 1996).

1.1.5.1 *Theileria annulata*

T. annulata causes tropical theileriosis in domestic cattle (*Bos taurus* and *Bos indicus)* and Asian water buffalo (*Bubalus bubalis*). It has been shown that the host range of *T. annulata* is limited to bovids since sporozoites were unable to infect peripheral blood mononuclear cells (PBMs) from other mammals in an experimental situation (Steuber, 1986).

The transmission vectors of *T. annulata* are ixodid ticks of the *Hyalomma* species. The natural disease vector in the Middle East and India is *H. anatolicum* but other vector species include *H. asiaticum, H. detritum* and *H. dromedarii* (Irvin, 1987). Ticks may feed on different hosts as adults, nymphs and larvae. *H. anatolicum*

is a three host tick, *H. detritum* is a two host tick whereby larvae and nymph feed from the same host (Sergent *et al.,* 1945). Ticks acquire *T. annulata* infection during a blood meal and transmit the parasite transtadially at the next stage of development when feeding on another bovine host.

The disease is restricted to areas where the tick vectors can survive and an endemic belt of tropical theileriosis ranges from Morocco to China. Indigenous cattle in endemic areas (*Bos indicus*) are relatively resistant to theileriosis with the mortality rate being less than 5% (Neitz, 1957). However, attempts to increase productivity and yields in these indigenous cattle by cross breeding with European breeds (*Bos taurus*) has led to increased mortality rates due to the higher susceptibility of these exotic and crossbreeds to theileriosis. Indigenous animals in endemic areas are exposed early to the parasite and if they survive then the immune protection is maintained through constant challenge. For newly introduced animals in endemic areas, rates of mortality reach up to 60% (Singh, 1991). There appears to be no inherent calf resistance and no maternal transfer of factors mediating resistance from mother to progeny. The number of animals at risk worldwide from theileriosis makes assessment of economic damage very difficult. Moreover, cattle which recover from infection suffer diminished milk yields, weight loss and fertility problems. This loss of productivity is a further constraint to the growth of local economies in endemic areas. Estimated losses to the Indian economy as a result of theileriosis is thought to be 10% of the livestock contribution to the gross national product (GNP) which places the dollar value of this loss in the range of tens of millions of dollars per annum (Singh, 1991).

1.1.5.2 *Theileria parva*

This species is the causative agent of East Coast Fever (ECF) in *Bos taurus* and African buffalo (*Syncerus caffer*). It has a higher pathogenicity than *T. annulata* and is prevalent throughout Central and Eastern Africa. Transmission is by the three host tick species, *Rhipicephalus appendiculatus* and *R. zambeziensus*.

Like *T. annulata,* exotic cattle have a higher susceptibility to *T. parva* than do the cattle indigenous to endemic regions. However, indigenous cattle originating from

non - endemic areas are severely affected by ECF. Once infected, mortality rates can be 80-100% for all age groups. Even for indigenous cattle in endemic areas the mortality rates can be as high as 50% with calves accounting for most of this figure (Irvin & Morrison, 1987).

Mukhebi *et al.* (1992) estimated the economical impact of ECF in 1989 to be of the order of $168 million with 1.1 million cattle killed by ECF. It is probable that the high rates of mortality stem from *T. parva* infecting T-cells which interferes with the effector response in the immune system (Morrison *et al.,* 1987). The cause of death in ECF is leucopenia.

Infections by *T. parva* and *T. annulata* can be distinguished morphologically between piroplasm stages. In *T. annulata* the piroplasms are predominantly round and oval shaped but in *T. parva* piroplasms are rod and comma shaped (Melhorn & Schein, 1984). There is no clinical need for this distinction given the lack of geographical overlap between these two species.

There is a trinomial nomenclature for the 3 subspecies of *T. parva*: - *T.p. parva* (East Coast Fever), *T.p. bovis* (Rhodesian theileriosis) and *T.p. lawrencei* (Corridor disease). From immunofluorescence using monoclonal antibodies generated against sporozoite surface antigens the three subspecies are indistinguishable from one another but the sporozoites differ in their ultrastructure (Fawcett, 1985).

1.1.5.3 *Theileria sergenti*

This species is endemic in areas of Eastern Asia and is transmitted by ticks of the *Haemophysalis* genus. The pathogenicity of infection is much milder than either *T. annulata* or *T. parva*. However when T. *sergenti* infection combines with other haemoprotozoic infections, mild pyrexia and anaemia can develop resulting in a large decrease in cattle productivity. It is the most common protozoan disease of grazing cattle in Japan.

Until most recently the two other benign species of *Theileria* which cause anaemia but not leucopenia have been linked taxonomically with *T. sergenti* in a group of *T. sergenti/orientalis* and *T. buffeli*. Based on differences in vector ticks at the sub

4

genus level, Fujisaki (1992) proposed that the classification triplet of *T. sergenti/orientalis/buffeli* be divided into two groups - *T. sergenti* and *T. orientalis/buffeli*. This has been confirmed by two dimensional PAGE protein analysis of piroplasm stages and by characterisation of genes encoding immunodominant proteins (Fujisaki *et al.*, 1994).

1.1.5.4. *Theileria mutans*

This species infects cattle (*Bos taurus* and *B. indicus*) and buffalo (*Syncerus caffer*) in sub-Saharan Africa and also in the Caribbean (Uilenberg *et al.*, 1983). Its tick vector belongs to the *Amblyomma* genus and the infection caused is benign theileriosis being only mildly pathogenic.

1.1.5.5. *Theileria taurotragi*

T. taurotragi infects cattle and other bovidae, being transmitted by ixodid ticks of the *Rhipicephalus* genus. It also occurs naturally in antelopes (*Taurotragus oryx*) (Stagg, 1983). It is widely found in Africa and can occasionally be pathogenic in cattle.

1.1.5.6. *Theileria velifera*

This is infectious for cattle and buffalo being transmitted by ticks of the *Amblyomma* genus. It is found in sub-Saharan Africa and the Carribean and is apathogenic.

1.1.5.7. Other species of *Theileria*

5

T. hirci (Dschunowsky & Uridschevich (1924), cited in Irvin 1987) infects sheep and goats via the *Hyalomma* vector. It has a similar geographical distribution to that of *T. annulata* and is highly pathogenic.

T camelensis infects camels but the vector and pathogenesis of the disease is unknown. It is found in Africa and parts of the former USSR.

A previously unidentified species of *Theileria* has been reported (Ngumi *et al.,* 1994). This parasite was isolated from cattle in Kenya and was shown to be antigenically distinct from other *Theileria* species by use of species specific monoclonal antibodies.

1.1.6 The Life Cycle of *Theileria annulata*

See Figure 1.1

1.1.6.1 Bovine Stages

Infection of the bovine host is initiated by an infected adult tick. Sporozoites contained within the tick vector salivary glands are injected into the bovine host when the tick begins to feed. Sporozoites then rapidly invade leucocytes (Jura *et al.,* 1983). Leucocytes susceptible to invasion by *T. annulata* sporozoites are those displaying major histocompatability complex (MHC) class II molecules - primarily B cells and monocytes/ macrophages (Glass *et al.,* 1989).

After leucocyte invasion the parasite develops into a uninucleate trophozoite stage which then undergoes a series of nuclear divisions to produce the multinucleated schizont composed of parasite membrane containing an average of 15 - 20 nuclei. As this development proceeds, the host cell divides in synchrony with the schizont by the schizont attaching to the host spindle apparatus (Carrington *et al.,*1995). The mechanism of this transformation has still to be fully elucidated and is discussed in more detail in section 1.1.11. After a finite number of cell divisions the enlarged macroschizont differentiates into microschizonts through the asexual stage of

6

merogony. Uninucleate merozoites are formed by nuclei migrating to the perimeter of the macroschizont and rhoptries appear in the schizont cytoplasm. The internal organelles then associate with the nucleus in the order found in the mature merozoite. Merozoites then bud out from the surface of the schizont and are liberated from the infected cell by breakdown of the host cell plasma membrane (Shaw & Tilney, 1992).

Merozoites then invade erythrocytes and undergo a further 2 rounds of division by schizogony to give the piroplasm stage (Conrad *et al.*, 1985). It has been proposed that piroplasms may be able to form merozoites which re-invade erythrocytes, as happens in *T. sergenti* but this has not been confirmed in any experimental studies. Piroplasms and infected erythrocytes are taken up by feeding ticks to complete the bovine stages of the life cycle.

1.1.6.2. The Tick Vector Stages

Ingested erythrocytes containing piroplasms are lysed in the tick gut. A proportion of the piroplasms undergo a sexual cycle (Cowdry & Ham, 1932, Melhorn & Schein, 1984). The free piroplasms differentiate into ray bodies and spherical forms which are the micro and macrogametes respectively. Syngamy of this pair forms a zygote. This and the succeeding kinete are believed to be the only diploid stages during the entire life cycle of the parasite. Morzaria *et al.* (1992) showed that recombinant parasites of mixed parental genotypes can be obtained from ticks fed on animals infected with two distinct parental stocks confirming sexual reproduction in *T. parva*. The motile kinete then passes through the haemolymph to the immature salivary gland cells where it transforms into a sporoblast undergoing multiple rounds of division. This stage remains dormant until the tick moults and resumes feeding (Schein *et al.*, 1975). The sporoblast then enlarges dramatically to give a multinucleate syncytium and uninucleate sporozoites form by cytoplasmic fission (Fawcett, Buscher & Doxsey, 1982). The sporoblast is probably the stage where meiosis occurs. Measurements of the DNA contents of the stages found in the tick gut showed that the gamete stages had half the DNA content of the zygote. This implies that fusion of the gametes occured in the gut of the tick, however in *T. parva*, the zygotes underwent a two step

meiotic division but a comparable division could not be detected in *T. annulata* (Gauer *et al.,* 1995). Sporozoites, merozoites and gametes are haploid while the multi-nucleated macroschizonts are polyploid. The sporozoites are released into the salivary gland and infection of the bovine host then occurs with the next blood meal (Purnell & Joyner, 1968, Reid & Bell, 1984).

1.1.7. Pathogenesis

The progress of the disease is charted by the destruction of lymphoid cells (as a result of parasite induced lymphoproliferation) and subsequent anaemia after the development of the piroplasm stages (reviewed in Irvin & Morrison, 1987).

In experimentally infected animals, the first manifestation of the disease is a swelling of the lymph nodes draining the site of sporozoite inoculation. As the parasitised cells proliferate and the macroschizont infected cell expand in number there is a marked fall in peripheral blood leucocytes (Preston *et al.,* 1992). This coincides with a fever of ~42°C occuring about 10 days after infection. By this point there is extensive destruction of both infected and non-infected cells in the lymphoid tissue which is probably linked to the expression of host matrix metalloproteinases in infected cells (Baylis *et al.,* 1992) which has been postulated to aid the dissemination of infected cells throughout the body (Adamson & Hall, 1996).

A second peak of fever after about 15 days can be correlated with the detection of piroplasms in blood smears. Fatalities occur ~20 days post infection from severe panleucopenia, anaemia and liver failure. Early autopsies showed several organs to be penetrated by lymphoblastoid cells - particularly liver, spleen, lungs, kidneys and gut (Sergent *et al.,* 1945).

Total elimination of the parasite from surviving animals is rare, thus maintaining a reservoir of infection. Low levels of parasitised erythrocytes are detectable in recovered animals (Neitz, 1957) hence a reservoir of infection is maintained. PCR is now the most sensitive means of determining the presence of the parasite in carrier cattle (D'Olivera *et al.,* 1995). Cattle used for these experiments

carried the infection for 12 and 15 months and could be shown, by PCR, to be diagnosed specifically for *T. annulata* even at parasitaemias as low as 0.00005%.

1.1.8. Chemotherapy and Control Measures

The three control measures currently available for tropical theileriosis are:-
a) Acaricides for tick vector control.
b) Chemotherapy
c) Vaccination/Immunisation using attenuated cell lines

1.1.8.1. Tick Vector Control

Acaricides provide a means of controlling tick vector populations. Due to expense and logistical problems they tend only to be used in areas suffering from a heavy tick infestation. All cattle must be treated in a comprehensive acaricide dipping programme. The disadvantage here is that if the programme is interrupted then cattle are again exposed to ticks and hence the disease. Furthermore, because this means of control does not provide natural immunity, cattle can become susceptible to theileriosis at a lower level of parasite challenge. There are also risks of ticks developing resistance to acaricides over long periods of treatment together with possible health risks to personnel from exposure to the acaricides together with the residues found in meat and milk (Drummond, 1976).

The major advantage of acaricides is that simultaneous control of all tick borne diseases is achieved, hence different control measures for different diseases become unnecessary.

1.1.8.2. Chemotherapy

Drugs currently available for the control of theileriosis include oxytetracyclin (Terramycin, Pfizer), halofuginone (Terit, Hoechst), parvaquone (Clexon, Coopers

Animal Health), buparvaquone (Butalex, Coopers Pitman Moore) and primaquin phosphate.

Oxytetracyclin, by inhibition of protein synthesis, suppresses macroschizont development if administered shortly after sporozoite innoculation. It preferentially affects parasite protein synthesis, probably through its effects on mitochondria. Host protein synthesis is only affected after long periods of treatment and at high doses (Spooner, 1990). It is ineffective against piroplasm or sporozoite stages and thus cannot be given therapeutically at the peak of parasitaemia and fever. It has been shown to be more effective against *T. parva* infections (Hashemi - Fesharki, 1992).

Halofuginone also targets macroschizonts but is more effective than oxytetracyclin at low dose rates. In an *in vitro* experiment, halofuginone was shown to reduce the numbers of schizont infected cells from 82% to 42% at a concentration of 0.025ppm (Schein, 1986). *In vivo* trials of the drug resulted in the complete elimination of schizonts four days post treatment (Schein & Voight, 1981).

Parvaquone and buparvaquone are both napthoquinone analogues of menoctone. They are potent against macroschizonts and are effective also against piroplasms. Parvaquone is more effective against *T. parva* infections (McHardy *et al.*, 1983), whereas buparvaquone is equally effective against both *T. annulata* and *T. parva*. It is believed to act as a specific inhibitor of the parasite mitochondrial electron transport pathway (Fry *et al.*, 1984). Large scale trials using buparvaquone and parvaquone have shown the efficacy of these drugs with cure rates ranging from 85 - 100% from a single dose (McHardy, 1992).

However the expense of chemotherapy remains a stumbling block but treated animals are often resistant to further infection. The drugs must be administered early in the course of infection to be of use.

1.1.9. Immunisation

Two methods are currently used for immunising cattle against theileriosis:-

a) Infection and treatment

b) Attenuated infected cell lines

1.1.9.1. Infection and Treatment

Infection is initiated by innoculation with sporozoites and concurrent tetracycline therapy. This method is currently used against *T. parva* (Radley *et al.*, 1975, Young *et al.*, 1992). For *T. annulata* the use of buparvaquone together with attenuated schizonts protects the cow against any likely tick exposure and provides appreciable immunity, probably by allowing an immune response against the schizonts to develop with the presence of the drug limiting any new infected cells developing (Grewal, 1992).

1.1.9.2 Attenuated Cell Lines

Cell line vaccines have been used successfully for a number of years to immunise cattle against theileriosis. The attenuated lines are derived from macroschizont infected cell lines, which through repeated passage have lost virulence (Pipano, 1981). By hybridisation with two polymorphic DNA probes Sutherland *et al.* (1996) showed that after 50-100 passages, *in vitro* selection of particular parasite genotypes occurs. This indicates clonal selection may contribute to loss of virulence. The same authors showed that continued passage of cloned cell lines derived from a virulent line led to the loss of reactivity with a monoclonal antibody which recognised the parental virulent line. This indicates that alteration of parasite gene expression takes place during attenuation, in addition to clonal selection.

Work by Baylis *et al.* (1992) showed that long-term cell culture caused a reduction in metalloproteinase activity when compared to newly infected cells. One of the attenuated cell lines (ODE) had reduced protease activity coupled with a decrease in the ability to produce merozoites. This may suggest that the proteases are also needed for merozoite production in addition to aiding the spread of infected cells. The reduction of these proteins and differences in gene expression may contribute to the

decreased pathogenesis seen with the attenuated vaccine lines which allows a protective immune response to develop.

Schizont vaccines are cryopreserved prior to administration. The need for refrigeration poses problems in endemic areas. One vaccine dose contains about 10^6 cells and is enough to give immunity to both natural and artificially heterologous infective challenges.

It has been much easier to immunise against *T. annulata* than *T. parva* using attenuated cell lines. This is probably because the transfer of macroschizonts from infected cell line to host cells is more efficient in *T. annulata* (Spooner *et al.,* 1989). Large scale vaccination programmes have been undertaken in many developing countries with considerable success.

Total eradication of the disease probably will depend on a successful subunit vaccine directed against the sporozoite stage as there is a known humoral immune response against this stage of the parasite. However, more must be learnt about the roles of the humoral and cell mediated immunity to the parasite before such an approach would yield results.

1.1.10. The Immune Response to *Theileria annulata*

Knowledge of the basis of immunity to theileriosis would greatly aid a rational approach to a subunit vaccine design. Some progress has been made on this front with the expression of the major 30kDa surface antigen of the merozoite stage (D'Olivera *et al.,* 1996) which could form part of a live subunit vaccine. The two arms of the immune system involved are the humoral and the cell mediated immune responses.

1.1.10.1 Humoral Immunity

Humoral immunity does not appear to play a primary role in immune protection. Antibodies directed against the sporozoite, macroschizont and piroplasm stages are produced but there is no evidence for immune sera reacting against the surfaces of infected host cells - either infected monocytes or erythrocytes (Hall,1988).

Recognition of the infected cell by sera would be the first step of antibody mediated cellular lysis. Antibodies that neutralise the infectivity of sporozoites have been detected in the serum of hyperimmunised cattle. This sporozoite neutralising activity was mainly present in sera from immune animals after a primary challenge (Preston & Brown, 1988).

Work with sporozoites has led to certain antibodies being shown to be able to block invasion (Williamson *et al.*, 1989). One antigen, SPAG-1 (sporozoite antigen 1), was identified by an inhibitory MAb. Western blots using this MAb recognise a series of polypeptides in sporozoite extracts which are thought to be the result of the proteolytic processing of a single gene product. The gene encoding SPAG-1 was found to contain regions with a high degree of homology to a bovine elastin repeat sequence (Hall *et al.*, 1992). Thus, it was proposed that sporozoites may be using mimicry to bind to the bovine elastin receptors as a means of invading cells. However, this region has since been found to be highly polymorphic (Katzer *et al.*, 1994) and *in vitro* sporozoite infection targeted elastin receptor positive and negative cell populations with an equal frequency, thus making the elastin receptor an unlikely binding ligand for the parasite (Campbell *et al.*, 1994). This molecule, though, is a candidate for inclusion in a subunit vaccine and has been analysed to determine the neutralising B- cell epitopes which lie towards the C- terminus (Boulter *et al.*, 1994)

1.1.10.2 Cell Mediated Immunity

The finding that immunity to *T. parva* could be transferred by innoculation of T cells from an immune calf into its naive twin (Emery, 1981) suggests that the mechanisms responsible for protective immunity are cell mediated. Work by McKeever *et al.* (1994) showed that the adoptive transfer of immunity was due to the CD8(+) fraction of class I MHC restricted cytotoxic T lymphocytes that recognise schizont infected cells. In *T. annulata*, Preston *et al.* (1983) showed there were two peaks of cytotoxic cells generated after challenge. The first peak appeared two weeks into the infection and was BoLA restricted (bovine MHC Class 1 antigens). The second peak, four weeks after challenge was not genetically restricted and was likely to be Natural

13

Killer (NK) cells. The second peak is associated with recovery from theileriosis since it is not detected in lethal infections. Attempts have been made to further characterise the BoLA restriction markers of the cytotoxic lymphocytes (reviewed in Morrison, 1996). More recent work (Oliver & Williams, 1996) has shown that BoLA class I antigens are modified on the cell surface of *T. annulata* transformed lymphoblastoid cells. This could explain the long term persistance of the parasite by modification of presented peptides thus providing a possible explanation for the avoidance of immune detection, since infection is controlled by the MHC class I restricted cytotoxic T cell killing of the infected cells.

Shiels *et al.* (1986) showed that one monoclonal antibody (4H5) recognised a polypeptide on the surface of schizont infected lymphocyte and that this antibody could mediate complement lysis of the infected cells (Preston *et al.*, 1986). It is unclear as to whether this antigen is host or parasite derived, although recent work indicates it to be host derived (C.Dando, unpublished work).

Mechanisms of immunity to the merozoite and piroplasm stages are still largely unknown, although antibodies in immune serum strongly recognise antigens from these stages such as the 30kDa merozoite surface antigen and the 117kDa rhoptry protein antigen (Dickson & Shiels 1993). These antigens are of considerable interest since a response to the merozoites would effectively limit the pathogenicity of the disease and the response to piroplasms could block the transmission of the parasite. Work in *Plasmodium* using a monoclonal against free gametes reduces the infectivity of the parasite to the mosquito vector (Carter *et al.*, 1990).

1.1.11. Activation of the host cell upon infection

Much work has focused on the ability of *Theileria* infections to induce lymphocytic proliferation in that infected monocytes can stimulate naive autologous T cells to proliferate. It has been shown that different *T. annulata* infected cell lines expressed different but constant levels of MHC class II but that there was no correlation between levels of MHC class II expression and levels of induced T cell proliferation (Brown *et al.*, 1995). Infected cells were shown to produce specific

mRNAs for IL-1α, IL-1β, IL-6, IL-10 and TNFα but not IL-2 or IL-4. One cloned line was found not to produce TNFα mRNA. The degree of proliferation of T cells stimulated by the infected cells paralled the amounts of IL-1α and IL-6 mRNA which are T -cell stimulatory cytokines.

However with *T. parva* infected cells, the mRNAs produced differ from the above in that IL-2, IL-4 and IFNγ mRNAs are produced together with IL-1α and IL-10. It is believed that IL-1α production by either *T. parva* or *T. annulata* infected cells acts as a major signal for the induction of non-specific T cell proliferation (Brown *et al.,* 1995).

1.1.12. The Cell Cycle in *Theileria annulata*

There are several proliferative stages during the life cycle of *Theileria* that undoubtably account for the pathogenesis seen during the course of the disease. These stages must involve the parasite's own cell cycle and in the bovine lymphocytes, it involves the host cell cycle also. The cell cycle has been extensively studied in higher eukaryotes and in yeasts but little is currently known about the cell cycle in protozoan parasites in terms of the degree of conservation of constituent molecules or the adaptions used to accommodate the complex parasite life cycles.

An introduction to the cell cycle follows and the aims of the project are given at the end of the cell cycle introduction.

Figure 1.1 The life cycle of *Theileria annulata*.

Diagram adapted from Tait & Hall, 1990. Infection starts upon inoculation of sporozoites into the bovine host upon feeding by the tick. These sporozoites then invade and transform leukocytes. The parasite then develops into a macroschizont which breaks down into merozoites. Merozoites invade erythrocytes and develop into piroplasms. This completes the life cycle within the bovine host. There are two main stages within the tick - gametogony and sporogony.

Host Cell Nucleus

Macroschizont

Merogony

Infected
Leucocyte

Proliferation

Merozoites

Sporozoite

Erythrocyte

Cow

Piroplasm

Blood
Meal

Tick salivary
gland

Sporoblast

Sporogony of
sporoblast cells
to produce
mature
sporozoites

Macro and Micro-
Gametes &
Zygote

Tick gut

Proliferation
in salivary
gland cells

Motile kinete
invades acinus
cells of tick
salivary gland

Gut
epithelial
cells

1.2.1 The Eukaryotic Cell Cycle

The cell cycle is a series of events that are necessary for a cell to replicate its DNA and then undergo mitosis. There are 4 stages to each cell cycle although processes such as meiosis or embryonic cell division may miss stages.
The 4 stages are :- S - replication of DNA

G2 - gap prior to mitosis

M - mitotic division

G1 - gap open to influence from external signals

Progress through the four stages is controlled by a family of serine/threonine kinases known as the cyclin dependent kinases (CDKs). The first isolated and best characterised CDK is p34^{cdc2} encoded by the *cdc2* gene (Cell Division Cycle 2) named from a temperature sensitive mutant of the fission yeast *Schizosaccharomyces pombe* (Nurse & Bisset, 1981). Homologues of *cdc2* have been cloned from the budding yeast *Saccharomyces cerevisiae* (CDC28) and higher eukaryotes by exploiting the high degree of conservation of this gene between species. For example the cloning of the human p34^{cdc2} homologue was achieved by complementation of the *S. pombe* temperature sensitive mutant (Lee & Nurse, 1987). p34^{cdc2} is also known as CDK1 in higher eukaryotes.

1.2.2. CDC2

The *cdc2* gene of *S. pombe* encodes a 34kD serine/threonine kinase. Together with cyclin B, p34^{cdc2} induces the G2 to M transition in response to a signal monitoring the completion of DNA replication (reviewed by Forsberg & Nurse, 1991). Certain residues conserved in other protein kinases are crucial for p34^{cdc2} function (Booher & Beach, 1986). Threonine 167 (Thr 161 in higher eukaryotes) is phosphorylated for the kinase to gain activity. Mutations at this site render the enzyme inactive and it cannot bind cyclin partners stabily (reviewed in Krek & Nigg, 1992). The cyclins bind a conserved PSTAIRE motif inducing a conformational change that allows Thr 161/167

17

to be phosphorylated. A final step of activation occurs by the dephosphorylation of a phosphorylated tyrosine residue Tyr 15 which is located in the ATP binding domain of the kinase. This reaction is mediated by CDC25 phosphatase. Arrest of DNA replication inhibits p34^{cdc2} by preventing this dephosphorylation step (Enoch & Nurse,1991).

S. pombe has only one CDK - p34^{cdc2} responsible for controlling progess through the cell cycle. When p34^{cdc2} is complexed with cyclin B the cell is in G2 and enters M phase after the kinase is activated. When cyclin B is destroyed upon exit from M phase, the yeast cells are then in G1 and can enter S phase once past the 'start' checkpoint. A temporal order is established due to a balance between the cyclin binding partners of cdc2 and its state of activation (reviewed in Nurse, 1994). Homologues of p34^{cdc2} are present in all eukaryotes and some have been designated as functional homologues. Figure 1.2 shows the conserved domains of cdc2- related kinases compared with human cdc2 (Hscdc2). The Trypanosoma brucei TbCRK3 and Theileria annulata ThaCRK2 have not been shown conclusively to be the cdc2 homologues in the protozoa but they are related to the CDK family based on the homology in the domains illustrated.

1.2.3   Cell Cycle Regulation in Aspergillus is by two Protein Kinases

In Aspergillus nidulans a second class of cell-cycle regulated protein kinases is required for progression into mitosis. These kinases are the NIMA kinases named from the mutant phenotype "never in mitosis"(reviewed in Osmani & Ye, 1996). Both cdc2/cyclin B and NIMA must be activated prior to mitosis in Aspergillus and both kinases must be proteolytically destroyed before completion of mitosis. There are a number of parallels between the NIMA and cdc2 kinases - their levels of the active kinase complexes fluctuate during the cell cycle, peaking in G2 and being inactivated upon mitotic exit. The regulation of these two kinases is very similar in order to achieve identical patterns of activity during the cell cycle - being regulated by cell cycle specific phosphorylation and being irreversibly inactivated during mitosis by proteolysis. With the NIMA kinase, the whole protein is destroyed unlike the p34^{cdc2}

kinase which is inactivated by the destruction of the cyclin B subunit. One mitosis specific role of NIMA could be to promote chromatin condensation whilst the cdc2 complex induces spindle formation. A number of NIMA related kinases (*nrk*) have been isolated in higher eukaryotes but the only identified functional homologue is from *Neurospora crassa*, another filamentous ascomycete. *Nrk* genes have been isolated from *T. brucei* (Gale & Parsons, 1993). Further work is needed to identify binding partners of NIMA in order to fully understand how NIMA and cdc2 co-operate in regulating the cell cycle in *Aspergillus*.

1.2.4. Other Members of the CDK family

In higher eukaryotes and certain protozoans there is a family of cyclin dependent kinases. Evidence for these first came about from work done with temperature sensitive *cdc2* mutant mouse cell lines. These cells were found only to arrest at the G2/M transition at the restrictive temperature. If the cells were immunodepleted of p34^{cdc2} they are unable to enter mitosis but showed no defect in DNA replication. The G1 cyclins were found to co-immunoprecipitate with a 34kDa protein which contained the PSTAIRE motif but differed from p34^{cdc2}. Using PCR, a total of twelve cdc2-related cDNAs were isolated from human cells (Meyerson *et al.*, 1992), two from *Drosophila* (Lehner & O' Farrell, 1990), two from *Xenopus* (Paris *et al.*, 1991), three from *T. brucei* (Mottram & Smith, 1995) and two from *Leishmania mexicana* (Mottram *et al.*, 1993 & Mottram, pers. comm.). The twelve cdc2 related genes are listed in Table 1.1 and three of these molecules were able to complement a CDC28 deficient yeast mutant (CDK1-3). To date no protozoan CRK has been shown to complement the CDC28 yeast mutant.

1.2.5. The Cyclin Family

These proteins serve as regulatory partners of the CDKs. Certain cyclins bind specific CDKs but others such as cyclin D can bind multiple CDKs (see table 1.1). The

cyclins are expressed at specific points of the cell cycle as shown in figure 1.4. Human cells contain at least fourteen cyclins with eight partner CDKs isolated to date (reviewed in Pines, 1996). Although the main role of the cyclin/CDK complex is in the regulation of the cell cycle, some other roles have been defined outwith the cell cycle: these include response to phosphate starvation in yeast (Kaffman *et al.,* 1994) and neurofilament phosphorylation in post-mitotic neurons (Lew *et al.,* 1992). There is now evidence that the binding of an alternative cyclin partner can lead to the expression of a different function. For example, expression of a specific subclass of cyclin A (cyclin A1) is restricted to germ cells in mouse and is found associated with cdc2/CDK2 indicating a probable functional role in meiosis (Sweeney *et al.,* 1996). Also the localisation of different cyclin subclasses suggests direction of different functions - cyclin B1 is localised to microtubules whereas cyclin B2 associates with the Golgi apparatus (Jackman *et al.,* 1995). The mechanism of activation of the cyclin dependent kinase subunit upon cyclin binding to the PSTAIRE box has been solved by X-ray crystallography - cyclin binding induces a conformational change in the CDK catalytic subunit which brings the bound ATP into the appropriate position to allow catalysis of the phospho-transfer reaction to the substrate (Jeffrey *et al.,* 1995).

The cyclins can be divided into two major classes - the mitotic cyclins and the G1 or START cyclins. Both classes share a common cyclin box - a region of ~100 amino acids involved in binding to the CDK partner. This is shown in Figure 1.3. The START cyclins include D and E and the mitotic cyclins are A and B1/B2. Cyclins A and B are specifically destroyed at mitosis through ubiquitination of a partially conserved 'destruction box' at the N-terminus. The START cyclins are inherently unstable and rapidly turned over due to the presence of a conserved PEST sequence in the C-terminal region of the proteins. However, yeast G1 cyclin destruction involves ubiquitin. So the sequential destruction of cyclins could be achieved by the specific induction of the ubiquitin turnover pathway at particular points of the cell cycle. More recent work has shed light on the nature of cyclin turnover (Jackson 1996). There is a family of proteins homologous to the yeast Cdc53 known as "cullins" which may be responsible for the targeting of cell cycle regulators, including cyclins, for destruction by ubiquitin-dependent proteolysis. Only the cyclin B/cdc2 complex has been defined as the primary mitotic complex responsible for the phosphorylation of components of

cellular architecture that are changed during mitosis (reviewed in Pines, 1995). Many proteins which have been shown to be *in vivo* substrates for the p34^{cdc2} kinase contain the substrate consensus sequence of S/T P X K/R (Kamijo *et al.*, 1992). These include many of the cytoskeletal proteins together with a number of protein kinases. Work with *Xenopus* egg extracts showed that the dynamics of spindle microtubules can be regulated by p34^{cdc2} kinase by phosphorylation of the microtubule associated protein p220 (Verde *et al.*, 1990). Immunofluorescence has shown some of the cellular p34^{cdc2} to be localised to the centrosome in Hela cells at the G2/M boundary which indicate a possible role for p34^{cdc2} in chromatin condensation and contraction of the spindle poles at mitosis (Bailly *et al.*, 1989, Riabowol *et al.*, 1989). The significance of histone H1 phosphorylation by the p34^{cdc2} kinase may be induction of changes in nucleosome packing allowing chromatin condensation but this has not been proven *in vivo*. The finding of the p34^{cdc2} substrate consensus motif in many DNA binding proteins has led to suggestions that the phosphorylation of the motif would abolish the DNA binding abilities of these proteins allowing the chromatin condensation to proceed - members of this group include the HMG (high mobility group) of transcription factors (Meijer *et al.*, 1991).

1.2.6. External controls and CKIs

In all eukaryotic cells, once a point in late G1 is passed, known as START in yeast, the cell cycle is closed to external influences such as mitogens which can control the commitment to S phase (Pardee, 1989). In higher eukaryotes, key regulators which link the cell cycle to external factors include the three D type cyclins which are produced only as long as growth factor persists and are rapidly degraded once the mitogenic stimulus stops (Matsushime *et al.*, 1991). The regulatory pathways converging on G1/S border are as shown in figure 1.5.

Key regulators of G1 progression in mammalian cells are the three D-type cyclins which assemble with CDK4 or CDK6 and cyclin E which combines with CDK2 later in G1(reviewed in Sherr, 1993). The three D type cyclins are induced in a cell lineage specific manner as part of the delayed early response to mitogens. They persist

throughout the cell cycle but are rapidly degraded if mitogenic signals cease. However, this will only regulate the cell cycle if the cells are in G1.

Cyclin E is expressed periodically with maximal levels at the G1/S border - associating in a complex with CDK2. Once cells enter S phase, cyclin E degrades and CDK2 associates with cyclin A. Like cdc2-cyclin B, both cyclin E - CDK2 and cyclin D - CDK4 complexes undergo phosphorylation on a single threonine residue to achieve activation. This phosphorylation is done by a CDK activating kinase (CAK) which may be composed of cyclin H and CDK7 (Fisher & Morgan, 1994), although this remains a matter of controversy as the cyclin H/CDK7 complex is also found associated with transcription factor TFIIH and is believed to phosphorylate RNA polymerase II and hence regulate transcription (Serizawa *et al.*, 1995).

The D type cyclins alone can bind retinoblastoma protein, pRb, which is believed to be an important point in the switch between proliferation and differentiation. Rb may act in cell cycle arrest by sequestering positive regulators of the cell cycle - transcription factors such as E2F. The cyclin D/CDK4 complex has been shown to phosphorylate members of the E2F transcription factor family (Fagan *et al.*, 1994) which are believed to regulate the cell cycle linked transcription of proteins required for S phase such as DNA polymerase α and ribonucleotide reductase.

1.2.7. Cyclin dependent kinase inhibitors

The cyclin dependent kinase inhibitors (CKIs) are a further class of control molecules in the cell cycle. These proteins co- purify with the CDKs isolated from mammalian cells (Xiong *et al.*, 1993). There are five distinct inhibitors which have been well studied so far and their inhibitory effects on different CDK/cyclin complexes is illustrated in figure 1.6.

The recent publication of the crystal structure of CDK2/cyclin A complexed with the p27 inhibitory subunit has done much to clarify the mode of action of CDK inhibitors (Russo *et al.*, 1996). The amino terminal of p27 binds to cyclin A and the carboxy region binds to the kinase small lobe, acting both to disrupt the conformation and to block ATP binding within the active site.

p21 is a universal CDK inhibitor in mammalian cells (Harper *et al.*, 1993). Its expression is directly regulated by p53 and is part of p53 induced G1 checkpoint control (reviewed in Sherr 1994). p53 is a tumour suppressor gene and levels of the p53 protein transiently increase in response to DNA damage (Kastan *et al.*, 1992) acting as a transcription factor activating the transcription of genes involved in arrest of the cell cycle such as p21. p21 forms a ternary complex with PCNA (proliferating cell nuclear antigen), a subunit of DNA polymerase δ and various CDK/cyclin combinations. The exact significance of the PCNA/CDK/cyclin complex is unclear although both p21 and p27 are implicated in linking mitogenic signals to the G1 phase of the cell cycle (Xiong *et al.*, 1993, Kato *et al.*, 1994). Recently it has been shown that specific removal of p27 by anti-sense DNA, prevented cell cycle arrest in response to mitogen depletion (Coats *et al.*, 1996).

The other main CKIs range from 15- 20kD and are specific inhibitors of CDK4. These may be differentially expressed as a response to a variety of anti- proliferative signals.

1.2.8. p13^{suc1}

The *suc1* gene of *Schizosaccharomyces pombe* encodes a small protein p13 whose role in the cell cycle is still largely unknown. It was originally identified as a gene capable of rescuing certain temperature sensitive mutants of cdc2 in *S. pombe* (Hayles *et al.*, 1986b), whereas deletion of *suc1* causes cells to arrest in mitosis (Moreno *et al.*, 1989). Homologous genes have been identified in budding yeast and other eukaryotes including human (Richardson *et al.*, 1990) and *Leishmania* (Mottram & Grant, 1996).

The ability of p13 to bind strongly with p34^{cdc2} and p33^{cdk2} *in vitro* (Arison *et al.*, 1988; Azzi *et al.*, 1992; Brizuela *et al.*, 1987; Draetta *et al.*, 1987, Duncommun *et al.*, 1991; Hadwiger *et al.*, 1989; Hayles *et al.*, 1986a; Meijer *et al.*, 1989) led to the development of a rapid affinity purification technique for p34^{cdc2}/cyclin B complexes from cell extracts (Labbe *et al.*, 1989; Pondaven *et al.*, 1990). Although *in vivo* only a

small porportion of the total cellular $p34^{cdc2}$ is found complexed with p13 (Brizuela *et al.,*1987).

Until quite recently the role of p13 in the cell cycle was largely undefined and simply portrayed as an oscillating factor in the mathematical models put forward for $p34^{cdc2}$ activation and turnover (Thron, 1992). Using fluorescently labelled p13 protein injected into stamen cells of *Transcantia*, Hepler *et al.,* (1994) showed that the protein is rapidly targeted to the nucleus. When the nuclear envelope breaks down the labelled protein is dispersed throughout the cell with no evident specific association with spindle elements. After division, p13 reconcentrates in daughter nuclei. In *S. pombe* p13 regulates two distinct forms of the mitotic cdc2 kinase, each binding different B type cyclins (Basi & Draetta, 1995). They also showed that it is required for M phase progression. Simon *et al.,* (1995) have shown that transcript levels of *Ckshs1* (one human homologue of *suc1*) are down regulated in certain cells after exposure to transforming growth factor β (TGF-β) which may suggest a role in growth arrest responses.

The structures of p13 and its human homologue, $p9^{Ckshs1}$, have been determined (reviewed in Endicott & Nurse, 1995). The p9 protein can oligomerise to a hexameric ring structure. It has been proposed that p9 can influence $p34^{cdc2}$ localisation and activity by this oligomerisation process (Parge *et al.,* 1993). However, p13 cannot form a hexamer and exists either as a monomer or dimer. Recently the crystal structure of human *suc1* homologue (*Ckshs1*) complexed with CDK2 has been determined (Bourne *et al.,*1996) and combined with mutational analysis, it has been shown that Ckshs1 only bound directly to the C-terminal large lobe of the kinase subunit. This effectively extends the area of the active site cleft. The binding does not affect the activity of the complex but possibly serves to target the CDK to regulatory molecules.

Recent work undertaken with the *Xenopus suc1* homologue, p9 (Patra & Dunphy, 1996) suggests that the consequences of depleting egg extracts of p9 depends on the stage of the cell cycle. In interphase extracts, depletion stops mitotic entry by the failure of Cdc2/cyclin B complex to activate by tyrosine dephosphorylation. Conversely, addition of recombinant p9 to extracts delays mitosis, again by inhibition of tyrosine dephosphorylation. Mitotic extracts depleted of p9 fail to exit mitosis because of a defect in cyclin B destruction. If these results are considered in the light of

24

the crystallographic data, then p9 could act as a "docking factor" for Cdc2 regulators such as Cdc25.

1.2.9. Protozoan Cyclin Related Kinases

A number of cyclin related kinases (CRKs) have been isolated from protozoan parasites - notably *Trypanosoma brucei* (Mottram & Smith, 1995), *Leishmania mexicana* (Mottram *et al.,* 1993), *Plasmodium falciparum* (Ross -MacDonald *et al.,* 1994), *Theileria annulata* and *Theileria parva* (Kinnaird *et al.,* 1996).

In *Trypanosoma brucei* there is a family of cdc2 related protein kinases (*Tbcrk1-3*). *Tbcrk1* encodes a 34kDa protein which is 54% identical to human cdc2 at the amino acid level. The putative cyclin binding region contains a PCTAIRE motif instead of the PSTAIRE motif. *Tbcrk2* encodes a 38kDa protein, with a 49% identity and a PSTAVRE motif. *Tbcrk3* encodes a 35kDa protein with a 54% identity and a PQTALRE motif. In *Leishmania mexicana,* two cdc2- related kinase genes have been isolated, and additionally, an unidentified kinase has been identified which is capable of binding to p13^{suc1} but is distinct from either of the two CRKs already cloned. The presence of a family of cdc2 related kinases in *Trypanosoma brucei* and *Leishmania mexicana* suggest that these proteins may have roles in controlling aspects of the cell cycle linked to the differentiation of the parasite during its life cycle. In *P. falciparum* the PfPK5 gene is at present the closest *cdc2* homologue isolated, with a sequence identity at the amino acid level of 60%. (Ross-MacDonald *et al.,* 1994). Work by Graser *et al* (1996a) showed that, while this kinase was capable of undergoing auto-phosphorylation *in vitro,* in order to produce the fully active kinase, binding of another protein, probably a cyclin was also necessary. In the slime mould *Dictyostelium discoideum* genes encoding a polypeptide highly related to cdc2 and a less closely related CRK with a PCTAIRE motif have been isolated (Michaelis & Weeks 1992, 1993). A possible *D. discoideum* cyclin B homologue has also been isolated (Luo *et al.,* 1995). Only the cdc2 like gene was able to complement a temperature sensitive CDC28 mutant of *S. cerevisiae* although growth of the transformants was slow and limited. Further work showed that the histone H1 kinase activity of the cdc2 like

protein varied during the development of *D. discoideum* and the activity correlates with the level of cyclin B protein. The level of cdc2 kinase activity was high in early development coincident with a period of mitosis but this activity was not associated with late development mitosis suggesting that another kinase may be involved. The mRNA levels of cdc2 and cyclin B are co-ordinately regulated during growth and early development and both mRNA species are reduced to undetectable levels during the terminal stages of differentiation (Luo *et al.,* 1995).

To date no protozoan CRK has been able to complement the *S. pombe* cdc2 temperature sensitive mutant that is the benchmark test for isolation of a functional cdc2 homologue. This may reflect the divergence between the yeasts and the protozoa or it may be that the functional cdc2 homologues have still to be isolated from these parasites. One means of isolating a functional cdc2 homologue would be to clone a parasite cDNA library in a yeast expression vector and select for complementation of a yeast cdc2 mutant phenotype (Mottram 1994).

In *Theileria* only one gene that is highly related to cdc2 has been isolated - ThaCRK2 (*T. annulata*) /ThpCRK2 (*T. parva*) (Kinnaird *et al.,*1996). The *T. annulata* gene was isolated from a cDNA expression library screen using an anti-PSTAIRE monoclonal antibody. Recently another related gene has been isolated by a degenerate PCR approach, using oligonucleotides to conserved kinase domains. This gene, ThaCRK3, is less related to p34^{cdc2} than to ThaCRK2 but has sufficient conservation of motifs to be classified as a member of the cdc2-related kinase family (Kinnaird *et al.,* unpublished results).

There has been only one cyclin isolated from a protozoan parasite - CYC1 from *T. brucei* (Affranchino *et al.,* 1993). It has a low homology to cyclins from higher eukaryotes but antibodies raised to it can immunoprecipitate an active kinase complex from *T. brucei* cell extracts.

1.2.10. ThaCRK2 and ThpCRK2

Monoclonal antisera raised against the highly conserved PSTAIRE region recognised a polypeptide of 34kD in Western blots of piroplasm extracts while an

antiserum specific for the C-terminus of mammalian cdc2 showed no reactivity in piroplasm extracts thus indicating that there is at least one protein in *Theileria* containing the PSTAIRE conserved motif but differing in the C-terminal region from the host cdc2 (Kinnaird *et al.,* 1996).

In order to isolate the gene encoding this molecule, a *T. annulata* cDNA library, generated using RNA prepared from an *in vitro* infected lymphocyte culture undergoing merogony was screened with a monoclonal anti-PSTAIRE antibody. Independently, a related gene was cloned from *T. parva* by screening a genomic library with the *P.falciparum* PfPK5 gene as a probe. These experiments led to the characterisation of both the cDNA clone from *T. annulata* (ThaCRK2) and the genomic clone from *T.parva* (ThpCRK2) by sequence analysis.

ThaCRK2 and ThpCRK2 show a high degree of interspecies conservation - 98% at the amino acid level and 91% at the nucleotide level. All amino acid substitutions are conservative and are located at the C-terminus which is the most variable region in cdc2 homologues from other eukaryotes. ThCRK2 has a 75% amino acid homology to the PfPK5 gene which suggests a functional conservation within the apicomplexan genes. There are five introns in the ThpCRK2 gene with the insertion points of four of these being identical to those in PfPK5, suggesting that the gene structure has been conserved since the evolutionary divergence of the parasites. It is possible that this single kinase is able to control karyokinesis and cytokinesis in *Theileria* by differential regulation of its activity.

The sequence of ThaCRK2 suggests it to be the functional equivalent of cdc2 by virtue of the conservation of homology over certain blocks of sequence common to the cdc2 kinase group. However, there are two regions in ThaCRK2 which differ significantly from the higher eukaryotic cdc2 homologues - the first being a tripeptide motif LQD in *S. pombe*, changed to LPA in *Theileria*. The second is the GDSEID motif which appears as GISEQD in ThCRK2. This motif is the site of interaction of the CAK (cdc2-activating kinase) which phosphorylates a conserved T167 residue. Thus, whilst the PSTAIRE cyclin binding motif is conserved, regions implicated in the control of kinase activity are not, suggesting the evolutionary divergence of the structure of certain regulatory proteins (See Figure 1.2).. This probably explains the

failure of the ThCRK2 gene to complement a yeast cdc2 mutant (Kinnaird *et al.*, 1996).

1.2.11. **Theileria induced lymphoproliferation**

The lymphoproliferation induced by invasion by sporozoites has been well documented but is poorly understood. Various theories to explain the clonal expansion have been put forward. Dobbelaere *et al.* (1988) proposed that *T. parva* infected T cells stimulate an autocrine loop by which infected cells secrete Interleukin-2 (IL-2). It was later shown (Heussler *et al.*, 1992) that nearly all *T. parva* infected cell lines express IL-2 mRNA and the Il-2 receptor (see section 1.1.11). The nature of the primary stimulus from the parasite or its level of interaction in the host cell are unknown.

Work with both *T. annulata* and *T. parva* showed that infected cells produce a range of cytokine mRNAs (section 1.1.11) the products of which probably act to induce the proliferation of non-specific T cells and possibly setting up autocrine loops stimulating the expansion of the infected cell population. Components of host signal transduction pathways have been cloned such as host casein kinase II (ole MoiYoi *et al.*, 1993) and a host metalloproteinase MMP9 (Baylis *et al.*, 1995). Levels of RNA and protein of both these molecules are specifically elevated in parasite infected cells. It is believed that the elevated levels of secreted host matrix metalloproteinases play a role in the pathology of the disease by allowing dissemination of infected cells throughout the body (Adamson & Hall, 1996). Baylis *et al.* (1995) also showed that there is up-regulation of the transcription factor AP-1 which may be involved in regulation of MMP9 transcription in infected cells. This is additionally significant given that elevated levels of AP-1 are a response to mitogenic stimulation and there is evidence for a role for this transcription factor in the G0/S and G1/S checkpoint controls (Muller *et al.*, 1993). But elevated levels of these and other factors in infected cell lines may simply be a result of stimulated proliferation. Certainly these factors contribute to the transformed cell phenotype but it is extremely difficult to pick out a single likely candidate for the parasite produced molecule(s) which stimulates

proliferation. Work by Carrington *et al.* (1996) using the toxin ricin, which specifically inhibits host cell protein synthesis, shows there to be exchange of polypeptides between the host and parasite within the infected cells.

Once intiated, host and parasite cell cycles appear to become synchronised in that host/parasite nuclear and cytoplasmic division must be linked to ensure even distribution of the parasite to daughter cells. This suggests that there must be some form of intracellular communication between host and parsite. *In vivo,* there seems to largely be a finite number of divisions before the development of the piroplasm stages after ~14 days. It may be that *in vivo* most infected cells don't achieve the balance of cell division seen with transformed cell lines grown *in vitro*. As the schizont enlarges during differentiation then the synchrony between host and parasite is lost as populations show a range of schizont sizes. The disruption of synchrony between the host cell division and the schizont nuclear division marks a switch in differentiation of the parasite to the merozoite stage (Shiels *et al.,* 1992) but it is not known if nuclear division is synchronous within a macroschizont.

Thus differentiation and also the use of the inhibitor colchicine which inhibits host but not parasite microtubule formation (Carrington *et al.,* 1995) demonstrates that schizont nuclear division can occur independently of host cell division. How this occurs is still a matter of speculation. In *P. falciparum*, it has been proposed that schizonts contain a ready pool of cyclins for activating all stages of the cell cycle and that the cell cycle is regulated independently in each nucleus (Leete & Rubin, 1996). A key factor in this is that each schizont nuclear membrane remains intact during division which would confine cyclin degradation to the nucleus and thus not deplete a cytoplasmic supply common to all nuclei. If the levels of cyclin remain high then the nuclei can continue with another round of division. Immunofluorescence could be used to confirm the existance of a cytoplasmic pool once suitable antibodies become available.

1.2.12 Project Aims

The fundamental mechanisms governing the cell cycle are likely to be similar in parasites to those elucidated in both higher and lower eukaryotes but there will

probably be novel aspects to the cell cycle in *Theileria*. There are several questions linking the cell cycle to gaps in our knowledge of the life cycle of the parasite. For instance, how is the parasite cell cycle linked to the transformation of the host leucocyte? What regulates the observed synchrony given that the lengths of the cell cycle stages of host and parasite are likely to be different? What causes the host cell division to cease as the parasite switches from division to differentiation inside the lymphocyte?

Knowledge of the specific interactions underlying growth and division of *Theileria* will lead to a better understanding of the interaction between host and parasite and may eventually offer up new targets for specific therapeutic agents.

Specifically the project aims were;

1. Kinases are highly likely to be involved in different life cycle events such as control of control of stage regulation and entry into the cell cycle from the G0 state (reviewed in Pines, 1996). As a means of characterising the kinases involved in different life cycle stages of *T. annulata,* yeast p13^{suc1} was used as a means of affinity purifying cdc2-related kinases from these stages. This approach would also lead to a means of establishing kinase activity and possibly, substrate specificity in the life cycle.

2. The interaction with the host cell cycle is important for the intralymphocytic stage of the parasite and this interaction changes as the parasite switches to differentiation. With a range of markers against both host and parasite molecules involved in the cell cycle it was possible to examine the changes occuring in both host and parasite cell cycles during the intralymphocytic stage.

3. Isolation and characterisation of other parasite genes encoding proteins associated with nuclear division and their possible means of regulation. These proteins are also possible targets for chemotherapeutics and the feasibility of these were considered for *T. annulata.*

Figure 1.2 Conserved domains of cdc2 related kinases.

This figure shows conserved domains of cdc2- related kinases compared with human cdc2 (Hscdc2). Dashes represent conserved residues and * indicates residues which undergo phosphorylation. Key - Tb - *Trypanosoma brucei,* Dd -*Dictyostelium discoidium,* Sp - *Schizosaccharomyces pombe* and Th - *Theileria.* The ThCRK2 and TbCRK3 are discussed in section 1.2.9.

	ATP Binding Domain **	Cyclin Binding Domain PSTAIRE Box	T-161 *	Control of T-161 P
Hscdc2	KIGEGTYGVV	EGVPSTAIREISLLKE	YTHE	GDSEIDQ
Spcdc2	--------------	------------------	-----	-------E
Ddcdc2	-L--------E-	D-------L--------	-----	--C----
Ddcrp	-L--------I-	E---C------------	-S--	-SGTS---
TbCRK3	IL----------	--I-Q--L--V--IQ-	-----	------G-
ThCRK2	--------------	--I--------------	-----	-I--Q---
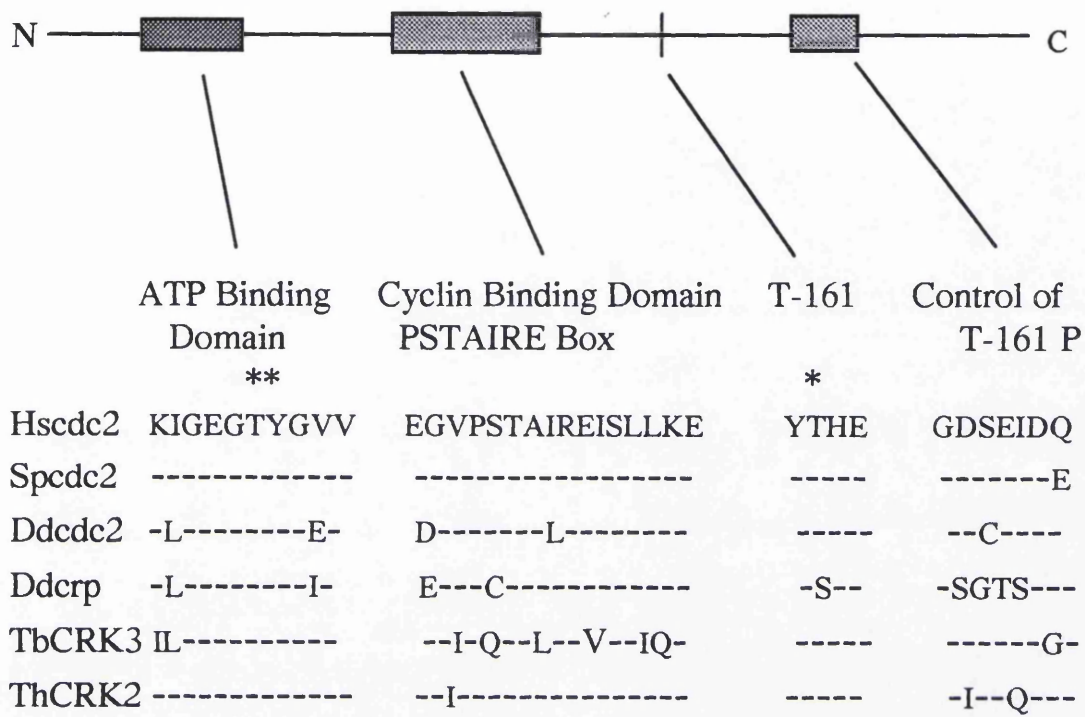
Figure 1.3 Members of the cyclin family

The mammalian cyclins A to H are shown together with the budding yeast Cln (G1 cyclins). The CDK7/Cyclin H complex is the CDK activating kinase CAK which phosphorylates a specific threonine residue (T161 in human cdc2, T160 in CDK2) which is phosphorylated in all active kinases. TFIIH contains the RNA polymerase II C-terminal domain kinase which has a role in transcription.

This diagram is adapted from Pines (1996).

Cyclin	Structure	Size	Function
A2	Destruction and Cyclin Box	48kDa	G2/M, S
B1	Destruction and Cyclin Box	48kDa	Mitosis
Cln	Cyclin box and PEST	66kDa	G1(START)
D	Cyclin box and PEST	32kDa	G1(R)
E	Cyclin box and PEST	44kDa	G1/S
F	Cyclin box and PEST	87kDa	G2?
G	Cyclin box	29kDa	?
H	Cyclin box	37kDa	CAK&TFIIIH
C	Cyclin box	33kDa	Transcription?

Figure 1.4 Periodicity of cyclin expression.

As shown in figure 1.3, cyclins are active at certain stages of the cell cycle. This figure shows the periodicity of cyclin expression - cyclin E is specifically synthesised and destroyed around the G1/S border. Cyclins A and B peak in G2 and M phase respectively. Cyclin D is synthesised in G1 and levels remain high throughout the rest of the cell cycle.
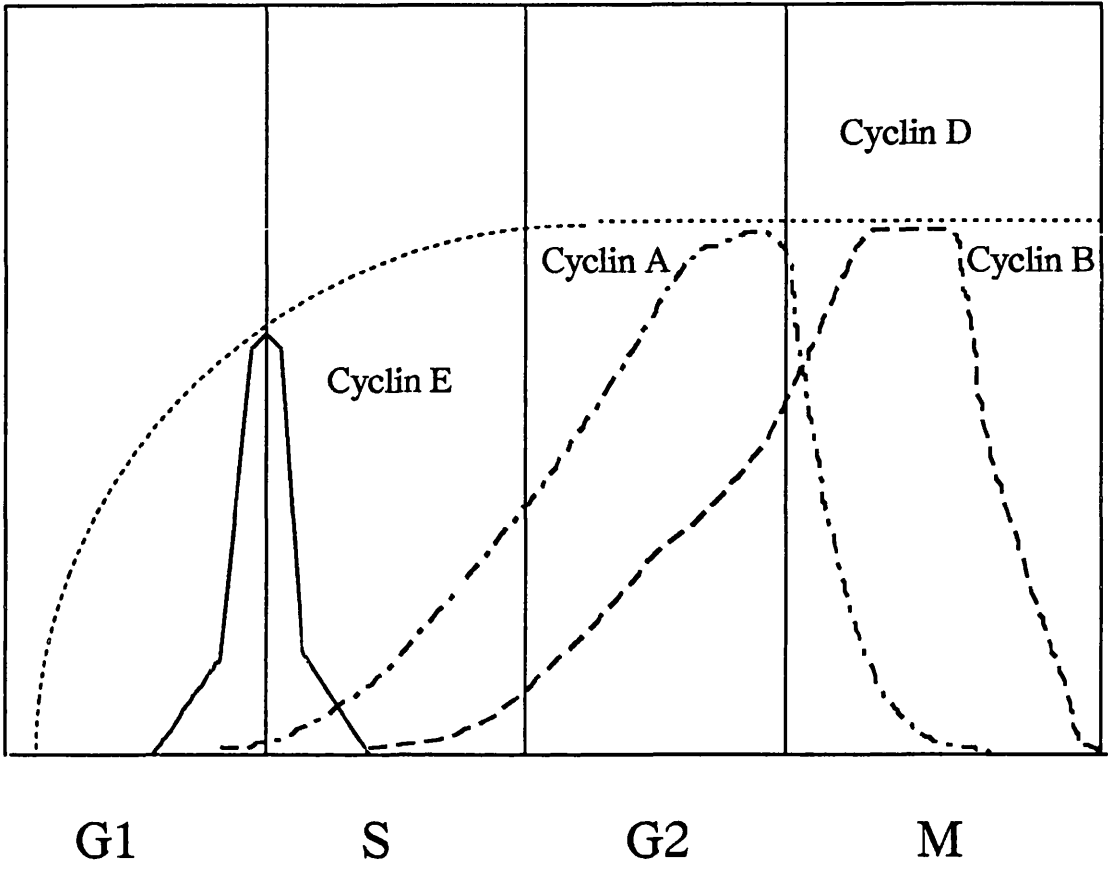
Figure 1.5 External controls influencing G1/S checkpoint.

This diagrams shows the interplay between various components of the cell cycle during the G1/S transition. The cycle is open to the influence of external factors at this point and the signalling pathway between these factors and the CDK complexes is shown.

The CDK7/Cyclin H complex is the CDK activating kinase CAK which phosphorylates a specific threonine residue (T161 in human cdc2, T160 in CDK2) which is phosphorylated in all active kinases. p27 is a CDK inhibitor that acts upon the CDK4/cyclin D complex by preventing its phosphorylation by CAK (reviewed in Pines 1996).

TGF-β is transforming growth factor beta.

cAMP - cyclic adenosine monophosphate

This diagram is adapted from Sherr (1994).
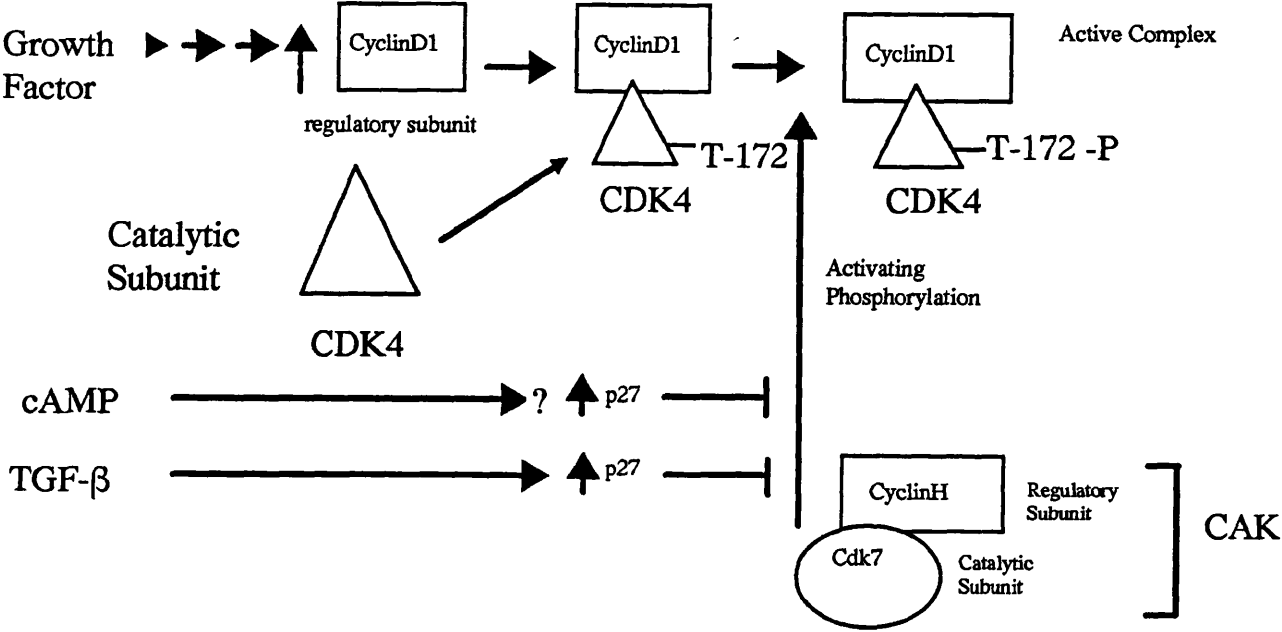
Figure 1.6 Cyclin kinase inhibitor subunits (CKI)

This figure shows cyclin dependent kinase inhibitor complexes, together with the stage of the cell cycle when active. p21 is active at all stages and appears to be a 'universal CDK inhibitor'.

Major Cyclin - Cdk Cell Cycle Complexes

Cell Cycle Stage	cyclin-Cdk complex	inhibitors				
		p15	p16	p18	p21	p27
G1	cyclin D -Cdk4/Cdk6	+	+	+	+	+
G1/S	cyclin E - Cdk2	-	-	-	+	+
S	cyclin A - Cdk2	-	-	-	+	-
G2/M	cyclin B - Cdc2	-	-	-	+	-

Table 1.1 CDKs and their activating cyclins with other cdc2-related cDNAs.

This table is from Pines & Hunter, 1995. For each CDK it shows the conservation of the PSTAIRE motif together with known cyclin partners. For some CDKs cyclin partners or stages of the cell cycle when active are unknown - this is indicated by N/D.

Key:

Xl - *Xenopus laevis*

Dm - *Drosophila melogaster*

Hs - *Homo sapiens*

CDK	PSTAIRE epitope	Associated Cyclins	Cell Cycle Stage	%Identity to human CRK1
cdc2Hs (CDK1)	EGVPSTAIREISLLKE	A, B	G2-M	100
cdc2X1	EGVPSTAIREISLLKE	A, B	G2-M	87
cdc2Dm	EGVPSTAIREISLLKE	A, B	G2-M	72
CDK2Hs	EGVPSTAIREISLLKE	A, D, E	G1-S, S	65
CDK2X1	EGVPSTAIREISLLKE	E	G1-S, S	64
Cdc2cDm	EGVPSTAIREISLLKE	E	G1-S, S	57
CDK3	EGVPSTAIREISLLKE	N/D	N/D	66
CDK4(PSKJ3)	GGLPV/ISTAIREVALLRR	D	G1-S, S?	44
CDK5(PSSLARE)	EGVPSSALREICLLKE	D	G1-S, S?	57
CDK6(PLISTRE)	EGMPLISTREVAVLRH	D	N/D	47
PCTAIRE 1-3	EGAPCTAIREVSLLKD	N/D	N/D	51-55
CHED(PITAIRE)	EGFPITAIREIKILRQ	N/D	N/D	42
CDK7	DGINRTALREEIKLLQE	H	N/D	40
p58-GTA	EGFPITSLREINTILK	N/D	N/D	32

Chapter Two

Materials & Methods

2.1 Cell Lines

BL20 is a bovine B cell lymphosarcoma cell line (Morzaria *et al.*, 1982). A *T.annulata* (Ankara) macroschizont infected cell line (TaA2) was isolated from an infected animal's peripheral blood mononuclear cells. A clone of this line, selected for its enhanced differentiation phenotype, is known as D7 (Shiels *et al.*, 1992).

Cell lines were maintained by culturing at 37°C with 5% CO_2 air in RPMI 1640 (Gibco-BRL) supplemented with 20% heat inactivated foetal calf serum (Gibco-BRL), $8\mu gml^{-1}$ streptomycin, $8U\ ml^{-1}$ penicillin, $0.6\mu gml^{-1}$ amphotericin B (ICN Flow), 0.05% $NaHCO_3$ and $10\mu M\ \beta$ mercaptoethanol (Brown, 1987). Cells were passaged by a five fold dilution every 48 hours.

2.2 Induction of *in vitro* differentiation

Differentiation of the D7 cell line was induced by shifting the culture temperature from 37°C to 41°C. The cell number was counted with a haemocytometer and adjusted to 1.5×10^5 cells ml^{-1} by dilution into fresh medium before induction and every 48 hours post induction.

2.3 Giemsa staining of induced cultures

Morphological examination of cultures at 41°C was carried out by light microscopy of Giemsa stained cytospin preparations. A $50\mu l$ sample was spun at 1500 rev min^{-1} (240g) for 5 minutes in a Shandon cytospin 2. The slides were then air dried and fixed in methanol for 30 minutes before staining in Gurr's improved R66 Giemsa stain (BDH) (4% solution in water).

2.4 p13^{suc1} Purification

Two methods of purification were used:

1. p13^{sucl} was prepared from an overproducing strain of *E. coli* (a gift of P. Nurse) by gel filtration on a Sephadex G100 column (Pharmacia). Fractions were analysed on a 15% SDS Page gel and the purest fractions pooled. These were concentrated by ammonium sulphate precipitation to 75% saturation and extensively dialysed against 50mM Tris pH8.0.

Final purification was by ion exchange fast protein liquid chromatography (FPLC) on a Q-Sepharose column (Pharmacia). p13^{sucl} was eluted with a continuous salt gradient of 0-500mM NaCl. Purified p13 was then coupled to an amino link gel (Pierce) according to the manufacturer's instructions. Unreacted sites on the gel beads were blocked with 1M Tris pH8.0. The concentration of coupling was 4mg of p13 to 1ml of gel.

2. The *sucl* gene was re-cloned into the pQE60 expression vector (Qiagen) which contains the sequence for a multiple Histidine tag at the 5' end of the cloning site thus allowing for an affinity purification of the expressed protein on nickel agarose (Ni-NTA, Qiagen). An overproducing strain of *E. coli* (a gift of Dr. K. Grant) was lysed by sonication and the supernatant was applied to an Ni-NTA column. The affinity bound protein was eluted in a 0-500mM imidazole gradient and fractions analysed on a 15% SDS-PAGE gel. The purest fractions were pooled and concentrated using a Centricon 10 filtration unit (Amicon) and dialysed against 50mM NaPO$_4$ pH8.0, 300mM NaCl to remove imidazole. Purified p13 was then coupled to an amino link gel (Pierce) according to the manufacturer's instructions. Unreacted sites on the gel beads were blocked with 1M Tris pH8.0. The concentration of coupling was 5mg of p13 to 1ml of gel.

2.5   Cell Lysis

Native protein extracts of uninfected host lymphocytes (BL20) and *Theileria annulata* piroplasms were prepared by resuspending cell pellets stored at -70 °C (BL20 cell pellets were obtained by centrifugation of 100ml cell cultures (1.5×10^5 cells/ml) at 3000rpm and removing the supernatant) in lysis buffer (50mM MOPS pH7.2, 100mM NaCl, 10mM EDTA, 1mM EGTA, 1mM sodium orthovanadate, 10mM NaF, 1% Triton X100) with protease inhibitors (1mM 1,10 phenanthroline, 5mM pepstatin A, 10mM leupeptin, 10mM phenylmethylsulfonyl fluoride) and incubating at 4°C for 30 min prior to centrifuging at 12000x g for 30 min. The supernatants were used for kinase assays and Western blotting.

Macroschizonts were prepared from *Theileria* infected lymphocyte line D7 at day 5 of differentiation using the Bio-nebuliser (Hoeffer). Pelleted cells were re-suspended in PBS at a concentration of 1×10^6ml^{-1} and passed through the nebuliser twice at a constant pressure of 20psi. The suspension was then centrifuged at 1000g through a 20% Percoll gradient (Pharmacia). The visible fractions from the Percoll gradient were checked for host cell contamination using cytospin preparations which were Giesma stained and examined by light microscopy at x1000. The preparation was found to contain traces of host nuclei and some intact cells. Macroschizont (schizont) protein extracts were prepared as described above.

Extracts were assayed for protein concentration (BioRad) and volumes adjusted to give equal protein loadings for affinity preparations of protein kinases.

2.6   Affinity Chromatography

50μl of p13^{suc1} and Tris- agarose coupled beads were added to a 2ml column (Pierce) and washed with 500μl of lysis buffer. 500μg of each protein extract was added to the p13 and Tris agarose beads and incubated at 4°C for 3 hours with mixing by rotation. The beads were then washed with 5x1ml of lysis buffer (supplemented with 10% glycerol) and 1x kinase assay buffer (KAB - see section 2.7) and re-suspended in 20μl of SDS-PAGE sample buffer or KAB.

Each set of agarose beads was then split 75/25 by volume for Western blotting and kinase assays respectively.

2.7 Histone H1 Kinase Assays

The beads were washed in 1x kinase assay buffer (50mM MOPS pH7.2, 20mM MgCl$_2$, 10mM EGTA) and preincubated in 25µl of KAB at 30°C for 10 mins. 20µl of kinase assay mix (KAM - 5µg histone H1 (Boehringer), 2.5µM ATP, 50nCi γATP (5000Ci/mmol) in KAB) was added and the mixture incubated at 30°C for 20 mins. The reaction was stopped by the addition of 20µl of 4x SDS sample buffer. Samples were then boiled and centrifuged prior to loading 25µl of supernatant onto a 12.5% SDS- PAGE gel. After electrophoresis gels were stained in Coomassie Brilliant Blue R-250 and destained in 30% methanol, 10% acetic acid and dried in an 'Easi-Breeze' Gel Drier (Hoeffer). The dried gel was then exposed to X-ray film (Fuji) at -70°C.

2.8 Electrophoresis of Protein Gels

2.8.1 SDS-Polyacrylamide Gel Electrophoresis

Denaturing polyacrylamide gel electrophoresis of proteins was performed according to the method of Laemmli (1970). The ratio of acrylamide:bis-acrylamide was 29:1 and was purchased ready mixed from Anachem. Polymerisation was catalysed by addition of 0.05% ammonium persulphate and 0.03% TEMED. Resolving gels were either 12.5% or 8% acrylamide in 375mM Tris-HCl (pH8.8), 0.1% SDS. Stacking gels were 4% acrylamide in 125mM Tris-HCl (pH6.8), 0.1% SDS. Gels were run at a constant voltage of 100V for 2-3 hours (mini-gels) or at 55V (~15 hours) for large gels until the dye front reached the bottom of the resolving gel. The electrophoresis buffer was 25mM Tris, 192mM glycine (pH 8.3), 0.1% SDS.

2.8.2 Tricine SDS Gels

In some circumstances it was more appropriate to use the Tricine SDS method of Schagger and von Jagow (1987). Here the gel buffer was 3M Tris-HCl (pH 8.45), 0.3% SDS. The anode buffer was 0.2M Tris-HCl (pH 8.9). The cathode buffer was 0.1M Tris, 0.1M Tricine, 0.1% SDS with the pH being adjusted to 8.25 by addition of Tricine. The running conditions are identical to those stated for the SDS-PAGE electrophoresis.

In both cases a glycerol/SDS sample buffer was added to the samples prior to loading on the gels. The sample buffer is composed of 50% glycerol, 5%SDS, 50mM Tris-HCl (pH 6.8) and 0.01% bromophenol blue. A minimum of 0.25 volume of the sample buffer was added to the samples prior to heating at 90°C for 5 minutes prior to loading. Low molecular weight markers (Sigma) were prepared as detailed in the manufacturer's instructions.

2.9   Western Blotting

Protein gels were blotted onto Hybond C membranes (Amersham). The blotting protocol was essentially that described by Towbin *et al.* (1979). The gel was laid over 3MM paper then covered with Hybond C paper prior to more 3MM paper being overlaid. The cassette was then immersed in an electroblot holder (Bio-Rad) with the Hybond C paper facing the anode of the tank. The transfer buffer was 25mM Tris, 192mM Glycine and 20% methanol and the transfer took place at 4°C. For small gels, the Mini-Protean system (Bio-Rad) was electrophoresed at 0.28A for 3 hours and the large gel blotter (gels of 9cm by 14cm) overnight at 0.1A. After transfer the Hybond membrane was stained in Ponceau S stain (0.2% Ponceau S (Sigma) in 3% trichloroacetic acid) to assess efficiency of transfer and equal loading of protein. The blots were pre-incubated in block buffer (5% low fat, dried milk, 10% horse serum in TBST (Tris buffered saline with Tween (100mM Tris-HCl pH7.5, 0.9% NaCl, 0.05% Tween 20)) for 1 hour at room temperature. Primary antibodies were diluted in blocking buffer to a working dilution and incubated with the blot for 3 hours at room temperature. The blots were rinsed twice then washed twice in TBS-Tween for 20

with the secondary antibodies (Horse radish peroxidase conjugates (Sigma)) prior to signal development with the ECL system (Amersham).

2.10   Immunoprecipitation

Immunoprecipitation of the ThaCRK2 polypeptide from piroplasm extracts was as follows; piroplasm extracts were lysed as in section 2.5 and the supernatant incubated with 10μl of affinity purified anti-ThaCRK2 antiserum (a gift of Dr. J. Kinnaird) at 4°C for 1 hour on a rocker. Then 40μl of a 50% slurry of Protein A-sepharose (Pierce) was then added and incubated for a further hour at 4°C. The Protein A-antibody-antigen complex was then collected by centrifugation at 12000g for 20 seconds in a microfuge and re-suspended in 10mM Tris HCl (pH 7.5), 0.1% NP-40 for 20 minutes at at 4°C. The centrifugation and wash steps were repeated twice and the final sepharose pellet re-suspended in 30μl of SDS-PAGE sample buffer, boiled for 5 minutes then centrifuged briefly prior to analysis on an SDS-PAGE gel.

2.11   Growth of bacterial strains

Unless otherwise stated, all liquid cultures were grown at 37^0C with vigorous shaking. Appropriate antibiotic selections for *E. coli* strains transformed with plasmid were: *E. coli* strain XL-1 Blue (Stratagene) - 100μg/ml ampicillin with 12.5ug/ml tetracycline.

2.12   Isolation of Plasmid DNA from *E.coli*

Small scale plasmid DNA purifications were performed using the Wizard Mini Prep kit (Promega) in accordance with the manufacturers protocol. For large scale preparations a Midi Prep kit (Qiagen) was used. For both these protocols, a stationary

phase culture was harvested by centrifugation at 12000g for 10minutes at 4°C. The pellets were then treated according to the kit instructions.

2.13   Lambda Phage Manipulations

The host bacteria PLK-17 (Stratagene) were first grown overnight in L-broth supplemented with 0.2% maltose and 20mM $MgSO_4$. The cells were then pelleted by centrifugation (5000g for 5 minutes at 4°C) and resuspended in 0.5 volume of sterile cold 10mM $MgSO_4$. The suspension was diluted if the Absorbance reading at 600nm was greater than 2 (i.e. >1.6 x 10^9 cells/ml). These plating bacteria were stored at 4°C and were viable for up to 3 weeks.

For determining the titre of the λ library used for screening, serial 10-fold dilutions of the phage stock were prepared in phage buffer (50mM Tris-HCL (pH7.5), 0.1M NaCl, 8mM $MgSO_4$, 0.01% gelatin). 100μl aliquots of each dilution were added to 100μl of plating bacteria and the samples were incubated at 37°C for 20 minutes. 3mls of top agarose (heated to 45°C) was then added and the mixture poured onto bottom agar plates. After cooling the plates were inverted and incubated overnight at 37°C. The plaques were counted and the titre determined from appropriate dilutions.

2.14   Library Screening

A λZAP cDNA library made from D7 total RNA was prepared by Dr. Kinnaird and plated at a density of 20000 plaques per large petri dish (12cm diameter) as described in section 2.13. Filter lifts of plaques were taken by allowing the filters to rest on the plaques for 1 minute. Alignment marks were made through the filter paper and the agarose using a needle. The filters were then removed with the plaque side up onto a pad of 3MM paper soaked in denaturation solution (1.5M NaCl, 0.5M NaOH) for 5 minutes. Next the filters were transferred to another pad soaked in neutralising solution (1.5M NaCl, 0.5M Tris-HCl (pH7.2)) for 5 minutes. This step was repeated with another pad soaked in the same solution. Finally the filters were washed in 2x

SSC (standard saline citrate, 1xSSC is 0.15M NaCl, 0.15M trisodium citrate, pH 7.0), transferred to dry 3MM paper and allowed to dry in air, colony side up. The filters were fixed using a UV transilluminator (Stratagene). The filters were hybridised to a radiolabelled DNA probe. Positive plaques hybridising to radiolabelled probes were cored from the plate using a sterile toothpick into SM buffer containing a drop of chloroform. Phage was allowed to diffuse out for 2-3 hours prior to replating a 10^{-2} and 10^{-4} dilution for a further round of screening. The process of filter lifts and hybridisations was repeated until all the plaques on a filter gave a positive signal with the radiolabelled probe. A single plaque was picked and the phage subjected to the *in vivo* excision protocol (Stratagene). This allows excision and re-circularisation of a pBluescript phagemid containing the insert by use of a 'helper phage' which initiates and terminates DNA replication from helper phage sequences inserted in the bacteriophage λ. Positive clones can then be identified as colonies on a plate containing ampicillin.

For large scale preparations of lambda phage DNA, the liquid lysate method was used (Sambrook *et al.*, 1989) with an equal multiplicity of infection for phage: bacteria and the DNA was isolated and purified using the Promega Magic Lambda Prep kit (Promega Corporation) according to the manufacturer's protocol.

2.15   Restriction Digests of DNA

Restriction endonuclease digests of plasmid DNA were done according to the procedures recommended by the manufacturer using the buffers supplied and the optimal temperature for activity of the enzyme. The reaction was terminated by heat inactivation of the enzymes at 70°C for 15 minutes or by the addition of agarose loading dye (0.025% bromophenol blue, 25% Ficoll, 50mM EDTA).

2.16   Agarose Gel Electrophoresis

DNA was visualised on horizontal agarose gels. Usually 1% gels were cast with 100ngml⁻¹ ethidium bromide and run in 1XTBE (0.09M Tris-HCl, 0.09M Boric acid, 2.5mM Na₂EDTA pH8.0) at a voltage of 10Vcm⁻¹ for 2 hours. Visualisation of DNA was on a UV transilluminator (302nm) and images were captured on a Gel-Imager system (Appligene) and stored on disk.

2.17   Recovery of DNA from Agarose Gels

DNA fragments were excised from agarose gels using a clean scapel blade and processed using the Qiaquick spin Kit (Qiagen). The fragment was eluted from the DNA binding column in 50μl TE (10mM Tris-HCl, 1mM EDTA, pH8.0) and stored at -20°C.

2.18   Quantification of Nucleic Acid

Concentration and purity of nucleic acid was determined on a spectrophotometer (Beckman) by measuring absorbance through a pathlength of 1cm @ 260nm and 280nm. An absorbance of 1 at 260nm is equivalent to a solution concentration of 50μgml⁻¹ of double stranded DNA. The ratio of A260/A280 indicates purity of the DNA preparation with a ratio of 1.8 being optimal.

2.19 Ligations

Ligations were performed in a final volume of less than 15μl in 1x T4 DNA ligase buffer (Promega) and 1-2 units of T4 DNA ligase (Promega). Generally, 25ng of vector DNA were used in each ligation, the amount of insert DNA used varied with the molar concentration of free ends in the reaction. Ligations were performed overnight at 16°C.

45

2.20 Transformations

Routinely, transformations were performed using 50µl of *E.coli* XL-1 blue supercompetent cells (Stratagene) and 25-100ng of ligated DNA according to the manufacturer's protocol. The transformed cells were selected using the antibiotic resistance marker carried by the plasmid (Amp^r). Where applicable, blue / white colony selection was also used to select transformants with plasmids containing inserts and for this, the agar media was also supplemented with 0.004% X-gal and 34µM IPTG (final concentrations).

Vectors used included pBluescript (Stratagene), pTZ19R and pGEX5-2 (both Pharmacia) and pTAG vector (R&D systems).

2.21 Southern Blotting

Capillary transfer of DNA from agarose gel to membrane (Amersham Hybond N) was as described in Sambrook *et al.* (1989). Agarose gels were washed twice in denaturing solution (0.5M NaOH, 1.5M NaCl) for 15 minutes per wash then twice again in neutralising solution (0.5M Tris-HCl pH 7.5, 3M NaCl). The gel was then placed on a platform of 3MM paper which had its ends immersed in 20xSSC. Hybond N membrane, cut to the same size as the gel was then laid on top and this was then covered with 3MM paper soaked in 2xSSC then paper towels and a weight. The transfer was allowed to proceed overnight. Blots were dried in air for an hour before cross-linking using a UV transilluminator.

2.22 Northern Blotting

RNA was electrophoresed through denaturing formaldehyde 1% agarose gels as described in Sambrook *et al* (1989). 10µg of total RNA was loaded per track. RNA standards (Gibco BRL) and an identical set of RNA samples were cut off and stained

in eithidium bromide after electrophoresis. The remainder of the gel was soaked for 15 minutes in transfer buffer (15mM NaH_2PO_4, 10mM Na_2HPO_4 pH 6.5) then transferred onto a Hybond N membrane overnight as described for Southern blotting except that the filter was not rinsed prior to cross-linking on a UV transilluminator.

2.23   Probe Labelling and Hybridisation

DNA probes were labelled by the random priming method (Feinberg & Vogelstein, 1983) using the Prime It II kit (Stratagene). Unincorporated radioactivity was removed by purifying the probes on the NucTrap column (Stratagene) according to the manufacturer's instructions. Blots were pre-hybridised in 0.5M sodium phosphate buffer pH 7.0, 0.5 % SDS (Church & Gilbert, 1984) at 65°C for 30 minutes using a rotating bottle in a hybridisation oven (Hybaid). This solution was replaced with a fresh solution containing the denatured labelled probe and hybridisation was allowed to proceed overnight at 65°C. The blots were then washed twice in 40mM sodium phosphate pH7.0.5% SDS for 10 minutes at 65°C then twice in 40mM sodium phosphate pH7.0.5% SDS for 10 minutes at 65°C before being wrapped in Saranwrap and exposed to X-ray film (Fuji). For re-probing the blots were placed in boiling 0.1% SDS solution allowed to cool in this solution to room temperature. Filters were exposed to X-ray film overnight to check that the probe had been properly removed.

2.24   DNA Sequencing

Sequencing was performed on both strands. Sequencing methods included the chain termination method of Sanger (Sanger *et al.,* 1977) with Sequenase kits (USB/Amersham) and (α-^{35}S) dATP (Dupont UK Ltd.) on a 6% gel run in a BaseAce apparatus (Stratagene); automated sequencing used the LiCor sequencer (LiCor Corp.) with samples prepared using the Fluoro Sequenase kit (CamBio) which uses fluorescently end-labelled primers; alternatively an ABI373 sequencer was used with samples prepared with the ABI Sequenase 2.0 kit on a Geneamp 2000 PCR machine

(Perkin-Elmer). Both the automated sequencer protocols use a PCR amplification step of the template DNA. The ABI method incorporates fluorescently labelled dNTPs in the PCR reaction which are then read by the computer as the DNA migrates in the gel. Commerical primers used included T3, T7 and Sp6 (Stratagene) with the pTAG 5' and pTAG 3' primers (R& D systems). In some cases specially designed oligonucleotide primers were used (Cruachem & Strathclyde University). Analysis of sequence data used the University of Wisconsin GCG package (Devereux *et al.,* 1984).

Gene Specific Primers for the *T. annulata* R1 subunit

Primers used for DNA Sequencing of the large subunit of ribonucleotide reductase from *T. annulata* are listed below. The position of the primer on the full length cDNA sequence (chapter 4) is shown.

Primer No.	Sequence	Sense	Position (cDNA)
1	3'GCTCCACGAG TGACACAGAG5'	anti	322-341
2	5'CTAGCAGCCA ACATCACCATA G3'	sense	444-464
3	3'CGAGGTGATC GAGGGACCTGT 5'	anti	500-520
4	3'CCCTGGCGGG AATCTTTAAC5'	anti	892-912
5	5'GGGAATCTTT AACACACACTG AGC3'	sense	899-921
6	3'GCCAATCCTA CAGTCCCAAA5'	anti	1386-1406
7	5'AGACCGATGG	sense	1711-1737

	GTGTAGGAGTA CAAGGT3'		
8	3'GCTGTGGGAC TGGGATAAACT TAAGGCAGA5'	anti	1949-1979
9	5'ATTACAGAAG GGTGTTGAGTG G3'	sense	2092-2114
10	5'CTTCAATATC ACAGGCTGGC3'	sense	2477-2496
11	3'GCTTCATGTG CTCATCGT5'	anti	2698-2716

2.25   Production of Antisera

Antibody against fusion proteins was produced in New Zealand white rabbits kept at Biological Services, Veterinary School, University of Glasgow. Standard immunisation protocols were followed (Harlow & Lane, 1988). Briefly, the GST-fusion protein in PBS at a concentration of 1mg/ml was mixed with an equal volume of a suspension of Alum (Pierce) added drop-wise with stirring for 30 minutes. Two rabbits were immunised with 500µg protein each and boosted after four weeks with 250µg protein, again in Alum. Test bleeds were assayed by Western blotting and boosting continued every three weeks until a satisfactory immune response was detected.

Commercial antisera used included:
The mammalian and avian specific anti HSP 60 antibody (Boehringer) is a monoclonal antibody recognising an epitope between amino acid residues 383-447 of the human HSP-60. It is reactive with both the constitutive and inducible forms of HSP-60 (manufacturer's data sheet).

The higher eukaryote specific anti-ribonucleotide reductase large subunit antibody (Biomedtek, Umea) is a mouse monoclonal antibody recognising an unmapped epitope from partially purified calf thymus R1 (manufacturer's data sheet).

Other antisera used are described in the results section.

2.26 Polymerase Chain Reaction

A: Rapid screening of bacterial transformants for plasmids with inserts

For colony screening of transformants plasmid DNA was used as template with T3 and T7 primers or other primers specific for the plasmid used in the ligation reaction. The reagents used as listed below:

Reagents	Final Concentration
Taq Polymerase 10X buffer (Promega)	1X
Taq DNA polymerase	1 unit/25μl
Acetylated BSA	100μg/ml
Magnesium Chloride	1.5mM
dNTP's (Promega)	200μM
Primers	4ng/μl

25μl of the reaction mixture was added to 0.5ml Eppendorf tubes and a sterile toothpick used to touch the colony on the transformation plates. The pick was then dipped into the reaction mixture before the mixture was overlaid with a drop of mineral oil and amplified over 25 cycles of 94°C for 30 seconds, 55°C for 30 seconds and 72°C for 2 minutes.

B: PCR amplification of the *suc1* homologue from *T. annulata*

DNA was amplified from piroplasm genomic DNA and cDNA and

the following conditions were used. These were based on those used to amplify the human p13 homologue *CksHs1* (Richardson *et al.,* 1990) and modified by Mottram & Grant (1996) to clone the homologue from *L. mexicana.*

For both these protocols, degenerate oligonucleotides were designed against conserved regions of p13^{suc1} as shown in figure 3.1.

For attempts to amplify the *Theileria* homologue two different reaction buffers were tried, both using the same primers as used for the cloning of the *L. mexicana* homologue. The primers are:

5'primer - AGAG<u>CTCGAG</u>TAYMGNCAYGTNATGYTNCC

3'primer - GAG<u>GAATTC</u>AANARNARDATRTGNGGYTCNGG

(N=G+A+T+C, Y=T+C, M=A+C, R=A+G and D=G+T+A , *XhoI* and *EcoR1* restriction sites are underlined). The 5' primer was 1000 fold degenerate and the 3' primer was 12000 fold degenerate for the cloning of the *L. mexicana* homologue. The buffers were:

1. 11.1X buffer - 45mM Tris HCl (pH 8.8), 11mM ammonium sulphate, 4.5mM MgCl$_2$, 6.7mM β mercaptoethanol, 4.4μM EDTA (pH 8.0), 1mM each of dATP, dCTP, dGTP and dTTP, 1 unit of *Taq* polymerase and 113μg/ml BSA.

2. The standard reaction buffer of Richardson *et al.* (1990) and Mottram & Grant (1996) of 50mM KCl, 10mM Tris-HCl (pH 8.3), 1.5mM MgCl$_2$, 0.01% gelatin, 0.2mM each of dATP, dCTP, dGTP and dTTP, 0.0025 units of *Taq* DNA polymerase, 10μg of primers and 5μg of template cDNA were used and the PCR parameters were 40 cycles of 94°C for 1 minute, 45°C for 2 minutes and 72°C for 3 minutes. The results of the PCR amplification are discussed in chapter 3 together with the various parameters tried.

2.27 5' Rapid Amplification of cDNA Ends (5' RACE)

5' RACE was performed using the GibcoBRL 5' RACE kit (GibcoBRL) according to the manufacturer's protocol with 1μg of total piroplasm RNA as

51

template. In brief, first strand cDNA was prepared from the total RNA using a gene specific primer for the large subunit of ribonucleotide reductase (TaR1). The resulting cDNA was dC-tailed using terminal deoxynucleotide transferase and the product, subsequently amplified by nested PCR. The nested PCR used another primer specific to for the TaR1 gene together with the Anchor Primer supplied with the kit, which annealed to the dC-tailed region of the cDNA. These primers are listed below. The PCR product was cloned into the pTAG vector using the A overhangs generated by the reaction.

Primers

5PRIME RACE 1 - 5' AGCGATAACTTCCTGATGCG 3' (antisense to position 289 - 308 of the TaR1 cDNA sequence.)

5PRIME RACE 2 - 5' AAATCGTGGTCCTCATAGCC 3' (antisense to position 127 - 146 of the TaR1 cDNA sequence.)

The protocol used was identical to that supplied by the manufacturer.

2.28 Indirect Immunofluorescence Microscopy

BL20 and D7 cells were cytospun onto poly-L-lysine coated slides and fixed in 4% formaldehyde in PBS for 10 minutes at room temperature before being permeabilised in 0.25% Triton X100 in PBS for a further 10 minutes. The cells were then preblocked in RPMI 1640 medium for 30 minutes in a humidified chamber at room temperature. The primary antibody at a dilution of 1/200 in RPMI 1640 was applied to the cytospin preparation and incubated for 3 hours, again in a humidified chamber. The slides were then washed with several changes in 0.1% NP-40 in PBS over 5 minutes. The FITC conjugated secondary antibody (Sigma) was diluted 1/500 in RPMI 1640 and incubated with the cells for a further hour. The slides were then washed again in 0.1% NP-40 before being mounted in DABCO (1,4-diazabicyclo[2.2.2.]octane (Sigma)) in 50% glycerol and viewed with a Zeiss Axioplan fluorescent microscope with an MC100 Spot camera attachment. Nuclei were localised

by staining with 1μgml^{-1} DAPI (4,6-diamino-2-phenylindole dihydrochloride), 1mgml^{-1} p-phenylene-diamine in DABCO/glycerol mountant.

An alternative method of fixation was tested using acetone at -20°C for 5 minutes followed by air-drying of the slides before incubating with the antibodies.

2.29 5-Bromo-2-deoxyuridine (BrdU) Incorporation

Cells were pelleted by brief centrifugation (at 300g for 5 minutes) and re-suspended in medium containing BrdU (Boehringer, final concentration of 10μM) at 2x10^6/ml for 60 minutes at 37°C. The cells were then again pelleted, washed three times in PBS then re-suspended in PBS with 5% albumin, cytospun onto poly-L-lysine slides and air-dried. The slides were fixed in 70% ethanol/50mM glycine pH2.0 at -20°C for 20 minutes. Slides were then washed three times in PBS before being incubated with a 1:10 dilution of the anti-BrdU antibody solution (Boehringer) for 30 minutes at 37°C (containing nuclease). Slides were washed again before incubating with anti-mouse IgG FITC conjugate for 30 minutes at 37°C. The slides were washed in PBS before mounting in DABCO/glycerol/DAPI to visualise nuclei using a Zeiss Axioplan fluorescent microscope with an MC100 spot camera attachment.

3.1.1 Introduction

As described in section 1.2.8 of the introduction, p13^{suc1} encodes a small protein whose exact role in the cell cycle has remained largely undefined. Very recent work with the *Xenopus* p13 homologue suggests it acts to regulate both the activity of cdc2/cyclin B at the G2/M boundary and inactivation of this complex at the metaphase/anaphase transition via degradation of cyclin B (Patra & Dunphy, 1996). The X-ray structure of a human p13 homologue complexed with CDK2 has also recently been defined (Bourne *et al.*, 1996) and this analysis led to the theory that p13 and its homologues may serve to direct CDKs to substrates or CDK regulatory proteins. Homologues have been identified from a variety of organisms (see Figure 3.1). The product of the *S. pombe suc1* gene is commonly referred to as p13 or p13^{suc1} while the gene encoding this protein is referred to as *suc1*.

The ability of p13 to bind strongly with p34^{cdc2} and p33^{CDK2} (Arison *et al.*, 1988; Azzi *et al.*, 1992; Brizuela *et al.*, 1987; Draetta *et al.*, 1987; Ducommun *et al.*, 1991; Hadwiger *et al.*, 1989; Hayles *et al.*, 1986; Meijer *et al.*, 1989) allows rapid affinity purification of the p34^{cdc2}/cyclin B complex from cell extracts (Labbe *et al.*, 1989; Pondaven *et al.*, 1990). CDK3 was shown to bind p13^{suc1} only weakly (Meyerson *et al.*, 1992).

Another protein, p15, has been isolated from starfish (Azzi *et al.*, 1994) and this was shown to be capable of binding CDK4 and CDK5 but incapable of binding p34^{cdc2} and CDK2. This p15 protein shows common properties with p13, particularly by being cross-reactive with anti-p13^{suc1} and anti-p9^{CKShs} antibodies and its ability to form stable complexes with CDK kinases which hint at it being another member of a possibly large family of p13 related proteins.

One cdc2-related kinase has been identified in *Theileria*, ThaCRK2 (Kinnaird *et al.*, 1996). Given that no other cdc2 like kinases had been isolated as part of that work via library screening and PCR, it is possible that *Theileria* only uses a single cdc2-like kinase for the control of its cell cycle, a situation analogous to that found in *S. cerevisiae*. However, more recently another cdc2-related kinase has been isolated from *Theileria* (ThaCRK3) but this is not highly related to p34^{cdc2} (Kinnaird, Logan & Langsley, in preparation).

The aim of the work reported in this chapter was to more fully characterise the cdc2-related protein kinases of *Theileria annulata,* by utilising recombinant p13^{suc1} as a means of affinity purifying and assaying kinases from different life cycle stages. While the genes encoding two CRKs have been characterised from the parasite, nothing is known about their enzyme activities, substrate specificies and interaction with other molecules. In the bovine life cycle stages of the parasite, each stage involves nuclear division. Initially the uninucleate trophozoite replicates its nuclei three to four fold to produce the multinucleate macroschizont which then continues to replicate in concert with the host cell but maintaining the nuclear number at ~10-15 parasite nuclei per cell. When differentiation to the merozoite is induced, a phase of rapid parasite division starts, leading to a schizont with over 500 nuclei which occupies much of the host cell. Merozoites are produced from this multinucleate schizont by budding of the membrane leading to uninucleate merozoites which then invade the erythrocytes and undergo a further two rounds of nuclear division to yield the piroplasm. It is not known how these complex series of nuclear divisions are regulated and whether different stages of the parasite life cycle regulate mitosis via different cell cycle associated kinases.

In order to address this question, an affinity purification based approach was undertaken to define the number and substrate specificity of cell cycle associated kinases present in the piroplasm stage using recombinant p13-sepharose chromatography and biochemical characterisation. As the affinity for p13 was low, experiments were undertaken to isolate the *Theileria* homologue of the *suc1* gene, the product of which would show a higher affinity for *Theileria* CRKs.

3.1.2   Expression and purification of p13^{suc1}

The yeast *suc1* gene was a gift of Prof. P. Nurse. The full length *suc1* gene was cloned into the pQE60 vector (Qiagen) and the plasmid used to transform M15[pREP4] *E. coli* (Qiagen) by Dr. K. Grant. Transformed cells were then induced to express p13 protein by induction with IPTG as detailed in chapter 2. The main method of purification of recombinant p13^{suc1} was by use of a Nickel-nitrilo-triacetic acid (Ni-NTA) agarose

column (Qiagen) via fast performance liquid chromatography (FPLC) with bound protein being eluted by an imidazole gradient.

Figure 3.2 shows stages of the induction and purification of p13. Panel A shows the cell supernatants after sonication and centrifugation. The supernatant (Lane 2) was then applied to the Ni-NTA column and fractions containing the purified p13 were eluted over the range of 200-300mM imidazole as shown in Panel B. The purified fractions were then pooled and dialysed (Panel C) prior to concentrating and cross-linking to Amino-link beads (Pierce) at a concentration of 5mg/ml. Control beads were prepared in an identical fashion by linking a 1M Tris pH7.4 solution in place of p13 according to the manufacturer's protocol.

3.1.3   Bovine CDK specifically binds to p13

Firstly it was necessary to show, as a positive control, that the p13 sepharose beads were capable of affinity purifying an active kinase complex from uninfected bovine cells (BL20). This was also carried out to standardise conditions of binding and washing which were then used in assays performed with parasite material. As mentioned in section 3.1 previous work had shown that in higher eukaryotes $p34^{cdc2}$ and $p34^{cdk2}$ were specifically bound to $p13^{suc1}$ and that the resulting complex was an active kinase.

Native extracts of BL20 cells were prepared and used in p13 binding assays followed by detection of the eluted polypeptides by Western blotting (figure 3.3). When specifically bound proteins were eluted from the p13-sepharose following extensive washing, there was a significant concentration of a 34kDa anti-PSTAIRE reactive polypeptide(s) (Panel A, lane 3). This concentration effect is not observed with the Tris coupled sepharose (lane 4). Similarly there is no depletion effect observed with the control beads (lane 2) compared to the p13 sepharose flow-through (lane 1). Panel B shows an identical immunoblot probed with a vertebrate specific cdc2 polyclonal antibody (Gibco). This antibody was raised against the C-terminal region of human $p34^{cdc2}$. Again, there is significant concentration of a 34kDa anti-cdc2 reactive polypeptide(s) with the p13 sepharose (lane 3). There is no specific binding of polypeptide(s) to the Tris-coupled sepharose (lane 4). It is difficult to distinguish

whether there has been a depletion of the reactive protein from the p13-sepharose flow-through lane (lane 1) because of a warping effect caused by overloading of the gel (lanes 1 & 2) based on Coomassie blue staining of the gels after transfer.

This result shows that the buffers and conditions used for lysis and binding are satisfactory for the extraction and purification of bovine CDK proteins. On the 12.5% acrylamide gel used for these blots it is not possible to resolve the small (<2kDa) size difference between the p34^{cdc2} and CDK2. However, this is seen in Figure 3.10 (Panel A, Lane 3) (8% acrylamide gel). Both bands are reactive with anti-PSTAIRE antibodies as they both contain this conserved motif. The next step was to show that the specific protein(s) bound to the p13 sepharose possessed kinase activity.

3.1.4   Purification of macroschizonts

As bovine cdc2 and CDK2 bind p13 it was necessary to purify macroschizonts to analyse parasite kinase binding to p13 in the infected lymphocyte stage of the life cycle. Macroschizonts were prepared by nebulisation of a differentiating D7 culture (5 days at 41°C) as the schizonts are larger at this point. The purified schizont material was stained by Giesma stain to assess host contamination. Figure 3.4 shows the material obtained with the nebulisation protocol. Panel B shows the host material fraction of the Percoll gradient after centrifugation, it contains intact schizonts indicating that the conditions used for nebulisation are satisfactory but that the Percoll gradient centrifugation has not separated the host and parasite material. From Panel C, which represents a higher band in the Percoll gradient, it can be seen that the schizont preparation used for the kinase assays in section 3.1.5 still contains host material and cell debris which would contaminate any assays undertaken with this material. The exact levels of contamination could be examined by immunoblotting of the schizont material but this was not done given the low yields of protein obtained.

3.1.5 An active kinase specifically binds to p13 sepharose from bovine and piroplasm extracts.

As the purified piroplasms were found to be free of significant host contamination and at least one parasite CRK was present in this stage, it was decided to base further experiments on piroplasm material.

3.1.8 Sypro orange stain detects p13 bound protein.

The binding experiments were repeated, eluting the bound protein in a small volume to maximise protein loading on an 8% SDS-PAGE gel. Figure 3.8 shows the binding of specific proteins from both bovine and piroplasm extracts to p13. The molecular weight markers are indicated on the right hand side of the figure. Sypro-orange is a protein stain which is as sensitive as silver staining (detection limit 2-5 ng of protein) and gels treated with Sypro-orange can be immunoblotted after staining which is not possible with silver stained gels.

With piroplasm extracts, elution after p13 binding (Lane 1) showed a 45kDa polypeptide was most clearly detected by the staining. The intensity of staining of this band suggests that this polypeptide is considerably concentrated by the p13-sepharose purification which hints at a high affinity interaction between yeast p13^{suc1} and the 45kDa molecule. This could be the ThaCRK3 kinase which has a predicted size of 45kDa. There are also some lower molecular weight polypeptides of approximately 31, 33 and 37kDa visible in the piroplasm eluate (Lanes 1) which would be in the correct size range for the CRK/CDK proteins. There are also higher molecular weight polypeptides of 70-80 and >100kDa. The 70kDa polypeptide is also present in BL20 cells and could be due to the presence of residual bovine serum albumin which was used to pre-block the p13-sepharose prior to binding. The >100kDa protein stains very strongly and is specific to piroplasms suggesting, again, a high affinity reaction. With bovine protein bound to p13 sepharose and eluted there is a band visible band at about 50kDa together with some minor polypeptide bands at around 34kDa which may be the cdc2/CDK2 proteins. Since p13 will bind the CRK/CDK protein complex, it is possible that some of the higher molecular weight polypeptides seen may represent components of this complex such as cyclins. This experiment was repeated with the gel western blotted after staining.

3.1.9 Immunoblotting with Sypro stained gel.

An identical set of experiments was undertaken to those in section 3.1.8 with the gel being immunoblotted after staining. The protein extract that was applied to the p13 column, the material eluted after binding to the column and the non-p13 bound material (flow-through) from both BL20 and piroplasms were run out on the gel. Both extracts applied to the column gave a heavy staining pattern (Lanes 1 & 4) while the non-bound material (tracks 3 & 6) show a prominent polypeptide at ~68kDa arising from the bovine serum albumin (BSA) used to pre-block the p13 column.

There are a number of proteins visible in the track containing piroplasm eluate from p13 sepharose (Lane 5) with the strongest being 45kDa similar to the profile seen in figure 3.8. The 35kDa polypeptide is also clearly visible.

Panel B shows an immunoblot of the stained gel in Panel A. Lane order is as above. There are two distinct proteins of molecular weights of 33 & 34 kDa reactive with the anti-PSTAIRE antiserum present in the BL20 p13 sepharose eluate (Lane 2) which probably represent bovine CDK2 and p34^{cdc2}. There is a concentration of bovine CDK seen in the BL20 eluate compared to the flow-through (Lanes 2 & 3). There is a fainter reactive polypeptide of 32kDa in piroplasm p13 sepharose eluate (Lane 5) showing again a PSTAIRE reactive protein binding to p13 from piroplasm extracts. The signal intensity of the 32kDa reactive protein is similar between the eluate and flow-through, despite the flow-through lane being higher in total protein. This indicates that the 32kDa protein is being concentrated to some extent by the p13 beads. Because the supernatant and flow-through lanes are so disproportionately loaded in both cases, it is not possible to assess the efficiency of depletion of CRKs from the supernatant by the p13 beads. Blotting a Sypro stained gel seems to reduce the signal strength from the immunoblot and so, the experiment was repeated using the same protein extracts for probing with the anti-ThaCRK2 antiserum but without staining the gel prior to blotting.

3.1.10 ThaCRK2 may bind p13 with a low affinity.

The immunoblotting was repeated using piroplasm and bovine supernatants prepared in section 3.1.9 to detect binding of parasite ThaCRK2 to p13 sepharose (figure 3.10).

Panel A shows the immunoblot profile with the anti PSTAIRE antiserum. There are two distinct bovine proteins of molecular weights 33 & 34 kDa, running as a doublet which are specifically binding to p13 and reacting with the anti-PSTAIRE antiserum - these are likely to be $p34^{cdc2}$ and CDK2 (Lane 3) (These are as seen in figure 3.9 Panel B lane 2). A parasite protein specifically concentrated by p13 binding also reacts with this antibody (Lane 1). The piroplasm supernatant also has PSTAIRE reactive polypeptides which look to be running as a doublet (Lane 2). There are other higher molecular weight polypeptides recognised by this serum which cross-react with the polyclonal anti-PSTAIRE serum. This blot was then stripped and re-probed with the anti-ThaCRK2 antiserum and the results are shown in Panel B. The lane order is as above. Again there is no cross reactivity with bovine protein (Lane 3). The antiserum shows strong reactivity with the 34kDa ThaCRK2 in the piroplasm supernatant track (Lane 2) but only faint reactivity visible after p13 binding and elution (Lane 1). This shows there may be a very weak interaction between ThaCRK2 and p13 and confirms the preliminary results shown in figure 3.8. Comparing the relative reactivities between lanes 1 & 2 using either the anti-PSTAIRE antibody (Panel A) or the anti-ThaCRK2 antibody (Panel B) suggests that there are, at least, two polypeptides in piroplasms with a PSTAIRE like motif. The difference in reactivities between lanes 1 & 2 with the anti-PSTAIRE antibody (Panel A) is less than the difference between the weak reactivity with anti-ThaCRK2 in lane 1 and in lane 2 (Panel B).Though it is difficult to be quantitative, anti-ThaCRK2 reactivity appears to be ~10 fold less than the supernatant (Panel B, lane 2). This suggested that there may be more than one anti-PSTAIRE reactive protein contributing to the signal with anti-PSTAIRE antibody. The 45kDa protein which was shown by Sypro staining to bind strongly to p13 is not reactive with anti-ThaCRK2 but may be slightly reactive with anti-PSTAIRE (Panel A, lane 1, arrowed).

Since there may be two parasite proteins capable of binding to p13, it was decided to immunoprecipitate the ThaCRK2 protein from piroplasm extracts to produce a depleted supernatant which was then used for binding assays.

3.1.11 Immunoprecipitation of ThaCRK2 from piroplasm extracts.

The anti-ThaCRK2 antiserum was used to immunodeplete piroplasm extracts of the CRK2 protein which had been shown to bind p13, albeit very weakly. Figure 3.11 shows the immunoprecipitation of the extract.

Lane 1 shows the reactivity of supernatant with the antibody prior to immunodepletion. There is no binding of ThaCRK2 to the Protein A sepharose (lane 2) as all reactivity remains in the supernatant from the control incubation of supernatant with Protein A sepharose only (lane 3). Lane 4 shows the supernatant from the immunoprecipitation reaction which has been nearly totally depleted of ThaCRK2. There is specific immunoprecipitation of ThaCRK2 by the anti-ThaCRK2 antisera (Lane 5). The immunodepleted supernatant (Lane 4) was then bound to p13 as previously described.

3.1.12 Immunodepletion removes ThaCRK2 from extracts but kinase activity remains

Immunodepleted and non-depleted extracts were then incubated with p13^{suc1} and p12^{cks1}, the recombinant polypeptide product of *L. mexicana* homologue of the *suc1* gene (a gift of Dr. K. Grant, Mottram & Grant, 1996). It was postulated that the *Theileria* CRKs may have a higher specific affinity for p12^{cks1} since it is from another protozoan. Specifically bound proteins were eluted from the beads and assayed by Western blotting. Figure 3.12 (Panel A) shows the resulting immunoblot probed with the anti-ThaCRK2 sera. Comparison of the flow-throughs from p12 and p13 binding to immunodepleted (lanes 5&7) and nondepleted extracts (lanes 6&8) showed a significant reduction in the levels of ThaCRK2 by the antibody. From this, it is possible to conclude that the immunoprecipitation has removed most of the ThaCRK2 from the extract. However, in the case of the depleted extract flow through after binding to p12-sepharose (Lane 5), there is a larger amount of ThaCRK2 present than in corresponding flow-through from p13. Any remaining ThaCRK2 in the depleted extracts has not bound either p13 or p12 to any detectable extent (Lanes 3 & 4). With non-depleted extract

eluates, there is possibly better binding of ThaCRK2 to p13 than to p12 though the difference in antibody reactivity is very small (Lanes 1 & 2).

This blot was then stripped and reprobed with a monoclonal antibody (5E1) raised against a predominant 30kDa protein present on both the merozoite surface and the piroplasm which showed that the difference in reactivity between non-depleted and depleted tracks (Lanes 8 & 7 and Lanes 6 & 5) was not simply due to protein loading. This is shown in Panel B. This also shows that the washing conditions are sufficiently rigorous to remove all traces of the 30kDa protein in the eluates. Since the reactive band is of equal intensity in lanes 5-8, it is possible to say that the decrease in reactivity of the anti-ThaCRK2 sera (Panel A) in the immunodepleted extracts is specific and that all samples had similar amounts of total piroplasm protein. The next step was to determine if the immunodepleted extracts still contained protein(s) capable of binding p13 and p12 sepharose which had kinase activity.

3.1.13 Immunodepleted piroplasm extract retains kinase activity.

The immunodepleted extracts were bound to p13 and p12 sepharose and assayed for kinase activity as described in section 3.1.6. The same three substrates were used to determine if there were any differences in substrate specificity between the depleted and non-depleted extracts after binding to p12 and p13 (figure 3.13).

Using ThaCRK2 depleted extracts, in the absence of added substrate there is a phosphorylated polypeptide of 45kDa (Panel A, lanes 1 & 5). With non depleted extract, there are 3 distinct phosphorylated proteins of 60, 45 and 35kDa (Panel B, lanes 1 & 5,) which undergo a heavier phosphorylation in the presence of p13 sepharose again indicating that an active ThaCRK2 may bind to p13 sepharose. Casein is heavily phosphorylated by the immunodepleted extracts bound to p13 (Panel A, Lane 2) but to a lesser extent by the p12 bound kinase (Panel A, Lane 6). Histone is equally phosphorylated by p13 and p12 bound kinase but less well phosphorylated with immunodepleted extract (Panel A, Lanes 3 & 7) when compared to the phosphorylation of histone by non-depleted extract (Panel B, Lanes 3 & 7). This may suggest the histone is a better substrate for the ThaCRK2 kinase. This could not be concluded from figure

3.6. Again, as seen in a previous assay (figure 3.6), there is poor phosphorylation of myosin light chains with both p13 and p12 bound kinases when added as an exogenous substrate. The absence of any decrease in casein phosphorylation by p13 bound protein from depleted extracts suggests the presence of another kinase with affinity for p13 and substrate specificity directed towards casein. It seems that p13 has a higher affinity than p12 for the unidentified parasite CRK polypeptide(s) as while similarly, there is no difference in the level of casein phosphorylation by p12 bound protein between immunodepleted and non-depleted extracts, it is much less than with p13. It could be that the unknown kinase does not phosphorylate histone at all as there was residual ThaCRK2 left in the extract after immunodepletion. Though this did not bind detectably bind to p13 or p12 (figure 3.12) there could be sufficient binding to account for the small amount of histone phosphorylation by the depleted extracts. There is definitely binding of ThaCRK2 since immunodepletion shows it clearly contributes to the phosphorylation of histone and no substrate phosphorylation profile. It is possible that the ThaCRK2 polypeptide can undergo auto-phosphorylation in the absence of exogenous substrate (Panel B, lane 1) or be phosphorylated by the other kinases bound to p13 as band Z corresponds to the size of ThaCRK2. The latter may be more likely as the non-depleted extracts bound to p12 show only very weak phosphorylation of Z. The 35kDa labelled polypeptide (Z) is removed upon immunodepletion of the extracts suggesting it is either phosphorylated by ThaCRK2 or is ThaCRK2 (Panel A, lane 1). A summary of the binding affinities and phosphorylation patterns is given in Table 3.1. Though it is not possible to be completely quantitative with this type of experiment, there appears to be a slightly higher level of casein phosphorylation in the immunodepleted p13 bound sample. This may reflect a degree of competition for the p13 binding sites by unidentified kinase and ThaCRK2. Thus when the majority of ThaCRK2 is removed, the p13 sepharose can bind more of the other kinase(s) hence a higher phosphorylation of casein. Also, the fact that the endogenous kinase activity in the absence of substrate is higher in non-depleted p13 bound protein suggests ThaCRK2 itself may have higher affinity for p13 than p12.

To determine if another PSTAIRE reactive protein was present in the ThaCRK2 immunodepleted extracts another set of immunoblots were undertaken using these supernatants and post-binding flow-through samples. These are shown in figure 3.14. Panel A shows the blot probed with the anti-ThaCRK2 antibody. Only the non-depleted

extracts react (lanes 1, 3 & 5). Panel B shows an identical blot probed with the polyclonal anti-PSTAIRE antiserum. In this case, there is reactivity in the ThaCRK2 depleted samples (lanes 2, 4 & 6). This indicates that although the immunodepletion has removed the majority of the ThaCRK2 reactivity, there remains another PSTAIRE reactive protein in these depleted extracts. A further binding experiment would need to be done with this depleted extract to prove that this PSTAIRE reactive protein was capable of binding p13 although the data from the kinase assays on the immunodepleted material suggests that it is capable of binding.

It is probable that ThaCRK2 would exhibit a higher affinity for the *Theileria* p13^{suc1} homologue. In order to clone and sequence the *Theileria suc1* homologue, primers were designed using conserved regions of *suc1* homologues from a range of species and PCR amplification undertaken.

3.1.14   PCR for *suc1* homologue in *Theileria annulata*

The oligonucleotide primers chosen were those used to clone the *L. mexicana suc1* homologue -(a gift of Dr. J. Mottram): The location of the primers within the gene sequence is shown in figure 3.1 (shaded region). The primers had the following sequences:

5'primer - AGAG<u>CTCGAG</u>TAYMGNCAYGTNATGYTNCC
3'primer - GAG<u>GAATTC</u>AANARNARDATRTGNGGYTCNGG

The 5'primer corresponds to a perfectly conserved amino acid sequence EYRHVMLP and the 3'primer encodes PEPHILLF as seen in figure 3.1. (N=G+A+T+C, Y=T+C, M=A+C, R=A+G and D=G+T+A , *XhoI* and *EcoR1* restriction sites are underlined). The 5' primer was 1000 fold degenerate and the 3' primer was 12000 fold degenerate. This is considerably smaller than the degeneracies of similar primers used to clone *CksHs1* from human cDNA (Richardson *et al.*, 1990).

Figure 3.15 shows results of a PCR reaction using parameters cited in Mottram and Grant (1996) for the cloning of the *L.mexicana* homologue. A variety of different annealing conditions and PCR reagent concentrations were tried to amplify a homologue

from *Theileria*. These are given in Table 3.2 together with PCR reagent conditions used to clone the human and *Leishmania* homologues. Lane 3 shows the positive control used which was the pQE plasmid containing the full length *suc1* gene as template, this gives a predominant band of ~200 bps, the predicted size of the yeast PCR product. Two bands of 230 and 180bps were amongst a series obtained with *Theileria* genomic DNA These two fragments which were in the predicted size range were excised from the gel, purified and cloned into the pCR vector (Invitrogen) and sequenced using T7 and SP6 primers. The 180bp fragment was found to have high homology to a well conserved region of the large subunit of ribonucleotide reductase (chapter 4). The 230bp fragment had no significant homology to any protein sequences in the databases in any of the six reading frames. The lack of other regions well conserved between different *suc1* homologues makes the design of other primers for PCR difficult (shown in Figure 3.1) and the failure of PCR to amplify a *Theileria* homologue suggests that it may be sufficiently different in these regions to prevent amplification. Now that more *Theileria* genes have been sequenced, a statistical analysis of codon bias could be carried out which could allow codon bias for *Theileria* to be incorporated into the primers.

However this approach would not work if the *Theileria* homologue is not conserved in amino acid sequence in these regions and other means of isolating the *Theileria* homologue would be to screen a *Theileria* expression library with antiserum raised against p13^{suc1} . However, this was not considered a viable option as a Western blot of host and parasite extracts reacted with antiserum generated against recombinant yeast p13 did not detect any polypeptide of the expected molecular weight range either in bovine or parasite extracts as shown in figure 3.16. The p13 protein is detectable in *S. pombe* extracts used as a positive control (lanes 7 & 8). This result suggests that most of the immunogenic epitopes are not conserved across species. Interestingly though this serum does cross-react with a macroschizont specific polypeptide of 28kDa and a piroplasm specific polypeptide of 45kDa, but it is highly unlikely that these polypeptides represent the *suc1* homologue. It would be of interest to determine if the reactive polypeptides seen in the piroplasm extracts could be blocked by pre-incubating the serum with p13. Another approach would be to undertake a low stringency heterologous library screen with a *L. mexicana* or *S. pombe* probe. The failure of the PCR approach and the difficulties associated with a library screen led to abandoning the cloning of the *suc1*

homologue in *Theileria* and to concentrate on the large subunit of ribonucleotide reductase since it is an essential enzyme in the DNA replication machinery and by its nature closely linked to the cell cycle.

3.2   Discussion and Conclusions

The work presented in this chapter focuses on the existence of at least two p13^{suc1} binding proteins with kinase activity that are present in piroplasm stage extracts of *Theileria annulata*. Prior immunodepletion of the ThaCRK2 from piroplasm extracts gave a reduction in histone phosphorylation significantly using p13 and slightly less with p12 bound proteins. This indicates that one of the proteins capable of binding p13^{suc1} is ThaCRK2. This gene was isolated using a monoclonal anti PSTAIRE antibody (Kinnaird *et al.,* 1996). The reactivity profile of this anti-serum on Western blots shows a predominant polypeptide of 34 kDa in piroplasm extracts and at least two polypeptides in infected lymphocytes, probably representing the bovine p34^{cdc2} and p32^{cdk2} homologues (Kinnaird *et al.,* 1996). Both the bovine p34^{cdc} and p32^{cdk2} are capable of binding to p13 (Figure 3.9 Panel B) and both presumably bind as part of an active kinase complex although it is not possible to discriminate between their relative activities in any of the assays undertaken. This binding shows that the p13 beads functioned as a specific affinity tag for cdc2-related kinases in the experiments performed in this chapter. The anti-ThaCRK2 reactivity of the p13 eluated material is very weak whilst the anti-PSTAIRE reactivity is considerably stronger. As prior depletion of ThaCRK2 suggests the presence of more than one p13 binding kinase it is likely that one other bound kinase, at least, also has anti-PSTAIRE reactivity (figure 3.14). However because different anti-sera have different titres and the anti-ThaCRK2 reactivity is consistently weaker than anti-PSTAIRE polyclonal antiserum it is not possible to conclusively identify another kinase with anti-PSTAIRE reactivity binding and eluting from p13 beads (figure 3.10). However work by Kinnaird *et al.,* (1996) who undertook immunoscreening of a cDNA expression library with an anti-PSTAIRE monoclonal antibody, led to the identification of a large number of reactive cDNA clones from the late stages of differentiation to extracellular merozoites, all of which were ThaCRK2. If the second kinase was expressed at much lower levels than ThaCRK2 at this stage then library screening may not readily isolate this gene. Additionally, as the anti-PSTAIRE monoclonal can react with other kinases which have a degree of divergence in the PSTAIRE region (Meyerson *et al.,* 1992, Mottram & Smith 1995) such as PCTAIRE etc., it suggests that other kinases in *Theileria* could be divergent in the PSTAIRE motif. Also

immunoprecipitation from piroplasm extracts with anti-ThaCRK2 antibody removed the vast majority of polypeptide reactive with the anti-PSTAIRE monoclonal antibody (Kinnaird *et al.,* 1996). There are two alternative interpretations for this result: firstly, incomplete clearance of ThaCRK2 from the extract and secondly, the presence of another protein of exactly the same molecular weight that is weakly reactive with the anti-PSTAIRE monoclonal sera. The evidence presented here for the existence of another PSTAIRE reactive protein is based upon use of a polyclonal antibody but it is difficult to know why the corresponding gene was not isolated during the library screen with the monoclonal antibody. One difference is that the library was made from D7 differentiating cells and the experiments here used piroplasm extracts so it is possible that there could be differential expression of the kinases in different life cycle stages. Although both the PSTAIRE antibodies were raised against the same peptide, it is possible that they recognise different epitopes. Unfortunately, our stock of monoclonal anti-PSTAIRE is finished so it is not possible to repeat the experiment presented in figure 3.14 for comparison with this serum.

Another cdc2-related kinase (ThaCRK3) has recently been cloned from *T. annulata* (Kinnaird, Logan & Langsley, unpublished). This gene has the sequence HFTTLRE in the region corresponding to PSTAIRE, suggesting that it will bind a very different class of cyclin partner. Similarly to the expression of ThaCRK2, the gene is expressed in all intracellular bovine stages of the parasite. As a species specific antiserum is currently being generated it will be interesting to determine the affinity of ThaCRK3 for p13. However, based on the current literature regarding regions involved in p13 interaction, it is possible to make a prediction. The binding affinity for ThaCRK2 seems to be very low or highly unstable as judged by the low reactivity of the specific anti-sera against piroplasm stage p13 bound eluates compared to that of p13 eluates from BL20 extracts but the slight increase in p13 bound casein kinase activity in ThaCRK2 depleted extracts suggests ThaCRK2 does compete, to some extent, with the unknown kinase for p13 binding (section 3.10/3.11). There may be a number of reasons for weak binding - the first would be that the interaction between ThaCRK2 and p13 is unstable and easily removed by the washing procedure, designed to reduce non-specific binding. Alternatively, only a small amount of ThaCRK2 could be available for binding to p13. This could be due to a competitive effect between the yeast p13 and the *Theileria* p13^{sucl}

homologue in the piroplasm extracts. The association of ThaCRK2, if already bound to the *Theileria* p13 homologue would not be easily disrupted by the presence of exogenous p13, especially if this has a lower specific affinity for parasite CRK relative to the parasite p13^{suc1} homologue. The consequence of this scenario is that most, if not all of the parasite CRK would be present in the flow-through fractions of the binding assays, being unavailable for binding to p13-sepharose. This could be easily determined if the parasite p13^{suc1} homologue had been isolated and could be used as an affinity tag. Binding affinities can be partly predicted by examining differences in the primary structure of ThaCRK2 and cdc2. As mentioned before, the binding affinity between p13 and ThaCRK3 is unknown and cannot be assessed due to the specific antiserum not being yet available. However, its structure is considered here in parallel with ThaCRK2 for its likely binding affinity for p13. A number of papers have studied the interactions between the cdc2 protein and its partners using an analysis of mutant phenotypes. Ducommun *et al.* (1991) used an alanine scanning mutagenesis method to look at the interaction between yeast p13^{suc1} and human cdc2, although use of the human *suc1* homologue p9^{Chsks1} gave similar results. This paper showed that there are several clusters of mutations on the p34^{cdc2} protein, including sites directly involved in catalytic activity that determine p13^{suc1} binding.

Figure 3.17 shows a pileup of ThaCRK2/3 with human and *S. pombe* p34^{cdc2}. Regions known to be involved in the p13 binding are highlighted in bold. These were present in both small and large lobes of cdc2. Marcote *et al,* (1993) defined these clusters more precisely by looking at the effects of single substitutions within some of these clusters. The rationale behind this is that gross changes involving several amino acids may have multiple effects and indeed he says that in general, single replacements tended to have less severe effects on binding. Specifically:

a) Within the cluster K^{21}GRHK^{25} (II), replacement of H^{24} by Ala had the largest effect on p13 binding in the assay (50% of wildtype). This residue is not conserved in ThaCRK2 (N) or in ThaCRK3 (D). The acidic residue in ThaCRK3 will considerably change the structure but being charged could still undergo bond formation albeit with a different residue. Neither are conservative substitutions and it is not possible to predict the effects on binding but although these might not be as severe as replacement with Ala. However the importance of this region is emphasised by analysis of charged → Ala clusters on

either side, E^2 - E^{12} and K^{33} - E^{42} both of which had virtually no effect on binding in the *in vitro* assay.

b). In the cluster $K^{56}ELRH^{60}$ (**IV**) replacement of H^{60} had the largest effect on binding of p13 (reduced to 20%). This residue is conserved in both *Theileria* kinases.

c). In the cluster R^{180} - D^{186} (**VIII**), which is not generally well conserved in *Theileria*, two specific replacements were analysed, R^{180} and D^{186}. $R^{180} \rightarrow$ Ala had almost no effect on binding but $D^{186} \rightarrow$ Ala reduced binding to 20% of wildtype levels. This residue is conserved in *Theileria* and is conserved in the cAMP dependent protein kinase in which, as shown from the crystal structure (Knighton *et al.*, 1993) it forms a bond with the backbone of the catalytic region. Similarly the residue E^{173} in the cluster R^{170} - E^{173} is predicted to form an internal ionic bond with R^{275} in the cluster D^{271} -R^{275} (**XIII**). Mutation of any of these three residues is likely to disrupt the conformation of the large lobe and thus indirectly affect p13 binding. As these residues are conserved in ThaCRK2 and ThaCRK3 it suggests that the conformation may not be that different and that binding affinity to yeast p13 may depend on direct interaction with specific residues. However effects of other differences on conformation cannot be ruled out.

d). In the cluster R^{215} - R^{218} (**XI**) replacement of R^{215} by Ala had a major effect on p13 binding. This residue is predicted to have a surface location in the large lobe and directly interact with p13. This region is quite well conserved in both ThaCRK2 and 3 and is therefore unlikely to affect binding to p13.

e). Certain residues in p34^{cdc2} have been predicted to be involved in binding of p13^{suc1} by Endicott (1994) from a structural model which was based on analysis of yeast mutant phenotypes combined with the X-ray crystal structure of the cAMP dependent protein kinase (Knighton, ibid). These p34^{cdc2} mutants can be rescued by over-expression of p13^{suc1}. The homologous wildtype residues in all 6 mutant alleles are conserved in ThaCRK2 and 3 (Figure 3.17 indicated by ▲). However, other residues as yet unidentified are probably also important in either direct binding of p13 or indirectly through tertiary structure.

f). A region represented by a deletion of 20 amino acids, S^{233} - H^{253} (**XII**), was characterised by Ducommun (1993) as abolishing 90% of the binding of human cdc2 to yeast p13. However, Alanine scanning mutagenesis of the small cluster K^{243} -K^{245} within this region had no effect on binding, suggesting that some of the other residues within the deletion are more important but it is equally possible that such a large deletion could have a disruptive effect on the conformation of the protein. This region has not been extensively analysed although in the crystal structure of the inactive form of human CDK2 some of the residues are predicted to have a surface location (de Bondt *et al.*, 1993) and therefore is likely to be a site of interaction with another protein. The region of this deletion is part of a 25 amino acid insertion that is not present in the cAMP dependent protein kinase but is typical of cdc2-related kinases. Because of this it was not been modelled in the 3-dimensional structure proposed by Marcote. While deletion of 20 amino acids suggests that it may be a point of p13 binding, a yeast mutant with a three amino acid deletion (L^{240}-D^{242} in *S.pombe*) contained within this insertion, had a dominant lethal phenotype when over-expressed causing cells prematurely enter mitosis without completing S phase. This led to the proposal that while the activity of the kinase was unaffected, it was likely that the mutant failed to interact with a negative regulator of mitosis , perhaps a CDK inhibitor (Labib *et al.*, 1995, Endicott *et al.*, 1994). This region is quite divergent in ThaCRK2 (19%, identical, 28% similar) and slightly less so in ThaCRK3 (29% identical, 35% similar), whereas *S. pombe* p34^{cdc2} and human cdc2 are over 50% identical, 57% similar. Given the possible importance of this area in p13 binding either through its effect on the conformation of the large lobe or direct interaction with p13, it seems possible that the degree of divergence in the *Theileria* CRK's may affect their affinities for yeast p13. In summary, on the basis of available information, this latter region and the cluster K^{20} -K^{24} containing the important H^{23} residue contain the differences most likely to influence p13 binding.

Very recently, the X ray crystal structure of human CDK2 complexed with a human p13 homologue, p9^{Ckshs1}, has been published (Bourne *et al.*, 1996). This has shed considerable light on the interaction of the two proteins and points to a possible role for p13 like molecules. The strong conservation amongst eukaryotes of key residues defined by the structure of the CDK2/ Ckshs1 complex suggested that the interaction will be very similar for other closely related CDKs and p13 homologues. The results of this

study also pin point certain residues which are not well conserved in the two *Theileria* kinases, again suggesting the affinity for yeast p13 is not optimal. The crystal stucture showed that Ckshs1 binds directly or "interfaces" with two domains in the C terminal lobe of CDK2. It does not appear to interface at all with the N-terminal lobe in which a small region of charged residues was implicated in p13 binding by the mutagenesis approaches of Ducommun (1991) and Marcote (1993) described above. In order to reconcile the apparently conflicting data the authors suggest that certain mutations in the N- terminus may have a conformational effect on the structure of the kinase which indirectly affects sub-unit binding. The domains in the CDK C-terminus extend over the residues G^{206} - L^{220} in human cdc2 (figure 3.17 region X) and residues S^{233} - P^{246} (XIII), part of the 25 amino acid insertion unique to cdc2-related kinase and which forms a loop structure. These regions have already been described as being divergent in ThaCRK2 and ThaCRK3 (here and Kinnnaird *et al.*, 1996). Specifically, within the region covering the 20 amino acid deletion described by Ducommun which is within the interfacing 25 amino acid loop sequence, Bourne *et al.* (1996) identified a conserved aromatic P residue which had been mutated in *S.cerevisae* CDC28 to L. This mutant is defective in p13 binding but still retains kinase activity. This residue is not conserved in either ThaCRK2 or 3 suggesting that this would abolish p13 binding. However the results presented here show that ThaCRK2 at least binds to p13 and thus possibly other substitutions may modify or stabilise the binding to some extent. To confirm cross species conservation several mutants of CksHs1 were created in the CDK2 contact region, all of which were defective in their yeast cdc2 binding affinities compared to the wild type CksHs1.

The side of CksHs1 away from the side that interfaces with CDK2 is also conserved between species and is positioned in the CDK2 catalytic cleft in such a way as to extend the surface area of the cleft. On this basis it is proposed that p13 like proteins function to target CDK's to substrates or kinase regulatory proteins.

Given the failure to PCR the *suc1* homologue of *Theileria* it is possible that the *Theileria* homologue differs quite extensively in the regions used to design primers. Thus other approaches would need to be employed to isolate the *suc1* homologue. It would then be of interest to determine if ThaCRK2 and ThaCRK3 would exhibit a higher binding affinity to the homologue compared to yeast p13 and I would suspect that they

quite probably will. This would perhaps also be the easiest way to determining the identity of the second kinase or kinases whose existence is suggested by the lack of reduction in casein kinase activity in piroplasm extracts immunodepleted of ThaCRK2 prior to p13 binding. One of these may be ThaCRK3 as analysis of protein sequence suggests it may bind p13. This will be confirmed with a specific antiserum. However, a 45kDa protein from piroplasm extracts was shown to bind strongly to p13 sepharose. This did not react with the anti-PSTAIRE antiserum. Rather interestingly, the predicted molecular weight of ThaCRK3 is 46kDa and it does not react with anti-PSTAIRE antiserum (Logan & Kinnaird, unpublished).

Work undertaken with *Paramecium tetraurelia* shows parallels with the findings here. Using an anti-PSTAIRE anti-serum it was shown that there were two polypeptides of 34 and 36kDa which were recognised by this antibody (Tang *et al.,* 1994). Both polypeptides exhibited different binding affinities for p13 sepharose with the 36kDa molecule possessing the higher binding affinity. Neither of these two molecules were recognised by sera against the C-terminal region of the human $p34^{cdc2}$ suggesting that there is divergence in this region. When the putative $p34^{cdc2}$ was cloned by PCR from *P. tetraurelia* it was shown to contain longer N and C-termini than the *S. pombe* polypeptide. Overall the homology between this homologue and other cdc2 proteins is only of the order of 50% at the amino acid level (Tang *et al.,* 1995). This protein was shown to be the 34kDa anti-PSTAIRE antibody reactive protein described in the earlier paper which did not show appreciable p13 binding. There is the possibility this gene from *P. tetraurelia* may not be the cdc2 homologue given that it is no more identical to human *cdc2* than it is to *cdk3* and that human *cdk3* had been shown to bind to p13 very weakly (Meyerson *et al.,* 1992). The authors state that the p13 binding sites as defined by Ducommun (1991) and Marcote (1993) are not conserved in the *P. tetraurelia* polypeptide. It is believed that this protein from *P. tetraurelia* possesses histone H1 kinase activity as a monomer although this may be an *in vitro* effect.(Tang *et al.,* 1994). Similarily work in *L. mexicana* showed the existence of at least two *cdc2* related kinases, *crk1* and *crk3* (Mottram *et al.,* 1993 and unpublished) together with another kinase capable of binding to p13 sepharose but which is distinct from either the *crk1* and *crk3* genes already isolated. Specific anti-serum raised against the crk1 polypeptide showed that this molecule bound weakly to p13 sepharose and although being able to bind the

Leishmania homologue p12 with a higher affinity, it was not responsible for the majority of the histone H1 kinase activity precipitable from the p12 sepharose (Mottram & Grant, 1996).

With respect to the second p13 bound kinase activity in *Theileria* identified by this work, a number of conclusions can be drawn about its identity on the basis of experiments detailed in this chapter. It has a relatively higher specific affinity for yeast p13 than *Leishmania* p12 and is more specific for casein as a substrate than histone. Although these substrates indicate a bias of different kinases, they are common substrates in kinase assays and, in many cases, the exact physiological substrate of the CDK's are unclear. It is probably reactive with a polyclonal anti-PSTAIRE serum (figs 3.10 & 3.14) suggesting that it possesses this conserved domain which, in turn, suggests that it is a member of a conserved cdc2-related kinase family. This result also suggests that it has similar molecular mass to ThaCRK2 and a mass typical for cdc2-related protein kinases. However, it must differ at the C-terminal region from the ThaCRK2 kinase since it does not cross react with the anti-ThaCRK2 sera. Further work would be productive in determining the identity of this kinase. One step would be to screen an expression library with the polyclonal PSTAIRE serum. It may also be feasible to isolate sufficient quantities of the protein by p13 purification and subsequent gel filtration for microsequencing allowing design of oligonucleotides and cloning via PCR amplification, using the PSTAIRE region to design the second oligonucleotide primer. In addition, given the high affinity of p13 for CDKs it may be possible to screen an expression library with recombinant Histidine tagged p13 with the 'p13 binding plaques' being detected by an antibody to the Histidine tag or to p13 assuming that the cDNA can express and fold properly in the bacterial expression system. The presence of phosphorylated proteins identified by SDS-PAGE following kinase assay in the absence of substrate suggests that bound kinases may autophosphorylate but other molecules in the CDK complex such as CKIs can be phosphorylated by the CDK to which they are bound (Morgan *et al.*, 1995).

Work by Tamaru and Okada (1996) showed there to be two major kinases associated with p13 in mature rat brain. These were characterised by an *in situ* SDS-PAGE gel kinase assay showing the sizes of the kinases to be 45 and 100kDa. The smaller kinase was purified to near homogenity and was shown not to cross-react with

anti-PSTAIRE sera. Its preferred substrates are histone H1 and myelin basic protein but there was poor phosphorylation of caseins and neurofilaments. It does not appear to need regulatory subunits for activity as it is active in a monomeric form. p45 is a possible member of the large family of proline-directed kinases. This work raises the possibility that there may be a range of kinases capable of binding to p13 which share little or no features of the CDK's.

In conclusion, there are at least two kinases in *Theileria annulata* which have different binding affinities for p13, possibly based either on differences in tertiary structure of the proteins or in specific residues that interact with p13. One of these is ThaCRK2 which is capable of binding to p13 as a part of an active kinase complex. ThaCRK2 is PSTAIRE reactive and was identified as binding through the use of a specific antiserum. Another anti-PSTAIRE polyclonal reactive kinase can also bind. This kinase may also be capable of undergoing autophosphorylation. A 45kDa polypeptide was identified by Sypro orange staining as binding to p13. This was not significantly anti-PSTAIRE reactive. It is possible that ThaCRK3, which has a predicted mass of 46kDa and does not detectably react with anti-PSTAIRE antiserum on Western blots (Kinnaird *et al.,* unpublished), could bind to p13. Further work should perhaps concentrate on the isolation of the second anti-PSTAIRE reactive kinase as a potential member of the cyclin related kinase family in *Theileria annulata*.

A strong histone specific kinase activity was present in piroplasms which is probably mainly due to the ThaCRK2. However, histone is a substrate commonly used in *in vitro* assays and may not reflect true substrate specificity. As *T. annulata* piroplasms show only limited division (Conrad *et al.,* 1985) and expression of genes known to be associated with DNA replication is low in the population as a whole (Chapter 6) it may be that this kinase activity fulfils a role not associated with nuclear division, such as organisation of the piroplasm for subsequent development in the tick into gametes.

Attempts to isolate the *Theileria suc1* homologue with a view to developing a more specific assay system were unsuccessful suggesting that it may be quite divergent.

Figure 3.1 Alignment of *suc1* homologues

Figure courtesy of Dr. J. Mottram. Key Cks1hs, Cks2hs - human p9 ^{CKS1} and p9 ^{CKS2}, Patsuc - *Patella vulgata* p9^{CKS1}, Cksphy - *Physarum polycelphalum* p9^{CKS1}, LmmCKS1 - *L. mexicana* p12^{CKS1}, Cks1 - *S. cerevisiae* p18^{CKS1} and suc1 - *S. pombe* p13^{suc1}.

Shaded blocks indicate highly conserved regions used for primer design.

```
         1                                                            50
Cks1hs                              MSHKQ IYYSDKYDDE EFEYRHVMLP
Cks2hs                              MA--- -------F-- HY--------
Patsuc                              M-AR- -------F-- D---------
Cksphy                              MPRDT -Q--E--Y-D K------I--
LmmCKS1  MPAKPAQDFF SLDANGQREA LIIIKKLQCK -L-----Y-D M-----I--
Cks1         MYHHYHA FQGRKLTDQE RARVLEFQDS -H--PR-S-D NY-------
suc1            MSKS GVPRLLTASE RERLEPFID- -H--PR-A-D -Y--------


         51                                                           91
Cks1hs   KDIAKLVPKT .........H LMSESEWRNL GVQQSQGWVH YMIHEPEPHI
Cks2hs   RELS-Q---- .........- ----E---R- -----L---- ----------
Patsuc   -----M---N .........- ----A---SI -----H--I- --K-------
Cksphy   P-V--EI--N ........R -L--G---G- ---------- -AL-R-----
LmmCKS1  --L-R---TS .........R ----M---Q- ---------- ----K---V
Cks1     -AML-VI-SD YFNSEVGTLR ILT-D---G- -IT--L--E- -EC-A-----
suc1     -AML-AI-TD YFNPETGTL- ILQ-E---G- -IT--L--EM -EV-V-----


         92
Cks1hs   LLFRRPLPKK PKK                                9 kDa
Cks2hs   ---------D QQ-                                9 kDa
Patsuc   -----KVTGQ                                   9 kDa
Cksphy   -----EV-MP AASLSHNP                          9 kDa
LmmCKS1  ---K--RT                                     12 kDa
Cks1     ---K---NYE AELRAATAAA (Q)16 HQTQSISNDMQVPPQIS 18 kDa
suc1     ---K-EKDYQ M-FSQQRGG                         13 kDa
```

Figure 3.2 Expression and purification of p13.

Recombinant clones containing the *suc1* gene within the pQE60
vector (Qiagen) were induced with 1mM IPTG for 5 hours at 37°C,
harvested and resuspended in sonication buffer (50mM sodium phosphate
buffer pH8.0, 300mM NaCl). The solution was then treated with lysozyme
(1mg/ml) at 37°C for 15 minutes prior to a freeze/ thaw cycle at -80°C
followed by sonication. Cellular debris was cleared by centrifugation at
40000g. The cleared supernatant was applied to a Ni-NTA agarose column
at 0.2ml/min. The column was washed in sonication buffer at a flow rate of
0.5ml/min, then with wash buffer (50mM sodium phosphate buffer pH6.0,
300mM NaCl, 10% glycerol) at the same rate. Bound protein was eluted
from the column using a linear gradient of 0 to 500mM imidazole in wash
buffer. Fractions containing purified p13 protein were pooled and dialysed
against 50mM sodium phosphate buffer pH6.0, 300mM NaCl and
concentrated using a Centricon-10 filter prior to coupling to Aminolink
beads (Pierce) at a concentration of 5mg/ml.

Panel A is a 15% SDS-PAGE gel showing the high speed centrifugation
pellet and supernatant fractions after sonication and application of
supernatant to the Ni-NTA column. Lane 1 is the pellet fraction. Lane 2 is
the supernatant fraction and lane 3 is the supernatant after passing through
the column.
Panel B shows aliquots of fractions eluted from the column analysed by 15%
SDS-PAGE gel.
Panel C shows the pooled protein from fractions 18-28 after dialysis prior to
concentration with the Centricon 10 filter. Tracks 1&2 show purified p13
protein.

A

1   2   3

13kDa

B

Fraction Number

M 2   4   6   8   10 12 14 16 18 20 22 24 26 28 30

Imidazole Concentration (mM)

0   100   200   300   350

97kDa →
66kDa →
45kDa →
29kDa →
14kDa →

C

1   2

13kDa
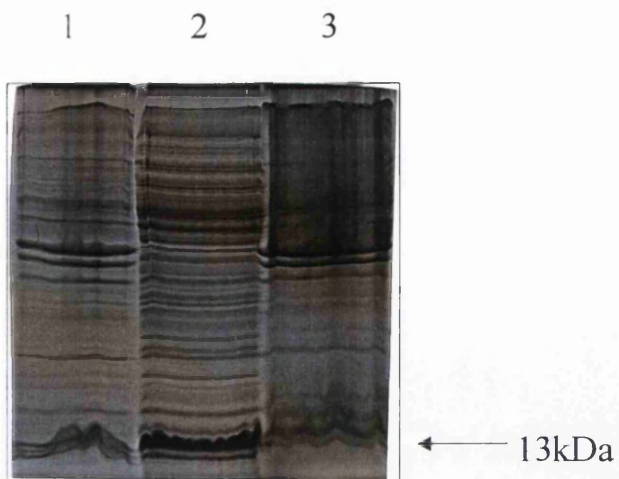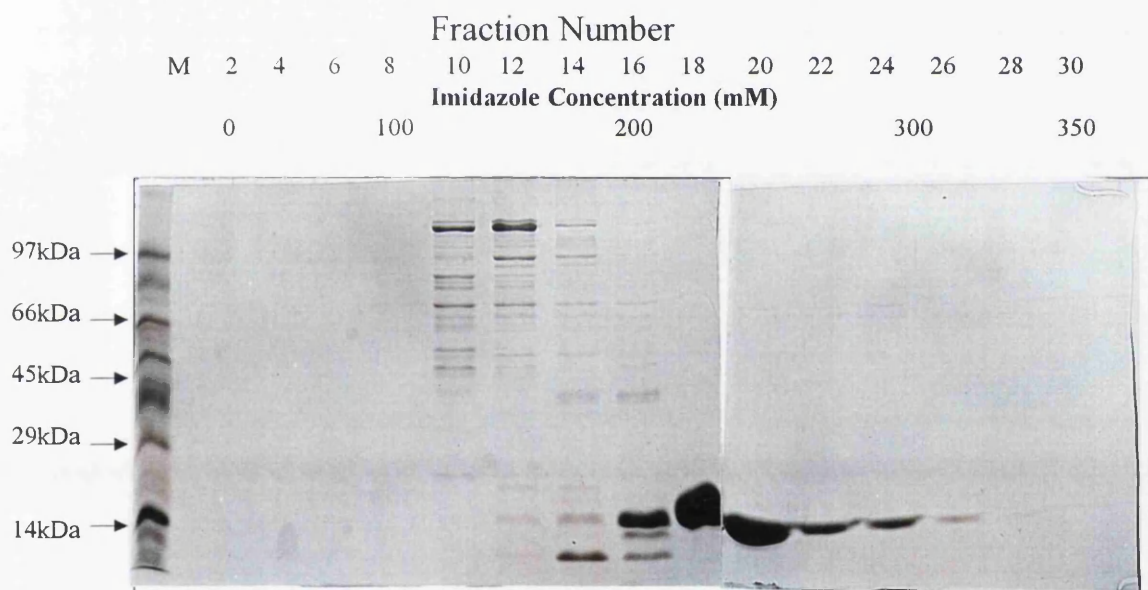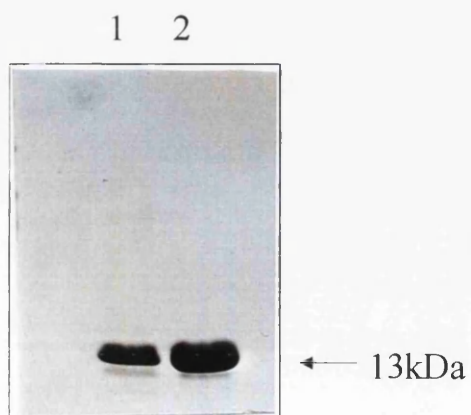
Figure 3.3   Affinity purification of bovine CDK on p13-sepharose.

Cell extracts from BL20 cells were incubated with control and p13 beads and washed as detailed in chapter 2.. The extracts were then separated on a 12.5% acrylamide gel, blotted onto Hybond N membrane and probed with sera as listed below. Signal development was carried out by chemiluminscence using the ECL detection system (Amersham).

Panel A shows a Western blot of extracts and p13 affinity purified protein using an anti-PSTAIRE monoclonal antibody.

Panel B shows a Western blot as in (A) only using an anti human cdc2 C-terminal polyclonal antibody (Gibco). The sizes are as shown on the right of the panels.

Key:

Lane 1   Flow through after p13 binding.

Lane 2   Flow through after Tris binding.

Lane 3   Eluate from p13 sepharose beads.

Lane 4   Eluate from Tris sepharose beads.

A

1   2   3   4

← 34kDa

B

1   2   3   4

← 34kDa
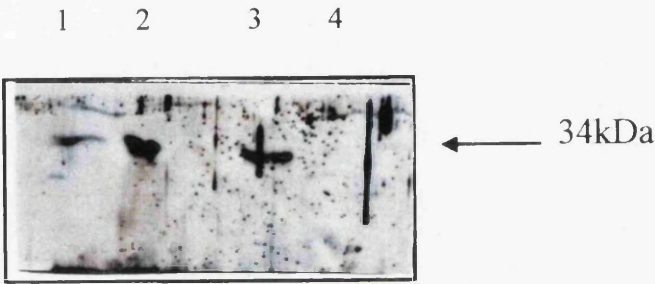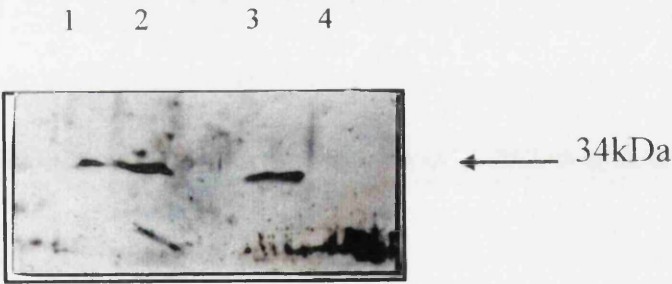
Figure 3.4 Purification of macroschizonts

A differentiating D7 culture (5 days at 41°C) was lysed by nebulisation and centrifuged through a Percoll gradient. The fractions were examined by Giesma staining to assess levels of purity.

Panel A shows the intact cells prior to nebulisation.

Panel B shows the host material after centrifugation.

Panel C shows the parasite material after centrifugation.

Key:

hn   host nucleus

ms   macroschizont

Magnification is X1000 with the scale bar representing 10μm.

A
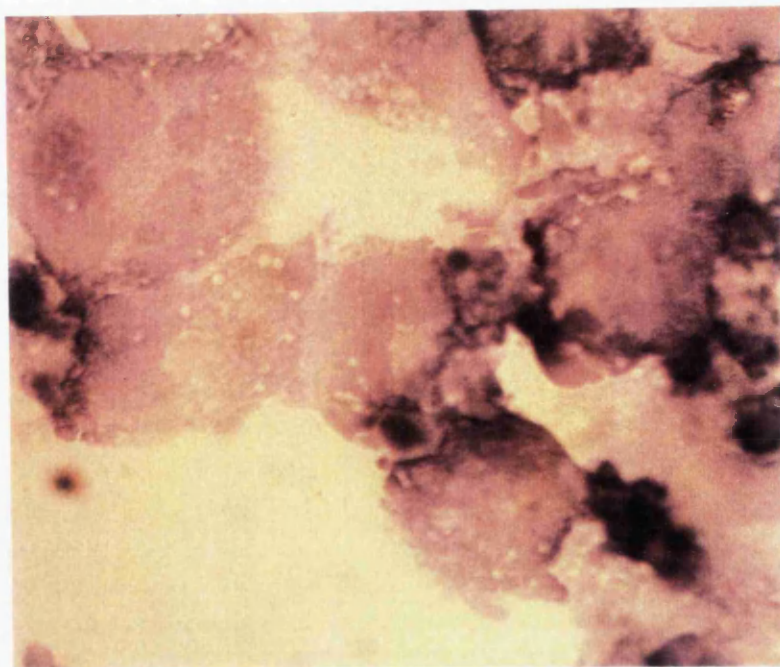
B
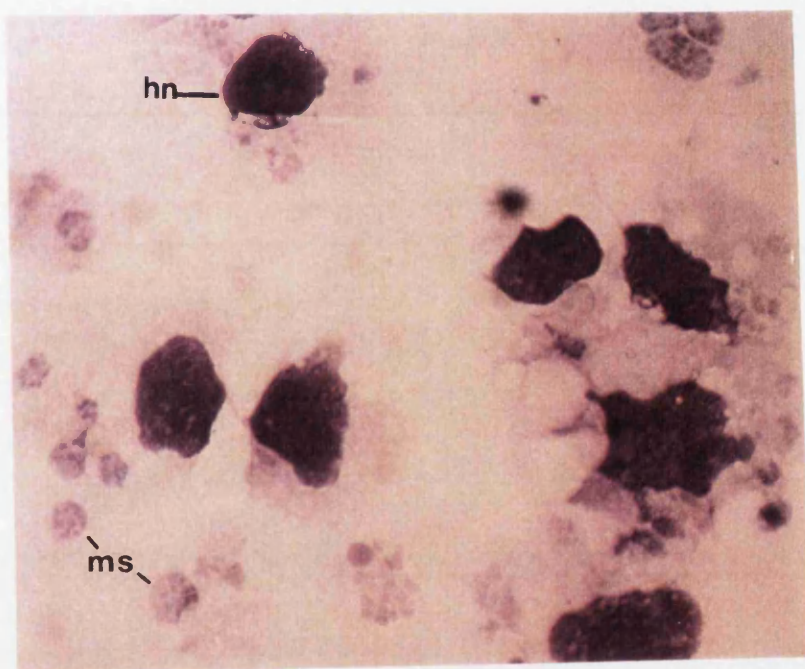
C
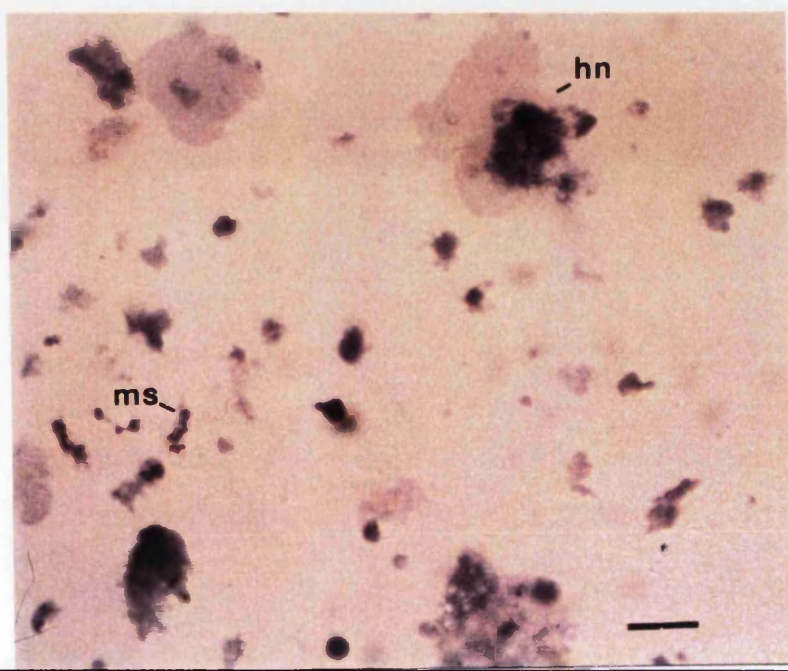
Figure 3.5. Histone H1 kinase assay of p13 sepharose and Tris sepharose bound protein from BL20, purified macroschizont and piroplasm extracts.

Cell extracts from BL20, macroschizonts isolated by nebulisation of D7 cells and piroplasm stage extracts were incubated with control and p13 beads. Kinase activity bound to beads, as assayed by the ability to phosphorylate histone H1, was detected after SDS/PAGE electrophoresis and autoradiography. Macroschizont preparation and purity of preparation is detailed in section 3.1.4.

Key:

Lane 1	BL20 p13 bound protein.
Lane 2	BL20 Tris bound protein.
Lane 3	Macroschizont p13 bound protein.
Lane 4	Macroschizont Tris bound protein.
Lane 5	Piroplasm p13 bound protein.
Lane 6	Piroplasm Tris bound protein.
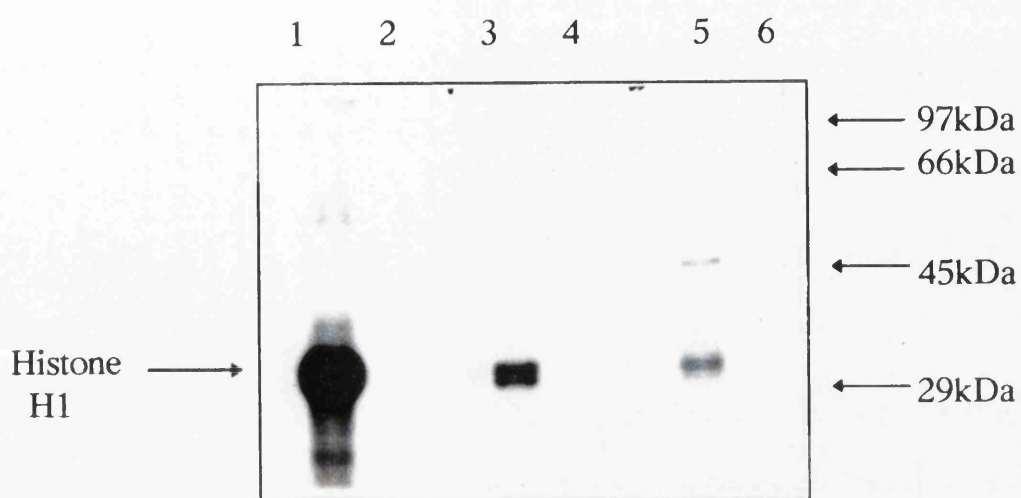
Figure 3.6 Kinase assay with p13 sepharose bound protein from piroplasm extracts using a variety of substrates.

Equivalent volumes of piroplasm p13 bound extracts were assyed for kinase activity in the presence of various substrates. Kinase activity was detected by SDS/PAGE and autoradiography as before.

Key:

Lane 1	No exogenous substrate added.
Lane 2	α casein as the exogenous substrate.
Lane 3	Histone as the exogenous substrate.
Lane 4	Myosin light chains as the exogenous substrates.

Arrows indicate bands X, Y and Z which are referred to in the text.
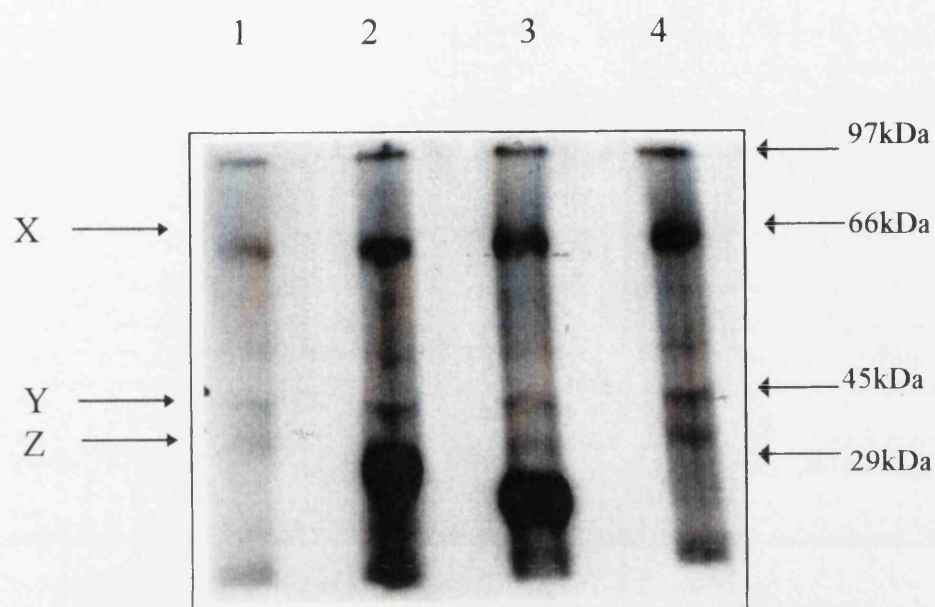
Figure 3.7. Reactivity profile of various cell extracts with anti-sera against vertebrate cdc2, ThaCRK2 C-terminal and PSTAIRE.

BL20, D7 and piroplasm extracts were prepared as detailed in chapter 2, normalised for protein concentration and separated on a 12% SDS/PAGE gel prior to blotting onto Hybond C membrane (Amersham.). Efficient transfer and equal loading was assessed by staining the nitrocellulose filter with 0.3% Ponceau S, in 5% TCA. Antibodies used to probe membranes are as detailed below. Secondary antibodies used for signal development were either anti-mouse or anti-rabbit IgG HRP conjugates. Signal development was carried out using chemiluminescence (ECL, Amersham).

Key:

Lane 1   BL20 extract.

Lane 2   D7 extract (undifferentiated - grown at 37 °C).

Lane 3   D7 extract (Day 6 of differentiation at 41°C).

Lane 4   Piroplasm extract.

Panel A shows a Western Blot probed with a vertebrate specific monoclonal anti-cdc2 antisera.

Panel B shows a Western blot reactivity profile of a polyclonal anti-ThaCRK2 antiserum.

Panel C shows a Western blot reactivity profile of a polyclonal anti PSTAIRE antiserum.

Sizes are as indicated to the right of the panels.
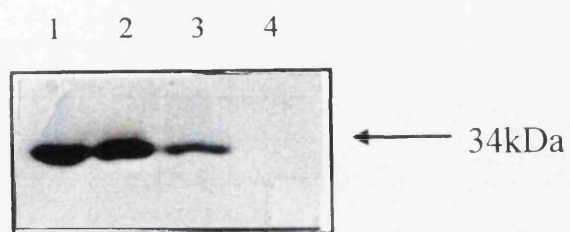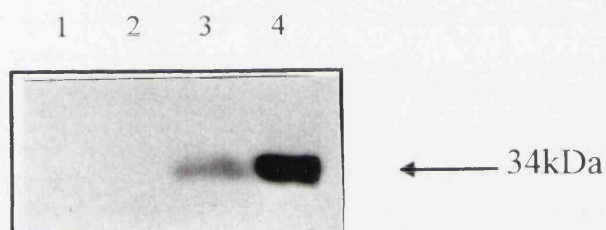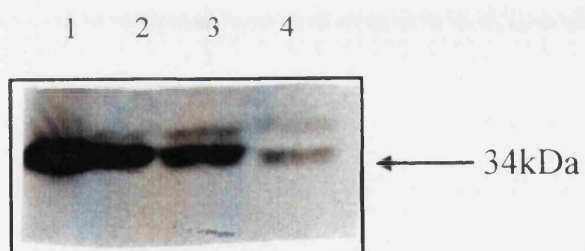
Figure 3.8 Sypro-Orange detection of protein binding to p13 from piroplasm and BL20 extracts.

An equivalent concentration of BL20 and piroplasm extract was added to equal volumes of p13 bead slurry and the eluate from each was separated on a 8% SDS polyacrylamide gel prior to staining with 1% Sypro-Orange stain (Bio-Rad).

Key:

Lane 1   Piroplasm protein bound and eluted from p13 sepharose.

Lane 2   BL20 protein bound and eluted from p13 sepharose.

The size markers are as shown on the right hand side.
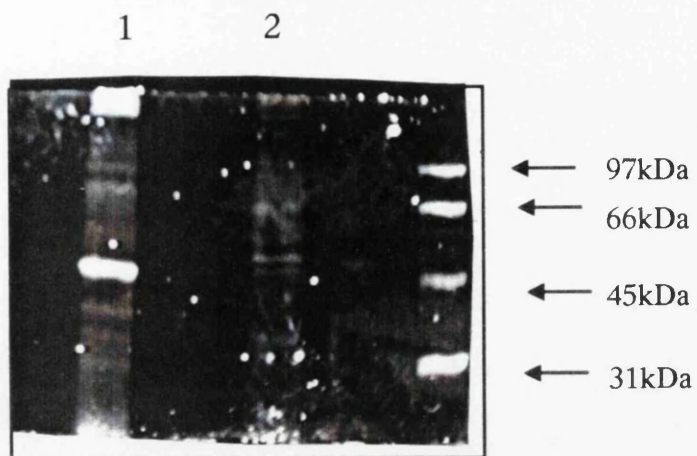
Figure 3.9 Sypro-Orange stained gel of piroplasm and bovine p13 bound proteins subsequently Western blotted and detected by anti-PSTAIRE antisera

Equivalent amounts of BL20 and piroplasm extracts were incubated with equal volumes of p13 bead slurry. The supernatant extract, flow-through and eluate from both BL20 and piroplasms were separated on a 12.5% SDS polyacrylamide gel. The gel was then stained in 1% Sypro-Orange stain (Bio-Rad) prior to immunoblotting. Detection of signal was via the ECL system (Amersham).

Key:

Lane 1   BL20 supernatant.

Lane 2   BL20 eluate after p13 binding.

Lane 3   BL20 flow-through after binding.

Lane 4   Piroplasm supernatant.

Lane 5   Piroplasm eluate after binding.

Lane 6   Piroplasm flow-through after binding.

Panel A shows the gel stained with Sypro-Orange.

Panel B shows the Western blot of the same gel probed with polyclonal anti-PSTAIRE antiserum. Lane order is as in Panel A.

Markers are as indicated by arrows.

A

| | 1 | 2 | 3 | | 4 | 5 | 6 |

97kDa →
66kDa →
45kDa →
31kDa →

B

| 6 | 5 | 4 | | 3 | 2 | 1 |

97kDa →
66kDa →
45kDa →
31kDa →
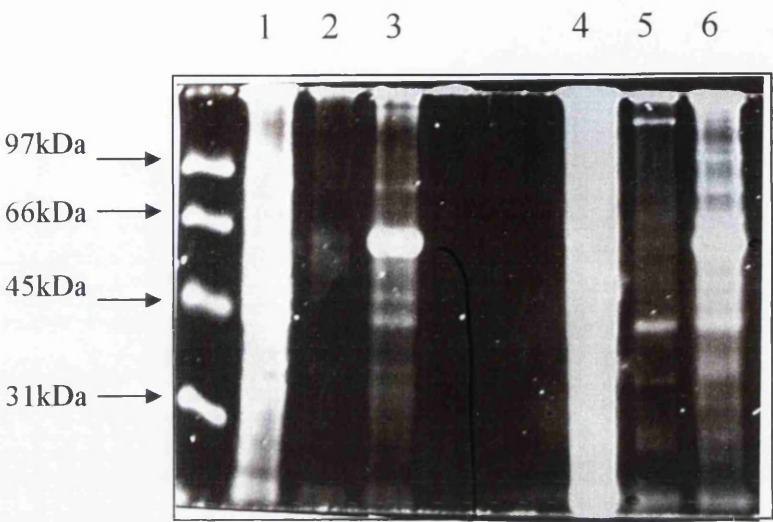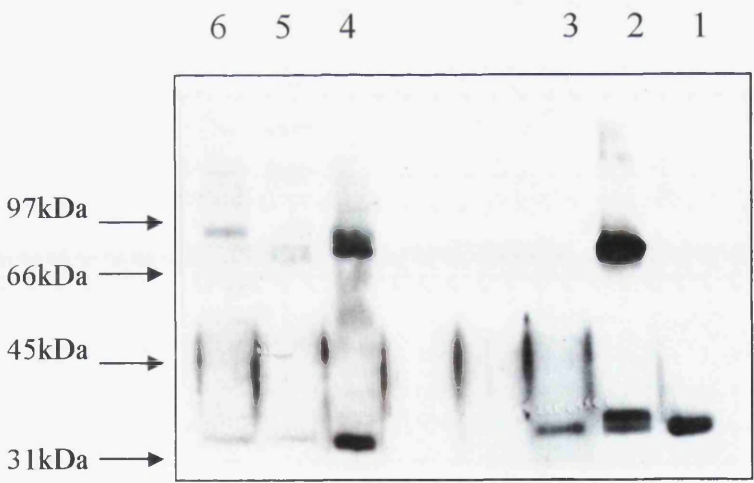
Figure 3.10 Western blot showing antibody reactivity of piroplasm and bovine proteins eluted from p13 sepharose

Equivalent amounts of BL20 and piroplasm extracts were incubated with equal volumes of p13 bead slurry. The extracts were identical to that used in figure 3.9. The supernatant extract and eluate from both BL20 and piroplasms were separated on a 10% SDS polyacrylamide gel and immunoblotted. Efficiency of transfer was verified by staining the nitro-cellulose filter in 0.3% Ponceau S, in 5% TCA. Detection of signal was via the ECL system (Amersham). The filter was stripped according to instructions supplied with the ECL kit and reprobed with the second antibody.

Key:

Lane 1   Piroplasm eluate.

Lane 2   Piroplasm supernatant.

Lane 3   BL20 eluate.

Lane 4   BL20 supernatant.

Panel A show the reaction profile of the polyclonal anti-PSTAIRE antiserum.

Panel B shows the same immunoblot incubated with the anti-ThaCRK2 antiserum.

Markers are as indicated by arrows.
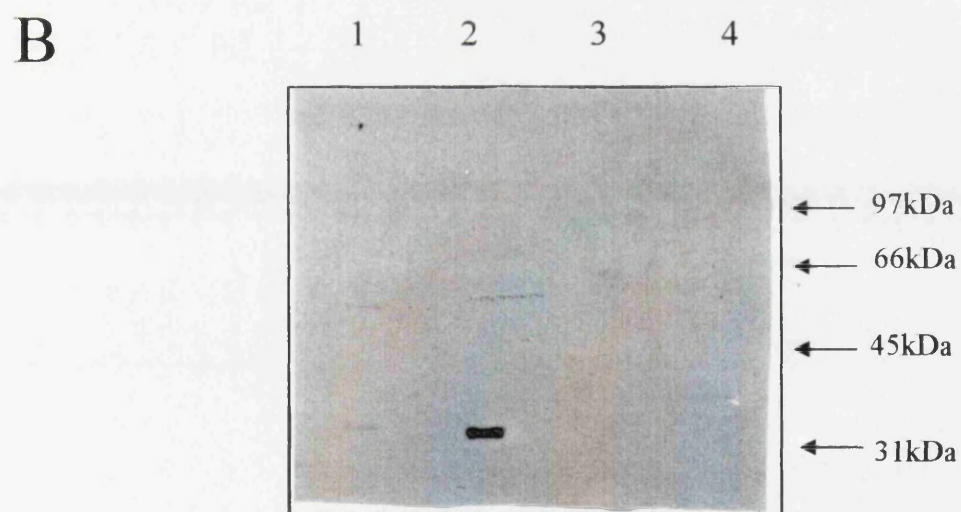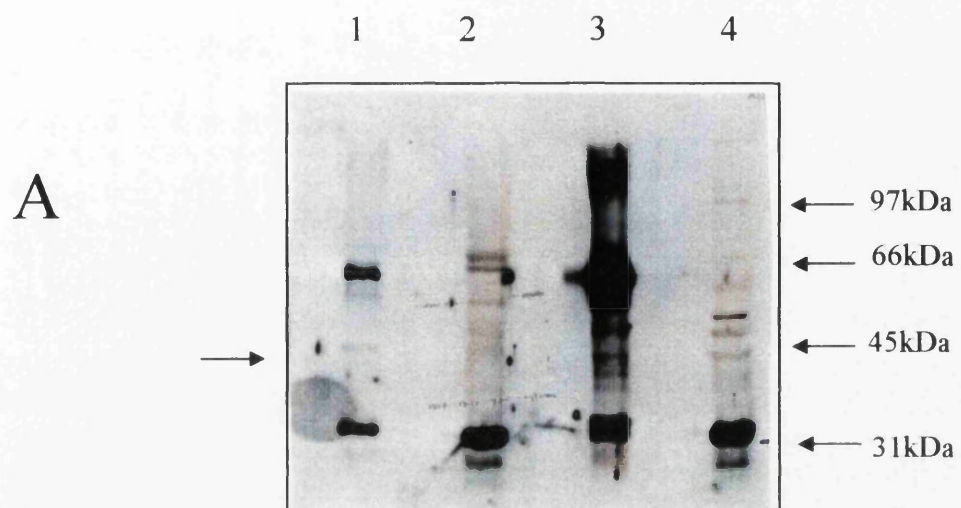
Figure 3.11 Immunoprecipitation of ThaCRK2 by anti ThaCRK2 sera.

10μl of affinity purified anti-ThaCRK2 antisera was incubated with piroplasm extract supernatant for 1 hour at 4°C with rotation. 10μl of a suspension of washed protein A beads (Pierce) were added and incubated for a further 1 hour. The supernatant was then collected by centrifugation and beads washed with 10mM Tris-HCl (pH7.5), 0.1% NP-40 for 20 minutes at 4°C. Elution of bound protein was by addition of an equal volume of 4X SDS/PAGE sample buffer. Samples were run on a 12.5% SDS polyacrylamide gel and immunoblotted after electrophoresis. Antibody used to develop the blot was the same anti-ThaCRK2 C-terminal anti-serum. Signal development was via the ECL Chemiluminescence system (Amersham).

Key:

Lane 1   Piroplasm supernatant after lysis.

Lane 2   Eluate from control binding to protein A sepharose alone (no ThaCRK2 antibody).

Lane 3   Supernatant from protein A control binding.

Lane 4   Supernatant from immunoprecipitation with ThaCRK2 antibody.

Lane 5   Eluate from ThaCRK2 immunoprecipitate from piroplasm extract.

The size of immunoprecipitated ThaCRK2 is indicated by the arrow.
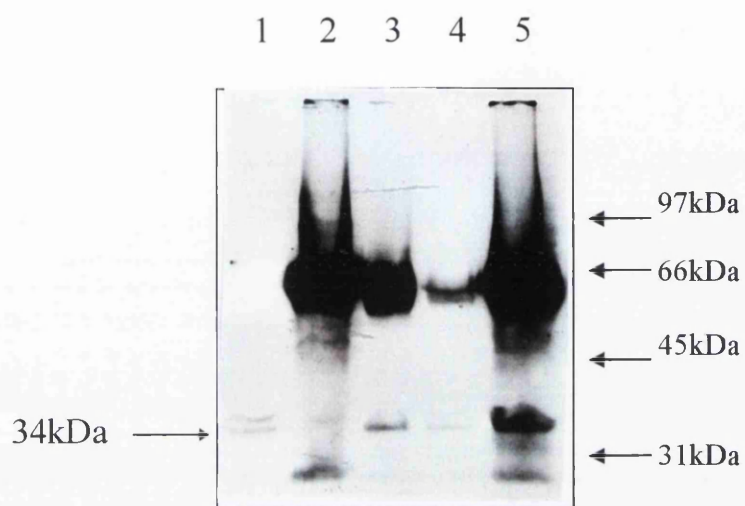
Figure 3.12 p13 binding profile of ThaCRK2 immunodepleted extracts.

Equivalent concentrations of piroplasm depleted and non-depleted extracts were incubated with equal volumes of p13 and p12 bead slurries. An aliquot of the flow-through and eluate from each sample were separated on a 12.5% SDS polyacrylamide gel and immunoblotted. Transfer was assessed by staining the nitrocellulose filter with 0.3% Ponceau S, in 5% TCA. Signal development was by the ECL/chemiluminescence system (Amersham).

Panel A shows the Western blot with immunodepleted and non-depleted piroplasm extract bound to p13 and p12 probed with the anti-ThaCRK2 anti-serum. The blot was then stripped and re-probed with a monoclonal antibody against the 30kDa merozoite antigen (5E1). This blot is shown in Panel B.

Key:

Lane 1	Eluate from p12 sepharose binding to non-immunodepleted extracts
Lane 2	Eluate from p13 sepharose binding to non-immunodepleted extracts
Lane 3	Eluate from p12 sepharose binding to immunodepleted extracts
Lane 4	Eluate from p13 sepharose binding to immunodepleted extracts
Lane 5	Flow through from p12 sepharose binding to immunodepleted extracts
Lane 6	Flow through after p12 sepharose binding to non-depleted extracts
Lane 7	Flow through after p13 sepharose binding to immunodepleted extract
Lane 8	Flow through after p13 sepharose binding to non-depleted extract

A

1 2 3 4 5 6 7 8

← 34kDa

B

8 7 6 5 4 3 2 1

← 30kDa
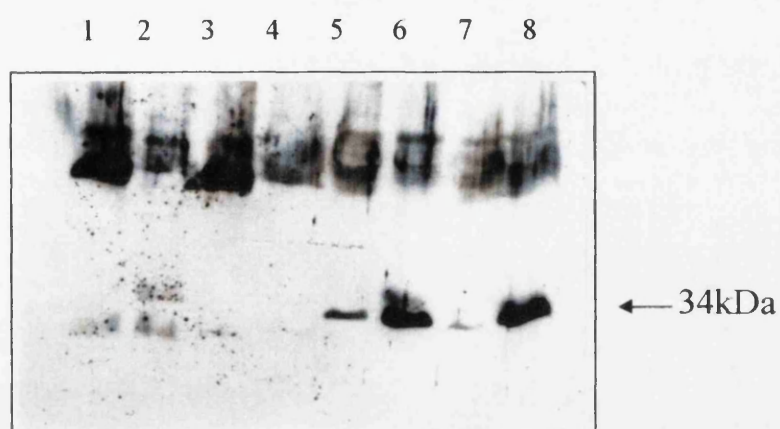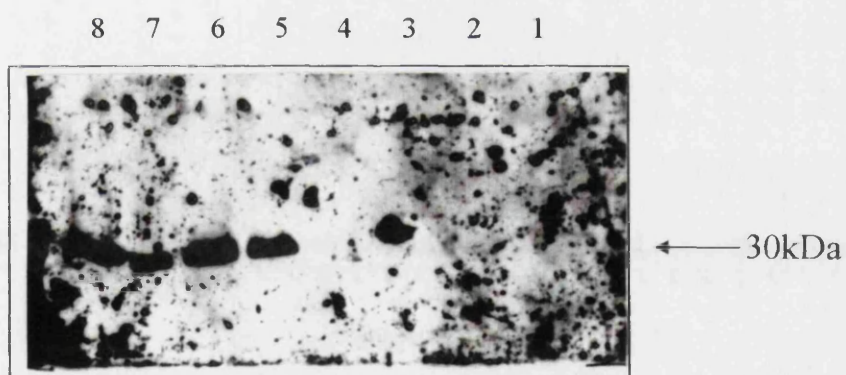
Figure 3.13 Kinase assay with p13 and p12 bound immunodepleted piroplasm extracts with a variety of substrates.

Equivalent volumes of piroplasm p13 and p12 bound extracts were asayed for kinase activity in the presence of various substrates as detailed for figure 3.6. Kinase activity was detected by SDS/PAGE and autoradiography.

Panel A shows kinase assay profiles with the use of immunodepleted extracts as prepared in Figure 3.12.
Panel B shows kinase assay profiles using non-depleted extracts as previously shown in Figure 3.6.

Key:

Lanes 1-4 are with assays with the piroplasm protein bound to p13 sepharose.

Lane 1   No exogenous substrate added to the reaction.

Lane 2   Histone with the exogenous substrate added.

Lane 3   α casein as the exogenous substrate added.

Lane 4   Myosin light chains as the exogenous substrate

Lanes 5-8 are identical to **Lanes 1-4** respectively but with p12 sepharose bound proteins. Lane order is identical for Panels A & B.

Bands X, Y and Z are discussed in the text.
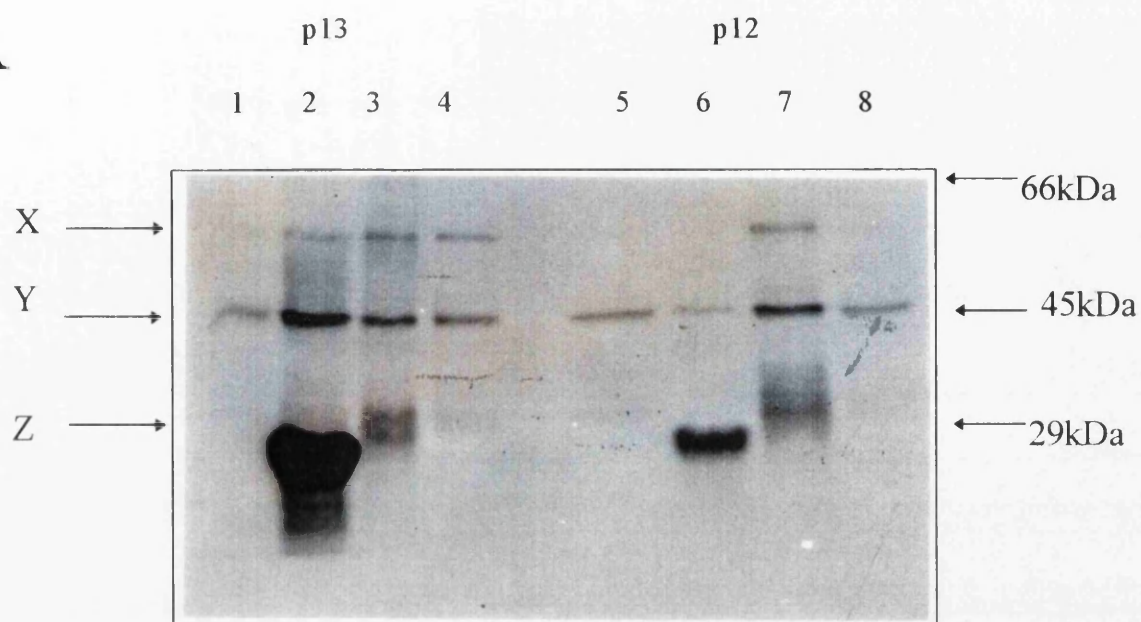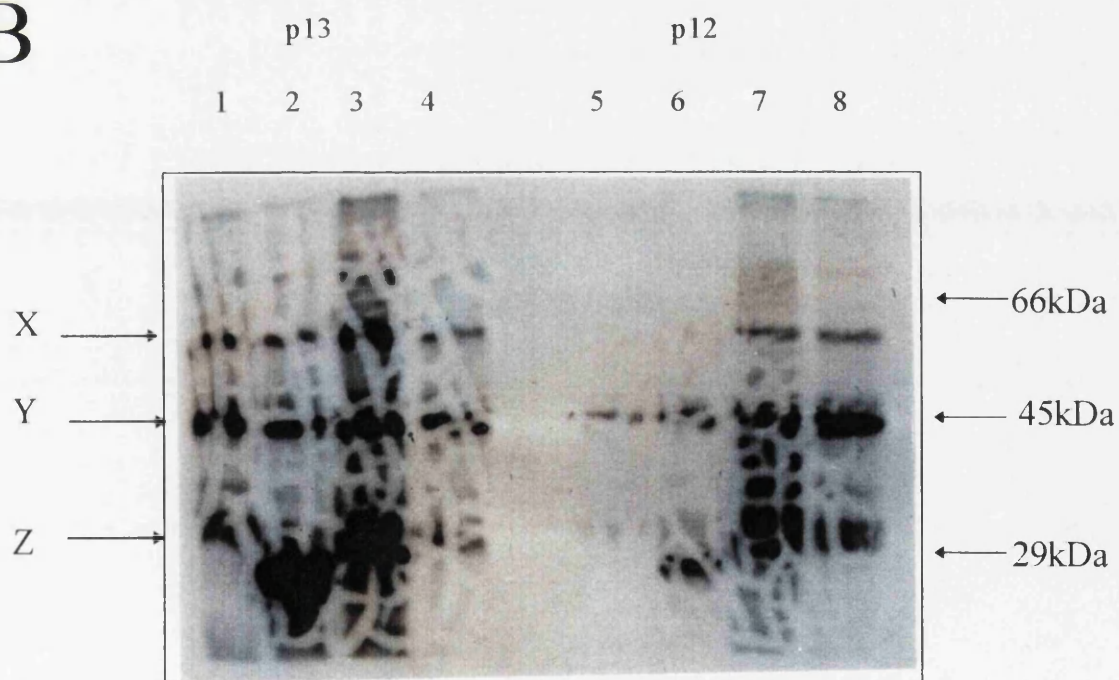
Figure 3.14 Immunoblotting of depleted extracts

Aliquots of the same supernatant and flow-through samples prepared in figure 3.12 were separated on a 12.5% SDS-PAGE gel, Western blotted and probed with anti-ThaCRK2 and anti-PSTAIRE antibodies are previous.

Panel A shows the immunoblot probed with the polyclonal anti-ThaCRK2 anti-serum.

Panel B shows an identical blot probed with the polyclonal anti-PSTAIRE anti-serum.

Key:

Lane 1:   Non depleted supernatant

Lane 2:   Immunodepleted supernatant

Lane 3:   Non-depleted flow-through after p13 binding

Lane 4:   Immunodepleted flow-through after p13 binding

Lane 5:   Non-depleted flow-through after p12 binding

Lane 6:   Immunodepleted flow-through after p12 binding

Molecular weights are as marked.

A

6 5 4 3 2 1

97kDa →

66kDa →

45kDa →

31kDa →   ← 34kDa

B

1 2 3 4 5 6

66kDa →

45kDa →

                           ← 34kDa
31kDa →
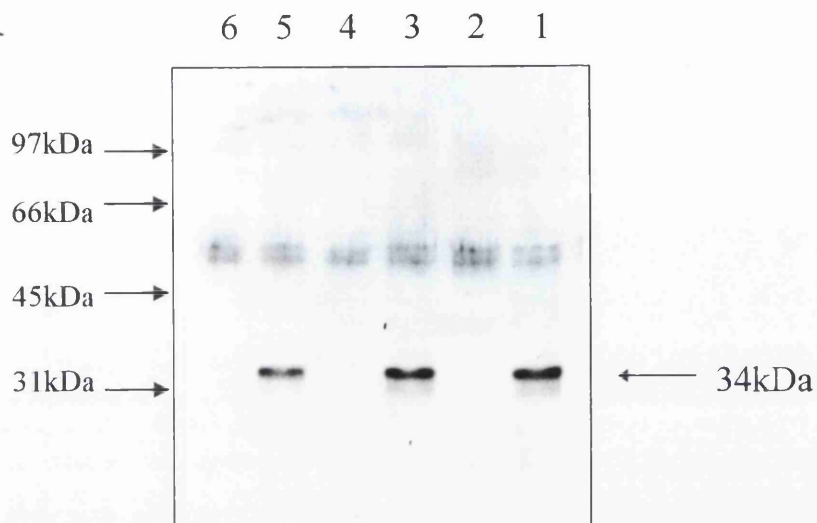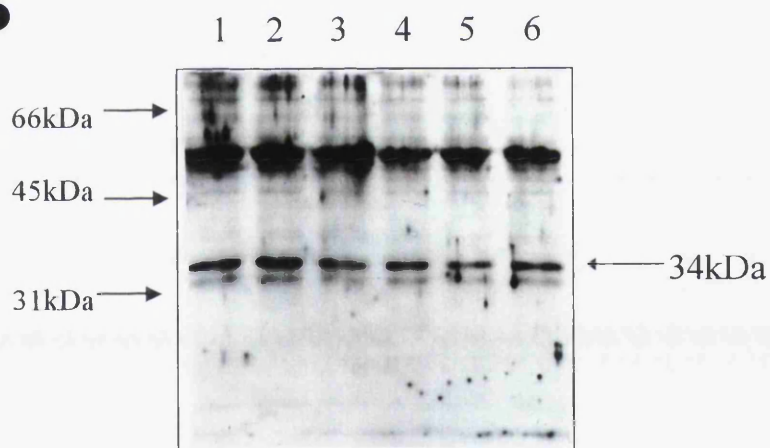
Figure 3.15 PCR for *suc1* homologue from *Theileria annulata*

Various parameters were tried as listed in Table 3.2. This reaction was done using the parameters listed in Mottram & Grant, 1996. The PCR cycling was done for 30 cycles of 94°C for 1 minute, 45°C for 2 minutes and 72°C for 2 minutes.

Key:

Lane 1   *T. annulata* genomic DNA from piroplasm stage

Lane 2   *T. annulata* cDNA made from RNA purified from D7 cells after 6 days at 41°C.

Lane 3   Yeast *suc1* cloned into the pQE60 vector (positive control)

Sizes are as indicated on the left of the figure.

298bps

226/201bps

154/134bps
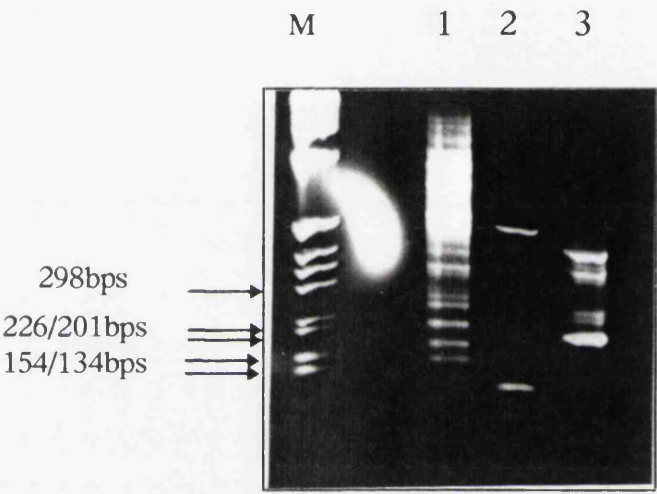
Figure 3.16 Anti-p13 antisera reactivity with bovine and parasite extracts

A Western blot of various extracts was probed with a polyclonal anti-p13 antiserum (a gift of P. Nurse).

Key:

Lane 1   BL20 extracts

Lane 2   D7 @ 37°C extracts

Lane 3   D7 (4 days at 42°C) extracts

Lane 4   D7 (7 days at 42°C) extracts

Lane 5   D7 (10 days at 42°C) extracts

Lane 6   Piroplasm extracts

Lane 7   *S. pombe* extracts

Lane 8   *S. pombe* extracts

The location of the yeast p13 is indicated by an arrow.
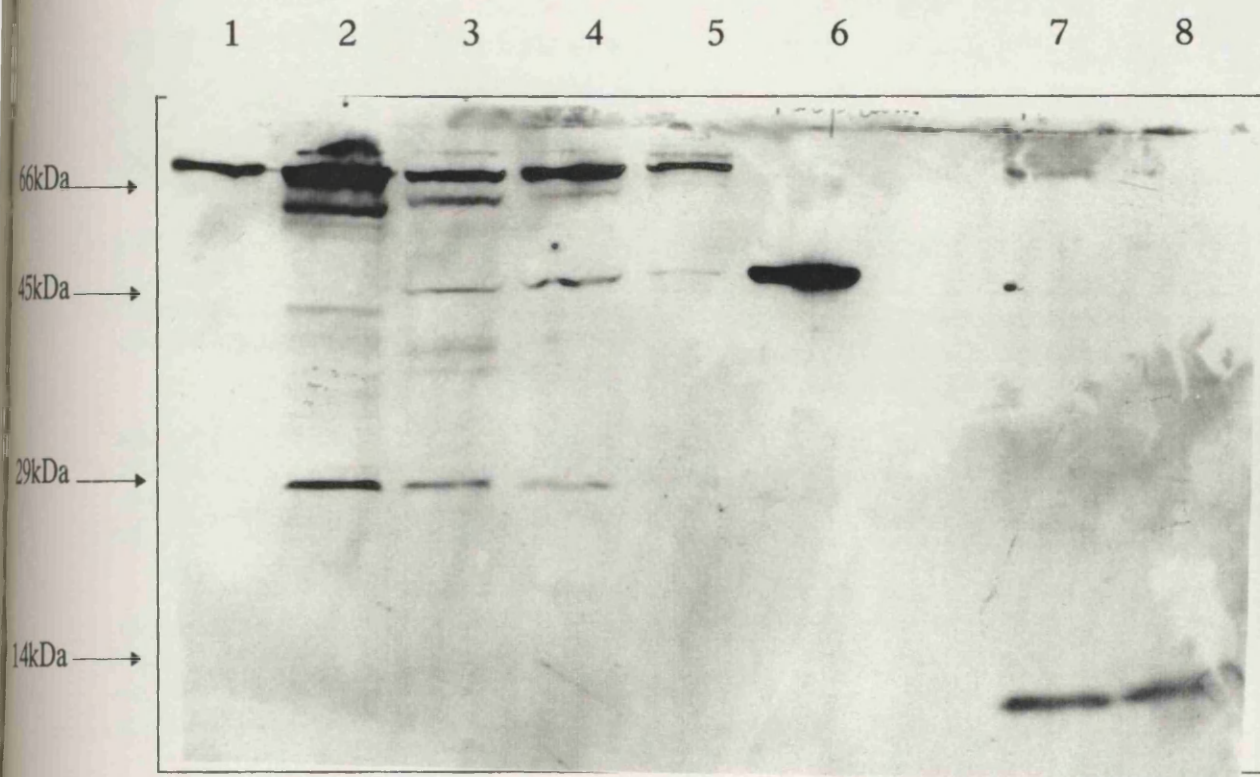
Figure 3.17 Pileup of ThaCRK2, ThaCRK3, human and *S. pombe* cdc2 showing regions important for p13^{suc1} binding

This figure shows the regions important for interactions between CDK and p13^{suc1}. Regions in bold are listed from **I** to **XIII**. Other important residues conserved across species are highlighted in grey. Mutation of these residues which are involved in internal bond formation in the large lobe affect binding indirectly by causing a conformational change. An arrow marks residues defined by Endicott *et al.*, (1994) by mutational analysis as being important in CDK and p13^{suc1} interaction.

```
ThaCRK2   ..........  ..........  ..........  ..........  ..........
ThaCRK3   MVKRVKKSAE  KTGKARKLNE  GVKLKEEKDD  EIKSENTETV  EDSKDLKNVD
cdc2h     ..........  ..........  ..........  ..........  ..........
Spcdc2    ..........  ..........  ..........  ..........  ..........
                                                               I

ThaCRK2   ..........  ..........  ..........  MRRYHKMEK.  IGEGTYGVVY  19
ThaCRK3   NVDKNVQKIN  EEVDDKQEDS  VTDSNGSDSL  DKRFTPVGKH  LGEGTYGQVI  100
cdc2h     ..........  ..........  ..........  MEDYTKIEK.  IGEGTYGVVY  19
Spcdc2    ..........  ..........  ..........  MENYQKVEK.  IGEGTYGVVY  19
                II            III

ThaCRK2   KAQNN.HGEI  CALKKIRVEE  EDEGIPS...  .........T  AIREISLLKE  56
ThaCRK3   KAMDTLTGKM  VAIKKVKNIE  YKKGVTKDRQ  LVGMVGIHFT  TLRELKVMTE  150
cdc2h     KGRHKTTGQV  VAMKKIRLES  EEEGVPS...  .........T  AIREISLLKE  57
Spcdc2    KARHKLSGRI  VAMKKIRLED  ESEGVPS...  .........T  AIREISLLKE  57
                IV            V              VI

ThaCRK2   L....HHPNI  VWLRDVIHSE  KCLTLVFEYL  DQDLKKLLD.  ...ACDGGLE  98
ThaCRK3   LS....HENL  MGLVAVYVKE  GSINIVMDIM  ASDLKKVVD.  ....AKVRLT  191
cdc2h     L....RHPNI  VSLQDVLMQD  SRLYLIFEFL  SMDLKKYLDS  IP..PGQYMD  101
Spcdc2    VNDENNRSNC  VRLLDILHAE  SKLYLVFEFL  DMDLKKYMDR  ISETGATSLD  107


ThaCRK2   PTTAKSFLYQ  ILRGISYCHD  HRILHRDLKP  QNLLINREGV  LKLADFGLAR  148
ThaCRK3   EPNVKCIMSQ  ILTGLSVLHA  SSFAHRDLSP  ANIFIDTFGV  CKIADFGLAR  241
cdc2h     SSLVKSYLYQ  ILQGIVFCHS  RRVLHRDLKP  QNLLIDDKGT  IKLADFGLAR  151
Spcdc2    PRLVQKFTYQ  LVNGVNFCHS  RRIIHRDLKP  QNLLIDKEGN  LKLADFGLAR  157
                            VII ↑      VIII         IX

ThaCRK2   AFAIPV....  ..........  ..RSYTHEVV  TLWYRAPDVL  MGSKKYSTAV  182
ThaCRK3   TVNPPIFRDC  SDLETMELNA  SRERMTSKVV  TLWYRAPELF  MGAECYHFAC  291
cdc2h     AFGIPI....  ..........  ..RVYTHEVV  TLWYRSPEVL  LGSARYSTPV  185
Spcdc2    SFGVPL....  ..........  ..RNYTHEIV  TLWYRAPEVL  LGSRHYSTGV  191
                    X            XI           ↑           ↑

ThaCRK2   DIWSVGCIFA  EMINGVPLFP  GISEQDQLKR  IFKILGTPNV  DSWPQVVNLP  232
ThaCRK3   DFWSVGCIFG  ELLSGKPLFP  GTNEIDQLGK  IYNLLGTP.E  NSWPQASKLP  340
cdc2h     DIWSIGTIFA  ELATKKPLFH  GDSEIDQLFR  IFRALGTPNN  EVWPEVESLQ  235
Spcdc2    DIWSVGCIFA  EMIRRSPLFP  GDSEIDEIFK  IFQVLGTPNE  EVWPGVTLLQ  241
                XII             ↑ ↑  ↑                  XIII

ThaCRK2   AYNPDFCYYE  KQAWSSIVPK  LNESGIDLIS  RMLQLDPVQR  ISAKEALKHD  282
ThaCRK3   LY.TQYSFSK  PKDLSLHFQH  ANSVTLDLLS  KLLKLNPNER  ISAKEALDHE  389
cdc2h     DYKNTFPKWK  PGSLASHVKN  LDENGLDLLS  KMLIYDPAKR  ISGKMALNHP  285
Spcdc2    DYKSTFPRWK  RMDLHKVVPN  GEEDAIELLS  AMLVYDPAHR  ISAKRALQQN  291


ThaCRK2   YF.......K  DLHRPSEFLN  GVH*......298
ThaCRK3   YFKVQPLKCK  PIDLPFDFIT  K*........410
cdc2h     YF.......N  DLDNQIKKM*  ..........297
Spcdc2    YL.......R  DFH*......  ..........297
```

Table 3.1 Binding affinities and substrate preferences of ThaCRK2 and other kinase.

	Affinity			Substrate Specificity			
	p13	p12		No Sub	Histone	Casein	MLC
ThaCRK2	++	+		++	+++	+	-
Kinase X	+++	+		+/-	+/-	++	-

Key:

+++   indicates relatively strong binding/ phosphorylation
+/-   indicates relatively poor binding/ phosphorylation
-        indicates no detectable phosphorylation
No sub - no exogenous substrate added to kinase assay
MLC - myosin light chains used as exogenous substrate

Table 3.2 Conditions used in attempt to PCR *suc1* homologue.

The primers used as listed in chapter 2. A number of different conditions were varied during the PCR experiments as listed in the table.

Parameters Used	Range of Parameters Tested
Source of DNA	Genomic and cDNA
Concentration of DNA	100ng to 1μg for both types
Annealing temperature	40 to 55°C
Primer concentration	1μM to 3μM
Magnesium concentration	1mM to 4.5mM
Use of detergent	Triton X100 added to 0.1%

Chapter Four

Isolation & Characterisation
of the
Large Subunit
of
Ribonucleotide Reductase
from
Theileria annulata

4.1.1 Introduction

Attempts were made to clone the *suc1* homologue from *T. annulata* by PCR amplification using degenerate oligonucleotide primers (a gift of Dr. J. Mottram). The primers were designed against two conserved regions of amino acid sequence present in a range of different organisms and had been used to clone a *suc1* homologue from *Leishmania mexicana*. (Mottram & Grant, 1996). Two PCR fragments of 230 and 180bps were isolated and cloned as described in section 3.14. The sequence of one fragment (180bps) had a high degree of homology to other ribonucleotide reductases in the sequence databases.

Although the isolation of this gene fragment was fortuitous, studies in a number of organisms have shown the transcription of this gene is regulated in a cell cycle specific manner (reviewed in Greenberg & Hilfinger, 1996, and discussed in the introduction to chapter 5) and, given its central role in DNA replication, further study would elucidate another aspect of the cell cycle regulation of *Theileria* since ribonucleotide reductase activity varies greatly during the cell cycle. It is highest when DNA synthesis occurs and is hardly detectable in quiescent cells. In higher eukaryotic cells the variation in RR activity at different stages is due to the fluctuation in R2 protein levels whereas the levels of R1 protein remains constant. It has also emerged as a potential chemotherapeutic target.

Ribonucleotide Reductase - a new therapeutic target

Ribonucleotide Reductase (RR) (EC 1.17.4.1-2) plays a central role in the biosynthesis of DNA. It converts ribonucleoside diphosphates into the corresponding deoxyribonucleotides (dNTPs) by catalysing the reduction of Carbon -2 on the ribose ring. dNTPS are used almost exclusively in the biosynthesis of DNA and hence, RR is subject to intricate regulatory mechanisms (reviewed in Thelander & Reichard, 1979, Stubbe, 1990). The chemical reduction of a ribonucleotide must be initiated by an organic free radical. Different means of achieving this have evolved and, to date, at least five different classes of reductases have been characterised, all with different primary protein structures (reviewed in Harder, 1993).

98

Class I enzymes include all known eukaryotic and viral reductases and some aerobic bacterial enzymes. The *E.coli* reductase is the best characterised. They all contain two subunits, the large (R1) and small subunit (R2) arranged in an $R1_2R2_2$ quaternary structure. Each R1 subunit (85 kD) has one substrate binding site with redox active thiols for ribose reduction and two separate allosteric sites. R2 has the tyrosyl radical from Tyr122 and each R2 polypeptide (43 kD) has an iron [Fe(III)] centre which generates and maintains the tyrosyl radical which initiates the chemical reduction reaction.

Studying the differences in biochemistry and protein structure of parasitic protozoa and their hosts can lead to the identification of rational targets for chemotherapy. By and large, the biochemical and metabolic pathways of protozoa have not been well characterised but some striking differences have already emerged (reviewed in Cox, 1993). For example, all parasitic protozoa studied to date are incapable of synthesising the purine ring *de novo* thus necessitating a unique set of salvage enzymes for the scavenging of host purines. Most are prototrophic for pyrimidine synthesis. However, *Trichinella vaginalis* and *Giardia lamblia* are obligatory deoxyribonucleotide scavengers suggesting that they lack a ribonucleotide reductase activity or possess a homologue with a very different substrate specificity to that of the mammalian counterparts.

A species specific anti-proliferative drug?

Pioneering work with the *Herpes simplex* virus RR showed that synthetic peptides corresponding to the first six amino acids at the carboxy terminus of the R2 subunit could inhibit the viral enzyme by preventing subunit association (Dutia *et al.,* 1985, Krogsrud *et al.,* 1993). This sequence is not well conserved between prokaryotic and eukaryotic subunits and so the inhibition is specific to the viral enzyme which makes it an ideal antiviral agent. Further work using chemically modified derivatives of the hexapeptide has produced much more potent inhibitors of the viral enzyme *in vivo* (Luizzi *et al.,* 1994) and some of these compounds have been cleared for clinical trials. Indeed many major pharmaceutical companies have therapeutic peptides

99

undergoing clinical trials for efficacy against a range of conditions (Kelley, 1996). Most of these molecules are highly potent hormones or their analogues (the smallest being a tripeptide, the thyrotropin-releasing hormone). Some peptide analogues are in pre-clinical trials and these include inhibitors against HIV and hepatitis viruses together with endotoxin neutralising peptides but problems may arise in terms of the quantities needed to be synthesised if used for clinical applications. This may necessitate new developments in the bio-synthesis of peptides since the traditional bulk peptide synthesis by adding a single amino acid in a stepwise fashion will not achieve an economy of scale comparable with those drugs produced by conventional drug manufacture.

Given the successful use of peptide analogues designed to block subunit assembly of the *Herpes simplex* RR, it may be possible to exploit the differences in R2 C terminus sequences to design species specific anti-proliferative peptides against a wide range of parasites.

In order to test whether the RR subunits of *Theileria* are sufficiently distinct from the mammalian counterparts and, therefore, whether RR could be considered as a suitable chemotherapeutic target, experiments were undertaken to fully characterise the large subunit. As studies in other organisms have shown that the enzyme activity and transcription are regulated in relation to the cell cycle, experiments were undertaken to analyse the expression and sub-cellular localisation of the molecule in *Theileria annulata*. As the promoter regions of other cell cycle regulated genes have been studied, a genomic clone encoding the R1 subunit of *T. annulata* was isolated with the aim of sequencing the region 5' to the start codon. This region, together with the regulation of the expression of R1, is considered in chapter 5.

This chapter focuses on the isolation and characterisation of the full length cDNA from a library using the PCR fragment generated (chapter 3) as a probe, isolation and restriction enzyme analysis of a genomic clone and analysis of the expression of the parasite gene in the bovine life cycle stages. A parasite specific region of the parasite cDNA was cloned into an expression vector to produce a fusion protein used for immunisation. This gave parasite specific serum which recognises a polypeptide of the predicted molecular weight of the large subunit on immunoblots. Expression and localisation of the R1 polypeptide during various stages of the life cycle were analysed by Western blotting and immunofluorescence.

4.1.2 Isolation of a *Theileria* Ribonucleotide Reductase PCR Fragment

The primers designed to amplify a conserved region of the *suc1* gene from *T. annulata* are described in section 3.14 and the conditions used are as described in Mottram & Grant (1996). Two fragments of 230 and 180 bps were cloned from PCR performed with piroplasm DNA as template. Both fragments were gel purified and ligated into the pCR vector (Invitrogen). When sequenced, the 180bp fragment was found to contain a single open reading frame (figure 4.1a) that had high homology to a conserved region of several eukaryotic large subunits of ribonucleotide reductase. This was determined by searching the SwissProt database using the GCG FASTA programme. This homology is shown in Figure 4.1b, using the species with the highest homology, *P. falciparum*, as an example.

4.1.3 Southern Blotting shows the PCR fragment is parasite derived

The TaR1 (*T.annulata* Ribonucleotide Reductase subunit 1) 180 bp PCR fragment was used to probe a Southern blot to confirm its parasite origin and to test for homology with the bovine R1 gene.

The probe hybridised strongly with the piroplasm DNA (Figure 4.2, Panel C) and weakly with the cloned macroschizont cell line D7 DNA (Panel B) which is predominantly host DNA. There are some faint bands hybridising to the BL20 DNA (Panel A) which are probably due to the probe hybridising to repetitive DNA sequence restriction fragments of the same mobilities seen on the ethidium stained gel (data not shown). This blot also showed that the gene is likely to be single copy in the parasite genome. The three restriction enzymes used do not have sites within the TaR1 PCR fragment used as the probe (see figure 4.3b). The cloned cell line DNA showed single hybridising bands of 8.6, 9 and 9.5kb with each enzyme and as this cell line is derived from a single parasitised cell it should contain a single parasite genome. The signal is fainter than that obtained with piroplasm DNA due to the small parasite contribution to

101

the total DNA isolated from the cell line. Piroplasms as they are isolated from an infected animal, are always composed of more than one genotype and hence there is polymorphism seen with the *BamHI* digest (Panel C Lane 1) giving three extra bands of 11, 9.2 and 2.7kb.

4.1.4 Isolation and characterisation of a full length cDNA clone

The PCR fragment was used to screen both cDNA and genomic libraries by filter hybridisation. The cDNA library was constructed in the λZAP II vector (Stratagene) from total RNA isolated from cell line D7 at day 7 during differentiation and the genomic DNA library was constructed in the λDASH vector (Stratagene) using purified D7 merozoite DNA. Both libraries were prepared by Dr. J. Kinnaird. A total of 20000 plaques were screened from the cDNA library of which 0.25% were positive after the first round of screening. Twenty plaques were selected for a second round of screening and, after two further rounds of screening, nine cDNA clones were isolated. The cDNA clones were *in vivo* excised and DNA purified from the resulting pBluescript vector. The DNA preparations were then restriction digested to determine insert size and two suitable inserts were selected for sequencing. One insert was 2 kb long while the other was possibly a full length clone of 2.9kb. For the genomic library screen, a total of 6000 plaques were screened and twelve clones were isolated after three rounds of screening. One of these was selected and studied in detail and was shown to contain the entire cDNA sequence by hybridisation and restriction mapping (section 4.1.6).

Initially sequencing was carried out from either end of the cDNA inserts using Sp6 and T7 primers. Sequencing from the T7 primer revealed an *SphI* site. Restriction mapping of the plasmid with *SphI* confirmed the presence of a 1.0kb *SphI* fragment which was subcloned into the pTZ19R vector (Pharmacia) and sequenced as before. Internal primers were designed from sequence data to complete the sequencing analysis of the cDNA on both strands due to the lack of any other suitable restriction sites for subcloning (shown on figure 4.3b). The sequence data was assembled and analysed using the GCG package (Devereux *et al.*, 1984).

The cDNA encoding the large subunit of ribonucleotide reductase of *T. annulata* is 2.8kb long and has an open reading frame of 2712 nucleotides encoding a polypeptide of 891 amino acids from the first in frame start codon with a predicted mass of 97kD. Figure 4.3a shows the full length cDNA sequence with the translated amino acid sequence.

The cDNA sequence contains three possible ATG translation start codons, all of which are in frame. The first **ATG** (M1, figure 4.3a) encountered in the ORF has the highest homology to a protozoan consensus sequence for translational initiation (see 4.1.5). There is an in frame TGA stop codon 39bps upstream from this most 5' ATG codon. As shown in figure 4.4, the pileup comparison with other eukaryotic R1 proteins suggests that the third **ATG** (M3) is the most likely start codon. As it has not yet been determined whether the sequence encoding this possible N-terminal extension is translated, this ATG (most downstream) will be referred to as 1 in future numbering. From this start codon there is an open reading frame of 2499 bps encoding a protein of 832 amino acids. At the 3' end, the eukaryotic polyadenylation signal AAUAAA is not present but a 20bp poly [A] tail is seen 60bp downstream of the first in frame stop codon.

R1 Sequence Conservation

There is a high degree of conservation in regions of functional importance. Table 4.1 shows the % identity and similarity between *T. annulata* R1 compared to other R1 subunits from other species present in the database calculated from M3, the third start codon (i.e. omitting the possible N-terminal extension). The *T. annulata* R1 (TaR1) has the highest identity to the R1 subunit from the related Apicomplexan, *P. falciparum* (PfR1 - 72%) but TaR1 is slightly more similar to mammalian R1 subunits than is PfR1 - for example - TaR1 is 70% identical to human R1 whereas PfR1 is only 66% identical to the human R1. Mammalian R1 subunits appear to be very highly conserved (97% identity between mouse and human). Rather surprisingly the fission and budding yeast subunits are only 76% identical to each other which perhaps reflects the evolutionary divergence

between the two yeasts. Generally, the overall degree of conservation is not high between eukaryotic / viral R1 subunits and *E. coli* R1 (22-33% identical) but when conservative substitutions are taken into account this rises to between 40 and 50%. Figure 4.4 shows a pileup comparison of the amino acid sequence of TaR1 with representative R1s from other phylogenetic groups. The regions important in the chemistry of the enzyme are discussed below, showing how these regions are conserved in the *Theileria* subunit.

From X-ray crystallography studies on the *E. coli* R1 subunit by Uhlin & Eklund (1994), it was shown that the R1 subunit is composed of three domains:

1) A mainly helical N-terminal domain of ~220 residues.

2) One α helix/β barrel domain of ~480 residues.

3) An $\alpha\beta\alpha\alpha\beta$ domain of ~70 residues.

Since all the eukaryotic R1 subunits show homology to the *E. coli* subunit over the length of the polypeptide, it is reasonable to assume they fit a similar three dimensional structure.

The active site contains one pair of cysteine residues which undergo oxidation during the reaction to form a disulphide bridge. However, as in many other thiol redox proteins, these are not located near to each other, but are separated by over 200 residues (Cys225 & Cys462 in *E. coli*). Both are present in the *Theileria* R1 (Cys216 & Cys442) and the surrounding regions are highly conserved. This cysteine pair come into close contact once the polypeptide chain folds, being on two adjacent β strands. A further cysteine (Cys439 in *E. coli*, Cys427 in *T. annulata*) acts directly on the substrate ribose ring to create a thiyl substrate radical. Figure 4.5 shows how these three cysteines and flanking sequences have been conserved between the prokaryotic and eukaryotic R1 subunits. Other highly conserved residues include those lining the pocket of the active site which flank the active cysteines as seen in figure 4.5. These residues are either polar or hydrophobic. There are no aromatic residues within the substrate cavity and the only charged residue is Glu441 in *E. coli* (Glu 429 in TaR1) which may serve to bind the ribose moiety of the substrate or function as a base in the redox reaction.

Uhlin & Eklund proposed the following mechanistic model for ribonucleotide reduction based on their structural studies of the R1 from *E. coli*.

1. Removal of the 3' Hydrogen atom by a thiyl radical of Cys439.

2. Protonation of the ribose ring 2'OH by the Cys225 with the resulting positive charge at O3 being stabilised by Glu441.

3. Redox reaction by Cys225 and Cys462.

4. Reduction of the disulphide bridge between Cys225 and Cys462 by the transfer of thiol exchange reactants via the flexible carboxyl terminal of R1. This involves two further conserved cysteines (Cys754 and Cys759) and effectively reactivates the enzyme. Two tyrosine residues (Tyr730 and Tyr731) aid in the electron transfer between the large and small subunit (Ekberg *et al.,* 1996). Tyr730 is hydrogen bonded to Tyr731 and Cys439. These are conserved in the Theileria R1 (Tyr 737 and 738) and Tyr731 lies close to where the R1 and R2 subunits interact. These three residues together with five in the R2 subunit form a hydrogen bonded network running through the holoenzyme complex. The degree of homology between prokaryote and eukaryote R1 subunits is remarkably high over these regions showing a conservation of mechanism common to all class I ribonucleotide reductases. (Figure 4.5). The divergence between *Theileria* R1 and other higher eukaryotic enzymes only becomes striking over the last 50 amino acids at the C- terminus and it was for this reason that this region was used as to generate parasite specific serum (see section 4.1.8).

Both the *Plasmodium* and *Theileria* N termini show differences from the mammalian R1s which may indicate that the allosteric regulation of the parasite enzymes differs from that of their mammalian hosts. If the putative extensions on the *Plasmodium* and *Theileria* R1s were shown to exist in the mature polypeptide then this may add weight to the possibility of the allosteric regulation being different to that of mammalian enzymes. The C terminal cysteines (Cys 817, 827 and 830 in *Theileria*) that interact with thioredoxin and glutaredoxin are conserved, together with the Asp 56 (Glu 54 in TaR1) which is involved in dATP feedback inhibition (Caras & Martin, 1988). The position of the last Cys residue is highly conserved being placed three residues 5' to the translational stop (except in HSV where it is two residues from the stop). Although the conservation of the first two (Cys 817, 827) is not obvious because of the gaps introduced to maximise the alignment, in all species there is a highly conserved spatial arrangement with the first and second being separated by 8-10 residues and the second being 2-4 residues from the last. *Plasmodium* and *Theileria* show a very high degree of spatial arrangement of these cysteine residues.

The R1/R2 Binding Site

It was shown that deletion of at least 6 residues from the carboxyl terminus of the *Herpes simplex* virus (HSV) R2 prevented subunit association (Filatov *et al.*, 1992). This has also been confirmed for the small subunit of ribonucleotide reductase from other species, intensifying interest in the use of peptidomimetric inhibitors as potential therapeutics.

Attempts to locate the site of binding of R2 on the large subunit have utilised NMR studies of purified mouse proteins (Lycksell *et al.*, 1994) which showed that the R2 C- terminus loses much of its free mobility after introduction of the R1 protein into the solution. More recent work has employed peptide protection assays and photoaffinity labelling (Davis *et al.*, 1994). Peptide protection assays mapped the R2 binding to residues C terminal to aa 325 in the mouse R1. Photoreactive R2 peptides labelled the R1 protein at positions 724-736 and 778-789 which lie very close to the C-terminal of the R1 subunit. As mouse R1 is likely to be very similar to the bovine R1 and since these regions are likely to be important for the design of species specific inhibitors, the degree of sequence conservation between mouse and *Theileria* was analysed in detail over these two regions (Figure 4.6). The homology in region 2 is not as high as that for region 1 and is displaced in the pileup comparison by an insertion of 30-40 residues in *Theileria* as seen in figure 4.4 though the positions relative to the extreme C-termini are very similar. However, this insertion may have a significant effect on the three dimensional structure assumed by the R1 subunit upon folding.

There is considerable variation between species in the C-terminal of R1 which is reflected in the R2 C terminal sequences. The actual position of the R2 subunit interaction is conserved in the 3D model of the *E.coli* and mouse R1 despite the regions involved having very low homology between the pro - and eukaryotes.

Region of R1 subunit dimerisation

Connor *et al.*(1993) made deletion mutants of the *Herpes simplex* R1 to map the

R1/R2 site of interaction and also to determine the region of R1 required for dimerisation. In HSV, residues required for dimerisation stretch from 421-434 but they conclude that other regions may also be necessary. The strength of interaction between the mutant R1 subunits was not determined. The homology over this region between the HSV and other R1 sequences is shown in figure 4.7. This region is not well conserved between species therefore it is not possible to infer that the same region is involved in dimerisation of other R1 subunits. It is possible that dimerisation is highly species specific. It would perhaps be more meaningful to compare regions known to be involved in R1 dimerisation in the higher eukaryotes given that the homology of *Theileria* to HSV R1 is only approximately 30% but to date this work has not been done in the higher eukaryotes.

4.1.5 Translation initiation site of TaR1

The open reading frame of the TaR1 cDNA clone extended for 229 base pairs upstream of the consensus ATG codon encoding the consensus N-terminal methionine of other eukaryotic R1 genes. Analysis of this region showed it to contain two additional upstream in frame ATG codons shown in figure 4.8. This hints at the possibility that this may be a possible N-terminal extension of the polypeptide.

A comparison of the nucleotide sequence around translation initiation sites (Kozak, 1987) has revealed an optimal sequence for vertebrates which is GCCACCatgG, although the most important effects on translation appear to be a requirement of a purine at the -3 and G at the +4 position. A similar database search was undertaken for the sequence flanking the translational initiation site in protozoa (Yamauchi 1991). For the sporozoans the consensus sequence was found to be

a/t t/a NTTNT t/a NAAAAATGA a/g a/t

If sequence flanking each of the three ATG codons in the upstream region are lined up with the above sequence and the % fit to the sporozoan consensus sequence is calculated (figure 4.8) then the first **ATG** codon encountered has the best fit to both

protozoan and Kozak consensus sequences. M1 and M3 both fit the minimum Kozak consensus of a purine at -3 and G at +4 which gave 60-90% efficiency of translation (Kozak, 1987). Yamauchi noted that the sporozoans exhibited a T bias in positions -13 to -5 (the A of the ATG codon is counted as +1) which could form a stem loop structure with the A residues flanking the ATG codon. If applied to the three sequences surrounding the start codons (M1-M3), the best fit with the Yamauchi consensus sequence is found with the 1st ATG codon (M1).

Sequencing of a 2.9kB *P. falciparum* R1 cDNA clone showed there to be another in frame start codon prior to the consensus eukaryotic start codon based on homology (Chakrabarti *et al.*, 1993). But, as with the *T. annulata* N-terminal region, this has not been shown as yet to be present in the mature polypeptide and it may be that these regions are untranslated (see chapter 5).

4.1.6 Restriction mapping of genomic clones

Of the 12 genomic clones isolate by library screening, one (λ3) was selected for further analysis. By Southern blotting and hybridisation this clone was shown to be very likely to contain the entire TaR1 gene sequence by hybridisation with 5' (*PstI/XhoI* fragment of 768bps) and 3' (*XhoI/XbaI* fragment of 170bps) specific probes prepared from the cDNA clone. Using various restriction enzyme digests combined with hybridisation analysis using 5' and 3' probes from the TaR1 cDNA clone (an example is shown in figure 4.9) it was possible to construct a restriction map of the entire genomic region - this is shown in figure 4.10. The whole insert is 16.5 kb and using double digests where one enzyme cuts in the λDASH polylinker, the fragments adjacent to the left and right arms of the λ vector could be positioned.

Subcloning from λ3

In order to begin a preliminary analysis of gene structure in relation to the cDNA, to obtain sequence for the study of possible promoter elements and to map the transcriptional start site (chapter 5), a suitable fragment was selected for sub-cloning from λ3. A 2.7 kb fragment, produced by digesting the λ3 clone with *BamHI* and *EcoRI*

which hybridised to the 5' probe only (figure 4.9 panel A lane 9), was predicted to contain sufficient 5' non-coding sequence and to extend to the *BamHI* site represented in the cDNA clone (at position 1211bp figure 4.3a+b). This was subcloned into the pBluescript vector, restriction mapped and partially sequenced. The insert was sequenced from either end using T3 and T7 primers. From the *BamHI* site used in the sub-cloning 266bps of sequence was obtained extending towards the 5'end of the gene. This was 99% identical to the cDNA clone and no introns were found (figure 4.10). Generally, introns in *Theileria*, tend to be small, ranging from 20-120 bps in the ThCRK2 for example (Kinnaird *et al.*, 1996). There is a single intron in the *P. falciparum* R1 gene of 184 bases further upstream from the region sequenced in *Theileria*. However it is possible that introns may be present elsewhere in the gene. Analysis of the 3'region would require a further subcloning step using a *BamHI/ HindIII* digest of the genomic lambda clone. Given that the location of four of the five introns in PfPK5 are conserved in the ThCRK2 gene, it is possible that the intron site found in the *P. falciparum* R1 gene is conserved in *T. annulata.*

4.1.7 Expression of TaR1 in bovine life cycle stages.

Since the large subunit of ribonucleotide reductase is involved with the production of deoxyribonucleotides for DNA replication, it follows that it should be expressed in those life cycle stages actively undergoing DNA replication. To investigate this experimentally, RNA was available from non-differentiating and late stage differentiated D7 cells and from piroplasms. The original TaR1 180bp PCR fragment was used to probe a Northern blot to determine its expression in different bovine stages of the life cycle (Figure 4.11, Panel A).

The gene is transcribed as a 2.8kb message in all intracellular bovine stages of the parasite with an apparent increase in transcript levels during the differentiation of the parasite to the merozoite stage and a decrease in the piroplasm stage. Because of the mixture of host and parasite RNA in the intralymphocytic stages it is difficult to estimate the absolute contribution of parasite RNA. Probing identical samples with a probe from the *T. annulata* DNA polymerase δ subunit (Panel B)(Smyth & Kinnaird, in preparation)

gave similar related levels between the two intralymphocytic stages but there was no comparable decrease in the piroplasm stage. With the *T. annulata* tubulin probe (Panel C) there is a similar pattern to the TaR1 signal is seen, with a decrease in signal in the piroplasm stage. The tubulin probe detects two abundant messages, one of which (1.8kb) corresponds to the predicted size of the tubulin mRNA. The origin of the second message is uncertain and is currently being investigated (Logan, pers.comm.). There was no cross-hybridisation with bovine RNA indicating that the hybridisation detected is parasite specific. Ethidium staining of an identical set of samples run in parallel on the same gel showed the relative contributions of host and parasite large and small ribosomal RNAs (Panel D).

4.1.8 Production of a parasite R1 specific antisera

Commercial antibodies are available, generated against the large subunits of higher eukaryote ribonucleotide reductase which also recognised the bovine R1 (see chapter 6). In order to distinguish between host and parasite molecules, it was important to produce a *Theileria* specific antiserum against the R1 for use in immunoblots and immunofluorescence assays. By comparing the pileup amino acid sequences between Theileria and higher eukaryotic R1, it was decided to express the 3' end of TaR1 in *E. coli* and use the resulting recombinant protein as an immunogen as this region differed extensively from any of the mammalian R1 subunits (see Fig. 4.4).

It was decided to use the GST fusion protein system (Pharmacia) as it allows for a single step purification by virtue of high affinity binding to glutathionine - sepharose. The protein is expressed fused to a portion of the glutathione S transferase (GST) of *Schistsoma japonicum*. The purified GST fusion protein is then eluted from a glutathione sepharose affinity column using 10mM glutathione. A GST expression vector (pGEX-5X-2) was digested with *BamHI* and *XhoI* and purified using the Wizard Clean Up Kit (Promega). A 270bp *Sau3AI-XhoI* at the extreme C-terminus of the cDNA clone (the *XhoI* site being in the polylinker) was compatible with the sites in the vector and was in frame. However, as *Sau3AI* cuts frequently in the cDNA clone, a 480bp *SphI-XhoI* fragment was isolated initially. This fragment was purified and then digested with *Sau3AI*

to give two fragments of 270bps and 210bps. Since only the 270bp fragment had compatible ends with the linearised vector the whole digest was used in the ligation. Transformants were screened for the presence of the 270bp insert and some were sequenced using a 5' pGEX specific primer to ensure that the insert was in the correct reading frame. A small scale expression was performed to optimise sonication and purification conditions prior to a large scale expression with 2 litres of culture. The stages of expression and purification are shown in Figure 4.12. On induction with IPTG, a prominent polypeptide of 36kDa was detected when extracts of the induced bacteria were analysed by SDS-PAGE gel electrophoresis. This is the predicted size for GST + TaR1 (26 kDa + 10kDa). The fusion protein was detectable in the supernatant of the sonicate (Lane 4) and was purified on a glutathione sepharose column. The purified protein was eluted using excess glutathione (Lane 5). The yield of fusion protein was approximately 3mg per litre. This was used to immunise 2 rabbits according to standard procedures (Harlow & Lane, 1988).

Sera from both rabbits were tested for reactivity against BL20 and piroplasm extracts by Western blotting and the results of are shown in Figure 4.13 together with the reactivity of the pre-immune serum. The final bleed of rabbit CM97 (figure 4.13 Panel B) recognises a protein of ~97kDa which is the predicted size for the R1 subunit from *Theileria*. No cross-reactivity with the bovine R1 was detected. It is not possible to determine if the size of this reactive protein could account for the presence or absence of the putative N-terminal extension due to the limits of resolution of the gels in this size range. The serum also recognises a smaller protein of approximately 45kDa which is not detected in the pre-immune serum. Serum from rabbit CM82 also recognises a 97kDa polypeptide (Panel A, final bleed lane 2) but less strongly than CM97 together with a faint 66kDa polypeptide but no 45kDa polypeptide. The background of the pre-immune serum was high with CM82 so it was decided to proceed mainly with CM97 serum for immunoblotting (Chapter 6).

If serum CM97 is pre-incubated with GST, the detection of the 97kDa and the 45kDa polypeptides is not blocked which eliminates the possibility of cross-reactivity of the rabbit serum with an epitope common to GST and an unknown parasite protein. Pre-blocking the serum with the fusion protein removes both reactive bands suggesting that an epitope on this part of TaR1 is present in parasite polypeptides of 97kDa and 45kDa.

111

It may be that immunoprecipitation of native protein would be specific for the R1 subunit, in that the serum may recognise a denatured epitope in the unknown polypeptide of 45kDa.

The antiserum was not subjected to any purification procedure since background was low at the dilutions used for Western blotting (1/200).

Immunolocalisation of TaR1

It was of interest to determine if the R1 subunit in *Theileria* localised to the cytoplasm as had been shown for mouse R1 (Engstrom *et al.*, 1984). Both sera were used successfully in immunofluorescence assays (IFA), although as before the background with serum CM82 was higher. Several different fixation protocols were undertaken (see chapter 2). Specific parasite reactivity was only obtained with cell preparations fixed with 4% formaldehyde followed by permeabilisation in 0.25% Triton X100. Figure 4.14 shows both the anti-TaR1 sera reacting specifically against the schizont nuclei. Panel A shows D7 cells stained with DAPI staining - clearly indicating host and parasite nuclei. Panel B shows the same cell with FITC detection of the CM82 anti-TaR1 antibody reactivity with the reactivity localised to all the parasite nuclei within the schizont. It seems that the nuclei are reactive with this serum although this should be confirmed by immunoelectron-microscopy. Panel C shows a BL20 cell stained with DAPI while panel D shows the same uninfected cell stained with FITC labelled TaR1 antibody from rabbit CM82. There is no specific reactivity, only background staining of the host cytoplasm. Panel F shows the CM97 anti-TaR1 serum reacting also with the schizont nuclei in D7 cells. This is a highly specific reaction as judged by the very low reactivity of D7 cell extracts on Western blots with the pre-immune serum from rabbit CM97. The fact that both rabbit anti-sera recognise schizont nuclei and the only common polypeptide reacting by Western blotting common to both sera is a 97kDa polypeptide, the predicted size of the TaR1 subunit, shows that this is a specific reaction with the TaR1 subunit. This appears predominantly localised to the parasite nuclei and all nuclei in every infected cell were reactive.

A monoclonal antibody against an unmapped epitope of mouse R1 was

purchased (Inro-Biomedtek, Sweden) and was used in IFA and immunoblot assays.
Figure 6.3 (Panel D) shows that this antibody recognises only a polypeptide of the
predicted molecular weight for the bovine R1 subunit. Figure 4.15 shows that the
antibody only reacts with the host by immunofluorescence. Panel A shows BL20 cells
stained with DAPI while panel B shows the same cells stained with FITC labelled MAb.
There is a diffuse staining throughout the cell cytoplasm, a location identical to that
found in studies undertaken with mouse MDBK and fibroblast cells (Engstrom *et al.,*
1984). Generally, the intensity of staining was uniform but a few cells were noted where
the intensity of reactivity in the cytoplasm was considerably brighter. Panel C shows a
D7 cell stained with DAPHI, Panel D shows the same cell with FITC labelled mouse R1
antibody. There is no cross-reactivity with the parasite macroschizont, some cells clearly
showing a reduction in the level of staining over the area occupied by the schizont and
localisation of the host R1 again is to be dispersed throughout the cytoplasm. The
fixation procedure is identical to that used by Engstrom *et al.* (1984) which showed that
the cytoplasmic reactivity is specific and not due to lack of permeabilisation of the
nuclear membrane by the fixation protocol. This was demonstrated with an antibody
directed against the polyoma virus large tumour antigen which was localised to the
nucleus in virus infected mouse fibroblast cells under the same fixation conditions. Thus
it is likely that for all higher eukaryotes, the R1 subunit is localised in the cytoplasm. This
contrasts with the localisation of the TaR1 subunit to the parasite nuclei in the D7 cells
(Figure 4.14 Panel B & F).

4.2 Discussion and conclusions

This chapter deals with the isolation of the large subunit of ribonucleotide reductase from *T. annulata*. The number of clones isolated during the library screen and the intensity of hybridisation signal suggests that it is very abundant in differentiating cells. However it is not clear as to whether the expression is up-regulated or whether the increase in signal intensity mirrors the increase in parasite nuclear content. The transcript pattern is most like that of β-tubulin with a similar signal intensity in D7 @ 37°C and a considerable increase at day 7 in differentiation but for the 1.8kb tubulin transcript this is not as high as TaR1. However, the picture is complicated by the presence of the 3.2kb hybridising RNA which is also strong with the tubulin probe. There is a greater decrease in hybridisation signal with the tubulin probe in the piroplasm stage. The increase in hybridisation with the polymerase δ probe from day 0 to day 7 is apparently less but the transcript levels are surprisingly high in the piroplasm stage given the limited division occuring in *T. annulata* piroplasms. As antibodies are not yet available for tubulin and polymerase δ, it is not possible to tell if these transcript levels are reflected in the protein concentration. It certainly seems that all three genes may be differently regulated in the piroplasm stage although it is possible that this could be due to differences in messenger stability. It should be possible to measure the relative transcription rates in these stages by preparing nuclei and performing nuclear run-on assays.

Both antisera generated against the GST-TaR1 fusion protein showed that TaR1 has a predominantly nuclear localisation in the macroschizont stage. All the nuclei in each macroschizont of infected cells were equally reactive. This in itself indicates that the protein level does not fluctuate significantly over the parasite nuclear division cycle, supporting the view that control of RR activity is by expression of the small subunit. It may ultimately be possible to demonstrate cyclical regulation of activity using synchronised parasite populations. However, because of difficulties in distinguishing host from parasite enzymes this will probably rely on specific immunoprecipitation of host and parasite enzymes.

The nuclear localisation is interesting and leads to the conclusion that deoxyribonucleotides are synthesised very near to the site of use. It is not possible to say how much of the dNTP synthesis pathway occurs in the nucleus or which molecules

can be transported across the nuclear membrane. It is probable in *Theileria* that the nuclear membrane does not break down at mitosis, a situation found in other lower eukaryotes (reviewed in Fantes, 1989). In mammalian cells, R1 is present in the cytoplasm and the nuclear membrane does not break down until early in mitosis and after DNA synthesis has taken place. The peak of RR activity is in S phase (Murphree *et al.,* 1969) suggesting that dNTPs are transported into mammalian cell nuclei across the nuclear membrane. There is no information in the literature of the subcellular localisation of R1 in other lower eukaryotes.

The cDNA clone isolated may encode a unique N-terminal extension which would make the polypeptide longer than any of the other higher eukaryote R1 subunits isolated to date. The fact that this extension contains an in-frame start codon which fits the Kozak and Yamauchi consensus sequences suggests that the translation start site lies here. It is necessary to confirm that this extension is present in the mature protein, possibly by producing a fusion protein to this region, raising anti-sera to this protein and then testing whether reactivity can be detected in parasite protein extracts. Certainly, it is interesting to speculate why *T. annulata* should contain this extension and whether it serves any function in the mature enzyme.

The reason for such a long N-terminal extension is unclear. It could be possible that the apicomplexan R1 mRNAs encode N-terminal extensions. This will become clearer when the sequencing of the *Toxoplasma gondii* R1 is completed (Kim, pers. comm.). Since it has postulated that the N-terminal region has a functional role in the allosteric regulation of the enzyme (Caras & Martin, 1988), it may be that the apicomplexans have a different means of allosteric regulation to that used by higher eukaryotes. Certainly, there may be some fundamental differences between the mammalian and the *Plasmodium* RR enzyme as might be expected in order to provide sufficient quantities of the dATP and dTTP for the replication of *Plasmodium* DNA given the AT richness of the *Plasmodium* genome. Whether this is via a different allosteric feedback mechanism or a differential sensitivity of the enzyme to feedback inhibition by dATP will require characterisation of the recombinant *Plasmodium* enzyme (J.Salem, pers. comm.).

Thus, I would conclude that the presence of a coding N-terminal extension may be a feature of the apicomplexan R1s and may indeed be a feature of protozoans R1s in

general. It is also possible that the presence of 3 ATG codons may indicate alternative translational starts sites which could be used in different life cycle stages to modulate the activity of the enzyme.

With respect to the differential expression of TaR1 in the bovine stages of the life cycle, it is possible that the increase in signal intensity during differentiation parallels the increase in size and RNA content of the macroschizont. This is a stage where there is considerable nuclear division occuring in the schizont and the increase in TaR1 RNA reflects this. It is constitutively expressed at all life cycle stages and appears to increase at day 7 rather more than for tubulin and considerably more than DNA polymerase δ. Scanning these Northern blots would allow these increases to be clarified in relation to one another. The piroplasm stage in *T. annulata* only undergoes two rounds of nuclear division (Conrad *et al.*, 1985) and the population is asynchronous. This would be reflected as a reduced requirement of the components of DNA synthesis and the reduction of the signal on the Northern blot suggests that the transcription of TaR1 is down-regulated when nuclear division is arrested. However, there is no similar decrease in hybridisation signal from the DNA polymerase δ probe, suggesting that its transcription is subject to a different regulatory mechanism in the piroplasm stage.

The region upstream of the consensus start ATG of TaR1 is 57% AT which is well below the mean %AT of 80% calculated by Yamauchi for the sporozoan mRNAs. It is possible that this high % plays a role specific for lower eukaryotes in translational efficiency. This figure is biased in favour of the large number of *Plasmodium* sequences in the database. If only *Babesia, Toxoplasma* and *Theileria* sequences are considered then the %AT falls to 60%. Coding regions tend to have 50-60% AT whilst non-coding intergenic regions contain ~70% AT. This suggests that the N-terminal region may well be translated. Complete clarification of the true translation start site will depend on further experiments aimed at direct N terminal sequencing of the purified protein from cell extracts or by generation of a specific anti-serum against either a peptide sequence from the putative N-terminal extension or a fusion protein made from this region.

The genomic sequencing could be completed which would show if there are any introns within in the genomic clone and if so, does the location match the intron site found in the *P. falciparum* R1 gene. The sequencing of the upstream region of the 5' end is discussed in chapter 5.

116

The identity of the cross-reacting protein of 45kDa seen on immunoblots with the CM97 anti-TaR1 anti-serum is unknown but it does appear to be parasite specific. It would be of interest to screen a library with this serum to try to isolate a cDNA clone expressing this molecule as results in chapter 6 suggests that it may be constitutively expressed in intracellular bovine stages at least.

Could Anti-sense oligonucleotides be targetted against TaR1?

One disadvantage of drugs interfering with protein function (i.e. postranslationally) is that usually only one or two point mutations are needed to cause resistance to the drug. Use of antisense deoxyribonucleotides (AS-ODN) to inhibit specific mRNA expression and translation would need several sequence mutations to destabilise binding of the AS-ODN and target sequence. The mechanism of action of AS-ODNs is either by steric blocking of gene expression or by activation of cellular RNAseH which cleaves the RNA component of the duplex. The blocking effect would prevent pre-mRNA splicing, polyadenylation or transport of the mRNA if the RNA/DNA hybrid forms in the nucleus. Within the cytoplasm the hybrid would block initiation of translation or ribosomal elongation (Sharma & Narayanan, 1995).

In vitro AS-ODN has been shown to inhibit the replication of *T. brucei* (Verspieren *et al.,* 1987) and *L. amazonensis* (Ramazeilles *et al.,* 1994). Work in *P. falciparum* using antisense oligos *in vitro* (Barker *et al.,* 1996) against a range of targets such as dihydrofolate reductase (DHFR), triose phosphate isomerase (TPI) and RR showed that they may have potential as chemotherapeutic agents but also as a molecular tool for examing gene function in relation to parasite biology. The oligonucleotides were modified by the addition of phosphorothioate bonds to reduce the nuclease sensitivity of the oligonucleotides. The inhibitory effects of the AS-ODNs on DNA synthesis was assayed by [^{3}H] hypoxanthine incorporation after addition of AS-ODN. A number of interesting conclusions arise from this study - antisense oligos are best designed against sequence downstream from the transcription start site and that they are specifically taken up into parasite infected erythrocytes. The exact mechanism of uptake is unknown but it probably involves changes in membrane permeability caused by the parasite. However, AS-ODNs will enter most cells and are now being used in clinical trials for HIV

117

treatment (Barker, pers.comm.). Work with AS-ODNs in *L. amazonensis* showed that linking the AS-ODN to a palmityl group enhanced the uptake into parasite infected macrophages which expressed an appropriate receptor on the surface(Mishra *et al.*, 1995). In *P. falciparum* the inhibitory effect of an AS-ODN complementary to the R2 mRNA sequence was assayed by labelled hypoxanthine incorporation. Significant inhibition was shown to occur at $1.0\mu M$ concentration for both asynchronous and synchronous cultures (Chakrabarti *et al.*, 1993). An alternative approach to blocking the expression of RR is to develop specific inhibitors of enzyme activity and Rubin (Univ.of Penn.) has been over-expressing the *P. falciparum* RR to provide sufficient material for inhibition assays (pers. comm.).

The only report of antisense RNA expression studies in *Theileria* is on *T. parva* infected cells by Eichhorn & Dobbelaere (1995). Their work builds on earlier findings that infected cells constitutively express IL-2 receptors which may be part of an autocrine loop for the continual proliferation of *T. parva* infected cells. Part of the bovine IL-2 α chain cDNA was cloned into a plasmid with an inducible promoter in both sense and anti-sense orientations. These constructs were transfected into *T. parva* infected cells and only the anti-sense configuration had a negative effect on growth rate under both induced and non-induced conditions. There was also a corresponding reduction in IL-2α chain mRNA in anti-sense transfected cells.

However, it may be difficult to get 100% inhibition of parasite growth with AS-ODN since they will be ineffective if the target enzyme is already present and has a long half life or if it is non-essential. Thus from what is known about the turnover of R1 and R2 in the mouse, it may well be that AS-ODN are not well suited for inhibition of the *Plasmodium* RR. However, nothing is known about the turnover in this parasite. The use of peptidomimetic inhibitors looks to be a more promising approach, particularly since they have been shown to be species specific inhibitors.

With respect to future work in *Theileria*, it will be necessary to isolate and characterise the small subunit. This will allow peptidomimetic inhibitors to be designed and tested on D7 cells. It may also be feasible, if the N-terminal extension was shown to be present in the mature polypeptide, to use peptides matching this region in inhibition assays as they are not likely to interfere with the host subunit.

Figure 4.1 Gap analysis of the predicted amino acid sequence of the 180bp PCR fragment to the *P. falciparum* R1 subunit

Figure 4.1a shows the predicted amino acid sequence of the PCR fragment. The GAP program was used to calculate the % identity and similarity over the region of the PCR fragment at the amino acid level to the R1 subunit from *P. falciparum* as shown on figure 4.1b.

Figure 4.1a

```
        CATATTGACGAAATCCCAAGCCACATCAAGGAACTATATAAAACTGTTTGGGAGATTAAG
   2221 ---------+---------+---------+---------+---------+---------+ 2280
        GTATAACTGCTTTAGGGTTCGGTGTAGTTCCTTGATATATTTTGACAAACCCTCTAATTC

a        H   I   D   E   I   P   S   H   I   K   E   L   Y   K   T   V   W   E   I   K    -

        CAGAAGCACATCATTGACATGGCAGCAGACCGTGGCATTTTCATTGACCAGTCACAGTCA
   2281 ---------+---------+---------+---------+---------+---------+ 2340
        GTCTTCGTGTAGTAACTGTACCGTCGTCTGGCACCGTAAAAGTAACTGGTCAGTGTCAGT

a        Q   K   H   I   I   D   M   A   A   D   R   G   I   F   I   D   Q   S   Q   S    -

        CTCAACATCCACATGGAACAGCCTACATTCAGTAAACTCACGAGCATGCACTTTTATGGC
   2341 ---------+---------+---------+---------+---------+---------+ 2400
        GAGTTGTAGGTGTACCTTGTCGGATGTAAGTCATTTGAGTGCTCGTACGTGAAAATACCG

a        L   N   I   H   M   E   Q   P   T   F   S   K   L   T   S   M   H   F   Y   G    -

        T
   2401 - 2401
        A

a        -
```

Figure 4.1b

```
        Gap Weight:   3.000       Average Match:    0.540
     Length Weight:   0.100    Average Mismatch:   -0.396

           Quality:   77.1              Length:      807
             Ratio:   1.285               Gaps:        0
 Percent Similarity: 86.667    Percent Identity:   80.000
```

```
  1 ................HIDEIPSHIKELYKTVWEIKQKHIIDMAADRGIFIDQSQSLNIHMEQPTFSKLTSMHFYG 60
                    .|.|||..:|||||||||||||:||||||||||||||||||||.::.|||.||.||||||
651 WDEDMKQQLIAHNGSIQYISEIPDDLKELYKTVWEIKQKNIIDMAADRGIFIDQSQSLNIYIQKPTFAKLSSMHFYG 750
```

Figure 4.2 Southern blot analysis of genomic DNA.

10 µg of BL20, cloned infected cell line D7 and 5µg of piroplasm DNA was digested with 3 different restriction enzymes and separated on a 0.8% agarose gel then transferred onto Hybond N membrane. The blot was then hybridised and washed by the Church & Gilbert SDS - phosphate method . The TaR1 PCR fragment was labelled by random priming with 50µCi of ^{32}P α dATP.

Key:

Panel A.	**Lane 1:**	BL20 genomic DNA digested with *Bam*HI.
	Lane 2:	BL20 genomic DNA digested with *Eco*RI.
	Lane 3:	BL20 genomic DNA digested with *Hind*III.
Panel B.	**Lane 1:**	D7genomic DNA digested with *Bam*HI.
	Lane 2:	D7 genomic DNA digested with *Eco*RI.
	Lane 3:	D7 genomic DNA digested with *Hind*III.
Panel C.	**Lane 1:**	Piroplasm genomic DNA digested with *Bam*HI.
	Lane 2:	Piroplasm genomic DNA digested with *Eco*RI.
	Lane 3:	Piroplasm genomic DNA digested with *Hind*III.

Sizes are as indicated to the left of the panel A in kb.

Size in
kB

10 →
9 →
8 →
7 →
6 →
5 →
4 →
3 →

2 →

```
                                                 M1
  1 TGATACAAACTCGTTATTTCCTTGATTGTTTTTAAAGTTAAGATGGATGCACATCAACAG 60
    *  Y  K  L  V  I  S  L  I  V  F  K  V  K  M  D  A  H  Q  Q

 61 GATCATAACAATACCACAAGTGGTTTTCCGCCTGAGGATGTGTCGGAAAGCTCACGTGGC 120
    D  H  N  N  T  T  S  G  F  P  P  E  D  V  S  E  S  S  R  G

121 TATGAGGACCACGATTTACCCTCAAATAAGTCCAGAGAGTCTGATCATGCCCACAATTCG 180
    Y  E  D  H  D  L  P  S  N  K  S  R  E  S  D  H  A  H  N  S

        M2                                  M3
181 CCAATGTTGAGTTTTTTTGGCGAGGCCGAGTCGAAGATAATGTACGTTATCAATAGGCAC 240
    P  M  L  S  F  F  G  E  A  E  S  K  I  M  Y  V  I  N  R  H

241 GGCGAGAAGGAAGATGTATCATTTGACAAGATTCTAAACCGCATCAGGAAGTTATCGCTG 300
    G  E  K  E  D  V  S  F  D  K  I  L  N  R  I  R  K  L  S  L

                             ←
301 GGACTGCACTCATTGGTGGATGCTCCACGAGTGACACAGAGCGTTATAAACGGAATGTAC 360
    G  L  H  S  L  V  D  A  P  R  V  T  Q  S  V  I  N  G  M  Y

361 ACAGGAATCCGAACGTCAGAACTGGACGAACTGGCTGCACAAACCTGCGCCTACATGGCT 420
    T  G  I  R  T  S  E  L  D  E  L  A  A  Q  T  C  A  Y  M  A

                                               →
421 GTGACGCACCCAGACTACTCTCGCCTAGCAGCCAACATCACCATAGATAACCTACACAAA 480
    V  T  H  P  D  Y  S  R  L  A  A  N  I  T  I  D  N  L  H  K

                     ←
481 AACACATCAAAAGATTTCAGCGAGGTGATCGAGGACGTGTATGATTATGTGAACGTTAAT 540
    N  T  S  K  D  F  S  E  V  I  E  D  L  Y  D  Y  V  N  V  N

541 GGACGGCCCTCAAGTCTGATAAGTGACGATGTGTTGGAGTTTGTTATGGAGAACAACGAC 600
    G  R  P  S  S  L  I  S  D  D  V  L  E  F  V  M  E  N  N  D

601 CGCTTGAACCGAGAAATAGACTATTCCCGTGATTTCCAGTACGACTACTTCGGCTTTAAG 660
    R  L  N  R  E  I  D  Y  S  R  D  F  Q  Y  D  Y  F  G  F  K

661 ACACTAGAGCGTTCGTATTTGCTGAACATTAACGGCAAGATCGTTGAGCGTCCACAGCAC 720
    T  L  E  R  S  Y  L  L  N  I  N  G  K  I  V  E  R  P  Q  H

721 ATGATAATGCGAGTTTCTGCAGGTATTCACTGCGGAGATTTGGAACGCACTATCCAAACA 780
    M  I  M  R  V  S  A  G  I  H  C  G  D  L  E  R  T  I  Q  T

781 TATCATCTTATGAGTCAGAGATATTTCACGCACGCGACCCCGACACTTTTCAATGCCGGC 840
    Y  H  L  M  S  Q  R  Y  F  T  H  A  T  P  T  L  F  N  A  G

                                               ←
841 ACCAAACACCCACAGATGTCGTCCTGTTTTCTTTTATCCATGAAAGACGACTCGCTGGCG 900
    T  K  H  P  Q  M  S  S  C  F  L  L  S  M  K  D  D  S  L  A

                                   →
901 GGAATTTTAACACACTGAGCCAGTGCGCCCTCATAAGTAAATCAGCTGGTGGGATAGGG 960
    G  I  F  N  T  L  S  Q  C  A  L  I  S  K  S  A  G  G  I  G

961 CTCGCGATTCACAAGATCAGAGCCAGCGGCTCGTACATTCGAGGTACAAACGGCATCTCA 1020
    L  A  I  H  K  I  R  A  S  G  S  Y  I  R  G  T  N  G  I  S

1021 AATGGGATTGTACCAATGCTAAAAATTTTTAACTCAACAGCCAAATATGTAGACCAGGGA 1080
    N  G  I  V  P  M  L  K  I  F  N  S  T  A  K  Y  V  D  Q  G

1081 GGTGGAAAGCGCAAAGGCTCGTTTGCGATATACCTGGAGCCCTGGCATGCTGACATTTTT 1140
    G  G  K  R  K  G  S  F  A  I  Y  L  E  P  W  H  A  D  I  F

1141 AAGCTGCTGGACCTCAGGAAAAACCACGGCTCAGAAGACCAGCGCGCACGCGACCTATTT 1200
    K  L  L  D  L  R  K  N  H  G  S  E  D  Q  R  A  R  D  L  F

1201 TACGCGCTTTGGATCCCCGACCTGTTCAGGAAACGTGTCGAGGCAAACAAGAACTGGACA 1260
    Y  A  L  W  I  P  D  L  F  R  K  R  V  E  A  N  K  N  W  T

1261 CTCATGTGCCCAGACGAGTGTCGAGGTTTGTATGAGGTCTGGGGAGACGAGTTCGAACGG 1320
    L  M  C  P  D  E  C  R  G  L  Y  E  V  W  G  D  E  F  E  R

1321 CTCTACACCCAGTACGAACAACAAGGGATGGGACGAAAAACAATTCCAGCCCAAAAACTG 1380
    L  Y  T  Q  Y  E  Q  Q  G  M  G  R  K  T  I  P  A  Q  K  L

              ←
1381 TGGTTCGCAATCCTACAGTCCCAAATCGAAACTGGGACCCCGTACATGTTATACAAGGAT 1440
    W  F  A  I  L  Q  S  Q  I  E  T  G  T  P  Y  M  L  Y  K  D

1441 GCATGCAACTCCAAGAGTAATCAGCAAAACTTGGGCACGATTAAATCTAGTAACCTGTGC 1500
    A  C  N  S  K  S  N  Q  Q  N  L  G  T  I  K  S  S  N  L  C

1501 TGCGAAATTGTTCAATTCACGAGCAAGGATGAGGTTGCAGTGTGTAATTTAGCGTCAGTA 1560
    C  E  I  V  Q  F  T  S  K  D  E  V  A  V  C  N  L  A  S  V
```

Figure 4.3a cDNA sequence of R1 subunit from *T. annulata*

This figure shows the nucleotide and predicted amino acid sequences of the cDNA clone encoding the large subunit of ribonucleotide reductase from *T. annulata*. The first three in frame start codons are marked in bold. Sequencing primers used are shown in greyscale with the direction of priming indicated by arrows. The *SphI* restriction sites used in the subcloning are shown by underlining. The *BamHI* site referred to in the genomic analysis is overlined. The *Sau3AI* site used in the cloning of the 3' end into the pGEX expression vector is shown overlined also. The location of the 180bp PCR fragment is indicated by the amino acid sequence in bold.

```
                                                M1
  1 TGATACAAACTCGTTATTTCCTTGATTGTTTTTAAAGTTAAGATGGATGCACATCAACAG 60
    *  Y  K  L  V  I  S  L  I  V  F  K  V  K  M  D  A  H  Q  Q

 61 GATCATAACAATACCACAAGTGGTTTTCCGCCTGAGGATGTGTCGGAAAGCTCACGTGGC 120
    D  H  N  N  T  T  S  G  F  P  P  E  D  V  S  E  S  S  R  G

121 TATGAGGACCACGATTTACCCTCAAATAAGTCCAGAGAGTCTGATCATGCCCACAATTCG 180
    Y  E  D  H  D  L  P  S  N  K  S  R  E  S  D  H  A  H  N  S

          M2                                    M3
181 CCAATGTTGAGTTTTTTTGGCGAGGCCGAGTCGAAGATAATGTACGTTATCAATAGGCAC 240
    P  M  L  S  F  F  G  E  A  E  S  K  I  M  Y  V  I  N  R  H

241 GGCGAGAAGGAAGATGTATCATTTGACAAGATTCTAAACCGCATCAGGAAGTTATCGCTG 300
    G  E  K  E  D  V  S  F  D  K  I  L  N  R  I  R  K  L  S  L

301 GGACTGCACTCATTGGTGGATGCTCCACGAGTGACACAGAGCGTTATAAACGGAATGTAC 360
    G  L  H  S  L  V  D  A  P  R  V  T  Q  S  V  I  N  G  M  Y

361 ACAGGAATCCGAACGTCAGAACTGGACGAACTGGCTGCACAAACCTGCGCCTACATGGCT 420
    T  G  I  R  T  S  E  L  D  E  L  A  A  Q  T  C  A  Y  M  A

421 GTGACGCACCCAGACTACTCTCGCCTAGCGGCGAACATCACCATTGATAACCTACACAAA 480
    V  T  H  P  D  Y  S  R  L  A  A  N  I  T  I  D  N  L  H  K

481 AACACATCAAAAGATTTCAGCGAGGTTGATCGAGGACCTGTATGATTATGTGAACGTTAAT 540
    N  T  S  K  D  F  S  E  V  I  E  D  L  Y  D  Y  V  N  V  N

541 GGACGGCCCTCAAGTCTGATAAGTGACGATGTGTTGGAGTTTGTTATGGAGAACAACGAC 600
    G  R  P  S  S  L  I  S  D  D  V  L  E  F  V  M  E  N  N  D

601 CGCTTGAACCGAGAAATAGACTATTCCCGTGATTTCCAGTACGACTACTTCGGCTTTAAG 660
    R  L  N  R  E  I  D  Y  S  R  D  F  Q  Y  D  Y  F  G  F  K

661 ACACTAGAGCGTTCGTATTTGCTGAACATTAACGGCAAGATCGTTGAGCGTCCACAGCAC 720
    T  L  E  R  S  Y  L  L  N  I  N  G  K  I  V  E  R  P  Q  H

721 ATGATAATGCGAGTTTCTGCAGGTATTCACTGCGGAGATTTGGAACGCACTATCCAAACA 780
    M  I  M  R  V  S  A  G  I  H  C  G  D  L  E  R  T  I  Q  T

781 TATCATCTTATGAGTCAGAGATATTTCACGCACGCGACCCCGACACTTTTCAATGCCGGC 840
    Y  H  L  M  S  Q  R  Y  F  T  H  A  T  P  T  L  F  N  A  G

841 ACCAAACACCCACAGATGTCGTCCTGTTTTCTTTTATCCATGAAAGACGACTCCCTGGCG 900
    T  K  H  P  Q  M  S  S  C  F  L  L  S  M  K  D  D  S  L  A

901 GGAATCTTTAACACACTGAGCCAGTGCGCCCTCATAAGTAAATCAGCTGGTGGGATAGGG 960
    G  I  F  N  T  L  S  Q  C  A  L  I  S  K  S  A  G  G  I  G

961 CTCGCGATTCACAAGATCAGAGCCAGCGGCTCGTACATTCGAGGTACAAACGGCATCTCA 1020
    L  A  I  H  K  I  R  A  S  G  S  Y  I  R  G  T  N  G  I  S

1021 AATGGGATTGTACCAATGCTAAAAATTTTTAACTCAACAGCCAAATATGTAGACCAGGGA 1080
    N  G  I  V  P  M  L  K  I  F  N  S  T  A  K  Y  V  D  Q  G

1081 GGTGGAAAGCGCAAAGGCTCGTTTGCGATATACCTGGAGCCCTGGCATGCTGACATTTTT 1140
    G  G  K  R  K  G  S  F  A  I  Y  L  E  P  W  H  A  D  I  F

1141 AAGCTGCTGGACCTCAGGAAAAAACCACGGCTCAGAAGACCAGCGCGCACGCGACCTATTT 1200
    K  L  L  D  L  R  K  N  H  G  S  E  D  Q  R  A  R  D  L  F

1201 CCAGCGCTTTGGATCCCCGACCTGTTCAGGAAACGTGTCGAGGCAAACAAGAACTGGACA 1260
    P  A  L  W  I  P  D  L  F  R  K  R  V  E  A  N  K  N  W  T

1261 CTCATGTGCCCAGACGAGTGTCGAGGTTTGTATGAGGTCTGGGGAGACGAGTTCGAACGG 1320
    L  M  C  P  D  E  C  R  G  L  Y  E  V  W  G  D  E  F  E  R

1321 CTCTACACCCAGTACGAACAACAAGGGATGGGACGAAAAACAATTCCAGCCCAAAAACTG 1380
    L  Y  T  Q  Y  E  Q  Q  G  M  G  R  K  T  I  P  A  Q  K  L

1381 TGGTTCGCAATCCTTACAGTCGCAAATCGAAACTGGGACCCCGTACATGTTATACAAGGAT 1440
    W  F  A  I  L  Q  S  Q  I  E  T  G  T  P  Y  M  L  Y  K  D

1441 GCATGCAACTCCAAGAGTAATCAGCAAAAACTTGGGCACGATTAAATCTAGTAACCTGTGC 1500
    A  C  N  S  K  S  N  Q  Q  N  L  G  T  I  K  S  S  N  L  C

1501 TGCGAAATTGTTCAATTCACGAGCAAGGATGAGGTTGCAGTGTGTAATTTAGCGTCAGTA 1560
    C  E  I  V  Q  F  T  S  K  D  E  V  A  V  C  N  L  A  S  V
```

```
1561 GCACTACCAAAATTCGTAAATACACAAACGAGGACATTTGACTTCAAAAAACTCTATGAA 1620
     A  L  P  K  F  V  N  T  Q  T  R  T  F  D  F  K  K  L  Y  E

1621 ATATGTCGTGTAATAACATACAACCTCAATAAAGTAATCGATAGGAATTATTACCCGGTG 1680
     I  C  R  V  I  T  Y  N  L  N  K  V  I  D  R  N  Y  Y  P  V

1681 AAACAAGCCAGGGCGTCTAATTTCAGACACAGACCCGATGGGTGTAGGAGTACAAGGTCTA 1740
     K  Q  A  R  A  S  N  F  R  H  R  P  M  G  V  G  V  Q  G  L

1741 GCAGATACGTTAGTGCTAATGAGTTACCCTTACAGTTCGACGGAGGCGAAAGAACTCAAC 1800
     A  D  T  L  V  L  M  S  Y  P  Y  S  S  T  E  A  K  E  L  N

1801 AAACGCATATTCGAAACCATGTATTATGCCTGTTTATCAGAGAGTATTGATTTGGCAAGA 1860
     K  R  I  F  E  T  M  Y  Y  A  C  L  S  E  S  I  D  L  A  R

1861 CAGTATGGAGCTTACGAGTCATATGTTGGGTCACCAGCTTCTAAGGGTTTACTACAATTT 1920
     Q  Y  G  A  Y  E  S  Y  V  G  S  P  A  S  K  G  L  L  Q  F

1921 GATATGTGGAACGCGAAAGTCCCAAATATGCTGTGGGACTGGGATAAACTTAAGGCAGAC 1980
     D  M  W  N  A  K  V  P  N  M  L  W  D  W  D  K  L  K  A  D

1981 CTACGTGAGCATGGGTTAAGAAATTCTTTATTTATTGCACCAATGCCTACAGCTAGTACC 2040
     L  R  E  H  G  L  R  N  S  L  F  I  A  P  M  P  T  A  S  T

2041 TCGCAGATTCTTGGTAACAATGAATCATTTGAGCCCTACACTAGCAACATTTATTACAGA 2100
     S  Q  I  L  G  N  N  E  S  F  E  P  Y  T  S  N  I  Y  Y  R

2101 AGGGTGTTAAGCGGTGAGTTTTTTGTGGTTAACCCTCATTTACTAAATGACCTGATTGAC 2160
     R  V  L  S  G  E  F  F  V  V  N  P  H  L  L  N  D  L  I  D

2161 TTGGGGCTCTGGAACGAGACAATGAAACAGAAGCTTATCGCCTACAACGGCTCACTAAAG 2220
     L  G  L  W  N  E  T  M  K  Q  K  L  I  A  Y  N  G  S  L  K

2221 CATATTGACGAAATCCCAAGCCACATCAAGGAACTATATAAAACTGTTTGGGAGATTAAG 2280
     H  I  D  E  I  P  S  H  I  K  E  L  Y  K  T  V  W  E  I  K

2281 CAGAAGCACATCATTGACATGGCAGCAGACCGTGGCATTTTCATTGACCAGTCACAGTCA 2340
     Q  K  H  I  I  D  M  A  A  D  R  G  I  F  I  D  Q  S  Q  S

2341 CTCAACATCCACATGGAACAGCCTACATTCAGTAAACTCACGAGCATGCACTTTTATGGC 2400
     L  N  I  H  M  E  Q  P  T  F  S  K  L  T  S  M  H  F  Y  G

2401 TGGAAAAAGGGTCTAAAAACAGGAGTTTACTACCTCAGGACTCAACCAGCCACAGATGCT 2460
     W  K  K  G  L  K  T  G  V  Y  Y  L  R  T  Q  P  A  T  D  A

2461 ATTAAATTCACAGTTGACGCGCTTCAATATCACAGCTGCGCAAAAAGCCGCGTGAAACCGGCC 2520
     I  K  F  T  V  D  A  S  I  S  Q  L  A  K  S  R  V  K  P  A

2521 AACTCAATCATGAGCGATGGTAACATGACTTCGATCATGAGTGACGGGACAATGTCAACG 2580
     N  S  I  M  S  D  G  N  M  T  S  I  M  S  D  G  T  M  S  T

2581 ACTGAAACTCTAGATGTGCTTCAACCCCTAGCATCAGTTGAAGAAACCAATAGAGACGAC 2640
     T  E  T  L  D  V  L  Q  P  L  A  S  V  E  E  T  N  R  D  D

2641 TTCGCCAGCGCCGACGAACCCCCAAATGTGTTCTCTAAATCCCAACCCCAACGAACCATGC 2700
     F  A  S  A  D  E  P  Q  M  C  S  L  N  P  N  P  N  E  P  C

2701 TTCATGTGGTCATCGTAGCCCACTAAAACTGTTGTAACCGGTTAAtttactaccaactttt 2760
     F  M  C  S  S  *  P  T  K  T  V  V  T  G  *

2761 ctttacataccaactttcacaaaaaaaaaaaaaaaaaaaaactca 2804
```

Figure 4.3b Restriction map of TaR1 cDNA
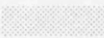
This figure shows the location of restriction sites in the TaR1 cDNA together with the region of the orginal PCR fragment isolated and the region of the 3' end used to make a fusion protein.

Scale: 1cm = 200bps

ATG - location of first methionine residue

■■■■ - location of PCR fragment isolated

** - stop codons

▭▭▭ - location of 3' region used for pGEX subcloning. *XbaI/ XhoI* fragment used as 3' probe for genomic analysis (170bps)

▬▬▬▬▬▬ - location of 5' probe used for genomic analysis (*PstI/XbaI* 770bps fragment).

▓ - multiple cloning site of pBluescript
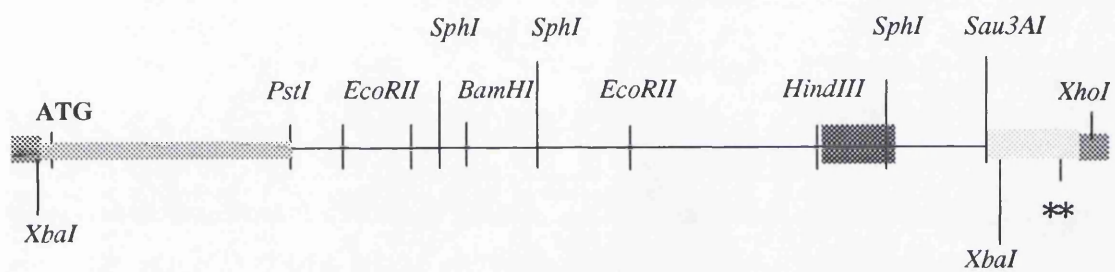
Figure 4.4 Pileup showing homology between prokaryotic and eukaryotic large subunits

This analysis was carried out using the PILEUP program in the GCG package. To generate optimal homologies between the subunits gaps are introduced - these are indicated by a dot. For clarity, only a selection of sequences available in the database have been used - a higher eukaryote, lower eukaryote, bacterium, viral and the 2 protozoan parasites. Numbering here is based on TaR1 using the third ATG as the start methionine based on homology. The region of TaR1 used to prepare a 3' specific fusion protein are listed in bold.

Key:

THEILERIA - *T. annulata*

PLASMODIUM - *P. falciparum*

HUMAN - *H. sapiens*

YEAST - *S. cerevisiae*

E. coli - *E. coli*

HSV - *Herpes simplex virus*

```
THEILERIA    *YKLVISLIV FKVKMDAHQQ DHNNTTSGFP PEDVSESSRG YEDHDLPSNK
PLASMODIUM   .......... .......... .......... ..MGDNVKRL PLPSENGEIK
HUMAN        .......... .......... .......... .......... ..........
YEAST        .......... .......... .......... .......... ..........
E. coli      .......... .......... .......... .......... ..........
HSV          .......... .......... .......... .......... ..........


                                           1                   27
THEILERIA    SRESDHAHNS PMLSFFGEAE SKIMYVINRH GEKEDVSFDK ILNRIRKLSL
PLASMODIUM   KSTSGRLSDD GIKRTPSGKP IQTMYVLNRK GEEEDISFDQ ILKRIQRLSY
HUMAN        .......... .......... ...MHVIKRD GRQERVMFDK ITSRIQKLCY
YEAST        .......... .......... ...MYVYKRD GRKEPVQFDK ITARISRLCY
E. coli      .......... .........M NQNLLVTKRD GSTERINLDK IHRVLDWAAE
HSV          .......... .......... .......... .......... ..........


             28                                            75
THEILERIA    GLH.SLVDAP RVTQSVINGM YTGIRTSELD ELAAQTCAYM AVTH.PDYSR
PLASMODIUM   GLH.ELVDPA RVTQGVINGM YSGIKTCELD ELAAQTCAYM ATTH.PDFSI
HUMAN        GLNMDFVDPA QITMKVIQGL YSGVTTVELD TLAAETAATL TTKH.PDYAI
YEAST        GLDPKHIDAV KVTQRIISGV YEGVTTIELD NLAAETCAYM TTVH.PDYAT
E. coli      GLHN..VSIS QVELRSHIQF YDGIKTSDIH ETIIKAAADL ISRDAPDYQY
HSV          .......... ........M SQETIISNLI DMLKVSAGW. ....DREANE


             76                                            124
THEILERIA    LAANITIDNL HKNTSKDFSE VIEDLYDYVN V.NGRPSSLI SDDVLEFVME
PLASMODIUM   LAARITTDNL HKNTSDDVAE VAEALYTYKD V.RGRPASLI SKEVYDFILL
HUMAN        LAARIAVSNL HKETKKVFSD VMEDLYNYIN PHNGKHSPMV AKSTLDIVLA
YEAST        LAARIAISNL HKQTTKQFSK VVEDLYRYVN AATGKPAPMI SDDVYNIVME
E. coli      LAARLAIFHL RKKAYGQFEP ..PALYDHV. VKMVEMGKYD NHLLEDYTEE
HSV          ISGRLFHKLM DMSSTETISQ YMSLF..... ......GPLL EPHILEFIQN


             125                                           164
THEILERIA    NNDRLNRE.I DYSRDFQY.. ....DYFGFK TLERSYLL.. NIN.GKIVER
PLASMODIUM   HKDRLNKE.I DYTRDFNY.. ....DYFGFK TLERSYLL.. RIN.NKIIER
HUMAN        NKDRLNSA.I IYDRDFSY.. ....NYFGFK TLERSYLL.. KIN.GKVAER
YEAST        NKDKLNSA.I VYDRDFQY.. ....SYFGFK TLERSYLL.. RIN.GQVAER
E. coli      EFKQMDTF.I DHDRDMTF.. ....SYAAVK QLEGKYLVQN RVT.GEIYES
HSV          YEQEIDEVCL EYRASYDFMC LRNCGILPAK RFYDTYVLPP RTEMNGKYES


             165                                           189
THEILERIA    PQHMIMRVSA GI.....HCG DLERTIQ... .......... .......TYH
PLASMODIUM   PQHLLMRVSI GI.....HID DIDKALE... .......... .......TYH
HUMAN        PQHMLMRVSV GI.....HKE DIDAAIE... .......... .......TYN
YEAST        PQHLIMRVAL GI.....HGR DIEAALE... .......... .......TYN
E. coli      AQFLYILVAA CLFSNYPRET RLQYVKR... .......... .......FYD
HSV          IPHFFARIAA YCAWNCIMCE PLKDTLVYVQ KRDWNVEIKT DMQIFKYFYK


             190                  216                  238
THEILERIA    LMSQRYFTHA TPTLFNAGTK HPQMSSCFLL SMKDDSLAG. IFNTLSQCAL
PLASMODIUM   LMSQKYFTHA TPTLFNSGTP RPQMSSCFLL SMKADSIEG. IFETLKQCAL
HUMAN        LLSERWFTHA SPTLFNAGTN RPQLSSCFLL SMKDDSIEG. IYDTLKQCAL
YEAST        LMSLKYFTHA SPTLFNAGTP KPQMSSCFLV AMKEDSIEG. IYDTLKECAL
E. coli      AVSTFKISLP TPIMSGVRTP TRQFSSCVLI E.CGDSLDS. INATSSAIVK
HSV          VISSQLVCCA TPVMRSAGVA GENLSSCFII APTLDTEKST ISSIFGELAP


             239                                           288
THEILERIA    ISKSAGGIGL AIHKIRASGS YIRGTNGISN GIVPMLKIFN STAKYVDQGG
PLASMODIUM   ISKTAGGIGV AVQDIRGQNS YIRGTNGISN GLVPMLRVFN DTARYVDQGG
HUMAN        ISKSAGGIGV AVSCIRATGS YIAGTNGNSN GLVPMLRVYN NTARYVDQGG
YEAST        ISKTAGGIGL HIHNIRSTGS YIAGTNGTSN GLIPMIRVFN NTARYVDQGG
E. coli      YVSQRAGIGI NAGRIRALGS PIRGGEAFHT GCIPFYKHFQ TAVKSCSQGG
HSV          LLASRSGVGV DVTKFSFGGK NIHSCLKLIN AQVEFF.... .......NDK


             289                                           338
THEILERIA    GKRKGSFAIY LEPWHADIFK LLDLRKNHGS EDQRARDLFY ALWIPDLFRK
PLASMODIUM   GKRKGSFAVY IEPWHSDIFE FLDLRKNHGK EELRARDLFY AVWVPDLFMK
HUMAN        NKRPGAFAIY LEPWHLDIFE FLDLKKNTGK EEQRARDLFF ALWIPDLFMK
YEAST        NKRPGAFALY LEPWHADIFD FIDIRKNHGK EEIRARDLFP ALWIPDLFMK
E. coli      V.RGGAATLF YPMWHLEVES LLVLKNNRGV EGNRVRHMDY GVQINKLMYT
HSV          SVRPVSVATY IEVWHCQIHE FLSAKLPENP D..RCNSIFQ GVCVPSLFFK
```

```
               339                                                382
THEILERIA   RVEANKN..W TLMCPDECRG LYEVW...GD EFERLYTQYE QQGMGRKT.I
PLASMODIUM  RVKENKN..W TLMCPNECPG LSETW...GE EFEKLYTKYE EENMGKKT.V
HUMAN       RVETNQD..W SLMCPNECPG LDEVW...GE EFEKLYASYE KQGRVRKV.V
YEAST       RVEENGT..W TLFSPTSAPG LSDCY...GD EFEALYTRYE KEGRG.KT.I
E. coli     RLLKGED..I TLFSPSDVPG LYDAFFADQE EFERLYTKYE KDDSIRKQRV
HSV         MYESDPNGLW YLFDPQDAPN LTRLY...GL EFEEEYLRLV SEKKY.KQSV

               383                               427 431
THEILERIA   PAQKLWFAIL QSQIETGTPY MLYKDACNSK SN.QQNLGTI KSSNLCCEIV
PLASMODIUM  LAQDLWFAIL QSQIETGVPY MLYKDSCNAK SN.QKNLGTI KCSNLCCEII
HUMAN       KAQQLWYAII ESQTETGTPY MLYKDSCNRK SN.QQNLGTI KCSNLCTEIV
YEAST       KAQKLWYSIL EAQTETGTPF VVYKDACNRK SN.QKNLGVI KSSNLCCEIV
E. coli     KAVELFSLMM QERASTGRIY IQNVDHCNTH SPFDPAIAPV RQSNLCLEIA
HSV         TLKSLMFSLI NTIIKTGSPY VISKEAMNKH HWYETQGEAI NCSNLCAEIV

               432             442                             465
THEILERIA   QFTSK..... ...DEVAVCN LASVALPKFV NT....... QTRTFDFKKL
PLASMODIUM  EYTSP..... ...DEVAVCN LASIALCKFV DL........ EKKEFNFKKL
HUMAN       EYTSK..... ...DEVAVCN LASLALNMYV .TSE....H. ...TYDFKKL
YEAST       EYSAP..... ...DETAVCN LASVALPAFI ETSE....DG KTSTYNFKKL
E. coli     LPTKPLNDVN DENGEIALCT LSAFNLGAI. .......... ....NNLDEL
HSV         QQPKQF.... .....TSTCN LANVCLPKCL NSSNFPYTCS NTAQFDFSKL

               466                                            515
THEILERIA   YEICRVITYN LNKVIDRNYY PVKQARASNF RHRPMGVGVQ GLADTLVLMS
PLASMODIUM  YEITKIITRN LDKIIERNYY PVKEAKTSNT RHRPIGIGVQ GLADTFMLLR
HUMAN       AEVTKVVVRN LNKIIDINYY PVPEACLSNK RHRPIGIGVQ GLADAFILMR
YEAST       HEIAKVVTRN LNRVIDRNYY PVEEARKSNM RHRPIALGVQ GLADTFMLLR
E. coli     EELAILAVRA LDALLDYQDY PIPAAKRGAM GRRTLGIGVI NFAYYLANDG
HSV         EYAVQAAVFI INACILSP.. SPTSSATVGQ RERSMGIGCH GLADVFSEMG

               516                                            563
THEILERIA   YPYSSTEAKE LNKRIFETMY YACLSESIDL AR..QYGAYE SYVGSPASKG
PLASMODIUM  YPYESDAAKE LNKRIFETMY YAALEMSVEL AS..IHGPYE SYQGSPASQG
HUMAN       YPFESAEAQL LNKQIFETIY YGALEASCDL AK..EQGPYE TYEGSPVSKG
YEAST       LPFDSEEARL LNIQIFETIY HASMEASCEL AQ..KDGPYE TFQGSPASQG
E. coli     KRYSDGSANN LTHKTFEAIQ YYLLKASNEL AK..EQGACP WFNETTYAKG
HSV         YGYLDLESEC LDRDIFETMY YTAVKTSSEI CSVGKGQPFA GFRKSKLAHG

               564                                            608
THEILERIA   LLQFDMWNAK VPN.....ML WDWDKLKADL REHGLRNSLF IAPMPTASTS
PLASMODIUM  ILQFDMWNAK VDN.....KY WDWDELKAKI RKHGLRNSLL LAPMPTASTS
HUMAN       ILQYDMWNVT .PT.....DL WDWKVLKEKI AKYGIRNSLL IAPMPTASTA
YEAST       ILQFDMWDQK .PY.....GM WDWDTLRKDI MKHGVRNSLT MAPMPTASTS
E. coli     ILPIDTYKKD LDTIANEPLH YDWEALRESI KTHGLRNSTL SALMPSETSS
HSV         VFHWATWDAM PQRVP....M KQWIHLQDNI KKFGVFNSQF IALMPTAGTS

               609                                            658
THEILERIA   QILGNNESFE PYTSNIYYRR VLSGEFFVVN PHLLNDLIDL GLWNETMKQK
PLASMODIUM  QILGNNESFE PYTSNIYYRR VLSGEFFVVN PHLLKDLFDR GLWDEDMKQQ
HUMAN       QILGNNESIE PYTSNIYTRR VLSGEFQIVN PHLLKDLTER GLWHEEMKNQ
YEAST       QILGYNECFE PVTSNMYSRR VLSGEFQVVN PYLLRDLVDL GIWDEGMKQY
E. coli     QISNATNGIE PPRGYVSIKA SKDGILRQVV PDY....... ..........
HSV         QLTGYTDSFY PYFANMSSKV SNKEEIMKPN ITFLKNVKPQ DL......CT

               659                                            707
THEILERIA   LIAYNGSLKH IDEIPSHIKE LYKTVWEIKQ KH.IIDMAAD RGIFIDQSQS
PLASMODIUM  LIAHNGSIQY ISEIPDDLKE LYKTVWEIKQ KN.IIDMAAD RGIFIDQSQS
HUMAN       IIACNGSIQS IPEIPDDLKQ LYKTVWEISQ KT.VLKMAAE RGAFIDQSQS
YEAST       LITQNGSIQG LPNVPQELKD LYKTVWEISQ KT.IINMAAD RSVYIDQSHS
E. coli     .......... .....EHLHD AYELLWEMPG NDGYLQLVGI MQKFIDQSIS
HSV         VRFYGGDVSM MPEDVSTRYK HFLTAFDYCP EAQ.MRRASI RAPYVDQSQS

               708                         737/738        750
THEILERIA   LNIHMEQPTF S.......KL TSMHFYGWKK GLKTGVYYLR TQPATDAIKF
PLASMODIUM  LNIYIQKPTF A.......KL SSMHFYGWEK GLKTGAYYLR TQAATDAIKF
HUMAN       LNIHIAEPNY G.......KL TSMHFYGWKQ GLKTGMYYLR TRPAANPIQF
YEAST       LNLFLRAPTM G.......KL TSMHFYGWKK GLKTGMYYLR TQAASAAIQF
E. coli     ANTNYDPSRF PSGKVPMQQL LKDLLTAYKF GVKT.LYYQN TRDGAEDAQ.
HSV         LTLFLTEENV QSAKY....L KDLLLLGFRL GLKTIMYYCR VKKTTKLLQL
```

```
          751                                        797
THEILERIA  TVD...ASIS QLAKSRVKPA NSIMSDGNMT SIMSDGTMST TETLDVLQPL
PLASMODIUM TVD...T... HVAKNAVKLK NA..DGVQIT REVSRETIST ESTV......
HUMAN      TLNK..EKLK DKEKVSKEEE EKERNTAAMV CSLENRDEC. ..........
YEAST      TID...QKIA DQATENVADI SNLKRPSYMP SSASYAASDF VPAAVTANAT
E. coli    .......... DDLVPSIQDD GCESGA.... .......... ..........
HSV        ECLKLDEHTK KDAQIVLADL ARELPDSHKT EDACPLDQSE CIACQ.....

          798                             828
THEILERIA  ASVEETNRDD FASADEPQMC SLNPNPNEPC F......... ..........
PLASMODIUM .......... .....TQNVC PLRRNNDEQC L......... ..........
HUMAN      .......... .......... .......... L......... PEVPAPTKNE
YEAST      IPSLDSSSEA SREASPAPTG SHSLTKGMAE LNVQESKVEV PEVPAPTKNE
E. coli    .......... .......... .......... .......... ..........
HSV        .......... .......... .......... .......... ..........

                                                    832
THEILERIA  .......... .......... .......... ...MCSS*
PLASMODIUM .......... .......... .......... ...MCSG*
HUMAN      .......... .......... .......... ...MCGS*
YEAST      EKAAPIVDDE ETEFDIYNSK VIACAIDNPE ACEMCSG*
E. coli    .......... .......... .......... ....CKI*
HSV        .......... .......... .......... .......
```

Figure 4.5 Functional conservation of residues implicated in thioyl transfer reaction of the large subunit.

This figure shows the conservation of several cysteine residues shown to be involved in the reaction mechanism of the *E. coli* R1 (Ekland *et al.*, 1996, Uhlin & Eklund, 1994). The first number refers to the amino acid sequence of the *E. coli* subunit, the second number in brackets corresponds to the *T. annulata* residue.

Block 1 Cys 225 (Cys 216)

```
E. coli       TRQFSSCVLI
THEILERIA     HPQMSSCFLL
PLASMODIUM    RPQMSSCFLL
HUMAN         RPQLSSCFLL
YEAST         KPQMSSCFLV
HSV           GENLSSCFII
```

Block 2 Cys 439 (Cys 427)

```
E. coli       RQSNLCLEIA
THEILERIA     KSSNLCCEIV
PLASMODIUM    KCSNLCCEII
HUMAN         KCSNLCTEIV
YEAST         KSSNLCCEIV
HSV           NCSNLCAEIV
```

Block 3 Cys 462 (Cys 442)

```
E. coli       GEIALCTLSAFNL
THEILERIA     DEVAVCNLASVAL
PLASMODIUM    DEVAVCNLASIAL
HUMAN         DEVAVCNLASLAL
YEAST         DETAVCNLASVAL
HSV           ...TSTCNLANVCL
```

Block 4 Cys 759 (Cys 830)

```
THEILERIA. ..MCSS*
PLASMODIUM...MCSG*
HUMAN       ...MCGS*
YEAST       ACEMCSG*
E. coli     ....CKI*
HSV         .......*
```

Block 5 Tyr730/731 (Tyr 737/738)

```
E. coli       GVKT.LYYQNTRDG
THEILERIA     GLKTGVYYLRTQPA
PLASMODIUM    GLKTGAYYLRTQAA
HUMAN         GLKTGMYYLRTRPA
YEAST         GLKTGMYYLRTQAA
HSV           GLKTIMYYCRVKKT
```

Figure 4.6 GAP program in GCG used to show homology between mouse and *Theileria* regions implicated in R1/R2 binding.

This figure shows the homology over 2 regions of the large subunits of mouse and *Theileria* RR which have been implicated in the binding of the large subunit to the small subunit. The second region (778-789 in the mouse R1) has a gaps introduced, indicated by dots to maximise the line up with the same region in the *Theileria* R1. The percentage similarity and identity is as calculated by the GAP program in the GCG package.

Region 1 - residues 724 - 736

```
Percent Similarity: 92%
Percent Identity:   85%


Mouse        724 HFYGWKQGLKTGM 736
                 ||||||.|||||:
Theileria    724 HFYGWKKGLKTGV 736
```


Region 2 - residues 778 - 789 (816 - 829 in TaR1)

```
Percent Similarity: 75%
Percent Identity:   50%

.
Mouse        778 VCSL..ENREECLM 789
                 :|||   : .|.|:|
Theileria    816 MCSLNPNPNEPCFM 829
```

Figure 4.7 Homology between region implicated in R1 subunit dimerisation from studies in HSV.

This figure shows a PILEUP of the eukaryotic R1 subunits with the region 420-440 of HSV R1 which was shown to be important in R1 subunit dimerisation (Connor *et al.*, 1993).

Region 421 - 434 of HSV R1 implicated in dimerisation in bold

```
HSV          NSSNFPYTCSNTAQFDFSKL
THEILERIA    NT.......QTRTFDFKKL
PLASMODIUM   DL.......EKKEFNFKKL
HUMAN        .TSE....H....TYDFKKL
YEAST        ETSE....DGKTSTYNFKKL
```

Figure 4.8 TaR1 cDNA clone contains 3 in frame ATG translational start codons

The cDNA clone encoding TaR1 extends for 229 bps upstream from the consensus start codon found in the higher eukaryotic R1 genes. This figure shows this region with the in frame start codons marked in bold. Below this is a comparison of the sequence flanking the putative translational start codons with the consensus sequence for a translational initiation site in protozoa (Yamauchi, 1991). The fit to this consensus is given to the right of the sequence, expressed as % of nucleotides matching the consensus.

```
  1   TGCTTCCTTC TGATACAAAC TCGTTATTTC CTTGATTGTT TTTAAAGTTA
          M1
 51   AGATGGATGC ACATCAACAG GATCATAACA ATACCACAAG TGGTTTTCCG

101   CCTGAGGATG TGTCGGAAAG CTCACGTGGC TATGAGGACC ACGATTTACC
                                                        M2
151   CTCAAATAAG TCCAGAGAGT CTGATCATGC CCACAATTCG CCAATGTTGA
                                          M3
201   GTTTTTTTGG CGAGGCCGAG TCGAAGATA ATG
```
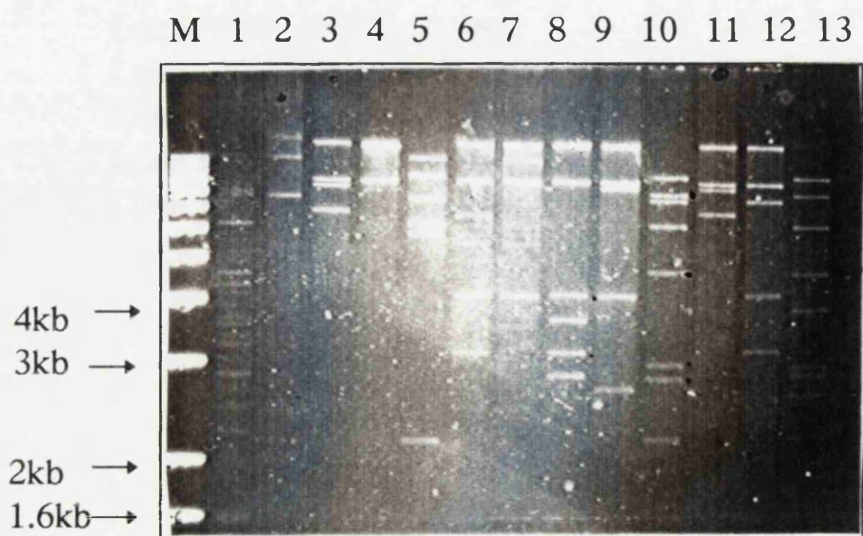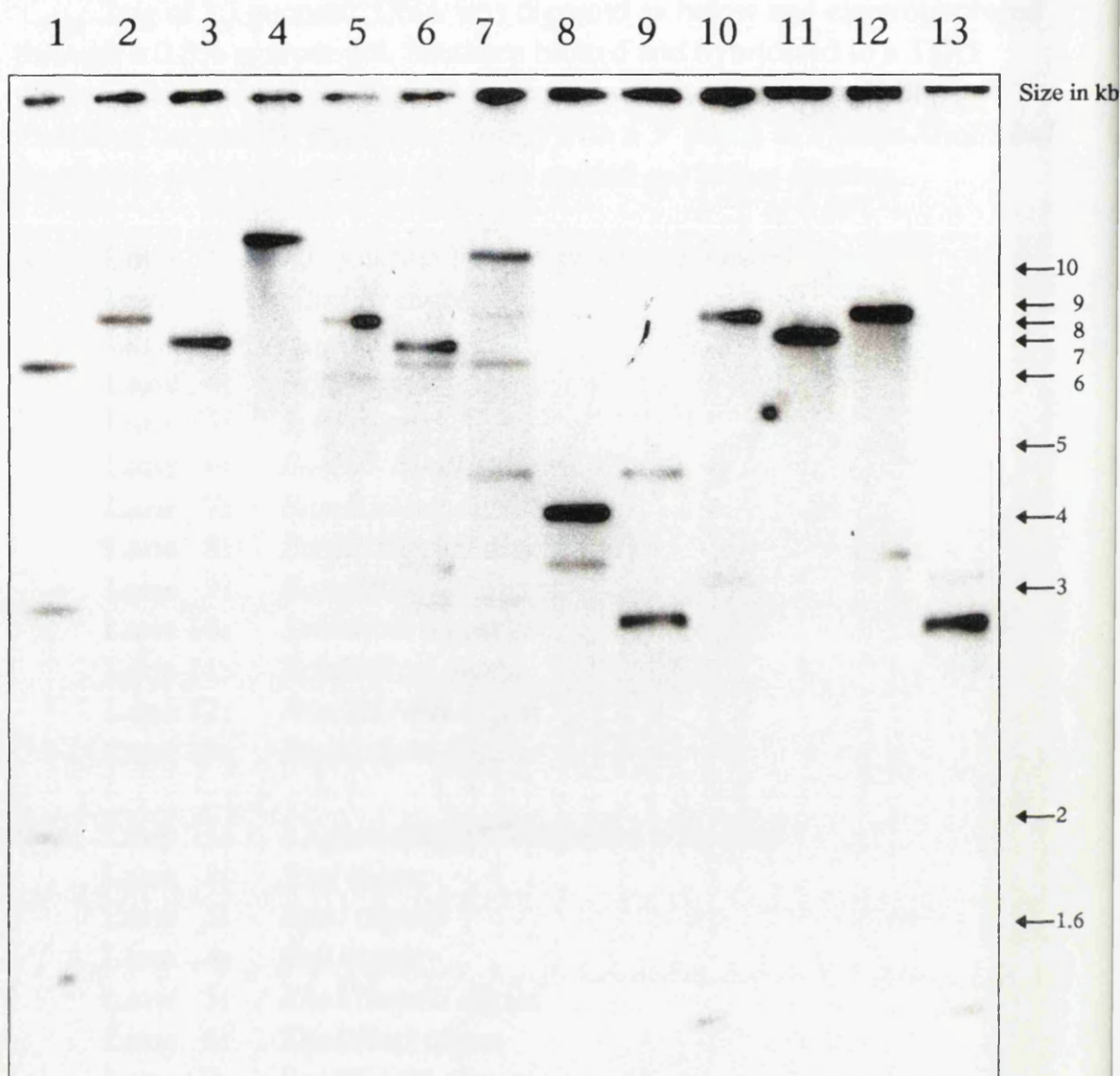
Consensus	a/t	t/a	NTTNT	t/a	NAAAAatgA	a/g	a/t	% Fit to consensus sequence
M1	T	T	TTAAA	G	TTAAGatgG	A	T	75%
M2	C	C	ACAAT	T	CGCCAatgT	T	G	37%
M3	C	G	AGTCG	A	AGATAatgG	T	A	56%

Figure 4.9 Southern blot analysis of genomic clone λ3.

1μg of λ3 genomic DNA was digested as below and electrophoresed through a 0.8% agarose gel, Southern blotted and hybridised to a TaR1 probe as detailed below. Panel A is probed with a 5' probe (a 770bps *PstI/XbaI* fragment). Panel B is probed with a 3' probe (a 170bps *XhoI/XbaI* fragment). Below each is the ethidium stained gel before blotting.

A. Lane 1: λ3 genomic DNA digested with *BamHI*
    Lane 2: *Hind III* digest
    Lane 3: *EcoRI* digest
    Lane 4: *NotI* digest
    Lane 5: *SphI* digest
    Lane 6: *BamHI/HindIII* digest
    Lane 7: *BamHI/NotI* digest
    Lane 8: *EcoRI/HindIII* digest
    Lane 9: *BamHI/EcoRI* digest
    Lane 10: *SphI/NotI* digest
    Lane 11: *EcoRI/NotI* digest
    Lane 12: *HindIII/NotI* digest
    Lane 13: *EcoRI/SphI* digest

B. Lane 1: λ3 genomic DNA digested with *XhoI*
    Lane 2: *SacI* digest
    Lane 3: *KpnI* digest
    Lane 4: *SalI* digest
    Lane 5: *XhoI/BamHI* digest
    Lane 6: *XhoI/NotI* digest
    Lane 7: *SacI/EcoRI* digest
    Lane 8: *SacI/NotI* digest
    Lane 9: *KpnI/EcoRI* digest
    Lane 10: *KpnI/BamHI* digest
    Lane 11: *SalI/EcoRI* digest
    Lane 12: *SalI/NotI* digest

A

1 2 3 4 5 6 7 8 9 10 11 12 13

Size in kb

←10
←9
←8
←7
←6
←5
←4
←3
←2
←1.6

M 1 2 3 4 5 6 7 8 9 10 11 12 13
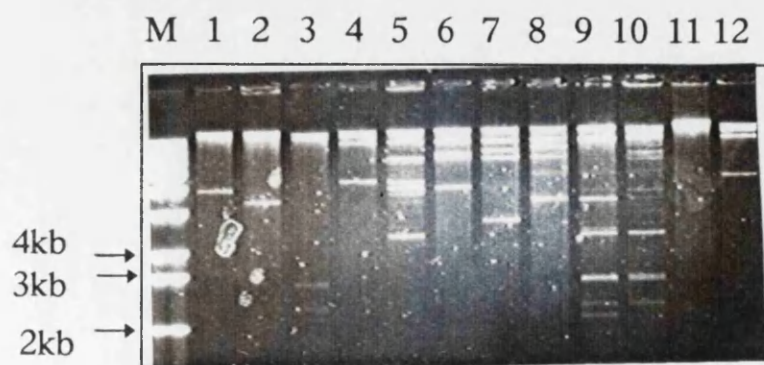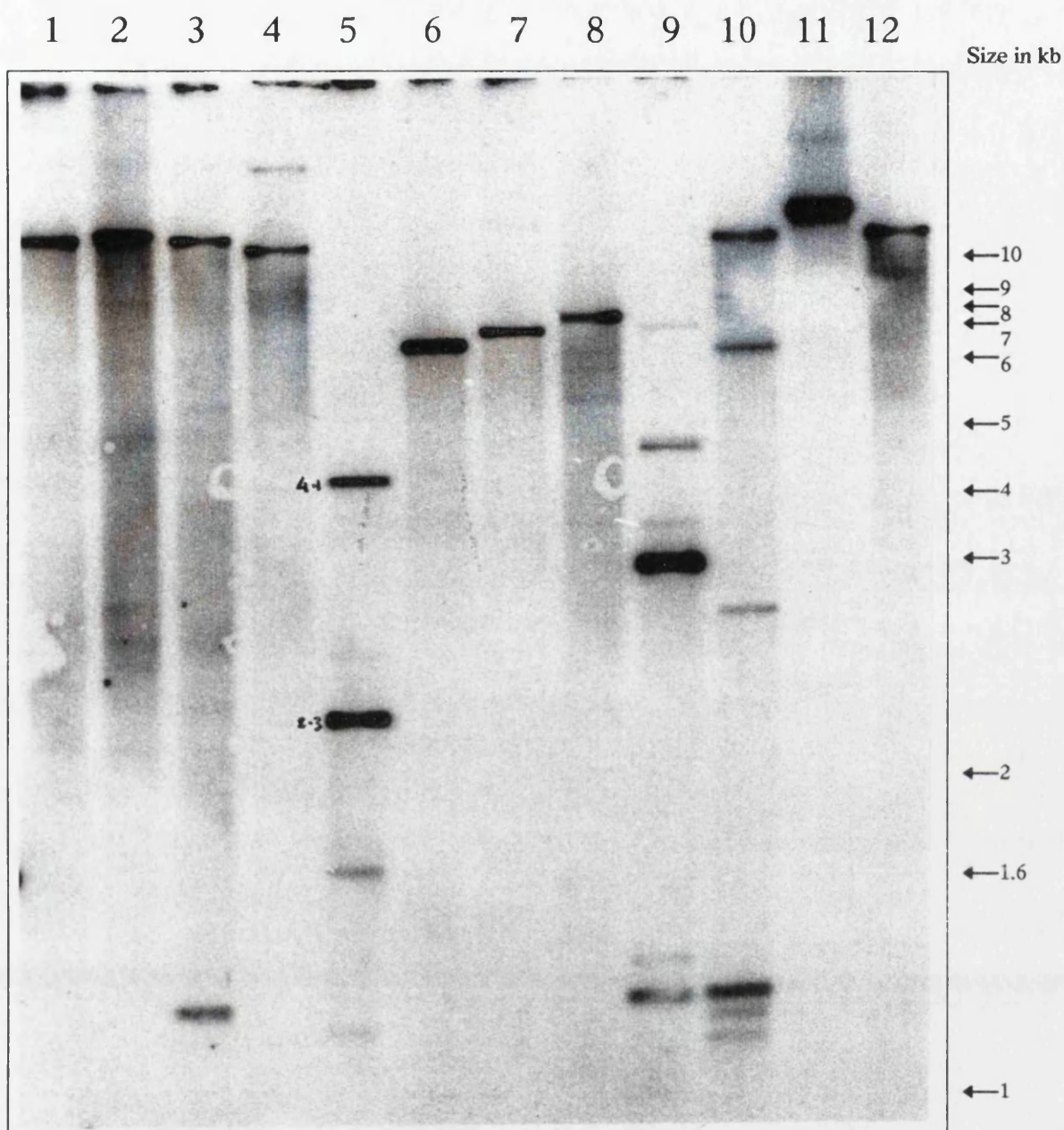
4kb →
3kb →

2kb →
1.6kb →

B

Figure 4.10 Restriction map of the TaR1 genomic clone (λ3)

This figure shows the restriction mapping of the genomic clone together with the regions hybridising with the 5' and 3' probes from the TaR1 cDNA clone. A 2.7kB *EcoRI/ BamHI* fragment was subcloned into the pBluescript vector for sequencing and restriction analysis. The hatched lines show the regions of the λ3 clone hybridising with TaR1 cDNA clones. The 5' sequence from the *BamHI* site is given below. The *BamHI* site is shown in bold.
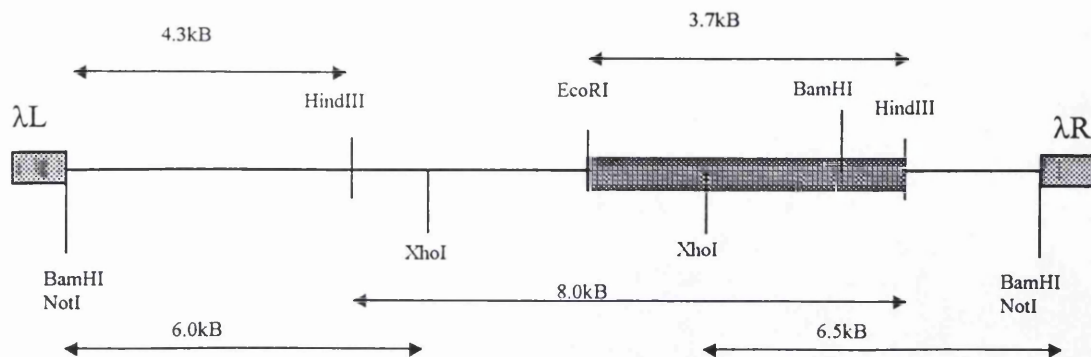
```
          G  I  G  L  A  I  H  K  I  R  A  S  G  S  Y  I  R  G  T  N
cDNA  TGGGATAGGGCTCGCGATTCACAAGATCAGAGCCAGCGGCTCGTACATtCGAGGTACAAA
      ||||||||||||||||||||||||||||||||||||||||||||||||||||||||||||
gDNA  TGGGATAGGGCTCGCGATTCACAAGATCAGAGCCAGCGGCTCGTACATTCGAGGTACAAA

          G  I  S  N  G  I  V  P  M  L  K  I  F  N  S  T  A  K  Y  V
cDNA  CGGCATCTCAAATGGGATTGTACCAATGCTAAAAATTTTTAACTCAACAGCCAAATATGT
      ||||||||||||||||||||||||||||||||||||||||||||||||||||||||||||
gDNA  CGGCATcTCAAATGGGATTGTACCAATGCTAAAAATTTTTAAcTCAACAGCCAAATATGT

          D  Q  G  G  G  K  R  K  G  S  F  A  I  Y  L  E  P  W  H  A
cDNA  AGACCAGGGAGGTGGAAAGCGCAAAGGCTCGTTTGCGATATACCTGGAGCCCTGGCATGC
      ||||||||||||||||||||||||||||||||||||||||||||||||||||||||||||
gDNA  AGACCAGGGAGGTGGAAAGCGCAAAGGCTCGTTTGCGATATACCTGGAGCCCTGGCATGC

          D  I  F  K  L  L  D  L  R  K  N  H  G  S  E  D  Q  R  A  R
cDNA  TGACATTTTTAAGCTGCTGGACCTCAGGAAAAACCACGGCTCAGAAGACCAGCGCGCACG
      ||||||||||||||||||||||||||||||||||||||||||||||||||||||||||||
gDNA  TGACATTTTTAAGCTGCTGGACCTCAGGAAAAACCACGGCTCAGAAGACCAGCGCGCACG

          D  L  F  Y  A  L  W  I  P  D  L  F  R  K
cDNA  CGACCTATTTTACGCGCTTT*GGATCC*CCGACCTGTTCAGGAAA
      ||||||||||  ||||||  ||  |||||||||
gDNA  CGACCTATTGTACGCCCTCT*GGATCC*
```

Figure 4.11 Northern blot analysis of TaR1 expression in bovine life cycle stages.

10μg of total RNA from BL20, D7@37 , D7@41(day7) cells and piroplasm were separated on a 1% formaldehyde agarose gel and blotted onto Hybond C membrane. Labelling of probe and hybridisations were as described in chapter 2.

Panel A shows the hybridisation signal with the 180bp PCR fragment used as a probe for TaR1.

Panel B shows the signal obtained with the *T. annulata* DNA polymerase δ subunit probe using a *HindIII* fragment from the coding region of the genomic clone.

Panel C shows the signal with the *T. annulata* tubulin probe.

Panel D shows the ethidium stained gel

Key:

Lane 1:   BL20 total RNA

Lane 2:   D7(37°C) total RNA

Lane 3:   D7(41 °C) total RNA
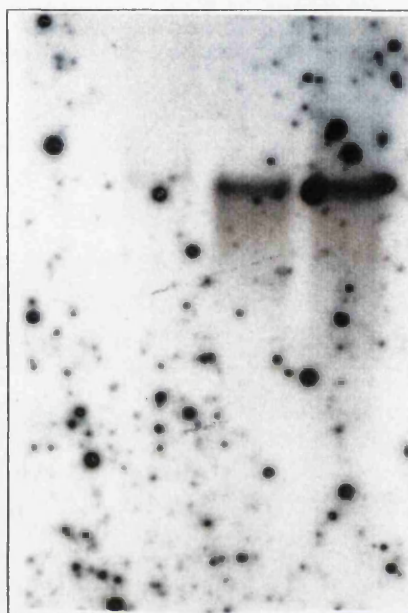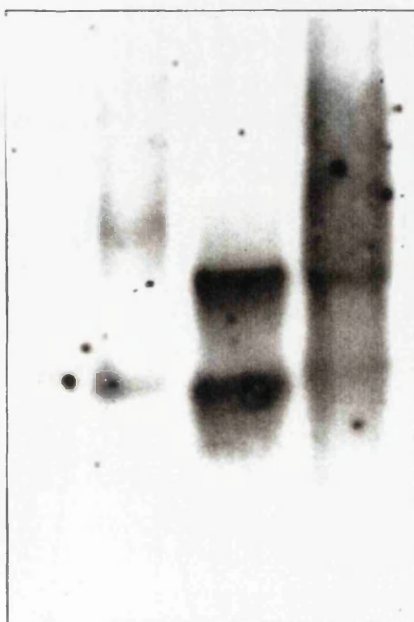
Lane 4:   Piroplasm total RNA

A

1   2   3   4

← 2.8kb

B

1   2   3   4

← 3.4kb

C

1   2   3   4

← 3.2kb

← 1.8kb

D

1 2   3 4

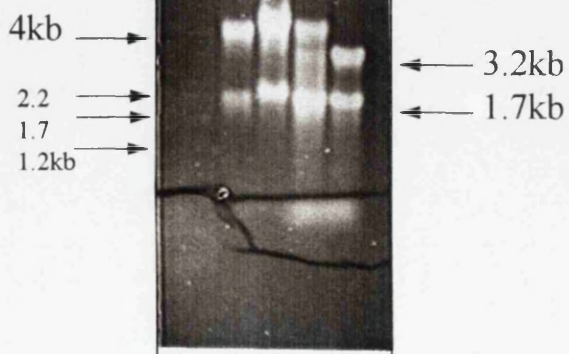4kb →

2.2 →
1.7 →

1.2kb →

← 3.2kb

← 1.7kb
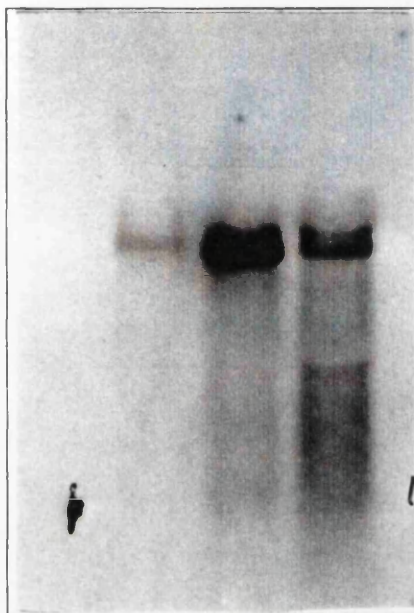
Figure 4.12 Expression and purification of TaR1 fusion protein.

Bacterial lysate was prepared by re-suspending cell pellets in SDS-sample buffer and running lysate on a 12.5% SDS-PAGE gel (lanes 2 & 3). The purified protein was prepared by resuspension of the bacterial pellet, sonication in non-denaturing buffer, centrifuging, then further purification from the supernatent (lane 4)by GST affinity chromatography according to the manufacturer's instructions (lane 5).

Key:

Lane 1   Protein molecular weight markers.

Lane 2   Clone containing expression plasmid prior to induction.

Lane 3   Clone after 2 hour induction.

Lane 4   Sonicate of induced clone.

Lane 5   Purified fusion protein after elution from GST column.

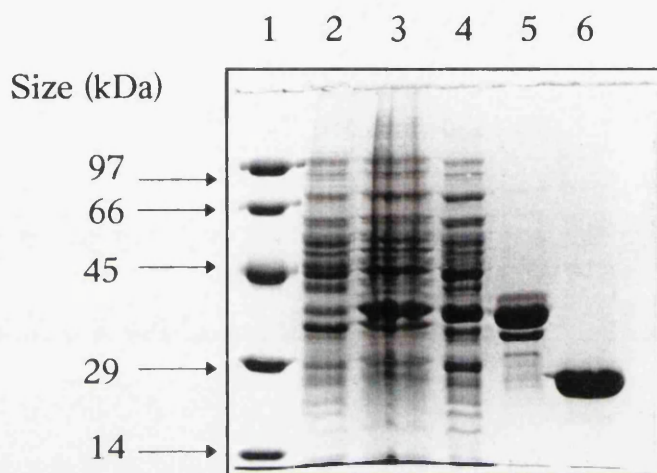**Lane 6**   Purified GST protein from vector only expression.

Figure 4.13 TaR1 sera recognises 2 proteins from piroplasm extracts only.

BL20 and piroplasm extracts were prepared as described in Section 2.5 and separated on an 8% SDS-Page gel. The proteins were then transferred onto Hybond C membrane (Amersham) and stained with 0.3% Ponceau S to assess equal protein loadings. The blots were then incubated with block buffer prior to the primary antibody being applied. Development of signal was using the ECL system (Amersham).

Lane 1:   BL20 extracts

Lane 2:   Piroplasm extracts

Panel A shows the reactivity of the CM82 pre-immune sera and sera from the final bleed. Sizes are as indicated next to panels. Both are at a 1/200 dilution.

Panel B shows the reactivity of the CM97 pre immune sera and sera from the final bleed at a 1/200 dilution. Lanes 1 and 2 are as above.

Panel C shows the reactivity of CM97 sera after pre-incubation with either purified GST protein or fusion protein.

A **CM82**

Pre Immune   Final Bleed

1   2   1   2

← 97kDa
← 66kDa

← 45kDa

B **CM97**

Pre Immune   Final Bleed

1   2   1   2

← 97kDa
← 66kDa

← 45kDa

C **CM97**

+GST protein   + fusion protein

1   2   1   2

← 97kDa
← 66kDa

← 45kDa

Figure 4.14 Immunofluorescence shows both CM82 &CM97 sera to react with schizont nuclei in D7 cells.

BL20 and D7 cells were transferred onto lysine coated slides by centrifugation in a Cytospin (Shandon Instruments). The slides were then fixed in 4% formaldehyde at room temperature for 10 minutes, prior to permeabilisation in 0.25% Triton X100 for 10 minutes again at room temperature. The slides were then pre-incubated with TBL medium for 1 hour in a humidified chamber then rinsed in PBS. The CM97 antibody was then applied at a dilution of 1/100 and incubated for 2 hours at room temperature. The slides were then rinsed in PBS and the FITC conjugated secondary antibody was then applied for 1 hour. The slides were rinsed for a final time, mounted with a DABCO/DAPHI solution and a coverslip attached. Pictures were taken on a MC100 spot camera attached to a Zeiss Axioplan microscope.

Panel A shows DAPHI staining of D7 cells.

Panel B shows the same D7 cells stained with the FITC conjugated antibody detecting labelling with CM82 antibody

Panel C shows BL20 cells stained with DAPHI.

Panel D shows the same cells in Panel C stained with the CM82 antibody via the FITC staining.
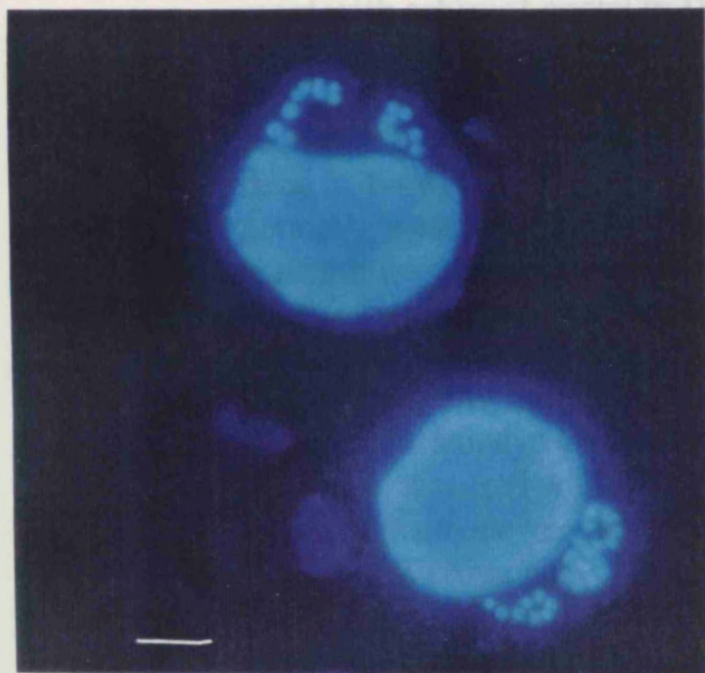
Panel E shows D7 cells reacting with DAPHI stain

Panel F shows the same cells reacting with CM97 antibody detected by FITC staining

Panel G shows D7 cells DAPHI stained

Panel H shows D7 cells reactive to the pre-immune sera from CM97 detected by anti-rabbit conjugated FITC anti-serum.

Magnification is at X100 (scale bar is 2µm) save for panels C+D which are at X40 (scale bar is 5µm).

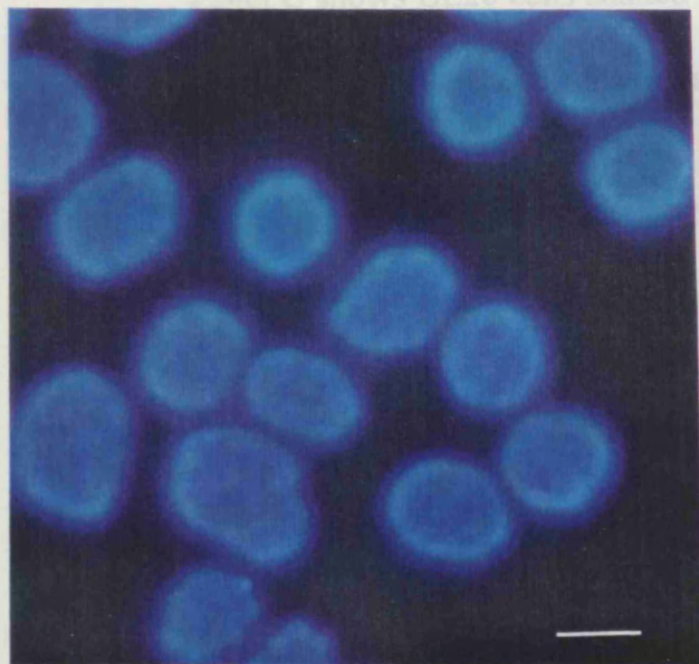**Figure** ... **Immunofluorescence shows both CM82 & CM97 sera to** ... **D7 cells** ...

Panel B shows the same D7 cells stained with the FITC conjugated antibody detecting labelling with CM82 antibody

Panel C shows BL20 cells stained with DAPHI
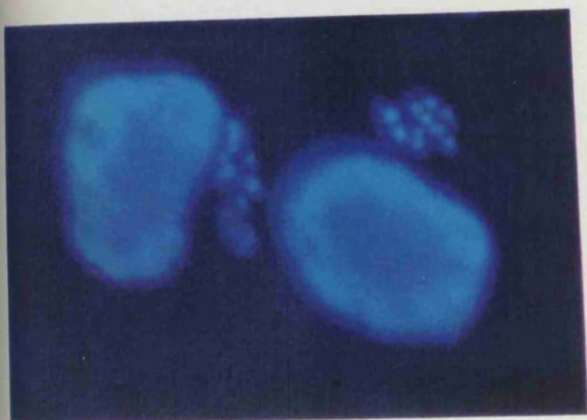
... save for panels C+D which ... at X40 (scale bar is 2μm)
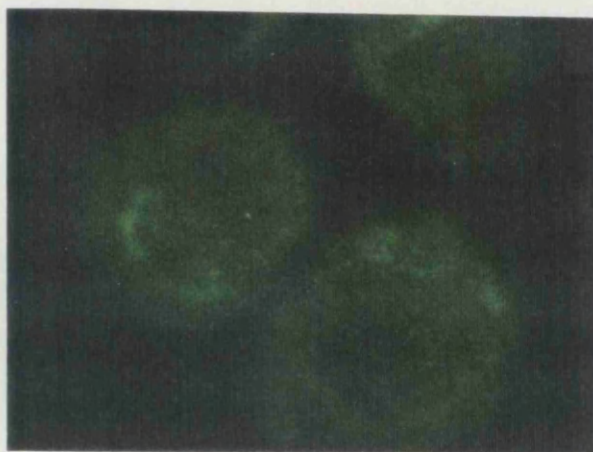
E

F

G

H

Figure 4.15 Immunofluorescence shows Ab0223 mAb to react with bovine cytoplasm only.

BL20 and D7 slides were prepared as detailed in Figure 4.12. The antibodies used were a mouse monoclonal against an unmapped epitope of the mouse R1 subunit and an anti-mouse FITC conjugate. Fixation and permeabilisation is as detailed in Fig. 4.12.

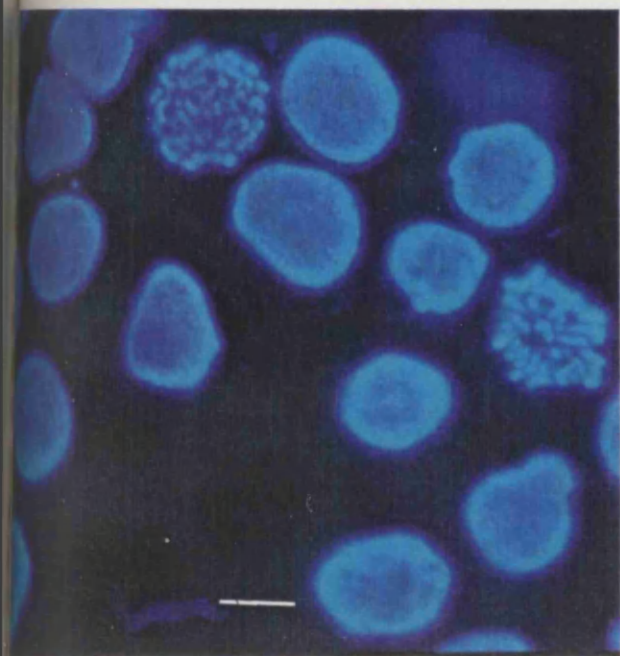Panel A shows DAPHI staining of BL20 cells.

Panel B shows the same BL20 cells stained with the FITC conjugated antibody.

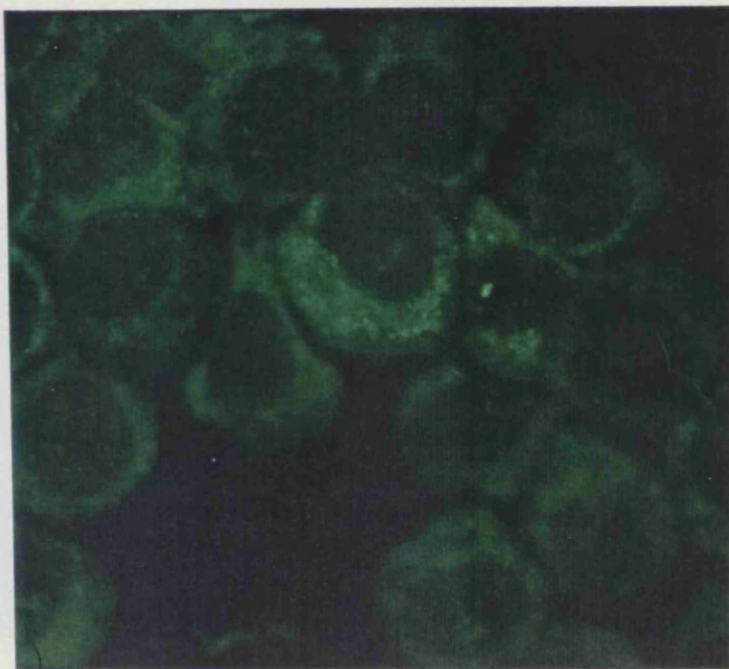Panel C shows D7 cells stained with DAPHI.

Panel D shows the same cells in Panel C stained with the monoclonal antibody via the FITC staining.

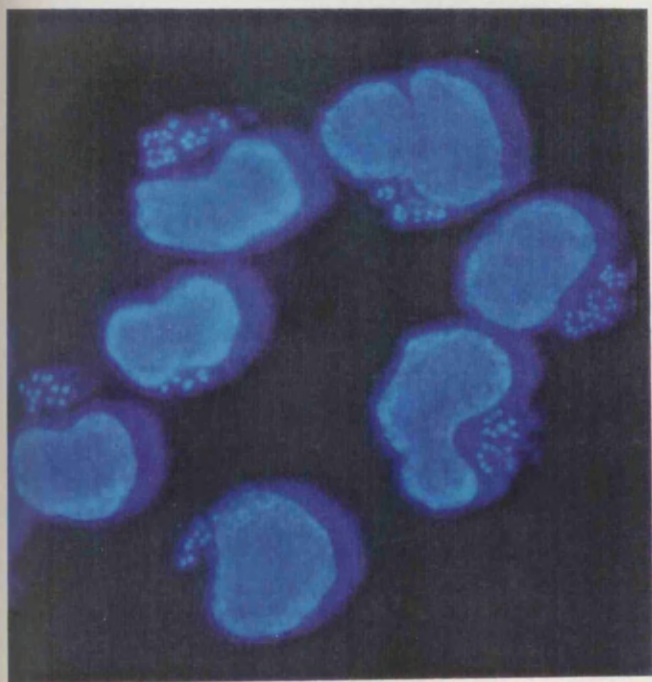Magnification is at X40 with the scale bar representing 5μm.
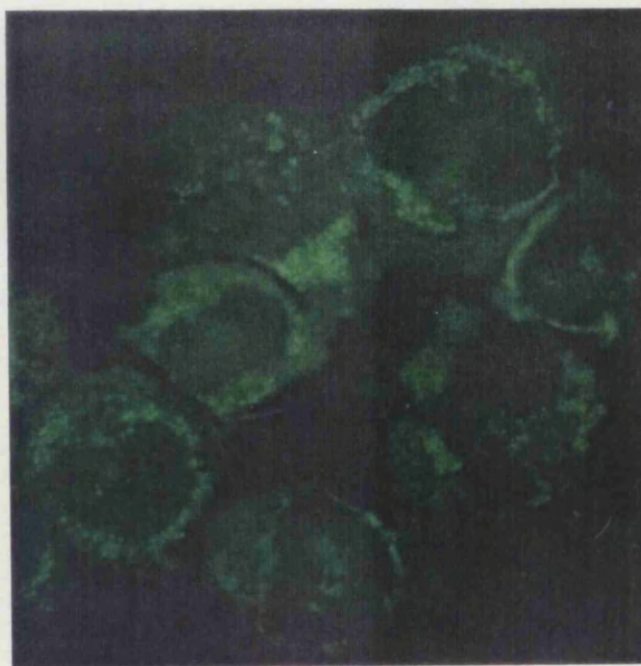
A

B

C

D

Table 4.1 Homologies at amino acid level of R1 subunits from various organisms

This table shows the homologies at amino acid level between the various R1 subunits isolated from different organisms present in the GenBank/EMBL database using the GAP analysis programme. For each comparative pair two values are given, the first is the % identity and the second is the % similarity. The % identity is a measure of absolute amino acid conservation between the pair and the % similarity takes account of conservative amino acid changes. The pairwise comparisons were carried out using the complete coding sequence from each species.

Key:

Ta - *Theileria annulata*

Pf - *Plasmodium falciparum*

Hs - Human

Mm - Mouse

Sp - *Schizosaccharomyces pombe*

Sc - *Saccharomyces cerevisiae*

Va - Vaccinia virus

Ec - *E. coli*

	Ta	Pf	Hs	Mm	Sp	Sc	Va	Ec
Ta	-	72/84	70/82	70/82	66/84	67/83	66/80	28/46
Pf	72/84	-	66/79	66/79	65/84	69/86	66/82	28/44
Hs	70/82	66/79	-	97/98	72/87	68/84	76/89	33/48
Mm	70/82	66/79	97/98	-	72/87	68/84	76/89	33/48
Sp	66/84	65/84	72/87	72/87	-	76/88	66/83	27/45
Sc	67/83	69/86	68/84	68/84	76/88	-	66/81	22/41
Va	66/80	66/82	76/89	76/89	66/83	66/81	-	29/48
Ec	28/46	28/44	33/48	33/48	27/45	22/41	29/48	-

Chapter Five

Regulation of Expression

of the

Large Subunit

of

Ribonucleotide Reductase

from

Theileria annulata

5.1.1 Introduction

This chapter considers possible mechanisms which could control expression of the TaR1 gene and polypeptide product and intially considers the regulation of ribonucleotide reductase expression in other eukaryotes which has been reviewed by Greenberg & Hilfinger (1996).

RR activity varies greatly during the cell cycle and is highest when DNA synthesis occurs but hardly detectable in quiescent cells. In higher eukaryotic cells the variation in RR activity at different stages is due to the fluctuation in R2 protein levels whereas the levels of R1 protein remains constant. In mice, the half life of R1 is >24 hours whereas for R2 it is only three hours. Activity is regulated by the S phase specific synthesis and breakdown of the R2 protein (Engstrom *et al.,* 1984). The R1 protein is constitutively expressed, remains at a constant level and is in excess throughout the cell cycle. The mRNA levels of both subunits rise in parallel in G1 reaching a peak as the cell progresses into S phase then declining into the G2+M phases (Bjorklund *et al.,* 1990). The S phase expression of the R2 mRNA is regulated by a cell cycle specific release of a transcriptional block which has been mapped to the 1st intron of the R2 gene. In S phase, a nuclear protein then binds just upstream of the block allowing full length transcripts to be produced (Bjorklund *et al.,* 1992). This protein may be MET1a1, a transcription factor which has been shown to play a role in transcription of the human complement protein C2 and *c-myc* (Ashfield *et al.,* 1991). Promoter analysis of the R1 gene in mice shows it to be a TATA less promoter but contains the TF-II binding elements common in cell cycle regulated genes (Filatov *et al.,* 1995).

In lower eukaryotes transcription of the large subunit also appears to be periodic over the cell cycle. Two R1 genes are present in *S. cerevisiae*. The transcription of one of these, RNR1, is cell cycle regulated as a result of an MCB box which contains a consensus *MluI* restriction site (Elledge & Davis, 1990). The MCB sequence element binds a transcription factor complex known as MBF or DSCI which promotes transcription (Johnston & Lowndes, 1992). The other large subunit gene, RNR3 is induced by DNA damage and is apparently not controlled by the MCB promoter system under these circumstances (Johnston & Johnson, 1995). Transcription of the single *cdc22⁺* gene present in *S. pombe* which encodes the large subunit of ribonucleotide

reductase, also shows cell cycle specific regulation, being maximally expressed at the G1/S boundary (Gordon & Fantes, 1986). The $suc22^+$ gene encodes the small subunit but two transcripts have been shown to hybridise to $suc22^+$, a smaller 1.5kb transcript that is constitutively expressed and a larger 1.9kb transcript that is induced upon blocking DNA replication with hydroxyurea (Fernandez-Sarabia *et al.*, 1993). This size difference is due to different transcript start sites (Harris *et al.*, 1996). Cell cycle expression of the larger transcript is under MCB control but is also induced by DNA damage and heat shock.

In *E. coli*, the two genes encoding ribonucleotide reductase are arranged in an operon and are transcribed as a polycistonic message in the order R1 then R2. The expression requires two proteins, dnaA and Fis binding to specific sites upstream of the mRNA start. Another AT rich site upstream of the start site is necessary for the coupling of expression to the replication cycle.

In the mouse, the R1 gene lies on chromosome 7. It lacks a TATA box but contains other sequence elements which link its expression to the cell cycle. There are several mRNA start sites and upstream of the first of these, there are two 23nt boxes which were shown to be important in gene expression using footprinting studies. Further work showed there to be three protein factors involved in binding to these two regions. One protein was an S phase specific protein, another was very similar to the Sp1 transcription factor while the identity of the third remains unknown. Although the level of mRNA is controlled at the level of transcription, there is evidence that there are further controls on the mRNA levels in addition to the transcriptional controls detailed above. There is a 49nt region in the 3'UTR which binds a 57kDa cytosolic protein. The binding of this protein increases the rate of degradation of the mRNA. Work with known PKC inhibitors such as staurosporine found that the PKC pathway exerts an influence on stability by decreasing the binding affinity of p57 for the 49nt sequence in the R1 3' UTR.

The stability of the R2 message is also regulated and a protein (p45) has been shown to bind to the 3' UTR with a resultant increase in the rate of degradation. This can be reversed by the action of TPA, a phorbol ester, in a similar manner to the PKC mediated stabilisation of R1 mRNA. Another protein, p75 binds further downstream in the 3'UTR but acts to stabilise the message. This protein is linked to the action of TGF-

β1, which has been shown to increase the levels of R2 protein in stimulated cells, via an increase in the R2 mRNA levels and via p75 mediated stabilisation of the R2 message.

Significance of the 3' UTR of human R1 and R2

It has been shown that the 3'UTR of the R1 and R2 mRNA contain sequences important in regulating gene expression through changes in message stability. It has been shown by transfection experiments that the R1 and R2 3' UTR can suppress tumourigenic properties of malignant mouse cells (Fan *et al.*, 1996). Cells expressing the R2 3'UTR had significantly reduced potential to disseminate in experimental metastasis assays. By some means the 3'UTR regions of R1 and R2 can modify tumour cell development and dissemination, possibly by the interaction of the mRNA with components involved in the regulation of cell growth. Thus, in conclusion, there are a wide range of means of controlling the transcription and translation of the R1 and R2 genes in both prokaryotes and eukaryotes. These pathways are linked to other signalling pathways within the cell showing that the expression of RR is intrinsically and intimately linked to the cell cycle.

As discussed in chapter 4, there is an upstream region in the TaR1 cDNA which contains two in frame ATG codons prior to the consensus start codon based on ribonucleotide reductase large subunit protein sequences from other eukaryotes. It is not known if there is an N-terminal extension in the mature polypeptide but it is possible that this sequence upstream of the eukaryotic consensus start methionine is not translated and serves a regulatory role in the expression of TaR1 at the translational level, possibly by forming an ordered secondary structure in the mRNA 5' region. This possibility will be considered in relation to what is understood about mechanisms for regulation of rate of translation in other eukaryotes. The *P. falciparum* RR has significant differences to the mammalian systems. The genes for PfR1 and PfR2 are located on the same chromosome and these genes have a different temporal order of expression than their mammalian counterparts, in that the PfR2 transcript appears earlier and persists for longer than the PfR1 transcript (Rubin *et al.*, 1993) in the schizont stage. No data is available on the half life of the subunits in *P. falciparum* or the sequence of the promoter regions. Thus there is relatively limited information on the regulation of RR expression in Apicomplexan

parasites. The aim of this chapter is to provide a preliminary analysis of the features that may determine the regulation of the *Theileria* RR. This chapter also considers the transcriptional regulation of TaR1 using aphidicolin, a DNA synthesis inhibitor, to block the cell cycle with the aim of determining whether the parasite R1 subunit transcription is under cell cycle control as has been shown for the mammalian and yeast systems.

The *Theileria* mRNA has only a small 3'UTR and there is no evidence for either alternative transcription start sites or variable length 3' UTR as there is only a single mRNA species detected by Northern blotting in different life cycle stages (Chapter 4). This is 2.8kb, very similar to the predicted size of the cDNA clone (2.79kb).

5.1.2 Mapping of the transcriptional start site of TaR1

As promoter sequence will be upstream of the transcription start site, it was decided to map the transcriptional start site of TaR1 using a PCR based method known as 5' Rapid Amplification of cDNA Ends (5'RACE). A description is given in the materilas and methods section. Two primers were designed to specifically amplify the 5' end of the TaR1 mRNA. The first primer annealed to a region downstream of the ATG codon representing the consensus translational start (M3). The second primer annealed to a region upstream of the 2nd ATG codon (M2). These are shown on Figure 5.2.

cDNA was prepared from a template of total piroplasm RNA using the first primer. Figure 5.1 shows the results of the PCR of reverse transcribed cDNA from the nested PCR reaction with the second primer, together with the control reactions supplied with the kit. The product was ligated into the pTAG vector and the one positive transformant was sequenced using pTAG specific primers. The DNA sequence of the RACE fragment is shown in figure 5.1. As only one positive transformant was obtained from the cloning of the PCR fragment, this does not exclude the possibility that the PCR fragment contained representatives with small size differences. S1 mapping would possibly enable finer mapping of the mRNA starting site and allow establishment of a conclusive transcriptional start site.

However, the end of the 5' RACE PCR fragment is 51 nucleotides further upstream from the end of the cDNA clone so it is likely that this is the true transcriptional start site. It is probable that the mRNA was not fully reverse transcribed during the library construction. The existence of this 5' untranslated region may be useful in designing anti-sense oligonucleotide inhibitors specific for the parasite gene given the results on anti-sense inhibition in *P. falciparum* published by Barker *et al.* (1996).

5.1.3 Is the 5' region of the TaR1 mRNA a means of regulation?

Northern blotting of *P. falciparum* RNA showed that the PfR1 mRNA was actually 5.4kb, with an ~ 2.9kb untranslated region (Rubin *et al.*, 1994) and although this has not been sequenced in its entirety, it is quite common for mRNAs in *P. falciparum* to possess a 5'UTR longer than the coding sequence.

Rather interestingly, if the 229bp upstream to the consensus start methionine (M3) of TaR1 is collapsed into a stable secondary structure using the FOLDRNA package of the GCG program, its free energy value (ΔG) is -52 kcal/mol which indicates a potentially very stable structure. The plot of the secondary structure is shown in Figure 5.3. The *P. falciparum* cDNA clone sequenced by Chakrabarti *et al.*, (1993) contains an upstream region of 123 base pairs before the consensus start codon is reached. If this is collapsed then the (ΔG) is -5kJ which suggests would not to be a stable structure. The full length mouse R1 cDNA possesses an upstream region of some 170bps in length (Thelander & Berg, 1986). If collapsed into a stable secondary structure with the FOLDRNA programme then the free energy value (ΔG) is -49kJ which indicates that a highly stable secondary structure can form. This ΔG value is rather similar to the value obtained for the TaR1 upstream sequence.

5.1.4 Analysis of the 5'non-coding sequence from λ3 genomic clone

The 2.7kb *BamHI/ EcoRI* fragment was subcloned from the TaR1 λ genomic clone (chapter 4) containing the entire gene. This was sequenced using the same gene

specific internal primers designed for mapping of the transcriptional start site on template cDNA by the 5' RACE method (figure 4.1). Approximately 250bps of upstream sequence was obtained on one strand only and is shown in figure 5.4a. The sequence is identical to the cDNA clone and to the 5'RACE product which mapped the transcriptional start site except for a single bp deletion and two adjacent bp deletions in the 5'RACE PCR product (marked as gaps ..). As the PCR product was sequenced on both strands, it is probable that these are artefacts of the amplification reaction. These three sequences are aligned in figure 5.4b for comparision. The genomic sequence upstream of the transcriptional start site was analysed for homology to known promoter sequences in the Eukaryotic Promoter Database (EPD) and the TFASTA transcription binding site server. Some homology to regions of vertebrate encoded transcription factors were found - namely OCT-1, GATA and TATA boxes. These are shown in figure 5.4. Next it was desirable to see if this region contained any of the *MluI* boxes (MCB elements) found in the upstream region of the *S. pombe* R1 gene and if there was any homology to the upstream sequence of the mouse R1 gene. The *MluI* boxes had been shown to be involved in the transcriptional regulation of the *S. cerevisiae* R1 gene at the G1/S border (Lowndes *et al.*, 1992). There was no significant homology between the *Theileria* R1 sequence and the mouse or yeast sequences. The best match to the consensus TATA sequence found in most eukaryotic promoters (TATAA/TA/T) is found at -33 from the transcription start site (figure 5.4b). This has the sequence TATTAGA and is not an optimum match though it is positioned at a typical point in eukaryotic promoters (usually ~25bps) upstream of the transcription initiation site. Interestingly there is no TATA box found in the mouse R1 promoter (Bjorklund *et al.*, 1993) or in the human R1 promoter (Parker *et al.*, 1995). It has been found that many genes involved in the cell cycle are regulated by the E2F transcription factor and that the regulation of this factor itself is subject to cell cycle control by a variety of other factors such as the tumour suppressor gene product p53 (reviewed in Muller, 1995). TATA boxes are present in genes transcribed by RNA polymerase II and are present in the *P. falciparum* PCNA gene (Horrocks & Kilbey, 1996) which shows differential expression in life cycle stages. The report of a gene encoding a divergent TATA binding protein from *P. falciparum* (McAndrew *et al.*, 1993) suggests that protozoan TATA box sequences may differ slightly from higher eukaryotes. With respect to other common

binding sequences present in the upstream R1 sequence there is homology to an OCT 1 box at -80 from the transcription start site and a perfect match to a GATA factor binding sequence at -70. GATA transcription factors are important in determining cellular differentiation patterns (Merika & Orkin, 1993; Orkin, 1995). There is also a GATA box present in the *P. falciparum* PCNA gene as well as a single match to the GATA consensus sequence found in the *Theileria* tubulin sequence. There is a partial match to the eukaryotic CAAT promoter sequence (consensus GGCCAATCT) at -110 (AGACAATTG) with 5/9 residues conserved. This sequence is involved in binding factors which regulate promoter efficiency and although the match is not well conserved, the distance from the transcriptional start site is typical for eukaryotic CAAT sequences (~-75). The fact that there are possible consensus sequences present in the upstream sequence of the TaR1 gene suggests that undertaking band shift assays with competing oligonucleotides and DNAse I footprinting studies against these regions would be informative in terms of defining whether these sequences are involved in the transcription of this gene. These sequences are highlighted in the upstream region of the TaR1 and tubulin genes as shown in figure 5.4.

5.1.5 Aphidicolin as a means of cell synchronisation

It is important to determine if the parasite genes coding for cell cycle related proteins are subject to cell cycle control of transcription in a manner similar to that found for some higher eukaryotic and yeast genes. For example, the human DNA polymerase α gene is expressed as cells enter the cell cycle from G0 and is then down-regulated after exit from the cell cycle (Pearson *et al.*, 1991). In budding yeasts the transcription of at least 17 genes encoding enzymes for DNA synthesis or precursor production are coordinately induced at the G1/S boundary. This is due to the presence of a conserved DNA sequence known as the MCB element or *Mlu* I cell cycle box (it contains a *Mlu* I restriction site). In *S. pombe* the expression of the large subunit of ribonucleotide reductase is induced at the G1/S boundary and also contains the *Mlu* I box. However, the transcript levels of the DNA ligase gene in fission yeast is expressed constitutively throughout the cell cycle as are the transcript levels of the DNA polymerase α and δ

genes (Park *et al.,* 1993) suggesting that, in *S. pombe,* there are at least two different regulatory modes for the expression of genes involved in the DNA synthesis. In order to investigate the regulation of cell cycle related genes, aphidicolin was used as a blocking agent to arrest cells at the start of S phase by specifically binding to the DNA polymerase α and δ subunits of the DNA replication machinery. Cells outside of S phase at the time aphidicolin is added, accumulate in S phase when they pass through the G1/S checkpoint (Johnson *et al.,* 1993). Aphidicolin affects the elongation activity of DNA polymerase but not initiation activity as shown by experiments done using aphidicolin sensititive and resistant CHO cells (Singleton & Mishra, 1995).

In *Theileria* infected cells, several objectives might be achieved through the study of aphidicolin inhibition. It is not known if *Theileria* DNA replication is sensitive to aphidicolin and if this is found to be the case, it should be possible to examine transcription of cell cycle associated genes and to analyse the effects of artificial synchronisation of host and parasite cell cycles.

5.1.6 BrdU labelling of D7 cells

In order to examine the effects of aphidicolin treatment on host and parasite it was necessary to develop a simple system for assay of DNA synthesis. There is no simple way of distinguishing host and parasite DNA synthesis using assay methods based on analysis of total cell extracts such as thymidine incorporation. It was decided to base the assay on microscopic detection of DNA synthesis in individual cells combined with counting of labelled host and parasite nuclei. This was done using 5-bromo-2-deoxyuridine (BrdU) incorporation followed by incubation with a specific antibody coupled with an immunofluorescent FITC labelled secondary antibody. As a control and baseline for using aphidicolin as a means of synchronising D7 cells in S phase, incorporation of BrdU was initially assessed in D7 cells growing at 37°C under normal conditions. The incorporation of BrdU was detected by immunofluorescence as shown in figure 5.5 and the results of the quantitative analysis are given in figure 5.6. Those host cells with reactive nuclei are those undergoing DNA synthesis during the course of the BrdU incorporation period (15, 30 and 60 minute incorporations were tried and it was

found that a one hour incubation was required to see parasite nuclear reactivity). As seen from figure 5.5 (Panel B), parasite nuclei rarely label in the absence of parallel host nuclei labelling. The numbers of cells containing labelled host nuclei only, labelled parasite nuclei only and both types of labelled nuclei were counted and then plotted as shown in figure 5.6. Macroschizonts with any degree or number of nuclei showing reactivity were scored as positive. In practice, it appears that parasite nuclei synthesise DNA synchronously within a macroschizont as most cells showing parasite BrdU incorporation have reactivity in all the nuclei based on comparison with the DAPHI staining pattern. However, it is not uncommon to see a cell where, compared to the DAPHI stain, there is a group or block of parasite nuclei showing reactivity and a group that does not (figure 5.5). At any one time there are approximately 60% of host cells synthesising DNA but only 20% of parasites . Of the parasites undergoing DNA synthesis most (~80%) do so in the presence of host DNA synthesis with relatively few parasites labelling in the absence of host DNA synthesis. As seen in figure 5.5, parasite DNA synthesis cannot be correlated with any particular intensity of host reactivity suggesting that parasite DNA synthesis is not closely linked to a specific point in the host S phase.

5.1.7. Aphidicolin blocking of D7 cells

The cells were treated with 1.5 mg/ml of aphidicolin for a period of 18 hours at 37°C, a concentration typically used for mammalian cells (Tobey *et al.,* 1988). The drug was then washed out and the cells resuspended in fresh fresh pre-warmed medium and sampled at 1, 2, 4, 5 and 6 hours post-release from aphidicolin for RNA preparation and BrdU incorporation. A sample of cells was also taken prior to resuspension in fresh media (time 0). For each time-point, a cytospin slide was prepared for BrdU incorporation counting and the remaining cells were used to prepare total RNA.

By counting the numbers of host and parasite nuclei with detectable BrdU incorporation, it was possible to achieve a measure of the efficiency of the aphidicolin treatment determining the frequency of positives. This should decrease as the cells move out of S phase and are no longer undergoing DNA replication. Figure 5.7 shows the incorporation of BrdU into D7 cells at time points 0 and 1 hour post release. At time 0,

there is very little detectable labelling of the parasite nuclei and low host reactivity (Panel B). The reactivity increases strongly in both types of nuclei as the cells move into S phase after release from the drug. The results of the cell counts for each time point are shown in figure 5.8 and plotted in the same figure. From the graph, it can be seen that not all host cells are arrested in S phase as the number of cells staining with the BrdU antibody is <100% after release from drug. The peak is at 1 - 2 hours post release with 76% of the host nuclei staining very brightly. This figure then decreases as the host cells move out of S phase. After 6 hours only 24% of the host nuclei are synthesising DNA. The degree of synchronisation is comparable to the 80 - 90% of S phase mammalian fibroblast cells cited in Tobey *et al.* (1988). The % of parasites showing nuclear staining peaks at 50%, 1 hour after release, decreases to 3.5% by 4 hours before increasing again to some 15% by 6 hours after release. Early after release, the majority of parasites showing BrdU incorporation do so in the presence of host DNA synthesis (85%). However, by the end of the time course the parasite component showing incorporation in the absence of host increases considerably (72%). Examples of cells seen following release from the aphidicolin block are shown in figure 5.7. From Panel C it can be seen that all the individual parasite nuclei are labelling and the host nucleus labelling is very strong, following release from the block but in Panel E only a proportion of the parasite nuclei are labelling one hour after release from block in this cell. It would be interesting, albeit difficult, to score the numbers of nuclei labelling in each schizont to determine how synchronous the parasite nuclear population is within a given host cell following aphidicolin treatment. The host cell seen in Panel E is larger than those seen in Panels A & C and it is possible that aphidicolin treatment makes cells more fragile so that this cell has been distorted by the presence of the drug. There could be two explanations for only 50% of the parasite nuclei being in S phase. The first being that the parasite may be less sensitive to the drug than the host; the increase to 50% from the 20% of parasites in S phase in the control culture suggesting S phase is slower or extended in the presence of this concentration of aphidicolin. This could be due to transportation of the drug into the macroschizont or the *Theileria* polymerase being insensitive to the drug, a situation found in Trypanosomes (Mutomba & Wang, 1996) and *Toxoplasma* (Makioka *et al.*, 1993). Secondly, the parasite may be sensitive to aphidicolin but because of the small size of the genome compared to the bovine (200 fold smaller), the time spent in S phase

is likely to be shorter and during drug treatment which causes an accumulation of parasites in S phase, some may manage to complete and exit S phase over the time of treatment.

5.1.8. Northern blotting of RNA prepared from aphidicolin treated D7 cells

RNA samples were prepared for five of the timepoints sampled and was used to prepare Northern blots for probing with TaR1 and parasite tubulin together with the ThaCRK2 and host cdc2 genes. Figure 5.9 shows the RNA time course Northern blot probed with the TaR1 and tubulin probes (Panels A & B respectively).

With the TaR1 probe the strength of the hybridisation signal increases following removal of the drug and peaks at the two hour time point, After this there is a small decrease in signal between four and six hours. Two - four hours post release is equivalent to the trough in parasite DNA synthesis as seen by BrdU incorporation (Figure 5.8, Panel A). Using a *Theileria* β tubulin cDNA clone as a probe, there is a similar increase in trancript levels immediately following removal of the drug. The hybridisation signal of 1.8kb reaches a maximum at 2hrs and does not decline significantly thereafter (Panel B). The blots were then stripped and re-probed with parasite ThaCRK2 and host cdc2 probes. Again, using the ThaCRK2 probe (Panel C), there is an increase in hybridisation signal 1 hour after removal of the drug which remains at a similar level over the rest of the time course,a pattern almost identical to that obtained with the β tubulin probe. The bovine cdc2 probe (Panel D) (Logan & Kinnaird, unpublished) hybridises to RNA species of 1.4 and 3.5 kb with the smaller of the two being the same size as the polyadenylated cDNA clone. The upper band is routinely present and may represent hybridisation to a closely related CDK RNA or an unspliced precursor of cdc2. The 1.4 kb transcript appears to show a marginal decrease 1 hour after removal of drug but then rises to a peak at 6 hours. This peak coincides with the exit from S phase of the majority of the host cell population. It has been shown that the human cdc2 promoter is activated in S phase (Dalton, 1992). As a control for synchronisation of the host, an attempt was made to hybridise the mouse R1 probe (a gift of L. Thelander) which is known to be transcriptionally regulated over the cell cycle

(Bjorklund *et al.*, 1992) but the probe fragment did not cross-hybridise with bovine RNA. It is possible that this region is quite divergent between mouse and bovine R1s. The increase in RNA levels could be analysed for parallel changes in polypeptide levels by immunoblotting of protein extracts prepared·from cells blocked and released from aphidicolin.

5.2 Discussion and Conclusions

The 229bps sequence in the TaR1 cDNA clone upstream of the consensus translational start codon (M3) has the potential to fold into an extremely stable secondary structure. While it is possible that this region could be translated and form an N-terminal extension to the typical eukaryotic R1 protein structure, it is equally possible that formation of a stable secondary structure at the 5' end of the mRNA could provide a means of regulating the rate of translation of the TaR1 RNA. This could occur either through preventing access to the ribosome or by binding of a protein factor to prevent translation. ATG burdened leader sequences are extremely rare on mRNAs encoding highly expressed proteins such as caseins, histone, immunoglobulins etc. Most of the mRNAs with a high ATG burden are also GC rich thereby reducing translation by virtue of a highly ordered secondary structure. Many vertebrate mRNAs can form sufficient secondary structure at the 5'end to repress translation which can become 'derepressed' upon a mitogenic signal inducing a specific protein binding to this region and thus changing the secondary structure or preventing the mRNA from maintaining the secondary structure. Whether this is an actual phenomenon used by *Theileria* as a means of translational regulation would need to be tested experimentally. This would require a *Theileria* based *in vitro* translational system using full length and truncated versions of the R1 mRNA.

The region of the DNA extending 225bps upstream of the transcription start site was sequenced and analysed for possible promoter sequences with homology to known eukaryotic promoter elements. It will also be interesting to determine if the various genes involved in the parasite cell cycle have a common promoter structure to enable co-ordination of expression. From the results of the aphidicolin experiments TaR1 may be subject to cell cycle regulation. It would be of interest to determine if the polymerase δ subunit shows the same pattern of expression in infected cells after exposure to aphidicolin. From the analysis of the upstream region of the genomic clone there is some homology to known promoter sequences found in higher eukaryotes such as the OCT1 and the TATA box, although the relative AT richness of these regions may account for artefactual homologies which resemble known transcription factor binding sites. In higher eukaryotes, the OCT1 transcription factor is preferentially expressed in early S

148

phase and up-regulates genes encoding enzymes involved in DNA replication. It has also been shown to be subject to regulation by phosphorylation during the cell cycle (Verrijer *et al.*, 1990).There is a perfect match to the GATA box known to be important as a binding sequence for a class of DNA binding proteins important in differentiation, although multiple GATA binding sites are required for erythroid cell specific trans-activation (Orkin, 1995). Interestingly the upstream region of the *P. falciparum* PCNA gene contains TATA boxes together with some regions showing strong homology to the OCT1 consensus sequence (Horrocks & Kilbey, 1996). There are also GC regions rich found in the promoter which are unusual given the AT richness of *Plasmodium*, however, the significance of these sequence elements is unknown. There is also a perfect GATA box found in the PCNA promoter but again, the significance of this is unknown. The *P. falciparum* PCNA promoter also contains a region with high homology to the initiator core promoter element consensus sequence (Javahery *et al.*, 1994). This initiator functions to localise a transcriptional start site and can co-operate with the TATA element if both are found in the same core promoter and are approximately 25bps apart. The consensus sequence is (T/C)(T/C)AN(T/A)(T/C)(T/C) with the matching sequence in the *P. falciparum* PCNA promoter being TTATATA and a TATA box being 25bps further upstream. This may indicate that the initiator element has been conserved in the protozoa and that the basal mechanisms of transcription are similar to that found in the higher eukaryotes. Comparing the TaR1 sequence (figure 5.4) there is a perfect initiator element TTAGACT found at the transcription start site but this could feasibly be a stand alone initiator element as they can operate in the absence of a TATA box. The *Theileria* tubulin gene contains a region with high homology to the TATA box about 25bps upstream of the transcriptional start site although this homology could be due to the high %AT found in intergenic regions. Earlier work by Horrocks *et al.* (1996) showed that PCNA and polymerase δ proteins are found at similar levels in trophozoites and schizonts despite the transcripts probably only being present in trophozoites. The promoter activity of these two genes is different despite the fact that, in both cases, the transcript and protein levels rise in parallel. Polδ is regulated at the level of transcription initiation whereas the PCNA transcript levels are regulated post-transcriptionally.

Looking for parallels with the *Theileria* R1 gene, it seems that the levels of protein and transcript rise in parallel throughout the course of differentiation with mRNA

levels remaining high in the piroplasm stage. However, given that promoter regions in *Theileria* have not been well characterised, it is difficult to postulate specific mechanisms involved in transcriptional regulation in *Theileria*. As a result of the work presented, it would now be possible to perform a detailed analysis of the TaR1 upstream region by deletion analysis and transient transfections to determine what sequences are necessary for promoter function once such techniques have been developed.

In order to investigate transcriptional regulation of cell cycle associated genes in *Theileria* and to investigate the relationship between host and parasite DNA synthesis, pilot experiments were carried out using the DNA synthesis inhibitor aphidicolin to block cells in S phase. In D7 cells growing at 37°C only ~20% of parasites are seen to be undergoing DNA synthesis at any one time. Aphidicolin treatment increases this to 50% by one hour following removal of the drug. Thus there is clearly an effect of aphidicolin on parasite DNA synthesis. However, it is impossible to distinguish whether this is a direct effect of the drug on the parasite DNA replication machinery or an indirect effect via the effect of the drug on host DNA synthesis. Since, under normal growth conditions at 37°C, most of the parasites that are synthesising DNA do so in the presence of host DNA synthesis, there may be some link with the host and parasite S phases- hence the effect of aphidicolin allowing host cells to accumulate in S phase may be transmitted to the parasite. Another possibility is that the parasite is less sensitive to the drug. This could be due to the requirement for transport of aphidicolin into the macroschizont or to the *Theileria* DNA polymerases being less sensitive, a situation found in *Toxoplasma gondii* (Makioka *et al.*, 1993). As *Theileria* species are in the same phylum, Apicomplexa, as *Toxoplasma* this may suggest that the *Theileria* polymerase subunits are aphidicolin insensitive. Conversely, work with the DNA polymerases from *P. falciparum* shows the activity to be aphidicolin sensitive (Inselberg & Banyal, 1984, Chavalitshewinkoon *et al.*, 1993). It would be necessary to purify the DNA polymerase enzymes from the parasite to determine the exact sensitivity of the *Theileria* DNA polymerase to aphidicolin by biochemical assay. An effect of a reduced sensitivity of *Theileria* to aphidicolin may manifest itself as lengthening of the parasite S phase sufficiently to give an accumulation of parasites in S phase but, because of the small genome size (10^7 base pairs, 200 fold less than the host genome size), a proportion manage to complete and exit S phase over the time of treatment. It appears that

aphidicolin may induce two peaks of parasite DNA synthesis within one host cell cycle. The evidence from nuclear counts (Shiels *et al.*, 1992) and the control D7 experiment indicate that two rounds of replication do not normally occur. This may reflect the artificial disruption of synchrony caused by the presence of the drug. If differentiating D7 cells are cultured in the presence of aphidicolin for 18 hours prior to the induction of differentiation at 41°C, the rate of differentiation is faster compared to control cells, lasting only four to six days (Shiels, pers. comm.).

For co-ordination of host nuclear division with parasite nuclear and schizont segregation to occur, the parasite gap phases may be elongated to allow for the completion of host S phase. How the parasite aligns itself with the host spindle for the division to occur is largely unknown though it has been suggested that attachment to host centrioles occurs (Carrington *et al.*, 1995). It has previously been shown by immunofluorescent detection of a schizont surface antigen that some parasite infected cells contain two macroschizonts (Carrington *et al.*,1995). These observations suggest that DNA synthesis is synchronous in all the nuclei within a schizont but not between schizonts in a single host cell. Definitive proof of this would require double labelling with detection of both the schizont surface antigen and BrdU labelled nuclei.

From the aphidicolin blocking of the D7 cell lines it is possible to draw some conclusions regarding the lengths of the host and parasite cell cycles. The probable existence of two peaks of DNA synthesis in this experiment would suggest that the nuclear division cycle of the parasite only lasts 3-4 hours. For the host, S phase lasts longer than 6 hours, given that incorporation of BrdU is still measurable 6 hours post release from the block. This fits with the 18-22 hour cell cycles typical of higher eukaryotes. However, it is possible the peak of parasite BrdU incorporation may have occurred within the 1st hour post-release from block which would only be detectable if earlier time points had been taken.

The Northern blotting experiments undertaken with RNA prepared from the aphidicolin blocked and released cells suggests that the parasite ThaCRK2 and β-tubulin are not under cell cycle control as transcript levels are steady in the 1-6 hour period after removal of drug.

It is interesting to note that the human cdc2 gene is TATA-less and is negatively regulated by the retinoblastoma gene product pRb which only associates with the E2F

transcription factor in G1 when transcription is blocked (Dalton, 1992) and a degree of transcriptional regulation of the bovine cdc2 gene was observed following release from the aphidicolin block. Here the peak transcript level was observed at 6hrs when most of the host cells were leaving S phase, a result identical to that obtained with human cdc2 transcription in synchronised HeLa cells (Dalton, 1992). This would parallel a requirement for cdc2/cyclin B at the G2/M phase boundary in mammalian cells with CDK2/cyclin B acting at G1/S phase. However, in fission yeast there is little if any cell cycle regulated transcriptional control of the cdc2 gene (Durkacz *et al.*, 1986). Relating this to the ThaCRK2 signal in the Northern blots of the aphidicolin blocked cells, it seems that there is again little regulation of transcription of this gene, a situation similar to that found in *S. pombe* and *Paramecium tetraurelia* (Tang *et al.*, 1995).

The pattern of expression seen for TaR1 following aphidicolin treatment may indicate that the transcript levels of TaR1 are cell cycle regulated. The results indicate that there may be a degree of regulation of TaR1 transcription over the nuclear division cycle in the macroschizont stage as there appears to be a peak in transcript level when DNA synthesis is low and just prior to the start of the next parasite DNA synthesis wave i.e. in preparation for the provision of dNTPs. As the peak is not striking, there may be several explanations as to why the effects of a transcriptional regulation may be masked: at one hour post release only ~50% of parasites were synthesising DNA which could contribute to a lack of sharpness of the peak. However, from a study of cell cycle regulation in *S. pombe* where a similar efficiency of synchronisation was obtained using an elutriation method (measured as 40% septated cells), there was a clear cell cycle regulation of histone 2A1 transcription (Park *et al.*, 1993). Therefore, it seems that this level of synchronisation should have been adequate to detect transcriptional regulation of gene expression during the nuclear cell division cycle in *Theileria*. It should be pointed out that the TaR1 transcript peak occurs after the first round of parasite DNA synthesis is complete and, as with all artificially induced synchronisation, it begins to break down after the first cycle. It might be expected that during the period of drug treatment, transcript levels of TaR1 would be elevated as S phase is prolonged but as the later peak appears to occur at the lowest level of parasite DNA synthesis i.e. prior to S-phase, an accumulation of RNA may not occur during an S phase block. In fact as all parasite transcripts assayed were at their lowest levels in the presence of aphidicolin, the period

of treatment needed to accommodate the long host cell cycle may have had a secondary effect on cell functions other than DNA synthesis such as protein synthesis. This has been found for some mammalian cell types following aphidicolin treatment (Schimke *et al.*,1991). Although the promoter sequence of R1 from *P. falciparum* has not been analysed, work with synchronised parasite cultures showed that the transcript levels of R1 & R2 are co-ordinately regulated during the cell cycle with a peak of expression occurring just prior to the entry of S phase (Rubin *et al.*, 1993). This is a similar situation to that found in mice where R1 & R2 transcripts increase in parallel correlating with DNA synthesis (Bjorklund *et al.*, 1990). However, it is not known if the half life of the *Plasmodium* R1 protein is longer than the R2 protein, a situation found in higher eukaryotic cells. There is very little homology between the *Theileria* R1 promoter sequences and those from mouse and human sequences which are very similar to each other. If anything, there are parallels between the *Theileria* R1 and *Plasmodium* PCNA promoters which may reflect the fact that both proteins are vital for DNA replication. More work with this region in *Theileria* could shed light on the means of regulation of cell cycle related genes by this parasite and how these relate to other members of the Apicomplexa. Certainly, this area has not been well investigated in *Theileria* and with only a few genes sequenced so far, it is not possible to draw any major conclusions about the mechanisms of transcriptional regulation at work in this parasite.

It is probable that there is a high degree of control over nuclear division in *Theileria* and this could extend to transcriptional control of expression of some associated genes such as TaR1. The evidence for this comes from the analysis of BrdU incorporation under non-drug conditions. These results show that in the non-differentiating macroschizont, DNA synthesis is synchronous between nuclei in a single schizont. This situation is found in higher eukaryotic syncytial cells eg in early *Drosophila* embryo development (Edgar *et al.*, 1994). However, this contrasts with schizogony in *P. falciparum* where the nuclear divisions are known to be asynchronous (reviewed in context in Leete & Rubin 1996). This, in itself, argues that regulation of nuclear replication may be more complex in *Theileria*.

The analysis of the upstream region of the TaR1 gene shows homology to some common motifs such as the TATA box and the GATA binding regions which may be important in the basal transcription apparatus of the parasite but further work is needed

to show that this upstream region acts as a functional promoter. Recent work with the *P. falciparum* PfPK5 protein which is highly homologous to the ThaCRK2 has shed some light on its role in the malarial cell cycle (Graeser *et al.*, 1996). Using aphidicolin treated cultures, it was shown that the immunoprecipitated PfPK5 kinase activity increased significantly in these blocked cells which suggests a role for this protein in the S phase of the cell cycle. The authors also showed that the PfPK5 is activated at the beginning of the nuclear division cycle and that the pool of cytoplasmic PfPK5 must be maintained for the newly formed nuclei. This may also hold true for the ThaCRK2 protein although further work needs to be done to confirm the role of ThaCRK2 in the division cycle in *Theileria*. This will be of interest if the DNA polymerases in *Theileria* are shown to be aphidicolin sensitive. Based on the results in this chapter it is not possible to state conclusively the effects of aphidicolin on the parasite DNA polymerases.

Work on the differentiation of neuroblastoma cells showed that addition of aphidicolin together with nerve growth factor acted to induce differentiation (Poluha *et al.*, 1996). This is interesting since prior treatment with aphidicolin induces differentiation in D7 cells. Further experiments showed that the neuroblastoma cells continued to express p21^{wafl}, a CDK inhibitor, after removal of aphidicolin and that the expression of p21 was required for the survival of these cells. This, perhaps, places control of differentiation in the context of negative regulators of the cell cycle which would be most interesting to look at from the view of parasite control of the host cell cycle and how the switch between proliferation and differentiation takes place. This is analysed in the next chapter.

To conclude, in *T. annulata* the host and parasite cell cycles are closely linked with the parasite S phase occurring within the host S phase. The genes encoding ThaCRK2 and β tubulin do not appear to be transcriptionally regulated during the nuclear division cycle but TaR1 may be subject to regulation. There is a partial degree of synchrony in the parasite induced by aphidicolin treatment but it is not clear from these experiments if the effect is mediated by a direct effect on the parasite DNA polymerase or indirectly as a result of the host cell cycle being blocked. Further experiments are necessary, particularly to define the sensitivity of the parasite to aphidicolin.

Figure 5.1 5' RACE with piroplasm RNA as template

Piroplasm total RNA was reverse transcribed according to the instructions supplied. The cDNA was then amplified using nested PCR with the second TaR1 specific primer together with the anchor primer and cloned into the pTAG vector. The DNA sequence of the product is shown in figure 5.2.

Panel A shows the RACE PCR reaction with the gene specific primer (5 PRIME RACE 2).

Lane 1:   PCR reaction with anchor primer and gene specific primer

Lane 2:   PCR reaction with anchor primer only

Lane 3:   PCR reaction with gene specific primer only

Panel B shows the control reactions showing 538bp bands obtained with the control RNA supplied with the kit.

M: DNA markers - 1kb ladder (Gibco-BRL)

Lane 1:   Control RNA with the first strand synthesis using GSP1 primer then nested PCR with GSP2 and GSP3 primers.
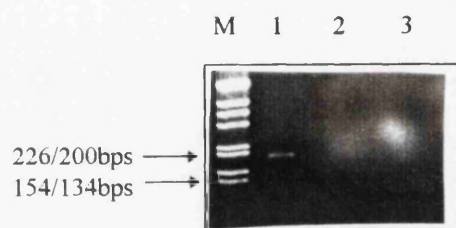
Lane 2:   Control RNA with the first strand synthesis using oligo-dT primer then nested PCR with GSP2 and GSP3 primers.

Primers

5PRIME RACE 1 - 5' AGCGATAACTTCCTGATGCG 3' (antisense to position 289 - 308 of cDNA sequence.)

5PRIME RACE 2 - 5' AAATCGTGGTCCTCATAGCC 3' (antisense to position 127 - 146 of cDNA sequence.)
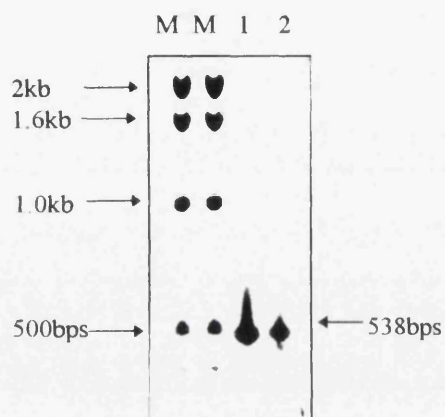
A

M 1 2 3

226/200bps →
154/134bps →

B

M M 1 2

2kb →
1.6kb →

1.0kb →

500bps → ← 538bps

Figure 5.2 5' RACE PCR maps likely transcriptional start site

The sequence of the RACE PCR fragment is shown opposite.

Key:

AGGA - mRNA sequence upstream of cDNA clone

AGGA - sequence of cDNA clone

<u>AGGA</u> - region of primer 2 used for second round of PCR

DNA Sequence from RACE fragment showing the upstream region from cDNA clone.

```
  1   TTAGACTATA TATTGTTTAT CTTTCGCTAT ATTTTTAAAT TATGCTTCTT
                                                        M1
 51   CTGATACAAA CTCGTTATTT CCTTGATTGT TTTTAAAGTT AAGATGGATG

101   CATCAACAGG ATCATAACAA TACCACAAGT GGTTTTCCGC CTGAGGATGT

151   GTCGGAAAGC TCACGTGGCT ATGAGGACCA CGATTT
```

Figure 5.3 FOLDRNA program shows upstream region of TaR1 cDNA clone can form a stable secondary structure

The FOLDRNA program of the GCG package was used to collapse the229bp region upstream of the consensus start ATG codon of the cDNA clone into a secondary structure. The ΔG value of -52kJ shows that this structure is exceptionally stable.

SQUIGGLES of: utr.connect March 16, 1996 14:56

FOLDRNA of: utr Check: 9419 from: 1 to: 229 March 16, 1996 14:33

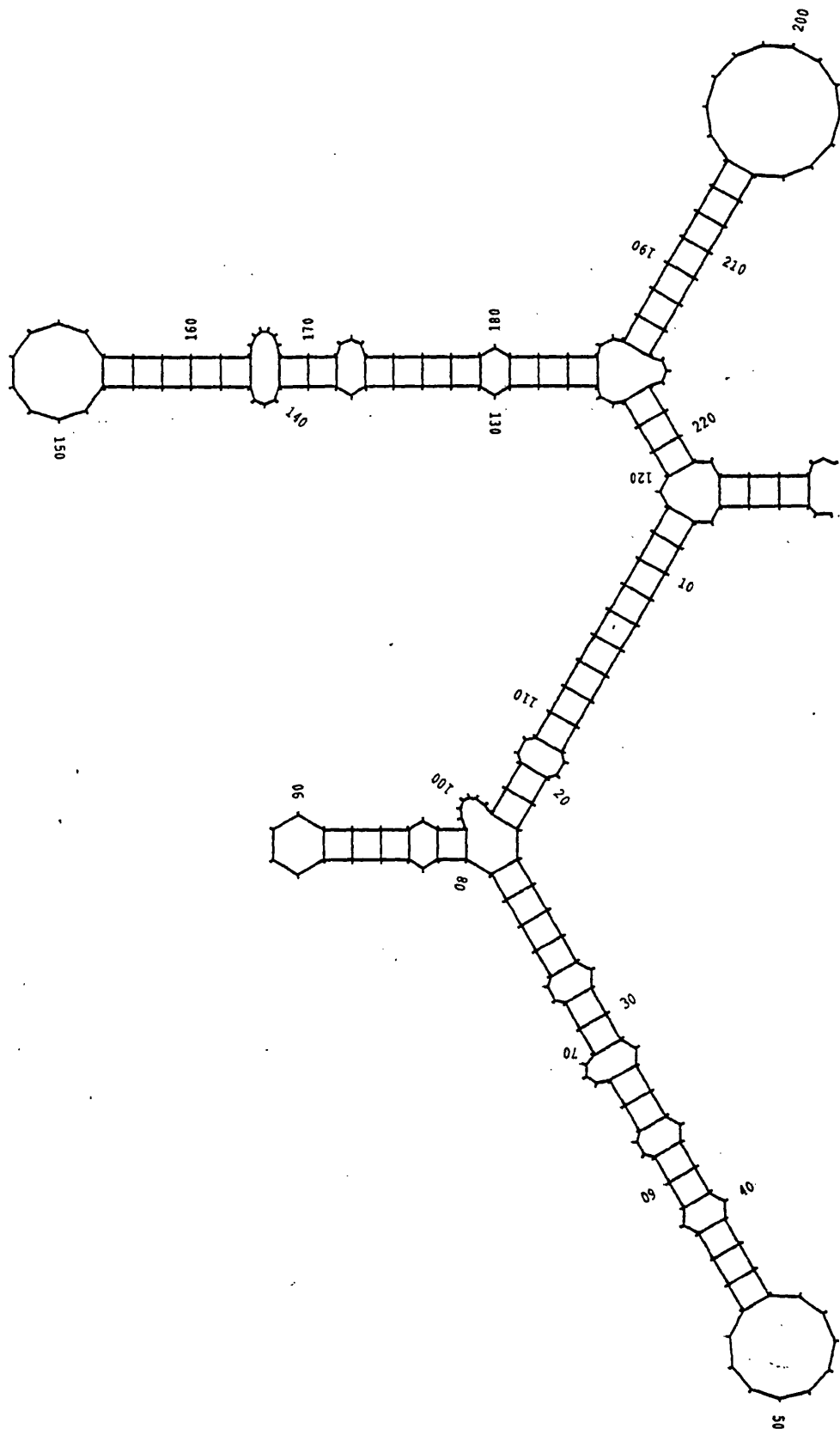Length: 229 Energy: -51.9

Figure 5.4a Alignment of genomic, RACE and cDNA TaR1 clone

This figure shows the alignment of the genomic, RACE PCR and cDNA clones of TaR1. The location of the first in frame ATG codon is marked in bold.

```
        1                                                               60
TaR1gen  AAAACCGAAA GTTCTATTTG GCAGAAAGAA TGCAGCTATT ACACACAAAA TAGGCAAGAT
RTPCR    ~~~~~~~~~~ ~~~~~~~~~~ ~~~~~~~~~~ ~~~~~~~~~~ ~~~~~~~~~~ ~~~~~~~~~~
TaR1cDNA ~~~~~~~~~~ ~~~~~~~~~~ ~~~~~~~~~~ ~~~~~~~~~~ ~~~~~~~~~~ ~~~~~~~~~~


        61                                                              120
TaR1gen  CTGTGATTAC AGTTGAAATG TAAAAAAgAT TAACANACAA TTGTTGAaAT AAAATTAGAC
RTPCR    ~~~~~~~~~~ ~~~~~~~~~~ ~~~~~~~~~~ ~~~~~~~~~~ ~~~~~~~~~~ ~~~~~~~~~~
TaR1cDNA ~~~~~~~~~~ ~~~~~~~~~~ ~~~~~~~~~~ ~~~~~~~~~~ ~~~~~~~~~~ ~~~~~~~~~~


        121                                                             180
TaR1gen  TCAAATTTAA GTGCAATGAT AGGAGTTAAC TAAGGGGTTT GGTACTGCCT GAATTaTTAG
RTPCR    ~~~~~~~~~~ ~~~~~~~~~~ ~~~~~~~~~~ ~~~~~~~~~~ ~~~~~~~~~~ ~~~~~~~~~~
TaR1cDNA ~~~~~~~~~~ ~~~~~~~~~~ ~~~~~~~~~~ ~~~~~~~~~~ ~~~~~~~~~~ ~~~~~~~~~~


        181                          ⟶                                  240
TaR1gen  ATTTGGATTG TGTGGCACGA TCACAAATTA GACTATATAT TGTTTATCTT TCGCTATATT
RTPCR    ~~~~~~~~~~ ~~~~~~~~~~ ~~~~~~~TTA GACTATATAT TGTTTATCTT TCGCTATATT
TaR1cDNA ~~~~~~~~~~ ~~~~~~~~~~ ~~~~~~~~~~ ~~~~~~~~~~ ~~~~~~~~~~ ~~~~~~~~~~


        241                                                             300
TaR1gen  TTTAAATTAT GCTTCCTTCT GATACAAACT CGTTATTTCC TTGATTGTTT TTAAAGTTAA
RTPCR    TTTAAATTAT GCTT.CTTCT GATACAAACT CGTTATTTCC TTGATTGTTT TTAAAGTTAA
TaR1cDNA ~~~~~~~~~T GCTTCCTTCT GATACAAACT CGTTATTTCC TTGATTGTTT TTAAAGTTAA
                          *
        301                                                             360
TaR1gen  GATGGATGCA CATCAACAGG ATCATAACAA TACCACAAGT G~~~~~~~~~ ~~~~~~~~~~
RTPCR    GATGGATG.. CATCAACAGG ATCATAACAA TACCACAAGT GGTTTTCCGC CTGAGGATGT
TaR1cDNA GATGGATGCA CATCAACAGG ATCATAACAA TACCACAAGT GGTTTTYCGC CTGAGGATGT
        M1
        361                             396
TaR1gen  ~~~~~~~~~~ ~~~~~~~~~~ ~~~~~~~~~~ ~~~~~~
RTPCR    GTCGGAAAGC TCACGTGGCT ATGAGGACCA CGATTT
TaR1cDNA GTCGGAAAGC TCACGTGGCT ATGAGGACCA CGATTT
```

Figure 5.4b Upstream sequence of TaR1 genomic clone

This figure shows the upstream sequence of the TaR1 gene derived from the RACE primer of the λ3 clone together with the upstream sequence from the tubulin gene (courtesy of M. Logan). Sequences of interest within this region are shown below:

Key:

TTAG   start of mRNA

<u>TATTAG</u>   TATA box and close match to consensus sequence of TATA(A/T)(A/T)

TGATAG   GATA boxes - matches to consensus sequence of (T/A)GATAR where R is a purine base (A or G)

ACTCAAAT   Oct-1 box - consensus sequence of ATGCAAAT

<u>*AGACAATTG*</u> CAAT box - consensus sequence of GGCCAATCT

Consensus binding sequences are as listed in Faisst & Meyer, 1992.

Large subunit of Ribonucleotide Reductase

```
  1   AAACGATATT TTGAGGGGAA AACCGAAAGT TCTATTTGGC AGAAAGAATG

 50   CAGCTATTAC ACACAAAATA GGCAAGATCT GTCATTACAG TTGAAATGTA

100   AAAAAGATTA ACAGACAATT GTTGAAATAA AATTAGACTC AAATTTAAGT

200   GCAATGATAG GAGTTAACTA AGGGGTTTGG TACTGCCTGA ATTATTAGAT

250   TTGGATTGTG TGGCACGATC ACAAATTAG
```


Tubulin upstream intergenic region

```
  1   TGAAAATTTG CTGATCTTTT TTTCCACCGA TGCGTCTCAC CTTTTTTTAC

 51   TGTACTAACT GTAGCATACA TTTTAATTGA TCAAATATCT AAATAAATTT

101   TACATTATAA TTAATTATAA AAATTATTAA CTTGCACAAT CAAGGATAAT

151   TTTTAGCATC AACATACAAG AAAAGCTCGA TCCTACACTA AGGAATCATA

201   AACAATTTTA AAATCCTTCG AATCGTAATC AAAATTAGAA TTCGAAGTAA

251   GTATTAACTA GAGTTATATA TACAACGTCG TAAGTATGTC GTGAAAAGTG

301   AAAGTACAAG TGTTTAAAAG TAATATGGGA ACCTTTGATA TTATAAACCC

351   ATTTTAAAAC TAAAATATTT TACTTTCATT TAAAAGGGGG CGTAACGATT

401   TTACTTATTT AGTGTTGTCT GTGTGTGGTA TAATTTGTAA TATATGTGAT

451   TGTAAATCAG TAAT
```

Figure 5.5 D7 cells stained with DAPHI and BrdU.

This figure shows D7 cells growing at 37°C stained with BrdU and DAPHI. Arrows indicates the location of a cell consisting of parasite nuclei staining in the absence of host staining (1), parasite and host nuclei both staining (2) and host nuclei staining alone (3).

Panel A shows the cells stained with DAPHI stain.
Panel B shows the same cells reactive against the anti-BrdU antibody.

Magnification is X20 and the scale bar represents 10µm.

A
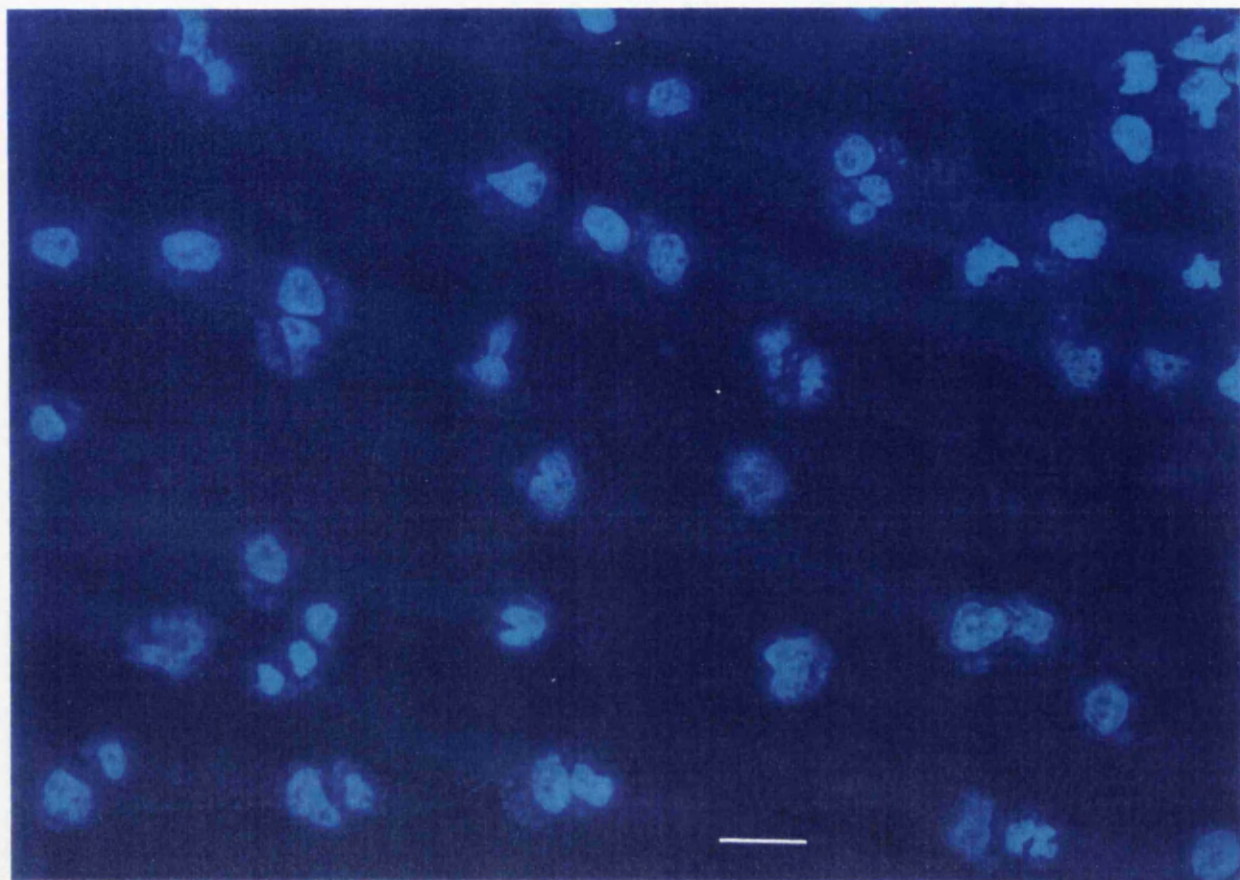
B
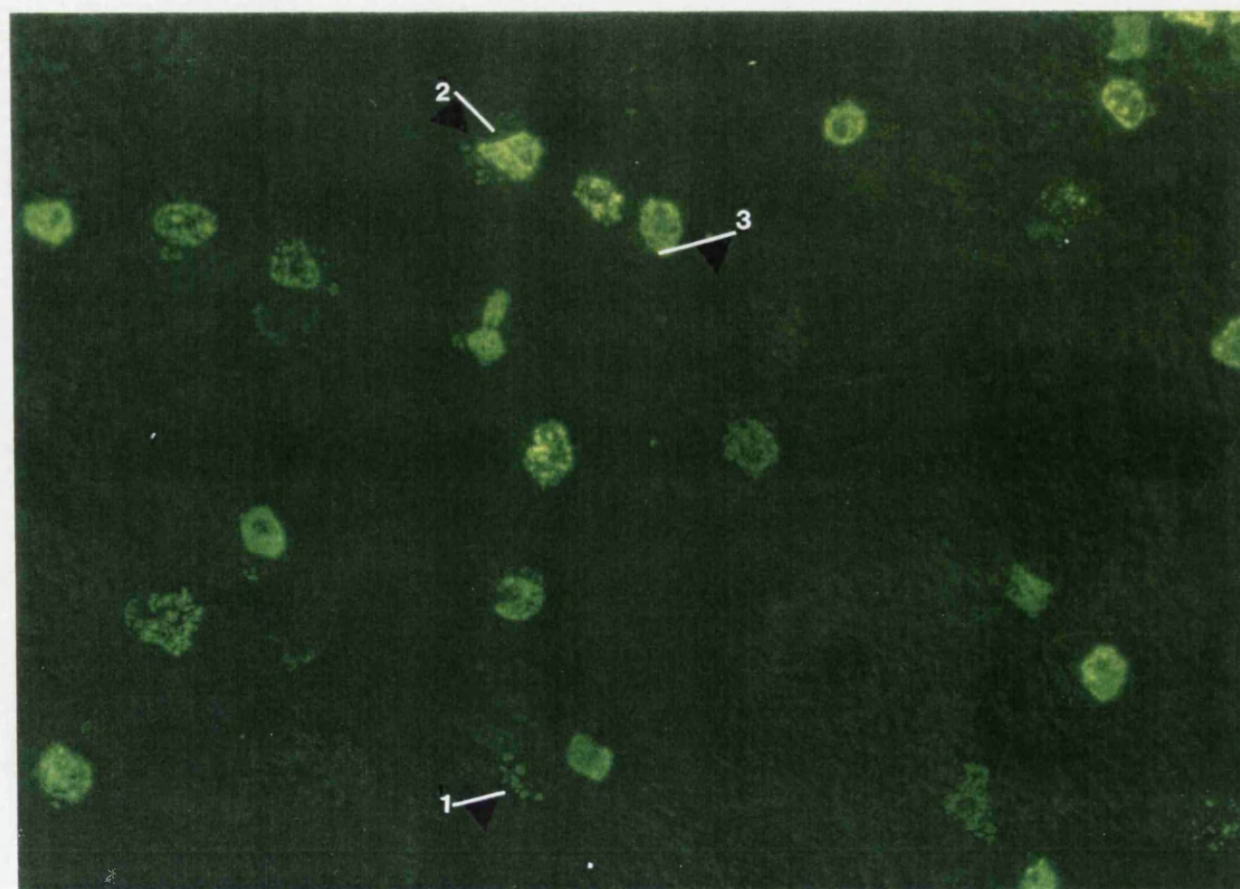
Figure 5.6 BrdU incorporation into D7 cells growing at 37°C

The table lists values for the total numbers of cells counted (as assessed by DAPHI staining) with the numbers of host nuclei and numbers of parasites with nuclei showing BrdU incorporation in D7 cells growing at 37°C. The data from the table is plotted below. This illustrates that parasite nuclear labelling rarely occurs in the absence of parallel host nuclear labelling. The y-axis shows the number of nuclei staining with BrdU expressed as a % of the total number of cells counted by DAPHI staining. The x -axis shows the host, parasite, parasite + host and parasite - host categories of nuclei staining.

Key to table:

In each row two figures are given, the first is the number of cells showing BrdU incorporation. The second is the first figure expressed as a % of the total number of cells counted.

Host nuclei   Host nuclei showing any detectable BrdU incorporation

Parasite nuclei   Parasite macroschizont showing any detectable degree of BrdU incorporation

Host + Parasite   Cells showing incorporation in both host and parasite

Host - parasite   Cells where parasite shows incorporation in absence of host labelling.

Table of BrdU incorporation into D7 cells growing at 37°C

Total number of cells counted - 222 by DAPHI staining.

host nuclei	parasite nuclei	Host + parasite	Parasite - Host
131	42	35	7
(59%)	(19%)	(16%)	(3%)

Nuclei staining with BrdU as a % of the total number
of cells counted by DAPHI staining

Nuclei staining with BrdU
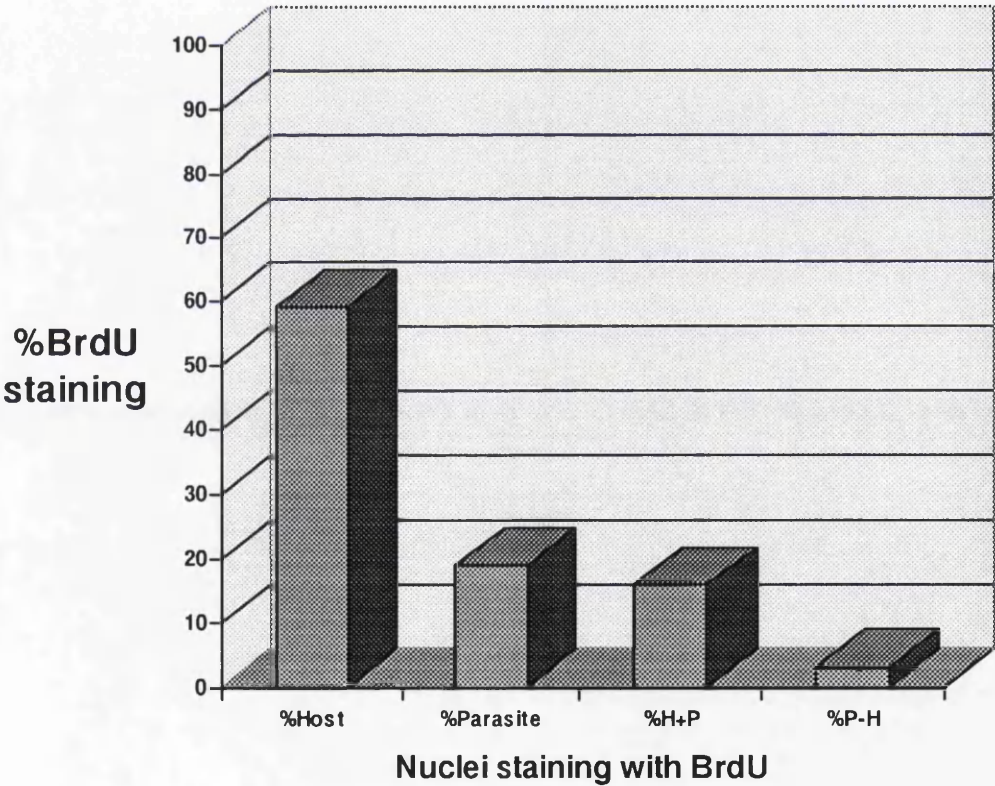
Figure 5.7 BrdU staining with D7 cells subjected to aphidicolin block

This figure shows the typical staining patterns encountered pre and post release from the aphidicolin block.

Panel A shows D7 cells prior to release from block stained with DAPHI. Panel B shows the same cells reactive with the anti-BrdU antibody.

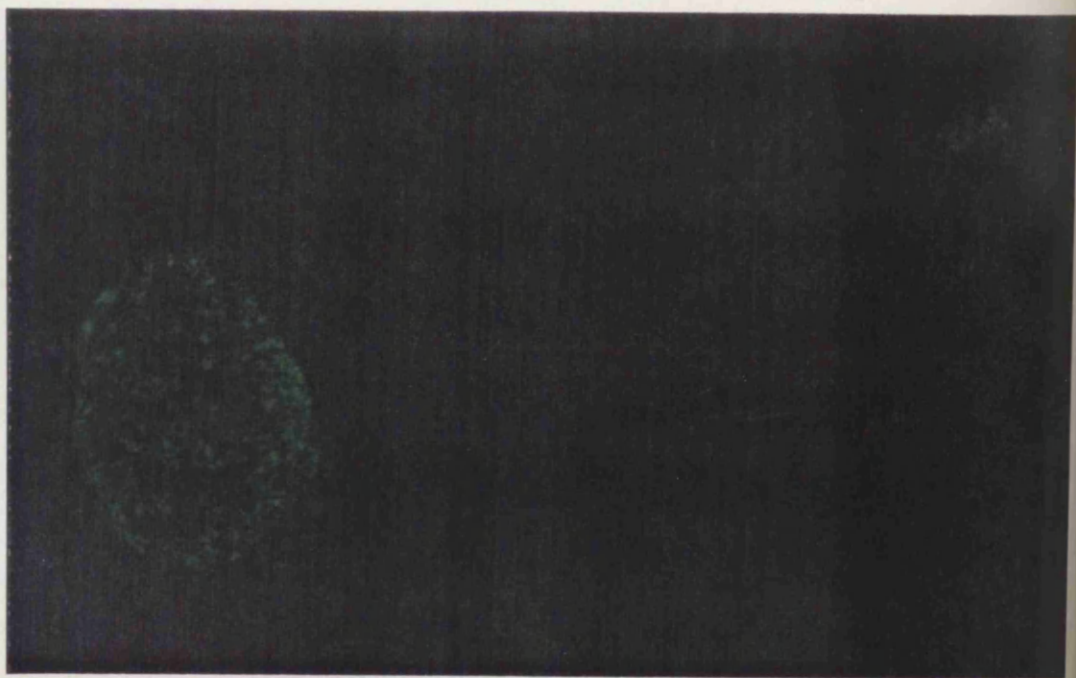Panels C & E show D7 cells sampled one hour post release from block, stained with DAPHI.
Panels D & F show the cells in panels C & E staining with the anti-BrdU antibody.

Magnification is X100 and the scale bar is 2µm.
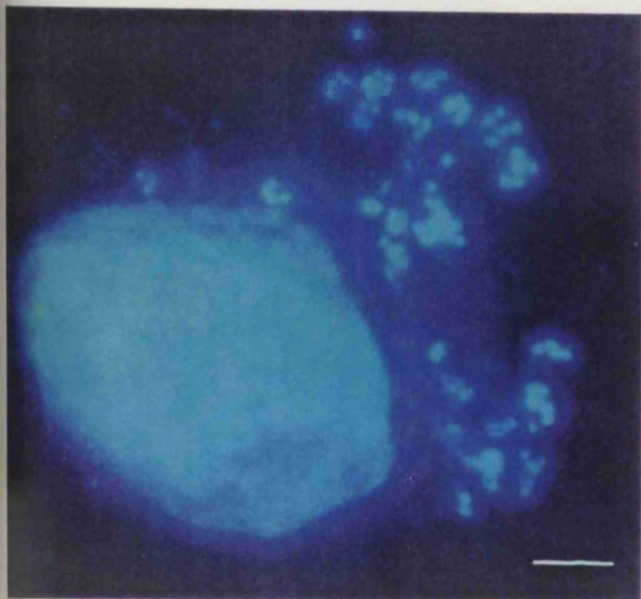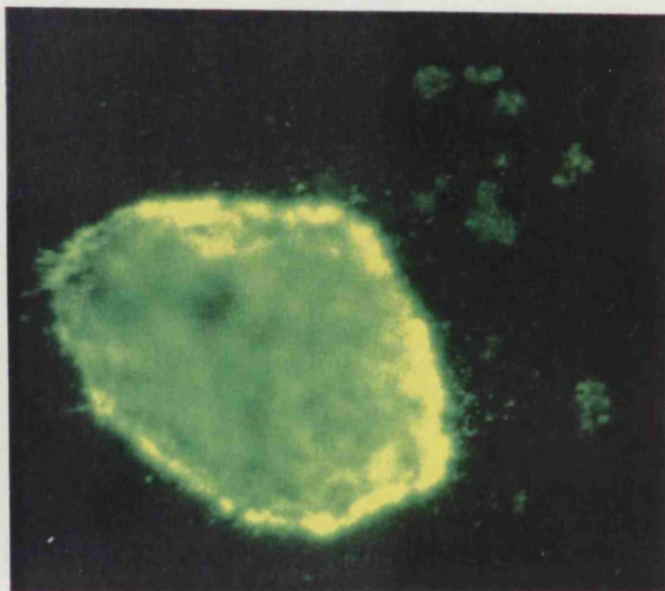
A
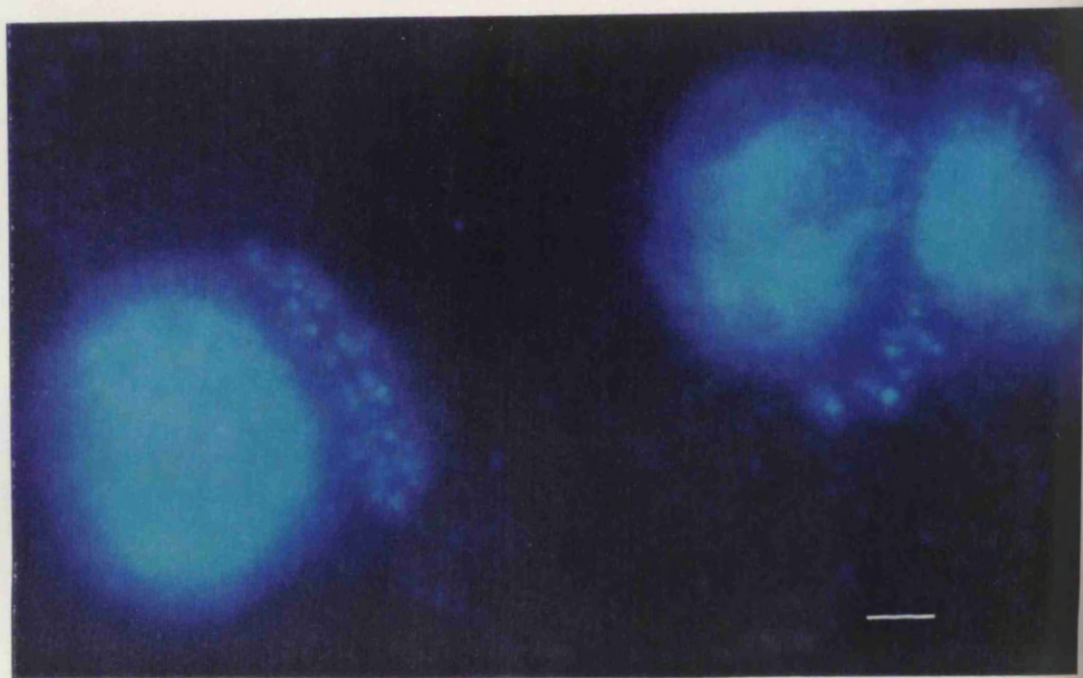
B

C   D
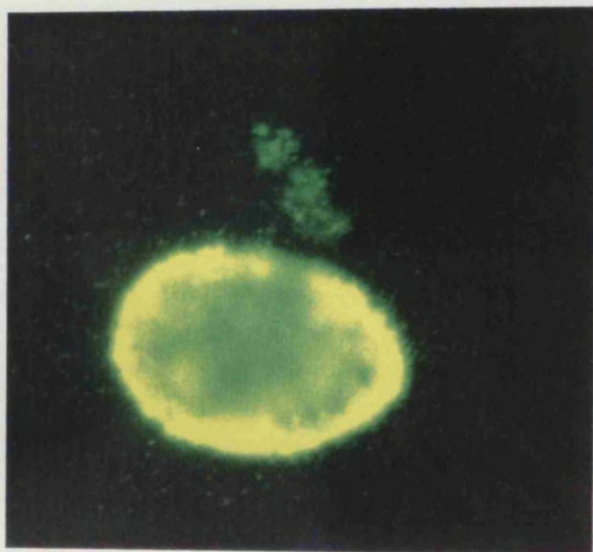
E   F

Figure 5.8 Bromo-deoxyuridine incorporation into D7 cells in the presence of aphidicolin

The table lists the values for the cell counts done at each of the 6 time points for the D7 cells blocked with aphidicolin for 18 hours at a concentration of 1.5µg/ml then released. The values for the host and parasite incorporations of BrdU are then plotted as % incorporating BrdU of total numbers of cells counted.

Key to Table:

DAPHI   Number of cells counted as stained by DAPHI

BrdU Host   Number of host nuclei staining with BrdU

% DAPHI   BrdU staining of host nuclei expressed as a % of the number of cells counted

BrdU P+H   BrdU staining of both parasite and host nuclei

BrdU P-H   BrdU staining of parasite in absence of host nuclei staining

Total P % of DAPHI   Total % of parasite nuclei staining with BrdU

Table of cell counts after release from aphidicolin block.

Time (h)	DAPHI	BrdU Host	% of DAPHI	BrdU P+H	BrdU P-H	Total P as % of DAPHI	P+H as % of positives	P-H as % of positives
0	284	132	45.0	10	0	3.5	100	0
1	235	179	76.0	100	18	50.2	85	15
2	483	367	76.0	18	7	5.0	72	28
4	1317	469	35.6	40	7	3.5	85	15
5	1091	433	39.6	54	38	8.4	59	41
6	416	100	24.0	18	46	15.3	28	72

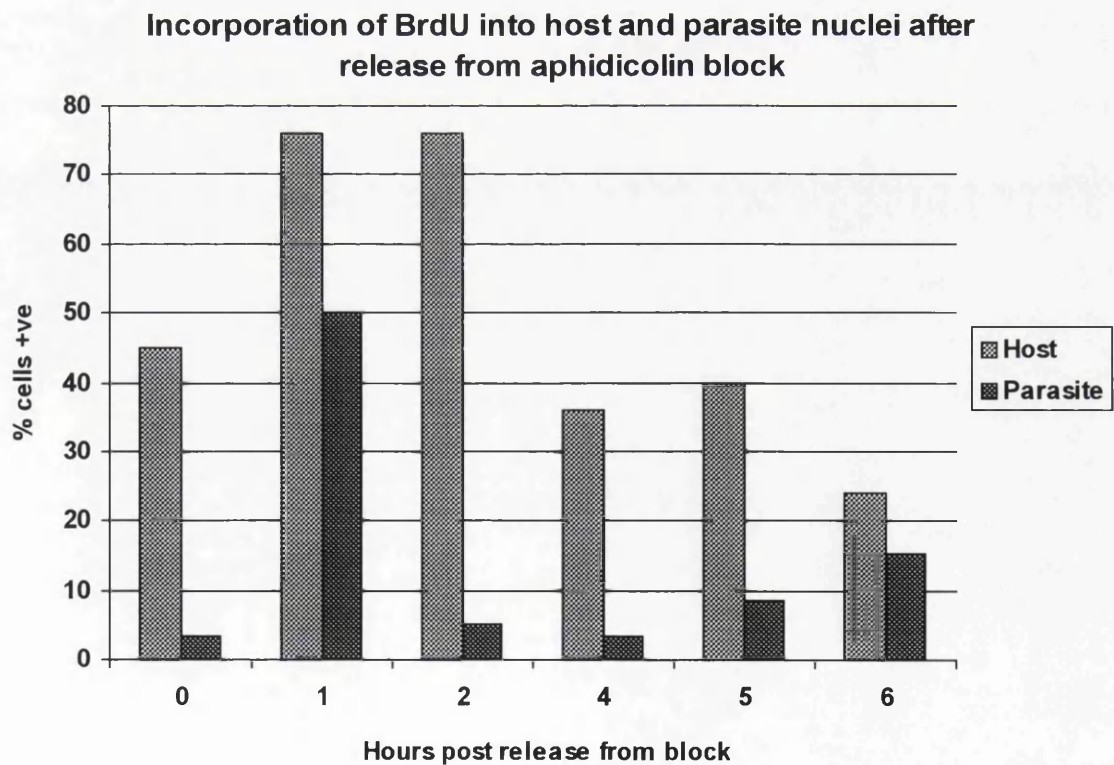Incorporation of BrdU into host and parasite nuclei after release from aphidicolin block

Figure 5.9 Northern blotting of RNA prepared from aphidicolin blocked D7 cells.

RNA from each sample was separated on a 0.8% denaturing formaldehyde gel and blotted onto Hybond N membrane (Amersham). The blots were then cross-linked and hybridised as described chapter 2.

Panel A shows the reactivity profile obtained with the TaR1 probe - a 0.75kb *XhoI/PstI* fragment excised from the pBluescript cDNA clone.

Panel B shows the profile with the parasite β-tubulin probe - a 1.0kb *BamHI* fragment excised from the pBluescript cDNA clone.

Panel C shows the profile with the ThaCRK2 probe - a 0.8kb *KpnI-XhoI* fragment from the pBluescript cDNA clone.
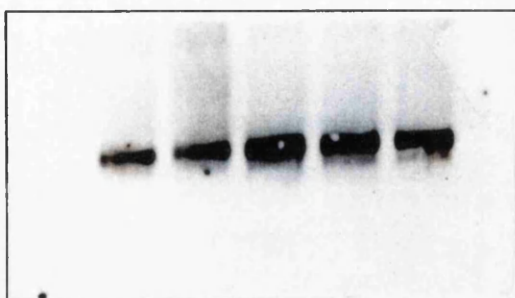
Panel D shows the profile with the host cdc2 probe - a 0.7kb *BglII/PstI* fragment excised from the pBluescript cDNA clone

Sizes are as indicated to the right of the panels.

A

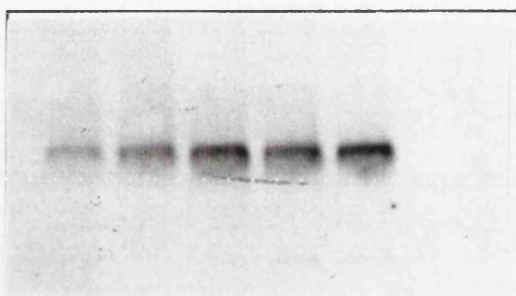Time post release of aphidcolin block
t0 t1 t2 t4 t6

← 2.9kb

B

Time post release of aphidcolin block
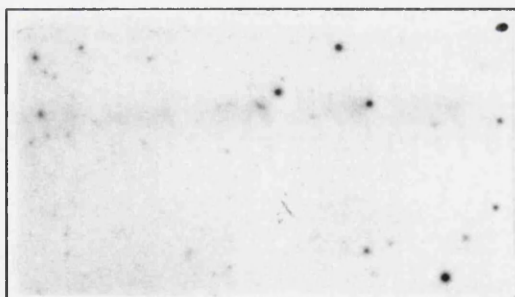t0 t1 t2 t4 t6

← 1.8kb

C

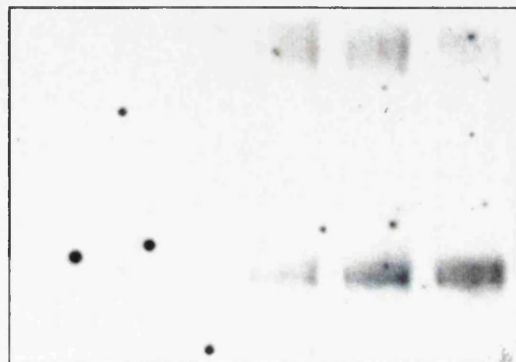Time post release of aphidcolin block
t0 t1 t2 t4 t6

← 1.3kb

D

Time post release of aphidcolin block
t0 t1 t2 t4 t6

← 3.5kb

← 1.4kb

Chapter Six

Expression of Cell Cycle Related Proteins during Differentiation

6.1.1 Introduction

Using a *T. annulata* infected cloned cell line D7 which has an enhanced differentiation phenotype, previous work had shown that during intra-cellular differentiation to the merozoite stage there is a point reached after which the parasite is committed to differentiation (Shiels *et al.,* 1992). The number of parasite nuclei per infected cell increases typically by up to 300% within 96 hours of the culture being shifted to 41°C and continues to increase until merozoites are formed prior to host cell lysis. During the early stages at increased temperature, the infected host cells continue to undergo a parasite induced proliferation with a concomitant increase in infected cell number of approximately four fold over the first 48 hours, then the rate of increase slows down as the parasite differentiates within the enlarged macroschizont, while the number of parasite nuclei continues to increase as the rate of infected cell division decreases. Thus the synchrony between the parasite and host cell cycles breaks down after approximately 2-4 days at 41°C. The rate of parasite nuclear division must continually be greater than that of host cell division after the breakdown of synchrony to account for the increase in parasite nuclei per infected cell. It is possible that in the final stages of differentiation, the host cell cycle may be shut down completely.

The unique ability of *Theileria* to induce immortalisation of the host cell has stimulated research into the mechanisms responsible for this. The gene encoding host casein kinase II, a component of the signal transduction pathway, has been cloned (oleMoiYoi *et al.,* 1993) as well as a gene coding for metalloproteinase MM9 (Baylis *et al.,* 1995). Both of these have elevated levels in infected cell lines but it is difficult to distinguish a specific effect, at this level, by the parasite from a general result of stimulated proliferation. It is extremely difficult to single out candidates for the 'factor' which stimulates proliferation. However, it seems probable that the 'factor' is a component of the external surface of the schizont or is a molecule that is actively transported out of the schizont into the host cytoplasm. Carrington *et al.* (1996) showed that by specifically blocking host protein synthesis with ricin some, as yet unidentified, parasite proteins are exported into the host cell. Many changes in gene expression take place in the differentiating cell (Glascodine *et al.,* 1990, Shiels *et al.,* 1993, Swan *et al.,* manuscript in preparation), some of which could be involved in effecting a change in

parasite induced host cell proliferation. It is not known if the reduction in host cell division during differentiation is due to the removal of parasite stimulation or to a physical or metabolic effect of the enlarged macroschizont. The aim of the work in this chapter was to characterise the decline in host cell division rate and the interaction between host and parasite cell cycles at the molecular level during differentiation at 41°C with a view to establishing if and when a specific down regulation of the host cell cycle occurs during differentiation.

The intial approach was to use anti-sera directed against components of the host and parasite cell cycles to determine alterations in the reactivity profiles of these proteins (by Western blotting) during differentiation.

6.1.2   Analysis of host /parasite cell cycle proteins during parasite differentiation.

A differentiation time course of D7 infected cells was prepared by placing a culture at 41°C. The culture was maintained by diluting into fresh medium every second day to $1.2-1.4 \times 10^5$ cells/ml until the growth rate had decreased at day 8. The fold increase in cell number at each time point is shown in figure 6.2 and the cell counts for each time point in Table 6.1. In this time course the growth of the population is maintained up to a slightly later time point than was observed in Shiels *et al.* (1992) (day 6). Samples were taken for preparation of protein extracts after 0, 2, 4, 6, 8, and 10 days at 41°C and Giesma stained slides were made from each of the D7 samples to assess the stage of differentiation. These are shown in figure 6.1.

Each sample was standardised to equal cell numbers (1.8×10^6 cells/track) by adjusting the resuspension volume of the cell pellet after centrifugation. The protein extracts from each time point were analysed by SDS-PAGE and Western blotting using a range of anti-sera. Standardisation on the basis of equivalent cell numbers rather than total protein was chosen as it should take account of possible alterations in the protein content of cells during the differentiation process. In practice, total protein content did not vary greatly as assessed by Ponceau S staining of Western blots. The anti-sera were selected to distinguish cell cycle events of both host and parasite. The sera used were higher eukaryote specific anti-cdc2 and ribonucleotide reductase (large subunit) and

166

Theileria specific ThaCRK2 and TaR1. In addition, control antisera for both host and parasite were used. These were a mammalian specific anti- HSP 60 antibody and the 45kDa parasite protein which cross-reacts with the TaR1 antisera (Chapter 4). The function of both of these proteins are thought to be unrelated to the cell cycle, and expression may, therefore, be differently regulated or unchanged during the differentiation time course. The reactivity profiles are as shown in figure 6.3.

Using the parasite specific anti-ThaCRK2 anti-serum (Panel A) the reactivity increases markedly after 4 days at the higher temperature (Lanes 4 - 7) and correlates with the most active period in terms of increase in numbers of parasite nuclei. Assuming that this protein is necessary for completion of the parasite cell cycle, it is present at a low concentration in non-differentiating cells and does not increase significantly during the early stages of exposure to the higher temperature (Lanes 3-4). From day 4 onwards, the size of the parasite macroschizont and nuclear content increase considerably (figure 6.1) and the increase in anti-ThaCRK2 signal may reflect this. However, after peaking at day 8 (Lane 6) the reactivity significantly decreases. This could reflect arrest of the parasite cell cycle prior to the rupture of the host cell and release of the mature merozoite stage which are non-dividing and do not react with anti-ThaCRK2 antibody by immunofluorescence (Kinnaird, unpublished). It is important to note that individual parasites in the cell population will be at various stages of differentiation, thus the process is not synchronous. These results indicate the trend of the population as a whole at a particular point in time. Hence at day 10, for example, the reduction in anti-ThaCRK2 signal largely represents the cells where merogony is complete but also includes some cells at earlier stages of differentiation. Similarily, it is difficult to determine if the apparently sharp rise in reactivity over days 6-8 reflects an upregulation in expression of ThaCRK2 or merely an increase in the size and nuclear content of the macroschizont. If it were possible to synchronise cell differentiation, this could be clarified.

An opposite effect is seen with the anti-cdc2 anti-serum which specifically recognises bovine cdc2 only (Panel B). During the early stages (days 2-4) of differentiation (Lanes 3-4) there is a gradual decrease in reactivity compared to that found in the D7 infected cells when maintained at 37°C (Lane 2), and by 6 days into differentiation the levels of host cdc2 protein are very low (Lanes 5 -7). At day 4-6 the

host cell division rate decreases (Shiels *et al.,* 1992) and this is reflected in the profile of host cdc2 and R1 reactivity.

The trends shown by the host cdc2 and parasite ThaCRK2 are mirrored almost exactly if the sera specific for the host and parasite large subunit of ribonucleotide reductase are used. Panel C shows the profile of the anti-TaR1 anti-serum (Chapter 4). As mentioned before there are two reactive bands seen with this antibody. It can be seen that for the 97kDa polypeptide, the predicted size of the *T. annulata* large subunit of ribonucleotide reductase, the reactivity increases most markedly over the later stages of the time-course (Lanes 5-7) though there is a small gradual increase over the early stages. This parallels the rise in ThaCRK2 reactivity over the same stage (Panel A Lanes 5-7), again with reactivity peaking after 8 days at the higher temperature (Lane 6). There is proportionally much weaker reactivity seen with piroplasm extracts (Lane 8) when compared to differentiating cells at day 8 (lane 6) than there is between the same two time points with the anti ThaCRK2 antiserum. However, the cross-reactive polypeptide of ~45kDa recognised by this sera exhibits a different profile of reactivity, remaining relatively constant throughout the experiment (Lanes 2-8). With the anti-mouse R1 antibody the situation is reversed (Panel D), there is a clear decrease in reactivity by 2 days after the shift to the higher temperature (Lane 3-7). This profile parallels that seen with the anti bovine cdc2 reactivity (Panel B), linking both these together. Panel E shows the reactivity of an anti-mammalian HSP60 antibody which was selected as a control (see 6.1.3 below) to show that the levels of host protein unconnected with the cell cycle remained similar throughout the time-course (Lanes 1-7). There is no cross-reactivity observed with this antibody against any parasite protein present in piroplasms (Lane 8).

6.1.3   Induction of host HSP60 upon heat shock

In order to establish the validity of the specific changes in cell cycle proteins during differentiation it was necessary to relate these results to control proteins which are known not to be involved in the cell cycle. Several antibodies were tested which might specifically react with bovine proteins. These included antibodies against HSP-90 and histone both of which cross-reacted with piroplasms and therefore would also

probably react with the parasite component of infected lymphocytes. An antibody raised against human glucose-6-phosphate dehydrogenase (a gift of P. Mason) was also tried but did not react against the bovine homologue. A commercial antibody against HSP-60 which was found to react exclusively with a bovine polypeptide of the expected size and showed no cross reactivity with piroplasms, was eventually selected. Of course it cannot be ruled out that a cross-reactive parasite HSP-60 protein is expressed in differentiating cells and not in piroplasms but this seems unlikely. HSP proteins are generally induced under stress conditions such as heat shock and previous work had shown that parasite HSP-70 RNA increased approximately three fold after the first 4 hours following heat shock at 41°C and thereafter remained at a stable level (Kinnaird *et al.*, unpublished). It was decided to test reactivity of the bovine HSP-60 antibody over a similar period to ensure that the reactivity did not change over the major part of the differentiation time course.

Equal numbers of cells were harvested from a culture at 0, 8, 32 and 48 hours at 41°C and analysed by SDS-PAGE and immunoblotting (Figure 6.4). By 32 hours there was an approximately 4-5 fold increase in HSP-60 protein which did not change by 48 hours. This shows that the reactivity increases once the cells are exposed to the higher temperature but that the reactivity remains relatively constant over the later stages of the heat shock. This validates the use of the antibody as a control in the experiments described in section 6.1.2. It would be ideal if another host specific antibody could be used in addition to the HSP60 as a means of measuring host protein contribution over the course of differentiation.

6.1.4   Densitometer scanning of reactivity profiles confirms decrease in host cell cycle related proteins.

The autoradiographs showing the reactivity profiles of the antisera in section 6.1.2 were scanned using a BioRad Densitometer II scanner and the results used to calculate relative ratios for each anti-body as a % of the day 0 value after the background value had been subtracted (Table 6.2). The values were then plotted on a graph over the period of days at the higher temperature, as shown in figure 6.5.

This quantative analysis confirms the qualitative observations made in section 6.1.2 which showed that two host cell cycle related proteins decreased very early in the time course of differentiation. The host cdc2 protein falls to less than 50% of its inital value after 2 days at 41°C but appears to increase between this point and the next sampling point (Day 4). This is probably a track loading artefact in the gel as the same Western blot when probed with the anti-ThaCRK2 serum, gave an unexpectedly low signal in this track. This is not mirrored with the bovine R1 or TaR1 signals at the same time point as these results were obtained from a second gel. However, it is clear that between days 2 - 4, there is an approximately 50% decrease in reactivity of bovine cdc2 and R1 antibodies which appears to occur slightly earlier than the sharp rise in the two corresponding parasite polypeptides which remains at low levels until day 4 - 6. By day 8, both the host cdc2 and R1 signals have fallen to less than 20% of their initial values.

With the parasite ThaCRK2 and TaR1 signals, both show similar trends over the course of differentiation with a peak of reactivity at day 8 prior to a fall of >40% by day 10 when many of the cells are producing mature merozoites and the host cells are disintegrating. The values obtained from the HSP60 antibody reactivity showed little variation over the time course.

6.1.5 Kinase activity over D7 differentiation

Using another D7 time course, extracts were prepared every 48 hours over a period of 10 days from D7 cells incubated at 41°C. The cell extracts were standardised for equal protein concentrations and each incubated with a constant volume of p13-sepharose beads then washed as described in chapter 3. The eluate from each time point was then assayed for kinase activity using histone H1 as the exogenous substrate. The activity profile is shown in figure 6.5. It can be seen that the phosphorylation of histone H1 remains quite constant throughout the time course. There is an additional polypeptide of 45 kDa present in the piroplasm extracts (marked as X, Lane 7) which also becomes apparent in the D7 extracts after 6 days at the higher temperature (Lane 4). This is not present in uninfected lymphocytes, only faintly in D7 infected or early stage differentiating cells. It was not detectable in purified schizonts. The profile of this

polypeptide parallels the Western blot data shown in section 6.1.2 where the levels of the ThaCRK2 protein are seen to increase over the course of differentiation. It has previously been shown that ThaCRK2 binds, albeit very weakly, to p13 sepharose (chapter 3). It follows, therefore, that phosphorylation of the histone H1 substrate may be as a result of the parasite proteins kinases expressed during the later stages of differentiation assuming that at this late stage of differentiation, the host protein contribution is minimal. The Western time course data indicates that the levels of the bovine cdc2 protein drops to between 5-10% of its day 0 value by day 6-8. As the mammalian cdc2 protein is present in excess and only a small porportion is complexed (Draetta & Beach, 1988; McGowan *et al.*, 1990) to give an active kinase *in vivo*, it is possible that the histone H1 kinase activity is due to host CDK's. It is difficult to extrapolate between extracts prepared from different time-course experiments but it is possible to draw trends in activity profiles that could form the basis for future experimental work.

6.2 Discussion and Conclusions

The work presented in this chapter deals with the differentiating parasitised cell. The immunoblotting shows that the switch between proliferation and differentiation could be related to levels of host CDK and other proteins involved in the cell cycle. The parasite proteins involved in proliferation rise quite spectacularly after 96 hours (around the point of commitment to differentiation (Shiels *et al.*, 1992)) in culture at 41°C when the host proteins have dropped to less than 50% of their initial levels. The parasite proteins remain relatively constant over the first 96 hours whilst the host cdc2 and R1 levels fall. Due to the cultures not being synchronous the rises may be staggered in that each individual cell will be at a different point in its differentiation at the sampling points. If the cultures could be synchronised in terms of the cell cycle then this could only be maintained over a short period at 41°C before the synchrony of division of host and parasite would break down, so that the trends seen in figure 6.3 would be similar.

This indicates that there is an early change in the expression pattern of host cell cycle genes measured at the protein level. While this could be due to changes in the rate of protein turnover or in the rate of translation, the most likely explanation is that there is a down regulation in the transcription of these genes. Future experiments should include an analysis of RNA levels by Northern blotting and nuclear run-on studies during the time course. The fact that there is still some host cdc2 reactivity after 10 days (Lane 7) suggests that the protein is still being synthesised by some intact host cells and/or the protein is quite stable as host R1 is not detectable at this stage. Previous work had shown that host cell division rate slows down around the commitment point of the parasite to differentiation at day 4 (Shiels *et al.*, 1992). In fact, these experiments (confirming and expanding on previous preliminary experiments, J. Kinnaird, unpublished results) showed a rather earlier decline in levels of host cdc2 and in host R1 suggesting that there is a change in the regulation of expression of some or all of the host cell cycle associated proteins as early as the first 24-48 hours at the elevated temperature. There was little change in a control bovine HSP-60 protein over the time course indicating that this effect could be specific to cell cycle proteins. However, this conclusion could be strengthened if at least one other reactive bovine antibody was available as a standard. It is not known if the reduction in the amount of the two host proteins is caused by an

equal reduction in all cells in the population or whether it is restricted to a certain class of cells. If the latter is the case, it would point to an alteration in the parasite control of the host cell division associated with entry into the asynchronous differentiation pathway. It should be possible to show this by quantitative immunofluorescence assay of individual cells in a population.

However, reduction of these molecules in all cells would perhaps suggest an effect of stress i.e. heat shock on the host cell cycle. In *S. cerevisiae* it has been demonstrated that heat shock causes a temporary cell cycle block (Rowley *et al.,* 1993). In response to elevated temperature cells accumulate in G1 prior to 'START' and that this is probably due to an effect of heat shock on the transcription of some cyclin genes. As the transcription of the transcriptional activator, SW14, required for the expression of these cyclin genes, is also transiently affected by heat shock they proposed that this may partially explain the effects. Therefore, a primary effect of heat shock on the host cell cycle could be sufficient to cause an imbalance between host and parasite growth and division leading to initiation and eventual commitment to the differentiation pathway. The latter hypothesis is attractive in that it does not rule out a second phase where differentiation of the parasite and division of the host cell become mutually exclusive i.e. the parasite has no further need for an actively dividing host cell for its proliferation hence the control over host cell division is shut down.

It is not possible to standardise the piroplasm track loading in terms of equal cell number as was done with the differentiating cells but protein loadings were equivalent as assessed by Ponceau S staining. It is possible, however, to obtain comparative ratios of protein levels in the piroplasm stage from reactivities of different antisera. Hence in the piroplasm stage, reactivity with anti-ThaCRK2 is at a similar level to day 8 differentiating cells and much greater than day 10. With TaR1 antisera the piroplasm reactivity is much less than that observed at day 8 or 10. As ThaCRK2 is not detectable in merozoites by immunofluorescence, it suggests that the gene is actively transcribed in the piroplasm stage and this conclusion is supported by the detection of high levels of specific mRNA and protein (Kinnaird *et al.,* 1996). The comparatively low reactivity of the TaR1 anti-sera in the piroplasm stage compared to the actively dividing stages of differentiation suggests that division is not a major feature of the asynchronous piroplasm population. This provides further evidence for the conclusions, made by Conrad *et al.,* (1985) based

on microscopic evidence, that *T. annulata* piroplasms only divide twice in the erythrocyte stage. The low levels of TaR1 reactivity, an essential enzyme of DNA synthesis, also tend to disprove the theory that *T. annulata* piroplasms can form merozoites which continually re-invade erythrocytes and develop into piroplasms, This is known to happen in *T. sergenti* (Uilenberg *et al.,* 1985) and it would be interesting to compare the relative levels of R1 protein in the piroplasm stage of the two species.

Certainly the parasite increases its rate of nuclear division during differentiation which would account for the rise in ThaCRK2 and TaR1 levels between day 4 and day 8. If this is the case, it raises the question as to why ThaCRK2 is highly expressed in piroplasms if it functions in the regulation of division. This points to an additional role for ThaCRK2, possibly directed by a different cyclin partner and, although it is premature to speculate, ThaCRK2 could play a role in organisation of the piroplasm nuclear structure in preparation for the tick vector stage or perhaps in gametocytogenesis which is likely to occur at this stage.

The histone H1 phosphorylation profile does not change greatly over the course of differentiation using proteins bound to p13 sepharose. It was previously shown (chapter 3) that bovine CDKs and, at least, two parasite kinases can bind to yeast p13. The amount of bovine cdc2 in the differentiating cell population has been shown to decrease considerably from early in differentiation. However, as cdc2 is always present in considerable excess in cells (Draetta & Beach, 1988, McGowan *et al.,* 1990) even a reduced amount of polypeptide may still show little reduction in activity, if other important proteins such as cyclins are still being expressed. It has also been shown that parasite ThaCRK2, a putative cdc2 homologue, rises greatly during differentiation and this also binds to p13 albeit weakly (chapter 3). Thus, ThaCRK2 may contribute to the p13 bound kinase activity seen here in the later stages of differentiation. However, immunodepletion of ThaCRK2 from piroplasm extracts (chapter 3) did not greatly alter the casein phosphorylation profile but did change the histone H1 phosphorylation profile. It was concluded that a second p13 bound kinase may be largely responsible for casein phosphorylation. As this parasite kinase is unidentified, its expression profile during differentiation is unknown. Clearly, p13 purification of cdc2 related kinases cannot distinguish clearly between host and parasite activities, especially as bovine cdc2/CDK2 may have a much higher affinity for p13. Therefore, this experiment does not clarify the

obvious decrease in amount of host cdc2 protein in terms of a parallel decrease in activity. A future approach would be to assay the different kinase activities over a time course using specific antisera for immunoprecipitation. Human cdc2 C terminal antibody will immunoprecipitate bovine cdc2 from native extracts to give a histone H1 kinase activity but it has not yet been possible to immunoprecipitate kinase activity for parasite CRK2 (J. Kinnaird, pers.comm.).

A polypeptide of 45 kDa was strongly phosphorylated in the p13 bound complex from piroplasm extracts and also in later stage differentiating cells. This polypeptide has the same molecular weight as the polypeptide identified as being specifically phosphorylated by a p13 bound complex from piroplasm extracts (chapter 3). Phosphorylation of this polypeptide was found to be considerably reduced in ThaCRK2 immunodepleted extracts and it was concluded that it may represent a component of the active ThaCRK2 kinase complex that is phosphorylated by ThaCRK2 or perhaps the second kinase bound to p13 could be a substrate for ThaCRK2.

The recent publication of Graeser et al (1996) found that the PfPK5 kinase, which is likely to be the P. falciparum homologue of ThaCRK2 because of the degree of identity, was possibly associated with S phase as activity was high in aphidicolin blocked cells. In the time course reported here, TaR1 antibody reactivity increases in parallel with ThaCRK2 again indicating that DNA synthesis is a major feature in post commitment differentiating cells.

With respect to the p13 bound kinase assays, there are other parasite proteins binding which seem to increase over the differentiation and are still present in the piroplasm stage. One of these may be the recently identified ThaCRK3 which could be assayed for p13 binding properties once a good anti-serum is produced. This could also be used to probe immunoblots of the p13 eluate fractions from D7 cells and piroplasms to determine if it is expressed at the protein level during differentiation.

To conclude, there is a very early decrease in two proteins associated with the host cell cycle. This occurs before a decrease in division rate and before commitment of the parasite to differentiation. It may suggest that the parasite derived mechanism which controls host cell proliferation is altered during the early stages of differentiation.

Figure 6.1 Giesma staining of D7 infected cell differentiation time course at 41°C used to prepare protein samples.

For each time point sample, 100µl of cells were centrifuged onto glass microscope slides using a cyto-spin (Shandon). The slides were then dried and fixed in methanol prior to staining in Giesma stain. The slides were then viewed and photographed at a X100 magnification.
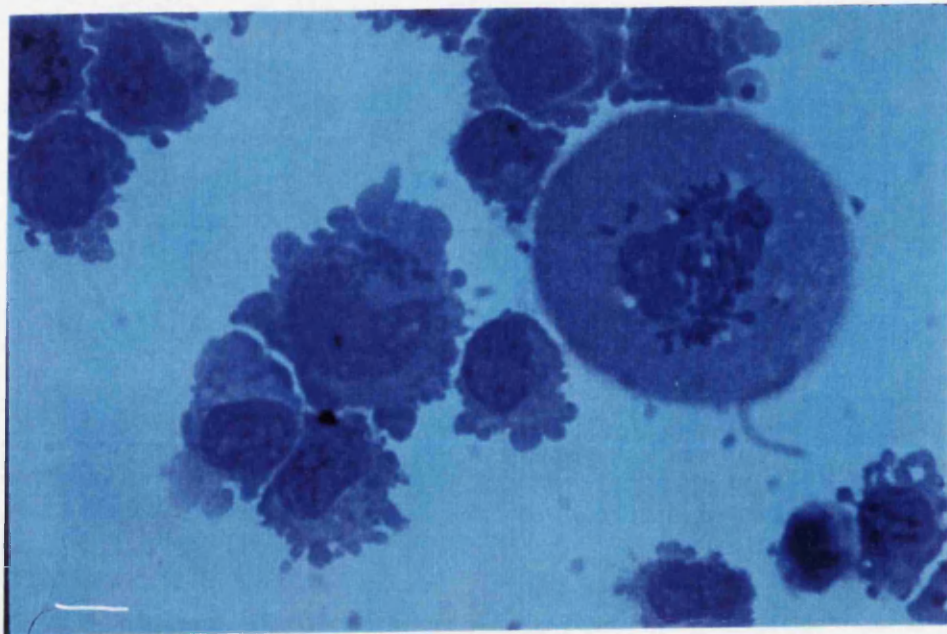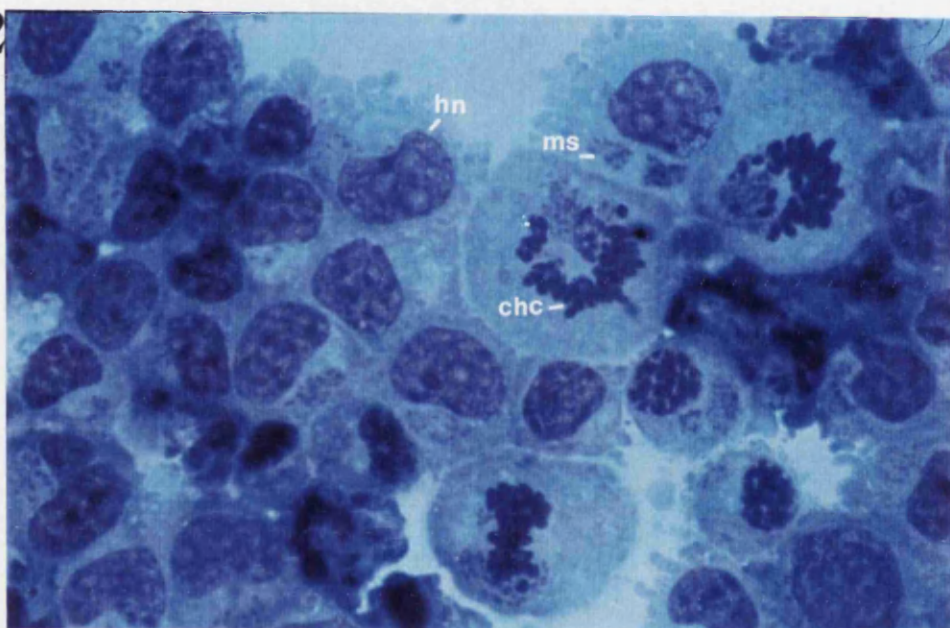Scale bar is 10µm.

Key:

Print 1	D7 @ 37°C
Print 2	D7 cells after 2 days at 41°C
Print 3	D7 cells after 4 days at 41°C
Print 4	D7 cells after 6 days at 41°C
Print 5	D7 cells after 8 days at 41°C
Print 6	D7 cells after 10 days at 41°C

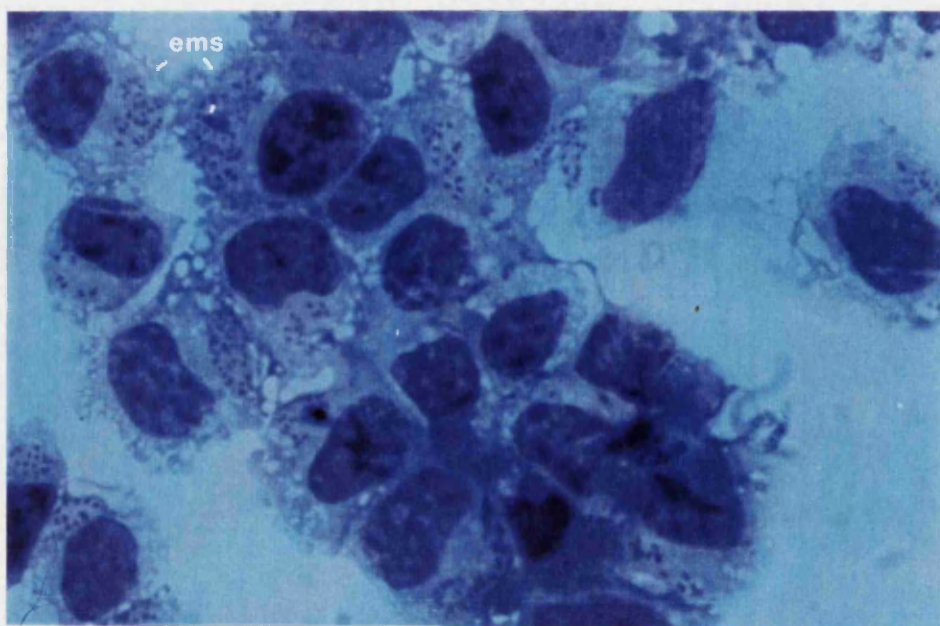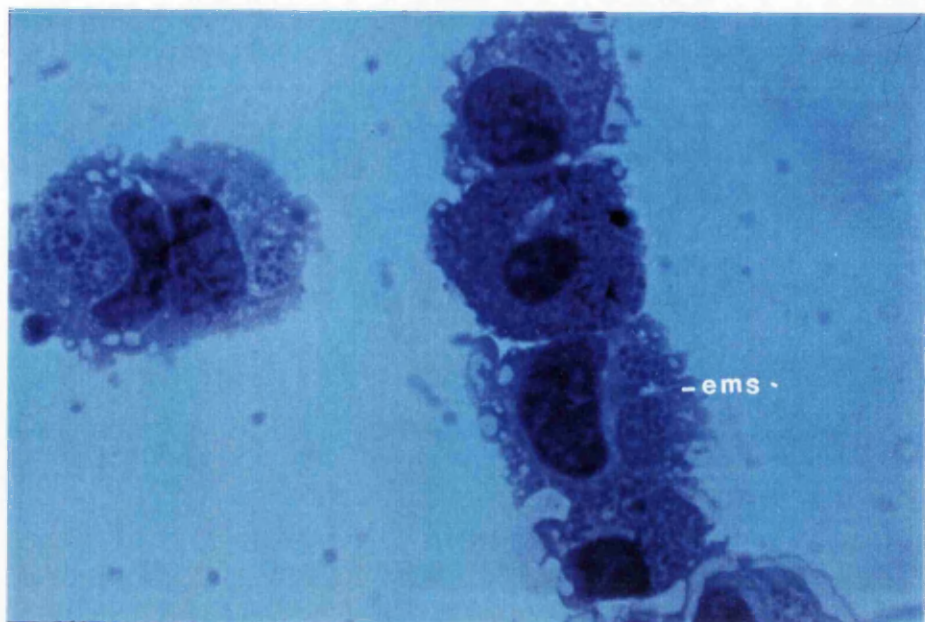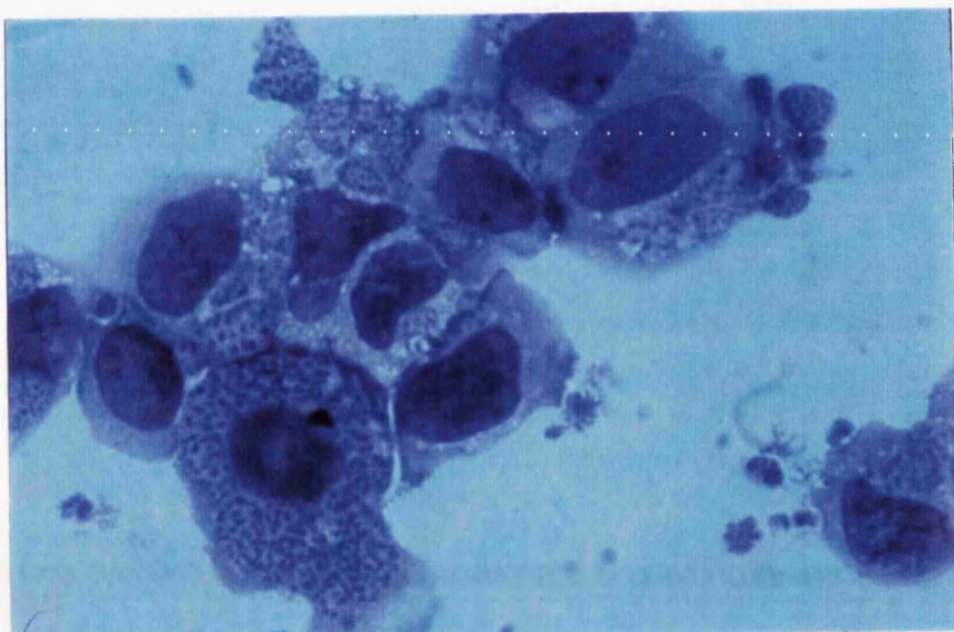|	
hn	Host nucleus
chc	Condensed host chromosomes
ms	Macroschizont
ems	Enlarged macroschizont
m	Merozoites

1

2
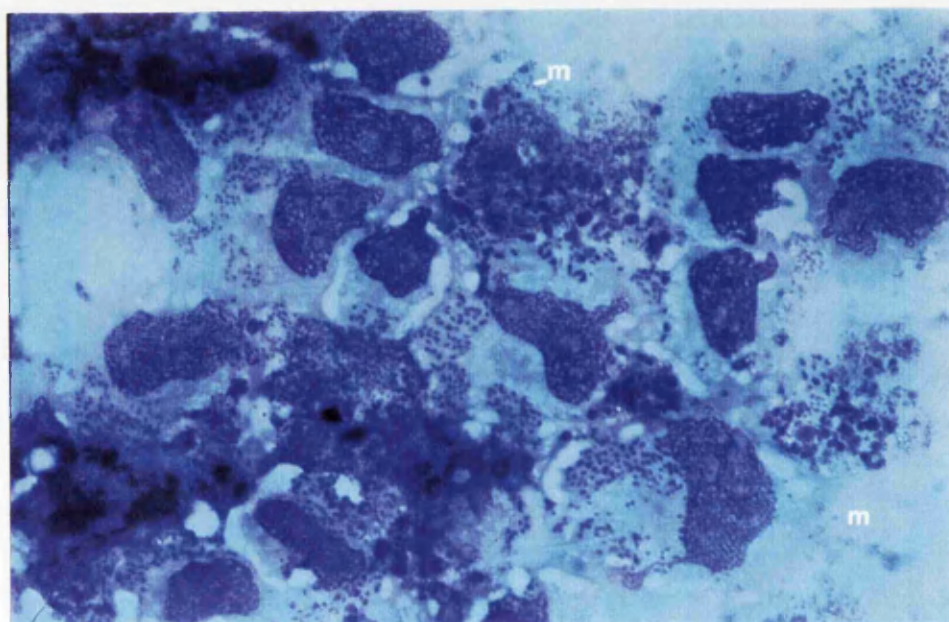

3

4

ems

5

6

m

m

Figure 6.2 Graph showing fold increase in cell numbers over course of differentiation

The values for the fold increase in cell number relative to day 2 were plotted against number of days at 41°C. The values are as in Table 6.1.
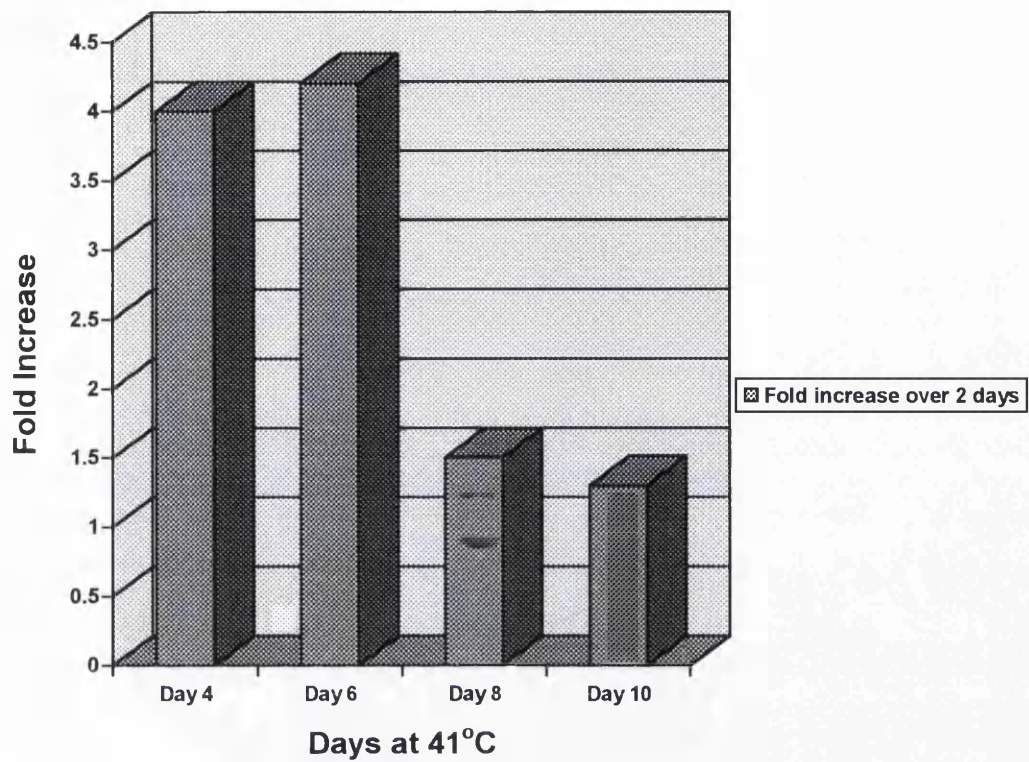
Figure 6.3 Reactivity Profile of anti-sera against cell cycle proteins during infected cell differentiation.

A time course of D7 infected cells were placed at 41°C and samples taken after 2, 4, 6, 8, and 10 days at 41°C. Samples were standardised for equal cell numbers at each of the sampling points. Samples of uninfected cells and D7 cells grown under standard conditions were also taken (BL20 and D7@37°C).

Samples from each sample were lysed in SDS-PAGE sample buffer and separated on 12.5% and 8% SDS-PAGE gels and immunoblotted Protein loadings were assessed by Ponceau S staining and samples are standardised for equal cell numbers at each time point.

Panel A shows the reactivity profile of the anti-ThaCRK2 anti-serum.

Panel B shows the same gel probed with the higher eukaryote anti-cdc2 anti-serum.

Panel C shows reactivity profile with the anti-TaR1 anti-serum.

Panel D shows the profile with the higher eukaryote specific anti-R1 antibody.

Panel E shows the profile with the higher eukaryotic specific anti-Heat Shock Protein (HSP-60) anti-serum (Sigma).

Key:

Lane 1   BL20 total cell extracts.
Lane 2   D7 infected cell extracts @ 37°C.
Lane 3   D7 cell extracts after 2 days at 41°C.
Lane 4   D7 cell extracts after 4 days at 41°C.
Lane 5   D7 cell extracts after 6 days at 41°C.
Lane 6   D7 cell extracts after 8 days at 41°C.
Lane 7   D7 cell extracts after 10 days at 41°C.
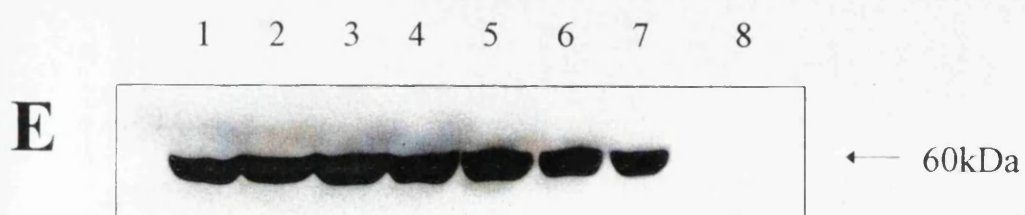**Lane 8**   Piroplasm cell extracts.

A   1 2 3 4 5 6 7 8 8   ← 34kDa

B   1 2 3 4 5 6 7 8   ← 34kDa

C   1 2 3 4 5 6 7 8   ← 97kDa   ← 45kDa

D   1 2 3 4 5 6 7 8   ← 90kDa
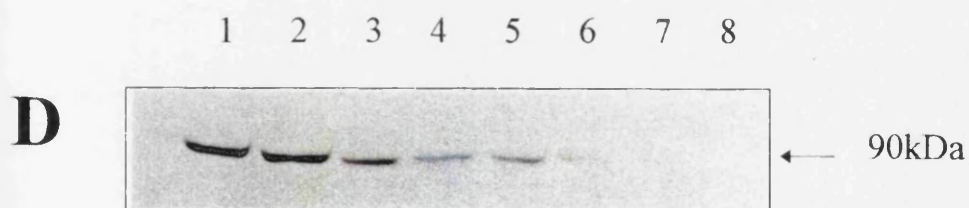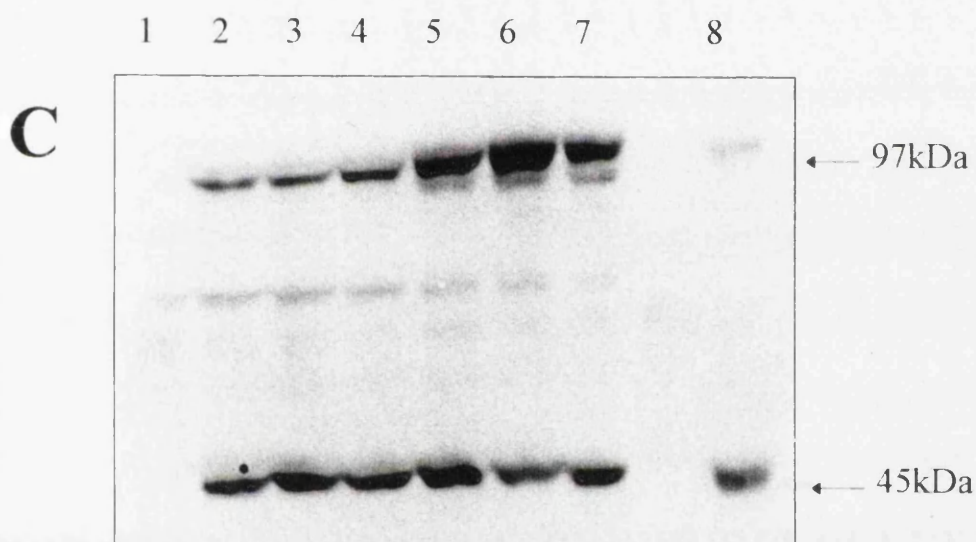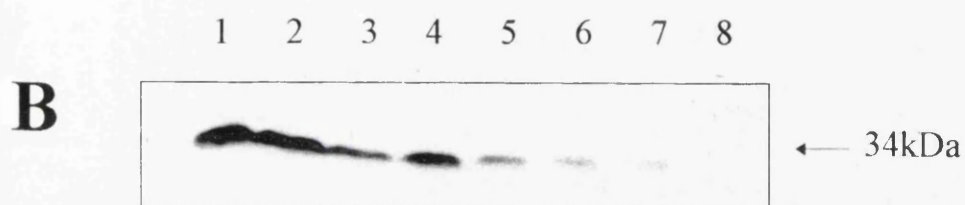
E   1 2 3 4 5 6 7 8   ← 60kDa
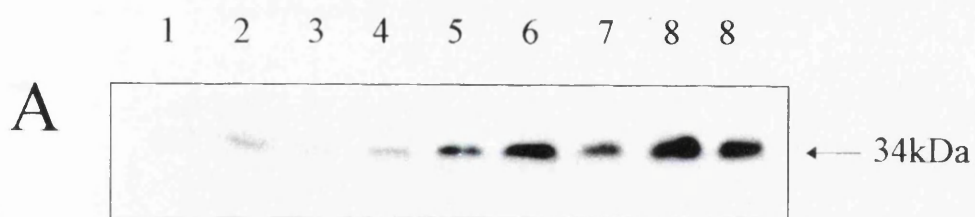
Figure 6.4 HSP-60 reactivity increases upon heat shock of D7 cells

The HSP-60 monoclonal antibody used in section 5.1 was shown to react specifically with host HSP-60 only. An immunoblot was done to assess the reactivity profile after the D7 cells had been placed at 41°C. Extracts were prepared from equal cell number samples of a D7 cell culture after 8, 32 and 48 hours at the higher temperature, separated on an 8% SDS-PAGE gel and immunoblotted. Equal protein loadings were assessed by Ponceau S staining after transfer.

This figure shows the profile obtained with the antibody over these sampling points. Sizes are as indicated on the left of the figure.

Panel A shows a 60 second exposure.

Panel B shows the same blot exposed for 5 minutes.

Key:

Lane 1	D7 cells at 37°C
Lane 2	D7 cells after 8 hours at 41°C
Lane 3	D7 cells after 32 hours at 41°C
Lane 4	D7 cells after 48 hours at 41°C
Lane 5	Piroplasm extracts

A

| 1 | 2 | 3 | 4 | 5 |

← 63kDa
← 60kDa

B

| 1 | 2 | 3 | 4 | 5 |

← 63kDa
← 60kDa

Figure 6.5 Densitometry results show decrease in host cell cycle proteins over differentiation

The values of the densitometry scanning analysis are plotted for both the parasite and host proteins.
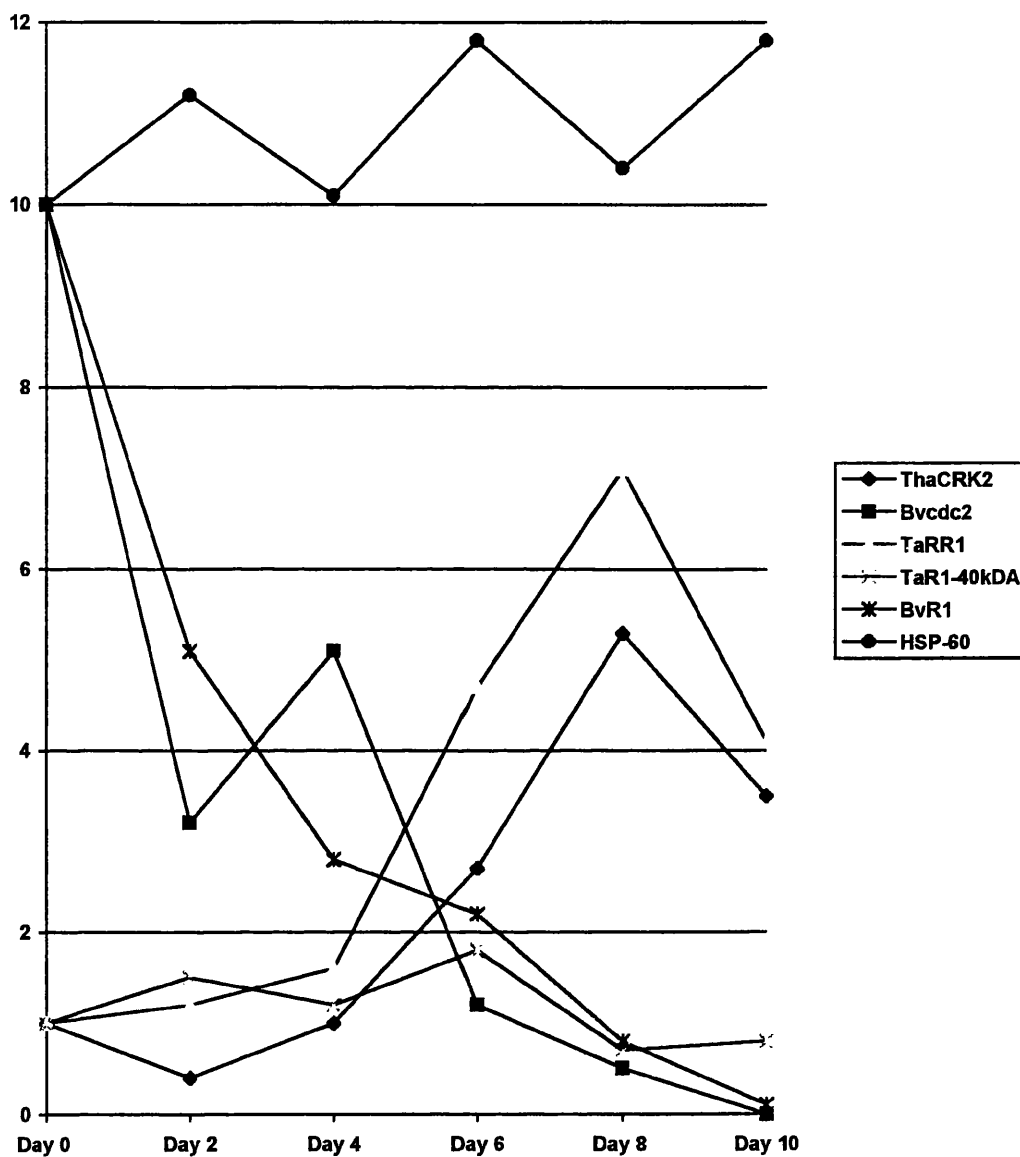
Day 0 normalised to 1.0 for parasite antibodies
Day 0 normalised to 10.0 for host antibodies

Based on equal cell numbers for each time point sampled

Figure 6.6 Kinase assay of differentiating cell extracts after p13 binding.

This figure shows differentiating D7 cell extracts assayed for kinase activity after binding to p13. Kinase assays were done using Histone H1 as the exogenous substrate as detailed in chapter 3. Two specific bands referred to in the text are labelled as X and Y.

Key:

Lane 1:   D7 extracts @37°C

Lane 2:   D7 extracts after 2 days at 41 °C

Lane 3:   D7 extracts after 4 days at 41 °C

Lane 4:   D7 extracts after 6 days at 41 °C

Lane 5:   D7 extracts after 8 days at 41 °C

Lane 6:   Schizont extracts

Lane 7:   Piroplasm extracts
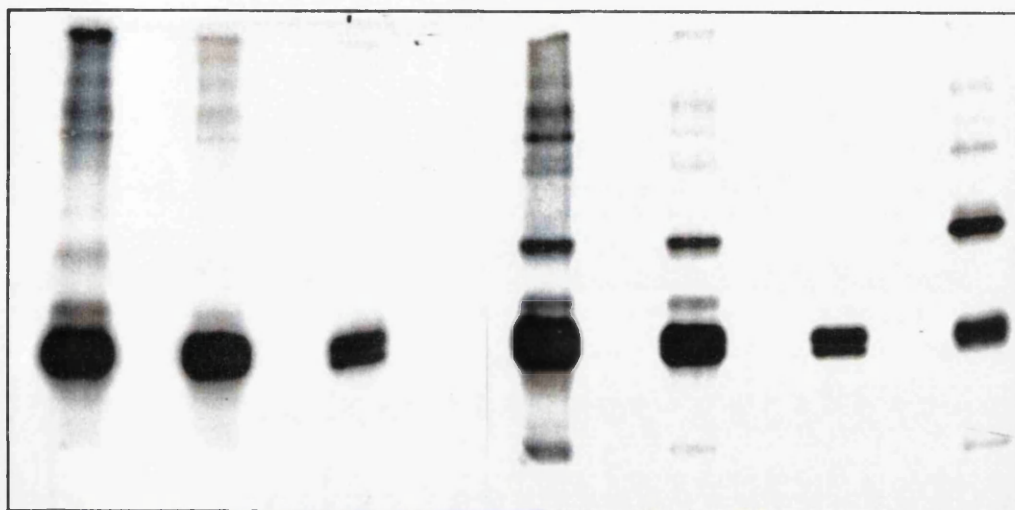
Table 6.1 Cell counts for the D7 time course

The cell counts for each sampling point are listed below together with the dilution used.

Days at 41°C	Cell Numbers/ml	Diluted to/ml	Fold increase
2	7.4×10^5	1.48×10^5	-
4	5.9×10^5	1.2×10^5	4.0
6	5.0×10^5	1.4×10^5	4.2
8	2.1×10^5	-	1.5
10	2.8×10^5	-	1.3

Table 6.2 Densitometer Scanning of Time course immunoblots

The immunoblots described in section 6.1.2 were scanned using a BioRad densitometer and the absorbance values for each antibody were used to plot a graph showing change of reactivity of the antisera over the course of differentiation.

For each antibody the values are calculated as a relative value compared to the Day 0 figure. For host antibodies the Day 0 value was normalised to 10 and for parasite antibodies this figure was normalised to 1.
Background absorbance was subtracted from each absorbance value (Abs) to give the true absorbance (Abs-B/gr.)
For plotting the graph (figure 6.4) only the D7 day 0 to day 10 values were used. The BL20 and piroplasm reactivity values were not used.

D. Anti-R1 anti-serum specific for host R1.

Background - 16.199

Sample	Absorbance	Abs-B/ground	Relative Value
BL20	20.508	4.309	-
Day 0	20.586	4.387	10.0
Day 2	18.398	2.199	5.1
Day 4	17.394	1.195	2.8
Day 6	17.131	0.932	2.2
Day 8	16.554	0.355	0.8
Day 10	16.243	0.044	0.1
Piroplasm	0.000	0.000	-

E. Anti-HSP-60 antibody.

Background - 20.236

Sample	Absorbance	Abs-B/ground	Relative Value
BL20	20.756	0.520	-
Day 0	20.805	0.569	10.0
Day 2	20.873	0.637	11.2
Day 4	20.815	0.576	10.1
Day 6	20.909	0.673	11.8
Day 8	20.826	0.590	10.4
Day 10	20.915	0.679	11.8
Piroplasm	-	-	

Chapter Seven

Summary

and

Future Perspectives

7. Summary and Future Perspectives

The *Theileria* life cycle is characterised by alternating phases of proliferation and arrest and the proliferative stages are associated with much of the pathogenic features of the disease. A detailed understanding of how parasite growth and division cycles are controlled will lead, ultimately, to the development of highly specific reagents for treatment of the disease. The work presented here attempts to address these issues.

The first stage of the work focussed on the use of yeast p13 sepharose as a means of affinity purification of p13 binding kinases from *T. annulata*. At least two different p13 binding kinase activities were demonstrated from the piroplasm stage of *T. annulata*. The substrate preferences of these kinases differs with the ThaCRK2 kinase showing a preference for histone. The other kinase whose existence was first inferred from the prior immunodepletion of ThaCRK2 binding studies exhibited stronger phosphorylation of casein and can possibly bind p13 with a stronger specific affinity than ThaCRK2. This other kinase may be encoded by the ThaCRK3 gene which was recently isolated. This will be confirmed once the anti-sera is available against this protein. Results presented here suggest that the binding of *T. annulata* kinases to yeast p13 was not optimal. It was not possible to isolate a *Theileria* homologue in this study but certainly, if a p13^{suc1} homologue could be isolated from *T. annulata* then this would be expected to show maximal affinity for *T. annulata* CRKs. It is possible that bovine CRK's would have a reduced affinity for a *Theileria* p13 homologue and this may provide a means for a more specific detection of parasite cdc2-related kinase activity from the intra-lymphocytic stage. Future attempts to clone this parasite homologue may include design of more suitable degenerate oligonucleotide primers for PCR amplification or using a *Theileria* CRK cDNA cloned in a suitable yeast expression vector as a trap in the yeast two hybrid system screen for interacting polypeptides. An alternative approach might be to screen a cDNA expression library with recombinant histidine tagged ThaCRK2 followed by specific detection of the histidine tag by a specific antiserum. However, this would depend upon correct folding of the proteins in bacterial expression systems.

Further refinement of the p13 sepharose purification system for CRK's and/or development of specific antibodies against parasite and host CRK's for

immunoprecipitation would allow comparartive assay systems to be established for testing different kinase inhibitors for differential effects on parasite and host.

Two cdc2-related kinases have been isolated so far from *T. annulata* and this shows that there is a family of cdc2-related kinases present in this parasite. This mirrors the situation in *Leishmania*, *Trypanosoma* and *Plasmodium*. It may be that there still remains a cdc2 homologue to be isolated from these parasites and the genes isolated so far may be related to other aspects of the parasite life cycle and may not be involved in the cell cycle. Gene knockouts with the *Leishmania* CRKs shows them to be essential (J. Mottram, pers. comm.) for parasite survival. Once the binding partners for these CRKs have been isolated and characterised, it may be possible to determine precise functional roles for these polypeptides in the individual parasite. Regarding cyclins, one has been cloned from *P. falciparum* and two from *T. brucei* (P. Neuville, pers. comm.). It is feasible that there will be significant differences in the regulation of parasite CRKs given the evolutionary distance between them and the higher eukaryotes.Although all the data so far suggests that the mechanisms of kinase regulation are conserved, the molecules involved may be different. It will be interesting to compare phylogenetic relationships between the CRKs and other genes involved in the cell cycle to assess how these differ compared to the classical phylogenetic relationships derived from rRNA genes (Gajadhar *et al.*, 1991). If rRNA genes are used to predict evolutionary relationships between the protozoa then *T. annulata* is close to *Sarcocystis muris*, a related Apicomplexan, but there is considerable divergence between *T. annulata* and *Plasmodium* which is surprising given the similarities between this pair in morphology and life cycles. The apicomplexans form a group with dinoflagellates and with ciliates which is separate from the other protist groups.

More information regarding the cellular localisation of the CRKs would point to possible functions of these proteins especially since work with PfPK5 (which is likely to be the homologue of ThaCRK2) suggests it to have a role in the nuclear division cycle in *P. falciparum* (Graeser *et al.*, 1996b). The authors immunolocalised PfPK5 to the edge of the parasite nuclei, possibly close to the centrosomes. Based on the knowledge of the localisation of cdc2/cyclin B to the mitotic spindles in HeLa cells, they postulated PfPK5 to have a role in mitosis, possibly in organisation of the spindle. Because of a higher activity of PfPK5 in aphidicolin blocked parasites, the authors speculated that PfPK5

may also have a role in DNA synthesis suggesting, as is the situation with cdc2 in higher eukaryotes, that PfPK5 may act at both G1/S and G2/M phases of the nuclear division cycle. In agreement with this, PfPK5 localised diffusely with DNA staining during S phase rather than as the discrete points at the sides of nuclei found later in the cycle. ThaCRK2 localises predominantly to the schizont cytoplasm, a situation found for PfPK5 by other workers (Ross-MacDonald *et al.*, 1994). This suggests that different fixation methods might bias localisation results, a situation found in HeLa cells (Bailly *et al.*, 1989; Riabowol *et al.*, 1989). It is possible that ThaCRK2 could also have a nuclear localisation which is beyond the limits of detection by the anti-serum. BrdU incorporation studies showed that very few parasites were synthesising DNA at any one point during growth at 37°C (10-20%). Hence, if transport of ThaCRK2 into the nucleus likewise only occured in a small percentage of parasites at any one time this would render detection in the nuclei even more difficult.

The isolation and characterisation of the large subunit of ribonucleotide reductase raises the possibility that this can be used as a target for a species specific therapeutic. The *Theileria* R1 subunit possibly possesses an N - terminal extension which is not present in the higher eukaryotes. This is interesting in terms of why is it present? Does it exist in the mature protein? If so, how would it affect the folding of the large subunit, its dimerisation and its interaction with the small subunit? Does this region have a role in the allosteric regulation of the parasite enzyme? If so, how does this regulation differ? Since the *P. falciparum* gene also contains an upstream region from the consensus eukaryotic start codon, it is possible that an N-terminal extension could be a feature of all Apicomplexan R1 subunits. It is interesting to speculate how the ribonucleotide reductase enzyme of *P. falciparum* may differ in terms of its allosteric regulation given the AT richness of the *Plasmodium* genome. Certainly if it were shown that this region is present in the mature protein, as is likely based on the most 5' translational start sequence having the best fit to the protozoan consensus start sequence, then it may be worthwhile testing anti-sense oligonucleotides and peptidomimetic inhibitors against this region as they shouldn't affect the host enzyme. As a first step in this latter direction it is necessary to show that the N-terminal extension is present in the mature protein either by purification of sufficient quantities of R1 for N-terminal sequencing or by generation of a specific antiserum. It would also be necessary to model the N-terminal extension on a 3-

dimensional structure prediction of the R1 subunit, in order to assess its effects on the tertiary and quaternary structure of the enzyme. Given the success of the peptidomimetic inhibitors against the *Herpes simplex* virus *in vivo* (Liuzzi *et al.*, 1994) then it may well be possible to use these against a range of intracellular parasites. If anything, *Theileria* could be the best *in vitro* system to use for this since there are easily maintained cloned cell lines available. As most peptidomimetic inhibitors are based on the sequence of the site of interaction in the small (R2) subunit, future work should center on isolation of this gene from *T. annulata*. Production of both recombinant subunits may allow an *in vitro* assay to be established for rapid testing of different inhibitors.

The localisation of the TaR1 subunit to the nucleus differs from the R1 subunit localisation in the host which is strictly cytoplasmic. Given this result, it is feasible that the DNA replication cycle of each nucleus is partly under individual control in that a supply of dNTP's does not come from a common pool but is synthesised within each nucleus. It is possible that the small subunit in *Theileria* plays a role in the regulation of ribonucleotide reductase activity as is found in the mouse, by the S phase specific synthesis and breakdown of the R2 protein (Engstrom *et al.*, 1984). The R1 protein in mice is constitutively expressed and remains at a constant level and is in excess throughout the cell cycle. It is possible that this situation occurs in *Theileria* as all nuclei were seen to label with the anti-TaR1 antisera by immunofluoresence. It is possible that the R2 subunit is synthesised in the cytoplasm every cell cycle and transported into the nucleus to combine with the large subunit, producing an active enzyme. If the small subunit is successfully cloned and specific antiserum raised to a fusion protein, it will be possible to carry out immunolocalisation studies which could test this hypothesis.

Northern blotting of RNA prepared from the aphidicolin treated cells showed that there was little change in the levels of the ThaCRK2 mRNA after release from block. However, there was a small but noticable peak in the amount of TaR1 mRNA after release from block. This coincided with the end of parasite S phase. The inference from this is that these ThaCRK2 gene is not under cell cycle control but the TaR1 gene may be subject to some form of transcriptional regulation. The sequencing of the upstream sequence from TaR1 shows there to be some common motifs but further experiments are needed to map which regions are important in expression and if these regions are capable of binding transcription factors.

Attempts made to synchronise D7 cells growing at 37°C using aphidicolin resulted in only 50% of the parasites being synchronised. The figure for synchrony of the host cell was higher given that mammalian DNA polymerases are known to be inhibited by aphidicolin. The situation in protozoa is different. Some such as the *P. falciparum* are known to be sensitive whilst others such as *T. gondii* and *T. brucei* are known to be insensitive. It was not possible to determine if the *T. annulata* polymerase is sensitive but there was a partial effect observed in the D7 cells used where drug treatment led to 50% of parasites entering S phase as opposed to the non-drug treated situation of 10-20%. This suggests that aphidicolin probably inhibits the parasite DNA replication. Parasite nuclei rarely labelled in the absence of parallel host nuclei labelling.

In the light of analysis of cell cycle protein levels in differentiating cells (Chapter 6) it is interesting how the levels of ThaCRK2 and TaR1 change over this period. The levels rise dramatically after 4 days at 41°C. This would just precede the reduction in host cell division and the massive enlargement of the macroschizont stage. This would provide pools of ThaCRK2 and TaR1 proteins needed for division and a higher rate of DNA synthesis occuring in the parasite nuclei. The levels of both drop at day 10 which would reflect the cell population completing differentiation into the merozoite stage which is non-dividing. The levels of the two host cell cycle markers, cdc2 and the large subunit of ribonucleotide reductase drop very early after the cells are shifted to the higher temperature. This is interesting as it indicates that synthesis of some of the host proteins essential for the cell cycle may be down-regulated before the commitment to differentiation. It is known that the stress of heat shock in yeast can cause a transitory arrest of the cell cycle in G1 and has an effect on transcription of genes such as R1. It is possible that this could be sufficient to provide the initial stimulus for a switch to a differential pathway by the parasite leading to a decline in the parasite induced host cell proliferation. A cell line, derived from the enhanced differentiating cloned cell line D7, has been isolated and does not differentiate to a significant extent at 41°C. The nature of the change is not known (Shiels *et al.,* unpublished). However, such a cell line would provide an ideal control for a parallel set of experiments to analyse the polypeptide changes in host and parasite cell cycle proteins over a time course at 41°C.

The experiments using BrdU incorporation to measure DNA synthesis showed this synthesis to be synchronous between nuclei in a macroschizont. The implications of

this would be that the division of each nucleus would only be synchronous if it were to rely on a common cytoplasmic pool of molecules needed for the intiation of replication. This allows for the speculation that the localisation of the ThaCRK2 to the cytoplasm is indictive of its role in the division of the nuclei in a manner similar to that postulated for PfPK5 (Graeser *et al.*, 1996b). Although there would need to be a control mechanism for the regulation of ThaCRK2 to ensure its activation at the correct stage. This could be achieved by specific cell cycle expression of cyclins and other regulatory molecules as found in higher eukaryotes. A possible theory for the control of parasite nuclear division can be made based on the results in this thesis. In D7 cells, BrdU incorporation showed that parasite nuclei within a macroschizont undergo synchronous DNA synthesis. R1 was localised to parasite nuclei and ThaCRK2 was already known to be predominantly in the cytoplasm. It is possible that control of RR activity may be due to cyclical synthesis and breakdown of the R2 subunit which would be relocated to the nucleus at each nuclear division cycle to allow for provision of dNTP's for DNA synthesis. Transcription of R1 and R2 may ultimately be under the control of a CDK such as ThCRK2 which could be activated in the cytoplasm, perhaps by a threshold concentration of cyclin binding partners. Activated ThaCRK2 would be transported to the nucleus to act on its substrate. Such a theory would accommodate the need for a common pool of a regulatory molecule to achieve co-ordination of DNA synthesis between nuclei. This may be a cyclin binding partner although other possibilities cannot be ruled out.

. This raises a question about how the timing mechanisms of S and M phase are then integrated. There may be a relative timing mechanism in that all the parasite nuclei undergo replication at the same time then mitosis would occur at a set time afterwards. There is a G2 size control phase operating under rapid growth conditions in fission yeast which integrates mitosis with cell size. The size at mitosis was found to be dependent on the *wee1:cdc25* ratio. As the cells grow during G2 the levels of *cdc25* mRNA and protein rise until mitosis is triggered which may mean that size control is a relative timing mechanism whereby mitosis occurs after a threshold level of Cdc25 is reached, activating cdc2 (reviewed in Lew & Kornbluth, 1996).

To conclude, this work has shown the existence of at least two kinases which are capable of binding to p13^{suc1}. These kinases, one of which is ThaCRK2, are likely to play a role in the cell cycle of *T.annulata*. The large subunit of ribonucleotide reductase has

also been isolated and gives optimism for use as a possible therapeutic target. It also has significant differences in its molecular and structural biology from that of the higher eukaryotic homologues which make a case for the further study of this molecule. The use of specific antisera has given an insight into the interplay between host and parasite cell cycle associated proteins during the intracellular differentiation of the parasite to the merozoite stage and raised questions about what means of control the parasite is using in its division cycle. Attempts with aphidicolin to synchronise infected cell populations merit further study.

More is known now about the proliferation and differentiation process in *Theileria annulata* and progress on the gene expression patterns within the macroschizont and the proof of exchange of polypeptides between host and parasite hint that the mechanism of transformation may soon be deduced.

References

References

Adamson, R. E. and Hall, F. R. (1996). Matrix metalloproteinases mediate the metastatic phenotype of *Theileria annulata*-transformed cells. Parasitology **113**: 449-455.

Affranchino, J. L., Gonzalez, S. A. and Pays, E. (1993). Isolation of a mitotic like cyclin homologue form the protozoan parasite *Trypanosoma brucei*. Gene **132**: 75-82.

Arison, D., Meijer, L., Brizuela, L. and Beach, D. (1988). *cdc2* is a component of the M phase specific histone H1 kinase: Evidence for identity with MPF. Cell **55**: 371-378.

Ashfield, R., Enriquez-Harris, P. and Proudfoot, N. J. (1991). Transcriptional termination between the closely linked human complement genes C2 and factor B - common termination factor for C2 and c-myc. EMBO Journal **10**: 4197-4207.

Azzi, L., Meijer, L., Ostvold, A. C., Lew, J. and Wang, J. H. (1994). Purification of a 15kDa cdk4- and cdk5- binding protein. Journal of Biological Chemistry **269**: 13279-13288.

Azzi, L., Meijer, L., Reed, S. I., Pidikiti, R. and Tung, H. Y. L. (1992). Interactions between the cell cycle control proteins p34^{cdc2} and p9^{CKSHS2} - evidence for 2 co-operative binding domains in p9^{CKSHS2}. European Journal of Biochemistry **203**: 353-360.

Bailly, E., Doree, M., Nurse, P. and Bornens, M. (1989). p34^{cdc2} is located in both nucleus and cytoplasm - part is centrosomally located at G2/M and enters vesicles at anaphase. EMBO Journal **8**: 3985-3995.

Barker, R. H., Metelev, V., Rapaport, E. and Zamecnik, P. (1996). Inhibition of *Plasmodium falciparum* malaria using antisense oligodeoxynucleotides. Proceedings of the National Academy of Sciences, USA **93**: 514-518.

Basi, G. and Draetta, G. (1995). p13^{suc1} of *Schizosaccharomyces pombe* regulates 2 distinct forms of the mitotic cdc2 kinase. Molecular and Cellular Biology **15**: 2028-2036.

Baylis, H. A., Megson, A., Brown , C. D. G., Wilkie, G. F. and Hall, R. (1992). *Theileria annulata* - infected cells produce abundant proteases whose activity is reduced by long-term cell culture. Parasitology **105**: 417-423.

Baylis, H. A., Megson, A. and Hall, R. (1995). Infection with *Theileria annulata* induces expression of matrix metalloproteinase 9 and trsnscription factor AP-1 in bovine leukocytes. Molecular and Biochemical Parasitology **69**: 211-222.

Bjorklund, S., Hjortsberg, K., Johansson, E. and Thelander, L. (1993). Structure and promoter characterisation of the gene encoding the large subunit (R1 protein) of mouse ribonucleotide reductase. Proceedings of the National Academy of Sciences, USA **90**: 11323-11326.

Bjorklund, S., Skogman, E. and Thelander, L. (1992). An S phase specific release from a transcriptional block regulates the expression of mouse ribonucleotide reductase R2 subunit. EMBO Journal **11**: 4953-4959.

Booher, R. and Beach, D. (1986). Site specific mutagenesis of $cdc22^+$, a cell cycle control gene of the fission yeast *Schizosaccharomyces pombe*. Molecular and Cellular Biology **6**: 3523-3529.

Bornemann, C., Drude, K. and Follman, H. (1996). Deoxyribonucleotide synthesis in green algae. Cell cycle fluctuation of ribonucleotide reductase is only moderate in the unicellular, exsymbiotic green algae, *Chlorella* sp. pbi. Plant Physiology **148**: 657-661.

Boulter, N., Knight, P. A., Hunt, P. D., Hennessey, E. S., Katzer, F., Tait, A., Williamson, S., Brown, D., Baylis, H. A. and Hall, R. (1994). *Theileria annulata* sporozoite surface antigen (SPAG-1) contains neutralising determinants in the C-terminus. Parasite Immunology **16**: 97-104.

Bourne, Y., Watson, M. H., Hickey, M. J., Holmes, W., Rocque, W., Reed, S. I. and Tainer, J. A. (1996). Crystal structure and mutational analysis of the human CDK2 kinase complex with the cell cycle regulatory protein CksHs1. Cell **84**: 863-874.

Brizuela, L., Draetta, G. and Beach, D. (1987). p13 suc1 acts in the fission yeast cell division cycle as a component of the p34^{cdc2} kinase. EMBO Journal **6**: 3057-3514.

Brown, C. G. D. (1987). Theileriidae. In "*In vitro* Methods for Parasite Cultivation" (A.E.R. Taylor and H.R. Baker, editors) pp230-253. Academic Press. :

Brown, D. J., Campbell, J. D. M., Russell, G. C., Hopkins, J. and Glass, E. J. (1995). T-cell activation by *Theileria annulata* infected macrophages correlates with cytokine production. Clinical and Experimental Immunology **102**: 507-514.

Brown, W. C., Lonsdaleeccles, J. D., Demartini, J. C. and Grab, D. J. (1990). Recognition of soluble *Theileria parva* antigen by bovine helper T cell clones - characterisation and partial purification of the antigen. Journal of Immunology **144**: 271-277.

Campbell, J. D., Brown, D. J., Glass, E. J., Hall, F. R. and Spooner, R. L. (1994). *Theileria annulata* sporozoite targets. Parasite Immunology **16**: 501-505.

Caras, I. W. and Martin, D. W. (1988). Molecular cloning of the cDNA for a mutant mouse ribonucleotide reductase M1 that produces a dominant mutator phenotype in mammalian cells. Molecular and Cellular Biology **8**: 2698-2704.

Carrington, M., Allsopp, B., Baylis, H., Malu, N. M., Shochat, Y. and Sohal, S. (1995). Lymphoproliferation caused by *Theileria annulata* and *Theileria parva*. In Molecular Approaches to Parasitology eds J.Boothroyd and R. Kommuniecki (Wiley -Liss) p43-46.

Carrington, M., Shochat, Y. and Gurnett, A. M. (1996). Use of toxin ricin to specifically inhibit host cell protein synthesis. Parasitology Today **12**: 492-495.

Carter, R., Graves, P. M., Keister, D. B. and Quakyi, I. A. (1990). Properties of epitopes of Pf 48/45, a target of transmission blocking monoclonal antibodies, on gametes of different isolates of *Plasmodium falciparum*. Parasite Immunology **12**: 587-603.

Cazzola, M., Bergamaschi, G., Dezza, L. and Arosio, P. (1990). Manipulation of cellular iron metabolism for modulating normal and malignant cellular proliferation: achievements and prospects. Blood **75**: 1903-1919.

Chakrabarti, D., Schuster, S. M. and Chakrabarti, R. (1993). Cloning and characterisation of subunit genes of ribonucleotide reductase, a cell cycle regulated enzyme from *Plasmodium falciparum*. Proceedings of the National Academy of Sciences, USA **90**: 12020-12024.

Chavalitshewinkoon, P., Devries, E., Stam, J. G., Franssen, F. F. J., VanderVliet, P. C. and Overdulve, J. P. (1993). Purification and characterisaton of DNA polymerases from *Plasmodium falciparum*. Molecular and Biochemical Parasitology **61**: 243-253.

Church, G. M. and Gilbert, W. (1984). Genomic sequencing. Proceedings of the National Academy of Sciences, USA **81**: 1991-1995.

Coats, S., Flanagan, W. M., Nourse, J. and Roberts, J. M. (1996). Requirements of p27^{kip1} for restriction point control of the fibroblast cell cycle. Science **272**: 877-880.

Connor, J., Furlong, J., Murray, J., Meighan, M., Cross, H., Marsden, H. and Clements, J. B. (1993). Herpes simplex virus type 1 ribonucleotide reductase large subunit: Regions of the protein essential for subunit interaction and dimerisation. Biochemistry **32**: 13673-13680.

Conrad, P. A., Kelly, B. G. and Brown, C. G. D. (1985). Intraerythrocyctic schizogony of *Theileria annulata*. Parasitology **91**: 67-82.

Cowdry, E. V. and Ham, A.W. (1932). Studies on East Coast Fever 1: The life cycle of the parasite in ticks. Parasitology **24**: 1-49.

Cox, F. E. G. (1993). Modern Parasitology, 2nd edition, Blackwell Scientific Publications, London. :

D'Olivera, C., Tijhaar, E. J., Shiels, B. R., Vanderweide, M. and Jongejan, F. (1996). Expression of genes encoding 2 major *Theileria annulata* merozoite surface antigens in *Escherichia coli* and a *Salmonella typhimurium* AROA vaccine strain. Gene **172**: 33-39.

Dalton, S. (1992). Cell cycle regulation of the human cdc2 gene. EMBO Journal **11**: 1797-1804.

Davis, R., Thelander, M., Mann, G. J., Behravan, G., Soucy, F., Beaulieu, P., Lavallee, P., Graslund, A. and Thelander, L. (1994). Purification, characterisation and localisation of subunit interaction area of recombinant mouse ribonucleotide reductase R1 subunit. Journal of Biological Chemistry **269**: 23171-23176.

deBondt, H. L., Rosenblatt, J., Jancarik, J., Jones, H. D., Morgan, D. O. and Kim, S. H. (1993). Crystal structure of cyclin dependent kinase 2. Nature **363**: 595-602.

Devereux, J., Haeberli, P. and Smithies, O. (1984). A comprehensive set of sequence analysis programmes for the VAX. Nucleic Acids Research **127**: 387-395.

Dickson, J. and Shiels, B. R. (1993). Antigenic diversity of a major surface molecule in *Theileria annulata*. Molecular and Biochemical Parasitology **57**: 55-64.

Dobbelaere, D. A. E., Coquerelle, T. M., Roditi, I. J., Eichhorn, M. and Williams, R. O. (1988). *Theileria parva* infection induces autocrine growth of bovine lymphocytes. Proc. Natl. Acad. Sci. **85**: 4730-4734.

Dobbelaere, D. A. E., Prospero, T. D., Roditi, I. J., Kelke, C., Bauman, I., Eichhorn, M., Williams, R. O., Ahmed, J. S., Baldwin, C. L., Clevers, H. and Morrison, W. I. (1990). Expression of Tac antigen component of bovine interleukin 2 receptor in different leukocyte populations infected with *Theileria parva* or *Theileria annulata*. Infection and Immunity **58**(12): 3847-3855.

Dobbelaere, D. A. E., Roditi, I. J., Coquerelle, T. M., Kelke, C., Eichhorn, M. and Williams, R. O. (1991). Lymphocytes infected with *Theileria parva* require both cell-cell contact and growth factor to proliferate. European Journal of Immunology **21**: 89-95.

Dolan, T.T. (1989). Theileriosis in Eastern, Central and Southern Africa. Ed. T.T. Dolan. ILRAD, Nairobi.

Dolan, T. T. (1992). Recent Developments in the Research and Control of *Theileria annulata*. Proceedings of a Workshop held at ILRAD, Nairobi, Kenya, 17-19 September 1990. (T.T. Dolan, editor). ILRAD, Nairobi.

Draetta, G. and Beach, D. (1988). Activation of cdc2 protein kinase during mitosis in human cells - cell cycle dependent phosphorylation and subunit rearrangement. Cell **54**: 17-26.

Draetta, G., Brizuela, L., Potashkin, J. and Beach, D. (1987). Identification of p34 and p13, human homologues of the cell cycle regulators of fission yeast encoded by cdc2 and suc1. Cell **50**: 319-325.

Drummond, R. O. (1976). Tick-bourne livestock diseases and their vectors. World Animal Review **19**: 28-33.

Dschunkowsky, E. and Luhs, J. (1904). Die Piroplasmosen der Rinder. Zentralblatt für Bakteriologie, Parasitenkunde, Infektionskrankheit und Hygiene, Abt I **35**: 486-493.

Ducommun, B., Brambilla, P. and Draetta, G. (1991). Mutations at sites involved in suc1 binding inactivate cdc2. Molecular and Cellular Biology **11**: 6177-6184.

Ducommun, B., Brambilla, P., Félix, M. A., Franza, B. R., Karsenti, E. and Draetta, G. (1991). cdc2 phosphorylation is required for its interaction with cyclin. EMBO Journal **10**(11): 3311-3319.

Dunphy, W. G. and Newport, J. W. (1989). Fission yeast p13 blocks mitotic activation and tyrosine dephosphorylation of the *Xenopus* cdc2 protein kinase. Cell **58**: 181-191.

Durkacz, B., Carr, A. and Nurse, P. (1986). Transcription of the cdc2 cell cycle control gene of the fission yeast *Schizosaccharomyces pombe*. EMBO Journal **5**: 369-373.

Dutia, B. M., Preston, V. G., Polfreiman, J. U. and Subak-Sharpe, J. H. (1984). Characteristics and physical mapping of *Herpes simplex* virus gene encoding for ribonucleotide reductase activity. Voprosy Virusologii **6**: 730-736.

Edgar, B. A., Sprenger, F., Duronio, R. J., Leopold, P. and O'Farrell, P. H. (1994). Distinct molecular mechanisms regulate cell cycle timing at successive stages in Drosophila embryogenesis. Genes & Development **8**: 440-452.

Eichhorn, M. and Dobbelaere, D. (1995). Partial inhibition of *Theileria parva* infected T cell proliferation by antisense IL2R α chain RNA expression. Research in Immunology **146**: 98-99.

Ekberg, M., Sahlin, M., Eriksson, M. and Sjoberg, B. M. (1996). Two conserved tyrosine residues in protein R1 participate in an intermolecular electron transfer in ribonucleotide reductase. Journal of Biological Chemistry **271**: 20655-20659.

Elledge, S. J. and Davis, R. W. (1990). Two genes differentially regulated in the cell cycle and by DNA damaging agents encode alternative regulatory subunits of ribonucleotide reductase. Genes and Development **4**: 740-751.

Emery, D. L., Eugui, E. M., Nelson, R. T. and Tenywa, T. (1981). Cell-mediated immune responses to *Theileria parva* (east coast fever) during immunisation and lethal infections in cattle. Immunology **43**: 323-336.

Endicott, J. A. and Nurse, P. (1995). The cell cycle and suc1: from structure to function. Structure **3**: 321-325.

Endicott, J. A., Nurse, P. and Johnston, L. N. (1994). Mutational analysis supports a structural model for the cell cycle protein kinase p34. Protein Engineering **7**(2): 243-253.

Engstrom, Y., Rozell, B., Hansson, H. A., Stemme, S. and Thelander, L. (1984). Localization of ribonucleotide reductase in mammalian cells. EMBO Journal **3**: 863-867.

Enoch, T. and Nurse, P. (1991). Coupling M phase and S phase:controls maintaining the dependence of mitosis on chromosome replication. Cell **65**: 921-927.

Fagan, R., Flint, K. J. and Jones, N. (1994). Phosphorylation of E2F-1 modulates its interaction with the retinoblastoma gene product and the adenoviral E4 19kDa protein. Cell **78**: 799-811.

Faisst, S. and Meyer, S. (1992). Compliation of vertebrate encoded transcription factors. Nucleic Acids Research **20**: 1-26.

Fan, H. Z., Villegas, C., Huang, A. P. and Wright, J. A. (1996). Suppression of malignancy by the 3' untranslated regions of ribonucleotide reductase R1 and R2 messenger RNAs. Cancer Research **56**: 4366-4369.

Fantes, P. (1989). In Molecular Biology of Fission Yeast ed Nasim, A., Young, P. & Johnson B.F. p128-204 Academic Press, London.

Fawcett, D. W., Buscher, G. and Doxsey, S. (1982). Salivary gland of the tick vector of East Coast Fever III. The ultrastructure of sporogony in *Theileria parva*. Tissue and Cell **14**: 183-206.

Fawcett, D. W., Young, A. S. and Leitch, B. L. (1985). Sporogony in *Theileria* (Apicomplexa: Piroplasmida). Journal of Submicroscopic Cytology **17**: 299-314.

Feinberg, A. P. and Vogelstein, B. (1983). A technique for radiolabelling DNA restriction fragments to high specific activity. Analytical Biochemistry **132**: 6-13.

Filatov, D., Bjorklund, S., Johanssen, E. and Thelander, L. (1996). Induction of the mouse ribonucleotide reductase R1 and R2 genes in response to DNA damage by uv light. Journal of Biological Chemistry **271**: 23698-23704.

Filatov, D., Ingemarson, R., Graslund, A. and Thelander, L. (1992). The role of *Herpes simplex* virus ribonucleotide reductase small subunit carboxyl terminus in subunit interaction and formation of iron tyrosyl center structure. Journal of Biological Chemistry **267**: 15816-15822.

Filatov, D. and Thelander, L. (1995). Role of a proximal NF-Y binding promoter element in S phase specific expression of mouse ribonucleotide reductase R2 gene. Journal of Biological Chemistry **270**(42): 25239-25243.

Fisher, A., Laub, P. B. and Cooperman, B. S. (1995). NMR structure of an inhibitory R2 C-terminal peptide bound to mouse ribonucleotide reductase R1 subunit. Nature Structural Biology **2**: 951-955.

Fisher, R. P. and Morgan, D. O. (1994). A novel cyclin associates with MO15/CDK7 to form the cdk activating kinase. Cell **78**: 713-724.

Forsburg, S. L. and Nurse, P. (1991). Cell cycle regulation in the yeasts *Saccharomyces cerevisiae* and *Schizosaccharomyces pombe*. Annual Review of Cell Biology **7**:227-237.

Fry, M., Hudson, A. T., Randall, A. W. and Williams, R. B. (1984). Potent and selective hydroxy-napthoquinone inhibitors of mitochondrial electron transport in *Eimeria tenella* (Apicomplexa:Coccidia). Biochemical Pharmacology **33**: 2115-2122.

Fujisaki, K. (1992). A review of the taxonomy of *Theileria sergenti/buffeli/orientalis* group parasites in cattle. Journal of Protozoological Research **2**: 87-96.

Fujisaki, K., Kawazu, S. and Kamio, T. (1994). The taxonomy of bovine *Theileria* species. Parasitology Today **10**: 31-33.

Gajadhar, A. A., Marquardt, W. C., Hall, R., Gunderson, J., Ariztia-Carmona, E. V. and Sogin, M. L. (1991). Ribosomal RNA sequences of *Sarcocystis muris, Theileria annulata* and *Crypthecodinium cohnii* reveal evolutionary relationships among apicomplexans, dinoflagellates and ciliates. Molecular and Biochemical Parasitology **45**: 147-154.

Galanti, N., Dvorak, J. A., Grenet, J. and McDaniel, J. P. (1994). Hydroxurea induced synchrony of DNA replication in the kinetoplastida. Experimental Cell Research **214**: 225-230.

Gale, M., Jr. and Parsons, M. (1993). A *Trypanosoma brucei* gene family encoding protein kinases with catalytic domains structurally related to Nek1 and NIMA. Molecular and Biochemical Parasitology **59**: 111-122.

Gauer, M., Mackenstedt, U., Melhorn, H., Schein, E., Zapf, F., Njenga, E., Young, A. and Morzaria, S. (1995). DNA measurements and ploidy determination of developmental stages in the life cycles of *Theileria annulata* and *Theileria parva*. Parasitology Research **81**: 565-574.

Glascodine, J., Tetley, L., Tait, A., Brown, C. G. D. and Shiels, B. R. (1990). Developmental expression of a *Theileria annulata* merozoite surface antigen. Molecular and Biochemical Parasitology **40**: 105-112.

Glass, E. J., Innes, E. A., Spooner, R. L. and Brown, C. G. D. (1989). Infection of bovine monocyte/macrophage populations with *Theileria annulata* and *Theileria parva*. Veterinary Immunology and Pathology **22**: 355-368.

Gordon, C. and Fantes, P. (1986). The *cdc22* gene of *Schizosaccharomyces pombe* encodes a cell cycle regulated transcript. EMBO Journal **5**: 2981-2986.

Graeser, R., Franklin, R. M. and Kappes, B. (1996). Mechanisms of activation of the cdc2-related kinase PfPK5 from *Plasmodium falciparum*. Molecular and Biochemical Parasitology **79**: 125-127.

Greenberg, G. R. and Hilfinger, J. M. (1996). Regulation of synthesis of ribonucleotide reductase and relationship to DNA synthesis in various systems. Progress in Nucleic Acid Research and Molecular Biology **53**: 345-395.

Grewal, A. S. (1992). Research developments in diagnosis and control of bovine tropical theileriosis in India. In "Recent Developments in the Research and Control of *Theileria annulata*:Proceedings of a Workshop held at ILRAD 17-19 September 1990" (T.T. Dolan, editor) pp 41-45. Nairobi, ILRAD.

Hadwiger, J. A., Wittenberg, C., Mendenhall, M. D. and Reed, S. I. (1989). The *Saccharomyces cerevisiae CKS1* gene, a homolog of the *Schizosaccharomyces pombe suc1+* gene, encodes a subunit of the Cdc28 protein kinase complex. Molecular and Cellular Biology **9**: 2034-2041.

Hall, F. R. (1988). Antigens and Immunity in *Theileria annulata*. Parasitology Today **4**: 257-261.

Hall, R., Hunt, P. D., Carrington, M., Simmons, D., Williamson, S., Mecham, R. P. and Tait, A. (1992). Mimicry of elastin repetitive motifs by_*Theileria annulata* sporozoite surface antigen. Molecular and Biochemical Parasitology **53**: 105-112.

Harder, J. (1993). Ribonucleotide reductases and their occurance in microorganisms: A link to the RNA/DNA transition. FEMS Microbiology Reviews **12**: 273-292.

Harlow, E. and Lane, D. (1988). Antibodies: A Laboratory Manual,. Cold Spring Harbor Laboratory Press, Cold Spring Harbor.

Harper, J. W., Adami, G. R., Wei, N., Keyomarsi, K. and Elledge, S. J. (1993). The p21-Cdk interacting protein Cip1 is a potent inhibitor of G1 cyclin dependent kinases. Cell 75: 805-816.

Harris, P., Kersey, P. J., McInery, C. J. and Fantes, P. A. (1996). Cell cycle, DNA damage and heat shock regulate $suc22^{+}$ expression in fission yeast. Molecular and General genetics 252(284-291):

Hashemi-Fesharki, R. (1992). Theileriosis due to *Theileria annulata* in Iran. In "Recent Developments in the Research and Control of *Theileria annulata*:Proceedings of a Workshop held at ILRAD 17-19 September 1990" (T.T. Dolan, editor) pp 15-18. Nairobi, ILRAD.

Hayles, J., Aves, S. and Nurse, P. (1986a). *suc1* is an essential gene involved in both the cell cycle and growth in fission yeast. EMBO Journal 5: 3373-3380.

Hayles, J., Beach, D., Durkacz, B. and Nurse, P. (1986b). The fission yeast cell cycle control gene *cdc2*:isolation of a sequence *suc1* that suppresses *cdc2* mutant function. Molecular and General Genetics 9: 2034-2041.

Heald, R., McLoughlin, M. and McKeon, F. (1993). Human wee1 maintains mitotic timing by protecting the nucleus from cytoplasmically activated cdc2 kinase. Cell 74: 463-474.

Hepler, P. K., Sek, F. J. and John, P. C. L. (1994). Nuclear concentration and mitotic dispersion of the essential cell cycle protein $p13^{suc1}$ examined in living cells. Proceedings of the National Academy of Sciences, USA 91: 2176-2180.

Heussler, V. T., Eichhorn, M., Reeves, R., Magnusson, N. S., Williams, R. O. and Dobbelaere, D. A. E. (1992). Constitutive IL-2 messenger RNA expression in lymphocytes infected with the intracellular parasite *Theileria parva*. Journal of Immunology 149: 562-567.

Horrocks, P., Jackson, M., Cheesman, S., White, J. H. and Kilbey, B. J. (1996). Stage specific expression of proliferating cell nuclear antigen and DNA polymerase δ from *Plasmodium falciparum*. Molecular and Biochemical Parasitology 79: 177-182.

Horrocks, P. and Kilbey, B. J. (1996). Physical and functional mapping of the transcriptional start sites of *Plasmodium falciparum* proliferating cell nuclear antigen. Molecular and Biochemical Parasitology 82: 207-215.

Ingemarson, R. and Thelander, L. (1996). A kinetic study on the influence of nucleoside triphosphate effectors on subunit interaction in mouse ribonucleotide reductase. Biochemistry **35**: 8603-8609.

Inselburg, J. and Banyal, H. S. (1984). *Plasmodium falciparum:* Synchronisation of asexual development with aphidicolin, a DNA synthesis inhibitor. Experimental Parasitology **57**: 48-54.

Irvin, A. D. (1987). Charcterisation of species and strains of _Theileria_. Advances in Parasitology **26**: 145-197.

Irvin, A. D. and Morrison, W. I. (1987). Immunopathology, immunology and immunoprophylaxis of *Theileria* infections. In "Immune Responses in Parasitic Infections:Immunopathology, Immunology and Immunoprophylaxis". (E.J.L. Soulsby, editor) pp223-274. CRC Press.

Irvin, A. D., Ocama, J. G. R. and Spooner, P. R. (1982). Cycle of bovine lymphoblastoid cells parasitised by *Theileria parva*. Research in Veterinary Science **33**: 298-304.

Jackman, M., Firth, M. and Pines, J. (1995). Human cyclins B1 and B2 are localised to strikingly different structures - B1 to microtubules, B2 primarily to the Golgi apparatus. EMBO Journal **14**: 1646-1654.

Jackson, P. K. (1996). Cell cycle: Cull and destroy. Current Biology **6**: 1209-1212.

Javahery, R., Khachi, A., Lo, K., Zenzie-Gregory, B. and Smale, S. T. (1994). DNA sequence requirements for transcription initiator activity in mammalian cells. Molecular and cellular biology **14**: 116-127.

Jeffrey, P. D., Russo, A. A., Polyak, K., Gibbs, E., Hurwitz, J., Massague, J. and Pavletich, N. P. (1995). Mechanism of CDK activation revealed by the structure of a cyclin A/CDK2 complex. Nature **376**: 313-320.

Johnson, R. T., Downes, C. S. and Meyn, R. E. (1993). The synchronisation of mammalian cells. In "The cell cycle - a practical approach" eds P.Fantes & R. Brooks IRL Press, London :

Johnston, L. H. and Johnson, A. L. (1995). The DNA repair genes RAD54 and UNG1 are cell cycle regulated in budding yeast but MCB promoter elements have no essential role in DNA damage response. Nucleic Acids Research **23**: 2147-2152.

Johnston, L. H. and Lowndes, N. F. (1992). Cell cycle control of DNA synthesis in budding yeast. Nucleic Acids Research **20**: 2403-2410.

Jura, W. G. Z. O., Brown, C. G. D. and B., K. (1983). Fine structure and invasive behaviour of the early developmental stages of *Theileria annulata in vitro*. Veterinary Parasitology **12**: 31-44.

Kaffman, A., Herskowitz, I., Tjian, R. and O'Shea, E. K. (1994). Phosphorylation of the transcription factor PHO4 by a cyclin-CDK complex, PHO80-PHO85. Science **263**: 1153-1156.

Kamb, A., Gruis, N. A., Weaver-Feldman, J., Lui, Q., Harshman, K., Tavtigian, S. V., Stockert, E., Day, R. S., Johnson, B. E. and Skolnick, M. H. (1994). A cell cycle regulator potentially involved in genesis of many tumour types. Science **264**: 436-440.

Kamijo, M., Yasuda, H., Yau, P. M., Yamashita, M., Nagahama, Y. and Ohba, Y. (1992). Preference of human cdc2 kinase for peptide substrate. Peptide Research **5**: 281-285.

Kastan, M. B., Onyekwere, O., Sidransky, D., Volgelstein, B. and Craig, R. W. (1991). Participation of p53 in the cellular response to DNA damage. Cancer Research **51**: 6304-6310.

Kato, J. Y., Matsuoka, M., Polyak, K., Massague, J. and Sherr, C. J. (1994). Cyclic AMP induced G1 phase arrest mediated by an inhibitor p27^{kip1} of cyclin dependent kinase 4 activation. Cell **79**: 487-496.

Katzer, F., Carrington, M., Knight, P., Williamson, S., Tait, A., Morrison, W. I. and Hall, R. (1994). Polymorphism of SPAG-1, a candidate antigen for inclusion in a subunit vaccine against *Theileria annulata*. Molecular and Biochemical Parasitology **67**: 1-10.

Kelley, W. S. (1996). Therapeutic peptides: The devil is in the details. Bio/Technology **14**: 28-31.

Kinnaird, J. H., Logan, M., Kirvar, E., Tait, A. and Carrington, M. (1996). The isolation and characterisation of genomic and cDNA clones coding for a cdc2-related kinase (ThCRK2) from the bovine protozoan parasite *Theileria*. Molecular Microbiology **22**: 293-302.

Knighton, D. R., Bell, S. M., Zheng, J. H., Teneyck, L. F., Xuong, N. H., Taylor, S. S. and Sowadski, J. M. (1993). 2.0 Angstrom refined crystal structure of the catalytic subunit of cAMP-dependent protein kinase complexed with a peptide inhibitor and detergent. Acta Crystallographa section D- Biological Crystallography **49**: 357-361.

Kozak, M. (1987). An analysis of 5' non-coding sequences from 699 vertebrate messenger RNAs. Nucleic Acids Research **15**: 8125-8148.

Krek, W. and Nigg, E. A. (1992). Cell cycle regulation of vertebrate p34^{cdc2} activity-identification of Thr161 as an essential *in vivo* phosphorylation site. New Biologist **4**: 323-329.

Krogsrud, R. L., Welchner, E., Scouten, E. and Liuzzi, M. (1993). A solid phase assay for the binding of peptidic subunit association inhibitors to the *Herpes simplex* virus ribonucleotide reductase large subunit. Analytical Biochemistry **213**: 386-394.

Labbe, J. C., Picard, A., Peaucellier, G., Cavadore, J. C., Nurse, P. and Doree, M. (1989). Purification of MPF from starfish: Identification as the Histone H1 kinase p34^{cdc2} and a possible mechanism for its periodic activation. Cell **57**: 253-263.

Labib, K., Craven, R. A., Crawford, K. and Nurse, P. (1995). Dominant mutants identify new roles for p34(cdc2) in mitosis. EMBO Journal **14**: 2155-2165.

Laemmli, U. K. (1970). Cleavage of structural proteins during the assembly of the head of bacteriophage T4. Nature **227**: 680-685.

Lee, M. G. and Nurse, P. (1987). Complementation used to clone a human homologue of the fission yeast cell cycle control gene *cdc2*. Nature **327**: 31-35.

Leete, T. H. and Rubin, H. (1996). Malaria and the cell cycle. Parasitology Today **12**: 442-444.

Lehner, C. F. and O'Farrell, P. H. (1990). *Drosophila* cdc2 homologues: a functional homologue is coexpressed with a cognate variant. EMBO Journal **9**: 3573-3584.

Levine, N. D., Corliss, J. O., Cox, F. E. G., Deroux, G., Honigberg, B. M., Leedale, G. F., Loeblich, A. R., Lom, J., Lynn, D., Merinfeld, E. G., Page, F. C., Poljansky, G., Sprague, V., Varva, J. and Wallace, F. G. (1980). A newly revised classification of the protozoa. Journal of Protozoology **27**: 37-58.

Lew, D.J. and Kornbluth, S. (1996). Regulatory roles of cyclin dependent kinase phosphorylation in cell cycle control. Current Opinion in Cell Biology **8**: 795-804.

Lew, J., Winkfein, R. J., Paudel, H. K. and Wang, J. H. (1992). Brain proline directed protein kinase is a neurofilament kinase which displays high sequence homology to p34^{cdc2}. Journal of Biological Chemistry **267**: 25922-25926.

Liuzzi, M., Deziel, R., Moss, N., Beaulieu, P., Bonneau, A. M., Bosquet, C., Chafouleas, J. G., Garneau, M., Jaramillo, J., Krogsrud, R. L., Lagace, L., McCollum, R. S., Nawoot, S. and Guidon, Y. (1994). A potent peptidomimetic inhibitor of HSV ribonucleotide reductase with antiviral activity in vitro. Nature **372**: 695-698.

Lowndes, N. F., McInerny, C. J., Johhson, A. L., Fantes, P. A. and Johnston, L. H. (1992). Control of DNA synthesis genes in fission yeast by the cell cycle gene $cdc10^+$. Nature **355**: 449-453.

Luo, Q., Michaelis, C. and Weeks, G. (1994). Over-expression of a truncated cyclin B gene arrests *Dictyostelium* cell division during mitosis. Journal of Cell Science **107**: 3105-3114.

Luo, Q., Michaelis, C. and Weeks, G. (1995). Cyclin B and cdc2 expression and cdc2 kinase activity during *Dictyostelium* differentiation. DNA and cell biology **14**: 901-908.

Lycksell, P. O., Ingemarson, R., Davis, R., Graslund, A. and Thelander, L. (1994). H1 NMR studies of mouse ribonucleotide reductase - the R2 protein carboxyl-terminal tail, essential for subunit interaction, is highly flexible but becomes rigid in the presence of protein R1. Biochemistry **33**: 2838-2842.

Makioka, A., Stavros, B., Ellis, J. T. and Johnson, A. M. (1993). Detection and characterisation of a DNA polymerase activity in *Toxoplasma gondii*. Parasitology **107**: 135-139.

Marcote, M. J., Knighton, D. R., Basi, G., Sowadski, J. M., Brambilla, P., Draetta, G. and Taylor, S. S. (1993). A three dimensional model of the cdc2 protein kinase: localisation of cyclin and suc1 binding regions an phosphorylation sites. Molecular and Cellular Biology **13**: 5122-5131.

Matsushime, H., Roussel, M. F., Ashmun, R. A. and Sherr, C. J. (1991). Colony stimulating factor 1 regulates novel cyclins during the G1 phase of the cell cycle. Cell **65**: 701-712.

McAndrew, M. B., Read, M., Sims, P. F. G. and Hyde, J. E. (1993). Characterisation of a gene encoding an unusually divergent TATA-binding protein (TBP) from the extremely A+T rich human malaria parasite, *Plasmodium falciparum*. Gene **124**: 165-171.

McGowan, C. H., Russell, P. and Reed, S. (1990). Periodic biosynthesis of the human M phase promoting factor catalytic subunit p34 during the cell cycle. Molecular and Cellular Biology **10**: 3847-3851.

McHardy, N. (1992). Chemotherapy of theileriosis: Field experience with butalex. In "Third Symposium on Tropical Animal Health and Production: Bovine Theileriosis. 9th October, 1992". Office for International Cooperation, Faculty of Veterinary Medicince, Utrecht.

McHardy, N., Hudson, A. T., Morgan, D. W. T., Rae, D. G. and Dolan, T. T. (1983). Activity of 10 napthoquinones, including parvaquone (993C) and menoctone, in cattle artificially infected with *Theileria parva*. Research in Veterinary Science **35**: 29-33.

McKeever, D. J., Taracha, E. L. N., Innes, E. L., MacHugh, N. D., Awino, E., Goddeeris, B. M. and Morrison, W. I. (1994). Adoptive transfer of immunity to *Theileria parva* in the CD8+ fraction of responding efferent lymph. Proceedings of the National Academy of Sciences, USA **91**: 1959-1963.

Meijer, L., Arion, D., Golsteyn, R., Pines, J., Brizuela, L., Hunt, T. and Beach, D. (1989). Cyclin is a component of the sea urchin egg M phase specific histone H1 kinase. EMBO Journal **8**: 2275-2282.

Melhorn, H. and Schein, E. (1984). The piroplasm: Life cycle and sexual changes. Advances in Parasitology **23**: 37-103.

Merika, M. and Orkin, S. H. (1993). DNA binding specificity of GATA family transcription factors. Molecular and Cellular Biology **13**: 3999-4010.

Meyerson, M., Enders, G. H., Wu, C. L., Su, L. K., Gorka, C., Nelson, C., Harlow, E. and Tsai, L. H. (1992). A family of human cdc2 related protein kinases. EMBO Journal **11**: 2909-2918.

Michaelis, C. and Weeks, G. (1992). Isolation and characterisation of a cdc2 cDNA from *Dictyostelium discoideum*. Biochimica et Biophysica Acta **1132**: 35-42.

Michaelis, C. and Weeks, G. (1993). The isolation from a unicellular organism, *Dictyostelium discoidium*, of a highly related cdc2 gene with characteristics of the PCTAIRE subfamily. Biochimica et Biophysica Acta **1179**: 117-124.

Mishra, R. K., Moreau, C., Ramazeilles, C., Moreau, S., Bonnet, J. and Toulme, J. J. (1995). Improved Leishmanicidal effect of phosphoborothioate antisense oligonucleotides by LDL-mediated delivery. Biochimica et Biophysica Acta **1264**: 229-237.

Moreno, S., Hayles, J. and Nurse, P. (1989). Regulation of the p34^{cdc2} kinase during mitosis. Cell **58**: 361-372.

Morrison, W. I. (1996). Influence of host and parasite genotypes on immunological control of *Theileria* parasites. Parasitology **112**: S53-S66.

Morrison, W. I., Goddeeris, B. M., Brown, W. C., Baldwin, C. L. and Teale, A. J. (1989). *Theileria parva* in cattle: Characterisation of infected lymphocytes and the immune responses they provoke. Veterinary Immunology and Immunopathology **20**: 213-227.

Morrison, W. I., Godeeris, B. M., Teale, A. J., Groocock, C. M., Kemp, S. J. and Stagg, D. A. (1987). Evidence for restriction by class I MHC determinants and parasite strain specificity. Parasite Immunology **9**: 563-578.

Morzaria, S. P., Roeder, P. L., Roberts, D. H., Chasey, D. and Drew, T. W. (1982). Characteristics of a continuous suspension cell line (BL20) derived from a calf with sporadic bovine leukosis. In Fifth International Sympoium on Bovine Leukosis, Tubingen, 1982. Straub, O.C. (editor), Commission of the European Communities Report Eur 8471EN pp519-528. :

Morzaria, S. P. and Young, J. R. (1992). Restriction mapping of the genome of the protozoan parasite *Theileria parva*. Proceedings of the National Academy of Sciences, USA **89**: 5241-5245.

Mottram, J. C. (1994). Cdc2 related protein kinases and cell cycle control in trypanosomatids. Parasitology Today **10**: 253-257.

Mottram, J. C. and Grant, K. M. (1996). *Leishmania mexicana* p12^{cks1}, a homologue of fission yeast p13^{suc1} associates with a stage regulated histone H1 kinase. Biochemical Journal **316**: 833-839.

Mottram, J. C., Kinnaird, J. H., Shiels, B. R., Tait, A. and Barry, J. D. (1993). A novel cdc2 related protein kinase from *Leishmania mexicana* LmmCRK1 is post translationally regulated during the life cycle. Journal of Biological Chemistry **268**(28): 21044-21054.

Mottram, J. C. and Smith, G. (1995). A family of Trypanosome cdc2 related protein kinases. Gene **162**: 147-152.

Mukhebi, A. W., Perry, B. D. and Kruska, R. (1992). Estimated economics of theileriosis control in Africa. Preventative Veterinary Medicine **12**: 77-85.

Muller, R., Mumberg, D. and F.C., L. (1993). Signals and genes in the control of cell cycle progression. Biochimica et Biophysica Acta **1155**: 151-179.

Murphree, S., Stubblefield, E. and Moore, E. C. (1969). Synchronised mammalian cell cultures, III. Variation of ribonucleotide reductase activity during the replication cycle of Chinese hamster fibroblasts. Experimental Cell Research **58**: 118-124.

Mutomba, M. C. and Wang, C. C. (1996). Effects of aphidicolin and hydroxyurea on the cell cycle and differentiation of *Tryapanosoma brucei* blood-stream forms. Molecular and Biochemical Parasitology **80**: 89-102.

Neitz, W. O. (1957). Theileriosis, gonderosis and cytauxzoonoses. A review. The Onderstepoort Journal of Veterinary Science **27**: 275-430.

Ngumi, P. N., Lesan, A. C., Williamson, S. M., Awich, J. R., Morzaria, S. P., Dolan, T. T., Shaw, M. K. and Young, A. S. (1994). Isolation and preliminary characterisation of a

previously unidentified *Theileria* parasite of cattle in Kenya. Research in Veterinary Science **57**: 1-9.

Norval, R. A. I., Fivaz, B. H., Lawrence, J. A. and Brown, A. F. (1985). Epidemiology of tick borne diseases of cattle in Zimbabwe.III. The *Theileria parva* group. Tropical Animal Health and Production **17**: 19-28.

Nurse, P. (1994). Ordering S-phase and M-phase in the cell cycle. Cell **79**: 547-550.

Nurse, P. and Bisset, Y. (1981). Gene required in G1 for commitment to cell cycle and in G2 for control of mitosis in fission yeast. Nature **292**: 558-592.

ole Moi Yoi, O. K., Brown, W. C., Iams, K. P., Nayar, A., Tsukamoto, T. and Macklin, M. D. (1993). Evidence for the induction of casein kinase II in bovine lymphocytes transformed by the intracellular protozoan parasite *Theileria parva*. EMBO Journal **12**(4): 1621-1631.

Oliver, R. A. and Williams, J. L. (1996). Altered expression of Class I major histocompatibility antigens on bovine cells infected with the protozoan parasite *Theileria annulata*. Veterinary Immunology and Immunopathology **50**: 173-179.

Orkin, S. (1995). Transcription factors and hematopoietic development. Journal of Biological Chemistry **270**: 4955 - 4958.

Osmani, A. H., van Peij, N., Mischke, M., O'Connell, M. J. and Osmani, S. A. (1994). A single p34^{cdc2} protein kinase (encoded by nimX^{cdc2}) is required at G1 and G2 in *Aspergillus nidulans*. Journal of Cell Science **107**: 1519-1528.

Osmani, S. A. and Ye, X. S. (1996). Cell cycle regulation in *Aspergillus* by two protein kinases. Biochemical Journal **317**: 633-641.

Papadopoulos, B., Perie, N. M. and Uilenberg, G. (1996). Piroplasms of domestic animals in the macedonia region of Greece. Veterinary Parasitology **63**: 41-56.

Pardee, A. B. (1989). G1 events and regulation of cell proliferation. Science **246**: 603-607.

Parge, H. E., Arvai, A. S., Murtain, D. J., Reed, S. I. and Tainer, J. A. (1993). Human cksHs2 atomic structure: A role for its hexameric assembly in cell cycle control. Science **262**: 387-395.

Paris, J., Le, G. R., Couturier, A., Le, G. K., Omilli, F., Camonis, J., MacNeill, S. and Philippe, M. (1991). Cloning by differential screening of a *Xenopus* cDNA encoding for a protein highly homologous to cdc2. Proceedings of the National Academy of Sciences, USA **88**: 1039-1046.

Park, H., Francesconi, S. and Wang, T. S. F. (1993). Cell cycle expression of two replicative DNA polymerases α and δ from *Schizosaccharomyes pombe*. Molecular Biology of the cell **4**: 145-157.

Parker, N. J., Begley, C. G. and Fox, R. M. (1995). Human gene for the large subunit of ribonucleotide reductase (RRM1): Functional analysis of the promoter. Genomics **27**: 280-285.

Patra, D. and Dunphy, W. G. (1996). Xe-p9, a *Xenopus* Suc1/Cks homolog, has multiple essential roles in cell cycle control. Genes & Development **10**: 1503-1515.

Pearson, B. E., Nasheuer, H. P. and Wang, T. S. F. (1991). Human DNA polyermase α gene: sequence controlling expression in serum stimulated cells. Mol. Cell Biol **11**: 2081-2095.

Pines, J. (1996). Cyclin from sea urchins to HeLas:making the human cell cycle. Biochemical Society Transactions **24**: 15-33.

Pines, J. and Hunter, T. (1995). Cyclin dependent kinases: an embarrassment of riches? In Cell Cycle Control ed C. Hutchinson and D. Glover IRL Press.

Pipano, E. (1981). Schizonts and tick stages in immunization against *Theileria annulata* infection. In "Advances in the Control of Theileriosis", (A.D. Irvin, M.P. Cunningham and A.S. Yound, editors) pp242-252. Martinus Nijhoff, The Hague.

Poluha, W., Poluha, D. K., Chang, B. C., Crosbie, N. E., Schonhoff, C. M., Kilpatrick, D. L. and Ross, A. H. (1996). The cyclin dependent kinase inhibitor p21^{wafl} is required for survival of differentiating neuroblastoma cells. Molecular and Cellular Biology **16**: 1335-1341.

Pondaven, P., Meijer, L. and Beach, D. (1990). Activation of M phase specific histone H1 kinase by modification of its p34^{cdc2} and cyclin components. Genes and Development **4**: 9-17.

Preston, P. M. and Brown, C. G. D. (1988). Macrophage mediated cytostasis and lymphocyte cytotoxicity in cattle immunised with *Theileria annulata* sporozoites or macroschizont infected cell lines. Parasite Immunology **10**: 631-647.

Preston, P. M., Brown, C. G. D., Bell-Sakyi, L., Richardson, W. and Sanderson, A. (1992). Tropical theileriosis in *Bos taurus* and *Bos taurus x Bos indicus* calves: Response to infection with graded doses of sporozoites of *Theileria annulata*. Research in Veterinary Research Science **53**: 230-243.

Preston, P. M., Brown, C. G. D. and Spooner, R. L. (1983). Cell mediated cytotoxicity in *Theileria annulata* infection of cattle with evidence for BoLA restriction. Clinical and Experimental Immunology **53**: 88-100.

Preston, P. M., McDougall, C., Wilkie, G., Shiels, B. R., Tait, A. and Brown, C. G. D. (1986). Specific lysis of *Theileria annulata* infected lymphoblastoid cells by a monoclonal antibody recognising an infection associated antigen. Parasite Immunology **8**: 369-380.

Purnell, R. E. and Joyner, L. P. (1968). The development of *Theileria parva* in the salivary glands of the tick *Rhipicephalus appendiculatus*. Parasitology **58**: 725-732.

Radley, D. E., Brown, C. G. D., Burridge, M. J., Cunningham, M. P., Kirimi, I. M., Purnell, R. E. and Young, A. S. (1975). East Coast Fever: Chemoprophylactic immunization of cattle against *Theileria parva* (Muguga) and five Theileria strains. Veterinary Parasitology **1**: 35-41.

Ramazeilles, C., Mishra, R. K., Moreau, S., Pascolo, E. and Toume, J. J. (1994). Antisense phosphorothioate oligonucelotides - selective killing of the intracellular parasite *Leishmania amazonensis*. Proceedings of the National Academy of Sciences, USA **91**: 7859-7863.

Reichard, P. (1988). Interactions between deoxyribonucleotide and DNA synthesis. Annual Review of Biochemistry **57**: 349-374.

Reichard, P. (1993). From RNA to DNA, why so many ribonucleotide reductases? Science **260**: 1773-1777.

Reid, G. D. F. and Bell, L. J. (1984). The development of *Theileria annulata* in the salivary glands of the tick vector *Hyalomma anatolicum anatolicum*. Annals of Tropical Medicine and Parasitology **78**: 409-421.

Riabowol, K., Draetta, G., Brizuela, L., Vandre, D. and Beach, D. (1989). The cdc2 kinase is a nuclear protein that is essential for mitosis in mammalian cells. Cell **57**: 393-401.

Richardson, H. E., Stueland, C. S., Thomas, J., Russell, P. and Reed, S. I. (1990). Human cDNAs encoding homologs of the small p34$^{CDC28/cdc2}$ associated protein of *Saccharomyces cerevisiae* and *Schizosaccharomyces pombe*. Genes and Development **4**: 1332-1344.

Ross-MacDonald, D. B., Graeser, R., Kappes, B., Franklin, R. and Williamson, D. H. (1994). Isolation and expression of a gene specifying a cdc2 like protein kinase from the human malarial parasite Plasmodium falciparum. FEBS European Journal of Biochemistry **220**: 693-701.

Rowley, A., Johnston, G. C., Butler, B., Werner-Washburne, M. and Singer, R. A. (1993). Heat shock mediated cell cycle blockage and G1 cyclin expression in the yeast *Saccharomyces cerevisiae*. Molecular and Cellular Biology **13**: 1034-1041.

Rubin, H., Salem, J. S., Li, L. S., Yang, F. D., Mama, S., Wang, Z. M., Fisher, A., Hamann, C. S. and Cooperman, B. S. (1993). Cloning, sequence determination and regulation of the ribonucleotide reductase subunits from *Plasmodium falciparum* - a target for anti-malarial therapy. Proceedings of the National Academy of Sciences, USA **90**: 9280-9284.

Russo, A. A., Jeffrey, P. D., Patten, A. K., Massague, J. and Paveletich, N. P. (1996). Crystal structure of the p27^{kip1} cyclin dependent kinase inhibitor bound to the cyclin A-CDK2 complex. Nature **382**: 325-331.

Sambrook, J., Fritsch, E. F. and Maniatis, T. (1989). Molecular Cloning: A Laboratory Manual (Cold Spring Harbor Lab. Press, Plainview, NY), 2nd Ed.

Sanger, F., Nicklen, S. and Coulson, A. R. (1977). DNA sequencing with chain terminating inhibitors. Proceedings of the National Academy of Sciences, USA **74**: 5463-5467.

Sarabia, M. J. F., McInerny, C., Harris, P., Gordon, C. and Fantes, P. (1993). The cell cycle genes *cdc22* and *suc22+* of the fission yeast *Schizosaccharomyces pombe* encode the large and small subunits of ribonucleotide reductase. Molecular and General Genetics **238**: 241-257.

Schagger, H. and von Jagow, G. (1987). Tricine - sodium dodecyl sulphate polyacrylamide gel electrophoresis for the separation of proteins in the range of 1 to 100kDa. Analytical Biochemistry **166**: 368-379.

Schein, E., Buscher, G. and Friedhoff, K. T. (1975). On the life cycle of *Theileria annulata* (Dschunkowsky and Luhs 1904) in the midgut and haemolymph of *Hyalomma anatolicum anatolicum* (Koch, 1884). Zeitschrift fur Parasitenkunde **47**: 165-167.

Schein, E. and Voight, W. P. (1981). Chemotherapy of theileriosis in cattle: In "Advances in the Control of Theileriosis" (A.D. Irvin, M.P. Cunningham and A.S. Young, editors), pp212-214. Martinus Nijhoff, The Hague.

Schein, E. B. (1986). *In vitro* screening of drugs against schizonts of *Theileria annulata*. In "Orienatation and Coordination of Research on Tropical Theileriosis". A workshop sponsored by the EEC.

Schimke, R. T., Kung, A. L., Rush, D. F. and Sherwood, S. W. (1991). Differences in mitotic control among mammalian cells. Cold Spring Harbor Symposia on Quantitative Biology, Volume LVI CSH Press : 417-425.

Sergent, E., Donatien, A., Parrot, l. and Lestoquard, F. (1945). Etudies sur les piroplasmoses bovines. Institut Pasteur d'Algerie, Alger.

Serizawa, H., Makela, T. P., Conaway, J. W., Weinberg, R. A. and Young, R. A. (1995). Association of CDK activating kinase subunits with transcription factor TFIIH. Nature **374**: 280-282.

Sharma, H. W. and Narayanan, R. (1995). The therapeutic potential of antisense oligonucleotides. Bioessays **17**: 1055-1063.

Shaw, M. K. and Tilney, L. G. (1992). How individual cells develop from a syncitium: Merogony in *Theileria parva* (Apicomplexa). Journal of Cell Science **101**: 109-123.

Sherr, C. J. (1993). Mammalian G1 Cyclins. Cell **73**: 1059-1065.

Sherr, C. J. (1994). The ins and out of RB: Coupling gene expression to the cell cycle clock. Trends in Cell Biology **4**: 15-18.

Shiels, B., Hall, R., Glascodine, J., McDougall, C., Harrison, C., Taracha, E., Brown, D. and Tait, A. (1989). Characterisation of surface polypeptides on different life cycle stages of *Theileria annulata*. Molecular and Biochemical Parasitology **34**: 209-220.

Shiels, B., Kinnaird, J., McKellar, S., Dickson, J., Ben miled, L., Melrose, R., Brown, D. and Tait, A. (1992). Disruption of synchrony between parasite growth and host cell division is a determinant of differentiation to the merozoite in *Theileria annulata*. Journal of Cell Science **101**: 99-107.

Shiels, B., McDougall, C., Tait, A. and Brown, G. C. D. (1986). Antigenic diversity of *Theileria annulata* macroschizonts. Veterinary Parasitology **21**: 1-10.

Simon, K. E., Cha, H. H. and Firestone, G. L. (1995). Transforming growth factor beta causes down regulation of Ckshs1 transcripts in growth inhibited epithelial cells. Cell growth and differentiation **6**: 1261-1269.

Singh, D.K. (1991). Theileriosis in India. In "Tropical Theileriosis - proceedings of the second EEC workshop on orientation and coordination of research." Eds D.K. Singh & B.C. Varshney.

Singleton, R. W. and Mishra, N. C. (1995). Genetic evidence that aphidicolin inhibits *in vivo* DNA synthesis in Chinese hamster ovary cells. Molecular and General Genetics **247**: 462-470.

Smeijsters, W. J. W., Zijlstra, N. M., deVries, E., Franssen, F. F. J., Janse, C. J. and Overdulve, J. P. (1994). The effect of (S)-9-(3hydroxy2phosphonylmethoxypropyl)

adenine on nuclear and organellar DNA synthesis in erythrocytic schizogony in malaria. Molecular and Biochemical Parasitology **67**: 115-124.

Spooner, P. R. (1990). Oxytetracycline inhibition of mitochondrial protein synthesis in bovine lymphocytes infected with *Theileria parva* or stimulated by mitogen. Parasitology **101**: 387-393.

Spooner, R. L., Innes, E. A., Glass, E. J. and Brown, C. G. D. (1989). *Theileria annulata* and *Theileria parva* infect and transform different bovine mononuclear cells. Immunology **66**: 284-288.

Stagg, D. A., Young, A. S., Leitch, B. L., Grootenhuis, J. G. and Dolan, T. T. (1983). Infection of mammalian cells with *Theileria* species. Parasitology **86**: 243-246.

Steuber, S., Frevert, U., Ahmed, J. S., Hauschild, S. and Schein, E. (1986). *In vitro* susceptibility of different mammalian lymphocytes to sporozoites of *Theileria annulata*. Zeitschrift für parasitenkunde **72**: 831-834.

Stubbe, J. (1990). Ribonucleotide Reductases. Advances in Enzymology **63**: 349-419.

Sutherland, I. A., Shiels, B. R., Jackson, L., Brown, D. J., Brown, C. G. D. and Preston, P. M. (1996). *Theileria annulata* -altered gene expression and clonal selection during continuous in-vitro culture. Experimental Parasitology **83**: 125-133.

Sweeney, C., Murphy, M., Kubelka, M., Ravnik, S. E., Hawkins, C. F., Wolgemuth, D. J. and Carrington, M. (1996). A distinct cycin A is expressed in germ cells in the mouse. Development **122**: 53-64.

Tait, A. and Hall, F. R. (1990). *Theileria annulata*: Control measures, diagnosis and the potential use of subunit vaccines. Rev. Sci. Tech. Off. Int. Epiz. 9(2): 387-403.

Tamaru, T. and Okada, M. (1996). Purification and characterisation of a p13^{suc1} bound serine/threonine kinase that is expressed in mature rat brain. European Journal of Biochemistry **238**: 152-159.

Tang, L., Pelech, S. L. and Berger, J. D. (1994). A *cdc2*-like kinase associated with commitment to division in *Paramecium tetraurelia*. Journal of Eukaryotic Microbiology **41**: 381-387.

Tang, L., Pelech, S. L. and Berger, J. D. (1995). Isolation of the cell cycle control gene *cdc2* from *Paramecium tetraurelia*. Biochimica et Biophysica Acta **1265**: 161-167.

Thelander, L. and Berg, P. (1986). Isolation and characterisation of expressible cDNA clones encoding the M1 and M2 subunits of mouse ribonucleotide reductase. Molecular and Cellular Biology **6**: 3433-3442.

Thelander, L. and Reichard, P. (1979). Ribonucleotide reductases. Annual Review of Biochemistry **48**: 133-158.

Thron, C. D. (1994). Theoretical dynamics of the cyclin B-MPF system: a possible role for p13^{suc1}. Biosystems **32**: 97-109.

Tobey, R. A., Valdez, J. G. and Crissmann, H. A. (1988). Synchronisation of human diploid fibroblasts at multiple stages of the cell cycle. Experimental Cell Research **179**: 400-416.

Towbin, H., Staehelin, T. and Gordon, J. (1979). Electrophoretic transfer of proteins from polyacrylamide gels to nitrocellulose sheets: procedures and some applications. Proceedings of the National Academy of Sciences, USA **76**: 4350-4354.

Uhlin, U. and Eklund, H. (1994). Structure of ribonucleotide reductase protein R1. Nature **370**: 533-539.

Uilenberg, G., Camus, E. and Barre, N. (1983). Existance in Guadaloupe (French West Indies) of *Theileria mutans* and *Theileria velifera* (Sporozoa, Theileriidae). Revue d'Elevage et de Medicine Veterinaire des Pays Tropicaux **36**: 261-264.

Uilenberg, G., Perie, N. M., Spanjer, A. A. M. and Franssen, F. F. J. (1985). *Theileria orientalis*, a cosmopolitan blood parasite of cattle - demonstration of the schizont stage. Research in Veterinary Science **38**: 352-360.

Verde, F., Labbe, J. C., Doree, M. and Karsenti, E. (1990). Regulation of microtubule dynamics by cdc2 protein kinase in cell free extracts of *Xenopus* eggs. Nature **343**: 233-236.

Verrijzer, C. P., Kal, A. J. and Van der Vliet, P. C. (1990). The DNA binding domain (POU domain) of transcription factor OCT-1 suffices for stimulation of DNA replication. EMBO Journal **9**: 1883-1888.

Verspieren, P., Cornelissen, A. W. C. A., Thoung, N. T., Helene, C. and Toulme, J. J. (1987). An acridine linked oligodeoxynucleotide targeted to the common end of trypanosome messenger RNAs kills cultured parasites. Gene **61**: 307-315.

Williamson, S., Tait, A., Brown, C. G. D., Walker, A., Beck, P., Shiels, B., Fletcher, J. and Hall, R. (1989). *Theileria annulata* sporozoite surface antigen expressed in *Eschericia coli* elicits neutralizing antibody. Proceedings of the National Academy of Sciences, USA **82**: 1585-1588.

Wright, J. A., Turley, E. A. and Greenberg, A. H. (1993). Transforming growth factor beta and fibroblast growth factor as promoters of tumor progression to malignancy. Critical reviews in oncology **4**: 473-492.

Xiong, Y., Hannon, G. J., Zhang, H., Casso, D., Kobayashi, R. and Beach, D. (1993). p21 is a universal inhibitor of cyclin kinases. Nature **366**: 701-704.

Xiong, Y., Zhang, H. and Beach, D. (1993). Subunit rearrangement of the cyclin-dependent kinases is associated with cellular transformation. Genes and Development **7**: 1572-1580.

Yamashita, M., Yoshikuni, M., Hirai, T., Fukada, S. and Nagahama, Y. (1991). A monoclonal antibody against the PSTAIR sequence of p34^{cdc2}, catalytic subunit of maturation promoting factor and key regulator of the cell cycle. Development Growth Differentiation **33**: 617-624.

Yamauchi, K. (1991). The sequence flanking transitional initiation site in protozoa. Nucleic Acids Research **10**: 2715-2720.

Young, A. S., Mutugi, J. J., Kariuki, D. P., Lampard, D., Maritim, A. C., Ngumi, P. N., Linyonyi, A., Leitch, B. L., Ndungu, S. G., Lesan, A. C., Mining, S. K., Grootenhuis, J. G., Orinda, G. O. and Wesonga, D. (1992). Immunisation of cattle against theileriosis in Nakuru district of south Kenya by infection and treatment and the introduction of unconventional tick control. Veterinary Parasitology **42**: 225-240.